The Modulation of Wound Healing for Glaucoma Filtration Surgery

A thesis submitted for the degree of

Doctor of Philosophy

Alastair Lockwood

Ocular Repair and Regeneration Biology Unit

UCL Institute of Ophthalmology and UCL School of Pharmacy

London

I, Alastair Lockwood confirm that the work presented in this thesis is my own. Where information has been derived from other sources, I confirm that this has been indicated in the thesis

For my Dad

"Do not go where the path may lead, go instead where there is no path and leave a trail"

Ralph Waldo Emerson

Abstract

Glaucoma is a leading cause of blindness worldwide. Surgical lowering of intraocular pressure (IOP) is frequently necessary, although scarring causes failure. Chemotherapeutics applied locally increase success but may have blinding complications, including hypotony and infections. Modifications in technique reduce risk, though intense monitoring is required postoperatively.

Matrix metalloproteinase inhibitors (MMPis) may be a less toxic anti-scarring alternative. Because the inhibition is reversible multiple injections are needed in experiments to maintain efficacy. Injections are uncomfortable, painful and costly however. The pharmacokinetic profile also shows concentration spikes and rapid drug clearance.

A sustained release preparation is therefore desirable. Here we show in chambers modeling aqueous flow that single pure ilomastat MMPi implants maintained a therapeutic concentration between 10 and 23 days. In the in vivo model, bleb survival appeared to be significantly prolonged, however a foreign body reaction existed to undissolved implants, with significant collagen deposition in the conjunctiva. To improve efficacy and reduce the proscarring nature of undissolved drug, implants of the more soluble MMPi marimastat and combination implants of ilomastat together with hyaluronic acid were formulated. These dissolved faster, but failed earlier. A combined implant of the anti-inflammatory dexamethasone and ilomastat appeared to prolong survival with less, but still considerable reaction. Coating ilomastat implants with a biocompatible polymer caused less reaction, but inflammatory foci existed around presumed polymer defects. A more hydrophilic polymer caused less reaction, though with macrophage infiltration.

During these experiments it became apparent that bleb appearance when using implants did not necessarily correlate with survival. Thus the notion of ‘bleb survival’ as an outcome was questioned and other outcomes tested. Dye to trace aqueous movement was too slow. Inducing ocular hypertension in the rabbit caused only a temporary, unpredictable pressure rise, and buphthalmos. Pooling IOP data from larger numbers after standard surgery appeared to be most accurate.

Acknowledgements

I am hugely grateful to many people during my time as a PhD student:

Thank-you Professors Peng Tee Khaw and Steve Brocchini. Your wisdom and guidance were invaluable in helping me develop ideas and providing encouragement at all points during my research. Your foresight gave me direction and your support strength to draw conclusions.

Thank-you Abeer Mohamed Ahmed, Ashkan Khalili, Daniel Paull, Hari Jayram, Surya and Sauparnika Rayapureddi, and Sumit Dhingra for your expertise and for being porter, anaesthetist, scrub and recovery nurse during in vivo experiments, often at unsociable hours! Thanks also to David Essex and Hodan Jama, who were invaluable, in particular when things went awry during the histological processing of the last experiments, and to Heidi Barnes who kept me safe and on my toes in the histology lab. Thank-you Sudershana for being so wonderful.

Thank-you Anya Vetter, Claire Ginn, Garima Sharma, Hala Fadda, Hanieh Khalili and Sahar Awwad for help and advice in experiments. Thank-you Dr David McCarthy for your expertise in electronmicrographs, Dr Rebecca Lever for allowing me to use her pristine lab for preparation for two of the in vivo experiments, Dr Hardyal Gill (Sunny) for all your patience with me, explaining high performance liquid chromatography and being able to point out the errors in my ways when it came to the HPLC machines.

Thank-you Professors Astrid Limb, Peter Shah, Andrew Dick and Phil Luthert for your inspiration and projection of ideas. Thank-you Jim Kirwan for all your fantastic support.

Thank-you Peggy Khaw for all your care, advice, and for making me part of the family in our unit.

Finally thank-you to Rebecca, William and Joseph, and my Mum for always being there and putting up with me.

Table of Contents

CHAPTER 1 INTRODUCTION 14

1.1 GLAUCOMA IN THE POPULATION 14

1.2 INTRAOCULAR PRESSURE (IOP) 15

1.3 GLAUCOMA FILTRATION SURGERY 17

1.4 AUGMENTATION WITH ANTIMETABOLITES 20

1.5 WOUND REPAIR 22

1.5.1 HAEMOSTASIS AND INFLAMMATION 23

1.5.2 RE-EPITHELIALISATION AND GRANULATION TISSUE FORMATION 24

1.5.3 TISSUE REMODELLING AND CONTRACTURE 24

1.5.4 MATRIX METALLOPROTEINASES 25

1.5.5 MMPS IN INFLAMMATION AND HEALING 28

1.5.6 MMPS AS CHEMOATTRACTANTS AND MODULATORS OF INFLAMMATION 29

1.5.7 MMPS AND GRANULATION TISSUE FORMATION 30

1.5.8 MMPS AND REMODELLING 31

1.5.9 MMPS AND CONJUNCTIVAL INJURY 31

1.6 MMP INHIBITION 32

1.7 MMP INHIBITION AS A THERAPEUTIC INTERVENTION AGAINST SCARRING 35

1.7.1 *IN VITRO* SCARRING MODEL 38

1.7.2 ANIMAL MODEL OF GLAUCOMA SURGERY 38

1.7.3 ILOMASTAT INJECTIONS PROMOTE BLEB SURVIVAL 40

1.8 THE ILOMASTAT "TABLET" IMPLANT 41

1.9 AIM AND SUMMARY OF EXPERIMENTS 42

CHAPTER 2 MATERIALS AND METHODS 46

2.1 IMPLANT FORMULATION 46

2.2 FLOW RELEASE STUDIES USING AN IN VITRO MODEL OF A BLEB 46

2.2.1 HPLC METHOD FOR ILOMASTAT 47

2.2.2 HPLC METHOD FOR MARIMASTAT AND ILOMASTAT / DEXAMETHASONE 48

2.2.3 STERILISATION OF IMPLANTS 48

2.3 FIRST IN VIVO EXPERIMENT IMPLANT FABRICATION 49

2.3.1 MODIFIED GLAUCOMA FILTRATION SURGERY 49

2.3.2 TREATMENT REGIMEN 51

2.3.3 CLINICAL ASSESSMENT 51

2.3.4 TERMINATION OF THE STUDY 52

2.3.5 HISTOLOGY 53
2.3.6 HAEMATOXYLIN AND EOSIN STAINING 53
2.3.7 PICROSIRIUS RED STAINING 55
2.4 SECOND IN VIVO EXPERIMENT IMPLANT FABRICATION 56
2.4.1 TREATMENT REGIMEN 57
2.4.2 ADDITIONAL SURGICAL TECHNIQUE 58
2.4.3 OUTCOMES 60
2.5 THIRD IN VIVO EXPERIMENT IMPLANT FABRICATION 61
2.5.1 TREATMENT REGIMEN 61
2.5.2 TERMINATION 62
2.6 FOURTH IN VIVO EXPERIMENT IMPLANT FABRICATION 62
2.6.1 TREATMENT REGIMEN 62
2.6.2 EXAMINATIONS 63
2.6.3 HISTOLOGY 64
2.7 FIFTH IN VIVO EXPERIMENT IMPLANT FABRICATION 65
2.7.2 TREATMENT REGIMEN 5TH IN VIVO 68
2.7.3 EXAMINATIONS 69
2.7.4 ICG DYE EVALUATION OF BLEB FUNCTIONALITY 69
2.7.5 TERMINATION 69
2.7.6 HISTOLOGY 69
2.8 SIXTH IN VIVO EXPERIMENT IMPLANT FABRICATION 70
2.8.1 HISTOLOGY 6TH IN VIVO 72
2.9 INVESTIGATION INTO INDUCING RAISED INTRAOCULAR PRESSURE TO BE USED A MEASURE OF SUCCESS IN VIVO 72
2.9.1 SURGICAL TECHNIQUE 73
2.10 APPENDIX 74
2.10.1 EQUIPMENT AND MATERIALS 74
2.10.2 TABLET FABRICATION 74

CHAPTER 3 RESULTS 77

3.1 EXCIPIENTLESS PURE ILOMASTAT TISSUE-TABLET IMPLANT STUDIES 77
3.1.1 ILOMASTAT IMPLANT IN VITRO EXPERIMENTS 77
3.1.2 *IN VIVO* RESULTS OF PURE ILOMASTAT 2 MM AND 1 MM IMPLANTS 89
3.1.3 DISCUSSION 102
3.2 OPTIMISATION OF MMPI RELEASE TO REDUCE INFLAMMATORY RESPONSE: A SECOND *IN VIVO* STUDY 110

3.2.1 *IN VITRO* RELEASE OF ILOMASTAT HYALURONIC ACID (VISIOL) IMPLANTS 111
3.2.2 EXPERIMENT TO OPTIMISE MMPI RELEASE *IN VIVO* RESULTS 113
3.2.3 DISCUSSION 121
3.3 INVESTIGATION INTO THE ANTI-SCARRING EFFICACY OF A MORE WATER SOLUBLE MMPI 126
3.3.1 FABRICATION OF MARIMASTAT IMPLANTS 126
3.3.2 IN VITRO RELEASE OF MARIMASTAT IMPLANTS 127
3.3.3 PILOT STUDY USING PURE MARIMASTAT IMPLANTS HARVESTING EYES AT 14 DAYS 128
3.4 INVESTIGATION INTO THE EFFICACY OF DEXAMETHASONE IN COMBINATION WITH ILOMASTAT AS A SLOW RELEASE ANTISCARRING AGENT 129
3.4.1 FABRICATION OF DEXAMETHASONE / ILOMASTAT IMPLANTS 129
3.4.2 *IN VITRO* RELEASE DATA FROM DEXAMETHASONE ILOMASTAT IMPLANTS 130
3.4.3 I*N VIVO* RESULTS OF DEXAMETHASONE / ILOMASTAT COMBINATION IMPLANTS AND PURE MARIMASTAT IMPLANTS AS ANTI-SCARRING AGENTS 134
3.4.4 BLEB MORPHOLOGY 139
3.4.5 HISTOLOGY 143
3.4.6 DISCUSSION 146
3.5 INVESTIGATION INTO THE RELEASE AND EFFICACY OF ILOMASTAT IN CONJUNCTION WITH DEXAMETHASONE, ILOMASTAT / HYALURONIC ACID COMBINATIONS AND POLYMER COATED ILOMASTAT IMPLANTS 155
3.5.1 SCANNING ELECTRON MICROSCOPE ANALYSIS 157
3.5.2 IN VITRO RELEASE 159
3.5.3 IN VIVO EXPERIMENT 167
3.5.4 BLEB VASCULARITY 170
3.5.5 BLEB MORPHOLOGY 171
3.5.6 TESTING OF BLEB FUNCTIONALITY USING INDOCYANINE GREEN 173
3.5.7 HISTOLOGY 176
3.5.8 DISCUSSION 179
3.6 INVESTIGATION INTO THE USE OF DIFFERENT POLYMER COATED IMPLANTS FOR ANTISCARRING THERAPY 183
3.7 INVESTIGATION INTO THE USE OF A HYDROPHILIC POLYMER COATED IMPLANTS 185
3.7.1 IN VITRO ANALYSIS OF PHOSPHORYL POLYMER COATINGS 186
3.7.2 IN VIVO ANALYSIS OF POLYMERS COATED 7 TIMES IN PC 1059 192
3.7.3 INTRAOCULAR PRESSURE 195
3.7.4 BLEB SURFACE AREA AND HEIGHT 196
3.7.5 TISSUE LEVELS OF ILOMASTAT 201

3.7.6 DISCUSSION 201
3.8 INVESTIGATION INTO BLEB FUNCTIONALITY 207
3.8.1 RESULTS 208
3.8.2 DISCUSSION 210

CHAPTER 4 DISCUSSION 213

CHAPTER 5 REFERENCES 218

List of Figures

FIGURE 1-1 AQUEOUS CIRCULATION IN THE EYE 15
FIGURE 1-2. HEALTHY NERVE AND GLAUCOMATOUS NERVE 16
FIGURE 1-3 GUARDED SCLEROSTOMY AND RESULTING BLEB 18
FIGURE 1-4 FAILED BLEB. 19
FIGURE 1-5 HISTOLOGY OF A FAILED BLEB AND FUNCTIONING BLEB 20
FIGURE 1-6 BLEB THINNING, BLEB LEAKAGE, INFECTION AND HYPOTONY 21
FIGURE 1-7 THE PHASES OF WOUND REPAIR 23
FIGURE 1-8 MMP STRUCTURE. 26
FIGURE 1-9 MONOCYTE MIGRATION ACROSS THE BLOOD BRAIN BARRIER 28
FIGURE 1-10 MMPS INVOLVED IN SUBCONJUNCTIVAL WOUND HEALING 32
TABLE 1-1 PHASE III CLINICAL TRIALS WITH MMPIS 35
FIGURE 1-11 ILOMASTAT 36
TABLE 1-2 KI VALUES FOR ILOMASTAT 37
FIGURE 2-1 THE DIFFERENT COMPONENTS OF THE PUNCH AND DIE SET. 46
FIGURE 2-2 FLOW RIG CHAMBER 49
FIGURE 2-3 SURGICAL STEPS. 50
TABLE 2-1 TREATMENT ARMS 51
FIGURE 2-4 USE PORTABLE SLIT LAMP 52
FIGURE 2-5 ORIENTATION OF GLOBE FOR HISTOLOGY 54
FIGURE 2-6 SAGITTAL SECTION THROUGH A GLOBE 55
TABLE 2-2 TREATMENT REGIMEN 2ND IN VIVO. 57
FIGURE 2-7 IMPLANT HYDRATION AND CONJUNCTIVAL INFLATION AT THE TIME OF SURGERY .59
FIGURE 2-8 HEALON V APPLICATION TO SCLERA BEFORE IMPLANT PLACEMENT. 60
FIGURE 2-9 SUTURE POSITION 2 MM ADJACENT TO THE DRAINAGE TUBE. 61
TABLE 2-3. TREATMENT ARMS. 63

TABLE 2-4, TREATMENT GROUPS. 68
TABLE 2-5 ADVANTAGES AND DISADVANTAGES OF DIFFERENT IN VIVO DESIGNS. 71
FIGURE 3-1 A 2 MM ILOMASTAT IMPLANT AFTER FABRICATION OF 2 MG MASS 78
TABLE 3-1 ILOMASTAT TISSUE-TABLET IMPLANT DIMENSIONS. 78
FIGURE 3-2 ILOMASTAT CONCENTRATION FROM SINGLE 3 MM ILOMASTAT IMPLANTS....79
FIGURE 3-3 CUMULATIVE MEAN PERCENTAGE RELEASE OF THE 3 MM IMPLANT 79
FIGURE 3-4. ILOMASTAT CONCENTRATION FROM SINGLE 2 MM ILOMASTAT IMPLANTS....80
FIGURE 3-5 CUMULATIVE MEAN PERCENTAGE RELEASE OF 2 MM ILOMASTAT IMPLANTS. 80
FIGURE 3-6 ILOMASTAT CONCENTRATION FROM SINGLE 1 MM ILOMASTAT IMPLANTS....81
FIGURE 3-7 CUMULATIVE MEAN PERCENTAGE RELEASE OF 1 MM ILOMASTAT IMPLANTS....81
FIGURE 3-8 ILOMASTAT CONCENTRATION FROM TWO 2 MM ILOMASTAT IMPLANTS 82
FIGURE 3-9 CUMULATIVE MEAN PERCENTAGE RELEASE OF TWO 2 MM IMPLANTS 83
FIGURE 3-10 CONCENTRATION OF ILOMASTAT WITH A FLOW RATE OF 1 μL / MINUTE 84
FIGURE 3-11 MEAN CUMULATIVE PERCENTAGE RELEASE OF 1 μL / MINUTE. 84
FIGURE 3-12 THE REYNOLDS NUMBER FOR FLUID FLOW BEHAVIOUR AROUND A CYLINDER. 87
FIGURE 3-13. THE PATTERN OF FLUID FLOW FOR DIFFERENT REYNOLDS NUMBERS. 87
FIGURE 3-14 REPRESENTATIVE PHOTOS OF BLEBS AT DAY 15....90
FIGURE 3-15 REPRESENTATIVE PHOTOS OF BLEBS AT DAY 30....91
FIGURE 3-16 BLEB SURVIVAL OF THE FOUR GROUPS. 91
FIGURE 3-17 MEAN BLEB SURFACE AREA OVER TIME 92
FIGURE 3-18 BLEB HEIGHT OF THE 4 GROUPS OVER TIME. 93
FIGURE 3-19 MEAN IOP OF OPERATED EYE WITH TIME....94
FIGURE 3-20 BLEB VASCULARITY POST SURGERY. 95
FIGURE 3-21 BLEB DISSECTION OF AN ILOMASTAT 1 MM TREATED BLEB.. 96
FIGURE 3-22 HAEMATOXYLIN AND EOSIN OF AN UNOPERATED EYE. 97
FIGURE 3-23 ETHYLCELLULOSE TREATED BLEB....98
FIGURE 3-24 MMC TREATED BLEB. 99
FIGURE 3-25 ILOMASTAT 2 MM TREATED BLEB. 100
FIGURE 3-26 ILOMASTAT 1 MM TREATED BLEB. 101
FIGURE 3-27 PICROSIRIUS RED STAINING OF THE FOUR TREATMENT ARMS 102
FIGURE 3-28 SCANNING ELECTRON MICROGRAPH OF CRYSTALLINE ILOMASTAT 104
FIGURE 3-29 MACROPHAGE ATTEMPTING TO INGEST AN ASBESTOS FIBRE. 105
FIGURE 3-30 FOREIGN BODY ENCAPSULATION OF AN IMPLANT 106
FIGURE 3-31 ILOMASTAT RELEASED FROM COMBINATION IMPLANTS....112
FIGURE 3-32 CUMULATIVE MEAN PERCENTAGE RELEASE OF ILOMASTAT 112
TABLE 3-2 TREATMENT REGIMEN 2ND IN VIVO. 113

FIGURE 3-33 REPRESENTATIVE PHOTOS OF BLEBS AT DAY 15 115
FIGURE 3-34 REPRESENTATIVE PHOTOS OF BLEBS AT DAY 30 115
FIGURE 3-35 BLEB SURVIVAL OF THE 7 DIFFERENT GROUPS 116
FIGURE 3-36 BLEB SURFACE AREA FOR THE 7 GROUPS OVER TIME. 116
FIGURE 3-37 BLEB HEIGHT FOR THE 7 GROUPS OVER TIME. 117
FIGURE 3-38 IOP FOR ALL 7 GROUPS OVER TIME. 118
FIGURE 3-39 BLEB VASCULARITY 119
FIGURE 3-40 HAMEATOXYLIN AND EOSIN STAINING OF PURE ILOMASTAT IMPLANTS. 120
FIGURE 3-41 HAEMATOXYLIN AND EOSIN STAIN OF BLEBS 121
TABLE 3-3. THE INHIBITORY PROFILE OF THE ILOMASTAT 124
FIGURE 3-42 THE CONCENTRATION OF MARIMASTAT RELEASED OVER TIME 127
FIGURE 3-43 CUMULATIVE RELEASE OF THE 2 MM MARIMASTAT IMPLANTS 127
FIGURE 3-44 HAEMATOXYLIN AND EOSIN STAINING OF THE TWO RABBITS 128
TABLE 3-4 DURATION OF RELEASE WHERE > 10 μM WAS MAINTAINED 130
FIGURE 3-45 MEAN CONCENTRATION RELEASED FROM ILOMASTAT AND DEXAMETHASONE .. 131
FIGURE 3-46 CUMULATIVE RELEASE OF ILOMASTAT AND DEXAMETHASONE 131
FIGURE 3-47 MEAN CONC. RELEASED FROM ILOMASTAT AND DEXAMETHASONE 132
FIGURE 3-48 CUMULATIVE RELEASE OF ILOMASTAT AND DEXAMETHASONE 132
FIGURE 3-49 MEAN CONC. RELEASED FROM ILOMASTAT AND DEXAMETHASONE 133
FIGURE 3-50 CUMULATIVE RELEASE OF ILOMASTAT AND DEXAMETHASONE 133
FIGURE 3-51 BLEB SURVIVAL OF THE FOUR GROUPS. 135
FIGURE 3-52 MEAN BLEB SURFACE AREA OVER TIME FOR THE FOUR GROUPS. 136
FIGURE 3-53 BLEB HEIGHT OF THE 4 GROUPS OVER TIME.. 137
FIGURE 3-54 MEAN IOP OF OPERATED EYE WITH TIME. 138
FIGURE 3-55 BLEB VASCULARITY POST SURGERY. 138
FIGURE 3-56 REPRESENTATIVE PHOTOS OF BLEBS AT DAY 15 139
FIGURE 3-57 SEQUENTIAL PHOTOS OF DEXAMETHASONE / ILOMASTAT TREATED BLEBS 140
FIGURE 3-58 OUTLINES OF THREE BLEBS OF THE ILOMASTAT / DEX. IMPLANT 141
FIGURE 3-59 SEQUENTIAL IMAGES OF THE BLEB OF R14 142
FIGURE 3-60 SECTIONS OF REPRESENTATIVE BLEBS 144
FIGURE 3-61 SECTIONS OF REPRESENTATIVE BLEBS 145
FIGURE 3-62 DIAGRAM ILLUSTRATING CONJUNCTIVAL ELEVATION 149
FIGURE 3-63 THE STAGES OF CUTANEOUS WOUND HEALING IN HUMANS. 152
FIGURE 3-64 SCANNING ELECTRON MICROGRAPH OF POLYMER COATED IMPLANT. 158
FIGURE 3-65 IMAGES OF INCREASING MAGNIFICATION OF THE IMPLANT SURFACE 159
FIGURE 3-66 ILOMASTAT AND DEXAMETHASONE RELEASED 160

FIGURE 3-67 CUMULATIVE MEAN PERCENTAGE RELEASE 160
FIGURE 3-68 MEAN CONCENTRATION OF ILOMASTAT 161
FIGURE 3-69 CUMULATIVE RELEASE OF ILOMASTAT OVER TIME FROM POLYMER 162
FIGURE 3-70 POLYMER SHELL AROUND IMPLANT REMNANT 162
FIGURE 3-71 ILOMASTAT RELEASE FROM THE COMBINATION IMPLANTS 163
FIGURE 3-72 CUMULATIVE RELEASE OF ILOMASTAT FROM HEALON GV 163
FIGURE 3-73. ILOMASTAT RELEASE FROM THE COMBINATION IMPLANTS 164
FIGURE 3-74 CUMULATIVE RELEASE OF ILOMASTAT FROM HEALAFLOW 164
FIGURE 3-75 SCANNNING ELECTRON MICROGRAPH OF A SANDWICH IMPLANT 165
FIGURE 3-76 CONCENTRATION OF ILOMASTAT RELEASED WITH TIME 166
FIGURE 3-77 MEAN CUMULATIVE ILOMASTAT RELEASE FROM THE SANDWICH IMPLANTS 166
FIGURE 3-78 BLEB SURFACE AREA OF THE SIX GROUPS. 168
FIGURE 3-79 BLEB HEIGHT OF THE SIX GROUPS OVER TIME. 169
FIGURE 3-80 INTRAOCULAR PRESSURE FOR ALL SIX GROUPS. 169
FIGURE 3-81 BLEB VASCULARITY FOR THE SIX GROUPS. 170
FIGURE 3-82 REPRESENTATIVE PHOTOGRAPHS 171
FIGURE 3-83 REPRESESNTATIVE PHOTOGRAPHS OF THE BLEB. 172
FIGURE 3-84 PRECIPITATION OF HEALAFLOW / ILOMASTAT 172
FIGURE 3-85(A) TRANSDUCER (T) AND ICG NEEDLE (N) INSERTION 174
FIGURE 3-86 CHANGES IN IOP WITH ICG INSERTION INTO THE ANTERIOR CHAMBER. 174
FIGURE 3-87 FLUORESCENCE FROM ICG DYE INJECTED 175
FIGURE 3-88 ICG HYPERFLUORESCENCE IN THE BLEB BLOOD VESSELS. 175
FIGURE 3-89. SECTIONS OF THE REPRESENTATIVE BLEBS 177
FIGURE 3-90. REPRESENTATIVE HISTOLOGICAL SECTIONS OF THE SANDWICH 178
FIGURE 3-91. ATTEMPTS TO SEAL A POLYMER POUCH USING CYANOACRYLATE GLUE 184
FIGURE 3-92. SEMS OF IMPLANTS COATED WITH THE POLYMERS PC 1059 186
FIGURE 3-93. MEAN CONC. OF ILOMASTAT RELEASED FROM SINGLE COATED PC 1059 187
FIGURE 3-94. CUMULATIVE RELEASE OF ILOMASTAT OVER TIME FROM PC 1059 188
TABLE 3-5. MEAN COATING THICKNESS AS DETERMINED BY SEM FOR N = 9 MEASURMENTS. 189
FIGURE 3-95. APPEARANCE OF IMPLANTS WITH 3, 5 AND 7 COATS 189
FIGURE 3-96 HYDRATED POLYMER PC1059. 190
FIGURE 3-97. MEAN CONC. OF ILOMASTAT FROM IMPLANTS COATED IN PC 1059 191
FIGURE 3-98. CUMULATIVE RELEASE OF ILOMASTAT OVER TIME 191
FIGURE 3-99. REPRESENTATIVE PHOTOS OF BLEBS AT DAY 15 193
FIGURE 3-100. REPRESENTATIVE PHOTOS OF BLEBS AT DAY 24 194
FIGURE 3-101. BLEB SURVIVAL OF THE 3 DIFFERENT GROUPS: 194

FIGURE 3-102 IOP FOR ALL 3 GROUPS OVER TIME..... 195
FIGURE 3-103 IOP FOR UNOPERATED EYE ALL 3 GROUPS OVER TIME. 196
FIGURE 3-104 BLEB SURFACE AREA FOR THE 3 GROUPS OVER TIME..... 197
FIGURE 3-105 BLEB HEIGHT FOR THE 3 GROUPS OVER TIME. 197
FIGURE 3-106 BLEB VASCULARITY. 198
FIGURE 3-107 HAEMATOXYLIN AND EOSIN..WATER (A), MITOMYCIN C (B), PC 1059..... 199
FIGURE 3-108 HAEMATOXYLIN AND EOSIN STAINING OF ALL BLEBS...PC 1059 200
TABLE 3-6 TISSUE LEVELS OF ILOMASTAT AT DAY 30. 201
FIGURE 3-109 THE EYES POST INJECTION OF HEALAFLOW OR MAGNETIC BEADS. 209
FIGURE 3-110 GRAPH TO SHOW THE IOP OF HEALAFLOW INJECTED EYES 209
FIGURE 3-111 GRAPH TO SHOW THE IOP MAGNETIC BEADS OVER TIME..... 210
FIGURE 4-1 CHEMICAL STRUCTURE OF LATANOPROST (A) AND ILOMASTAT (B)..... 212

Chapter 1 Introduction

1.1 Glaucoma in the population

Glaucoma is a term used to describe a group of conditions with an optic neuropathy, characteristic morphological changes in the optic nerve head and visual field defects. It remains a leading cause of blindness throughout the world and one of the most common neuropathies. It is estimated that 60.5 million people suffered from it in 2010 and 7 million believed to be bilaterally blind (Quigley and Broman, 2006). The number of people with glaucoma is projected to increase to 111.8 million in 2040 (Tham et al., 2014).

Over the last century, in fact, the proportion of blindness attributed to glaucoma in developed countries has changed very little (10%) (Taylor, 2009). In developed countries the main cause of blindness 100 years ago was corneal disease, fifty years ago it was cataract and in present day it is macular degeneration. That there has been no reduction in the proportion of blindness due to glaucoma is not simply because there have been no advances in treatment. A major factor is the ageing population. As a population becomes healthier and people live longer, the incidence of this degenerative optic neuropathy that reaches a clinically detectable threshold will increase. Furthermore, because screening is not cost effective a high proportion of patients remain undiagnosed (Wong et al., 2004). Optometrists perform tests for glaucoma of varying number and detail, according to their index of suspicion and capability. A recent study found evidence that the incidence of diagnosed patients with glaucoma was less than half that expected (Lockwood et al., 2010).

At present glaucomatous optic neuropathy is irreversible and therefore the mainstay of treatments involve trying to slow this degeneration. The biggest risk factor for accelerated progression is an increased level of intraocular pressure (IOP) and reducing this is the only proven therapy in everyday use.

1.2 Intraocular pressure (IOP)

The eye requires a pressure to maintain its structure and function. Under normal conditions aqueous fluid is produced by the ciliary body behind the iris. This flows through the pupil, and the majority exits via the trabecular meshwork. A small proportion of aqueous fluid uses the uveoscleral pathway to exit via the ciliary muscle and sclera (Figure 1-1). In a population with no visual symptoms the mean IOP has been determined as 15.5 mm Hg, derived from a study of 10000 individuals (20000 eyes) (Leydghecker et al., 1958).

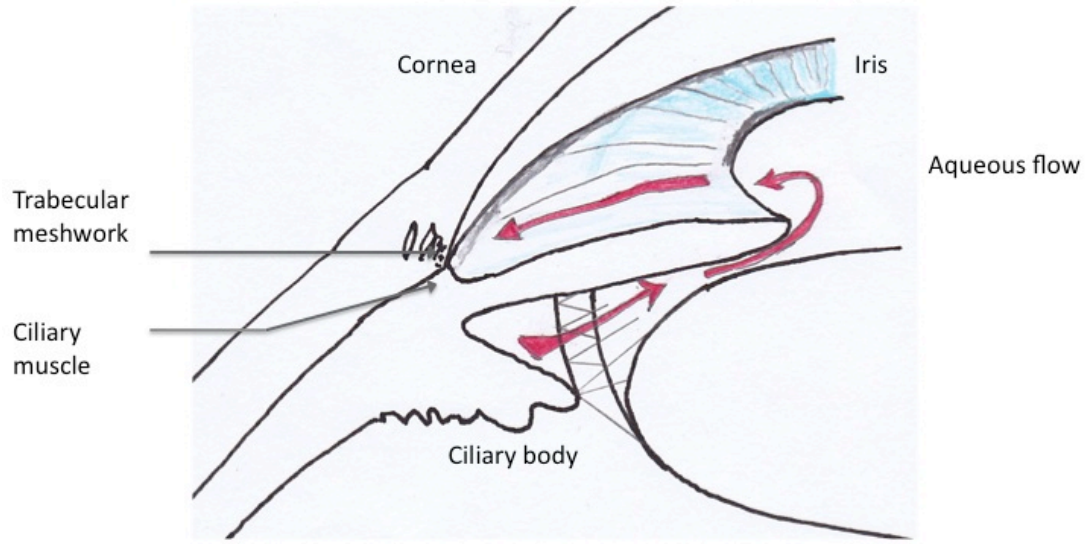

Figure 1-1 Aqueous circulation in the eye.

With an increased resistance to flow, most commonly due to intrinsic changes in the trabecular meshwork, the pressure increases. Too high a pressure results in accelerated optic nerve degeneration either through a direct mechanical effect or through ischaemia (Caprioli et al., 2010) or through a combination mechanism (Li et

al., 2015). The optic nerve changes in appearance from a pink healthy 'ring donut' shape to a deep pale 'cup' (Figure 1-2).

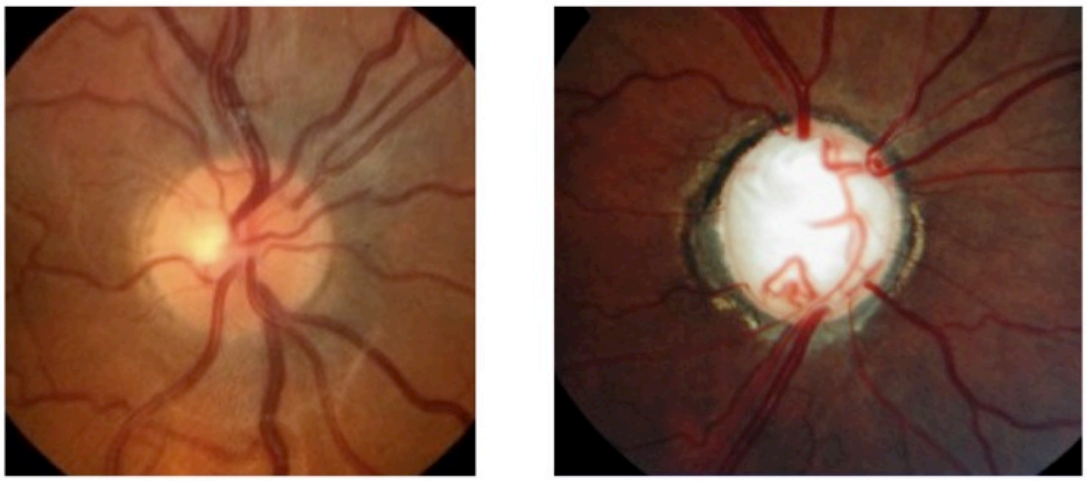

Figure 1-2. Healthy nerve (left) and glaucomatous nerve (right).

The human optic nerve consists of approximately 1.2 million ganglion cells. Even in people without glaucoma it degenerates at 0.5 % per year (Harwerth et al., 2008). Because the brain accepts a rate of degeneration as normal, the patient with glaucoma may only appreciate vision loss when the disease is very advanced. The time between awareness and blindness as a consequence can be relatively short. Therefore, unsurprisingly, a considerable proportion of patients present late, and to maintain lifelong reasonable visual function significant intervention is required.

Ultimately the aim of glaucoma management is to lower intraocular pressure (IOP) to a level at which optic nerve degeneration is slowed and the progression of vision loss minimised. Although the level of IOP that causes optic nerve damage varies between patients, studies have shown that reducing IOP consistently to less than 15

mm Hg minimises progression in patients with advanced disease (AGIS 7., 2000, Heijl et al., 2002).

Most medical therapy involves topical drop application of a drug to the eye on a regular basis, and either inhibits aqueous production or improves aqueous outflow. Typically the longest licensed interval between administrations is 24 hours. Systemic medications, such as carbonic anhydrase inhibitors, are often only used in the short term due to the common deleterious side effects. Despite maximal tolerated medical treatment however, a subset of patients' IOP remains above target, their glaucoma continues to progress, and if unchecked this leads to blindness.

Although the patient that exhibits relentless glaucomatous progression, despite medical treatment, has entered the 'surgical zone' one temporising measure is laser treatment. Historically laser treatment has been used to lower the intraocular pressure for many years. In general this has been through reducing aqueous production by cyclodestruction or improving outflow by treating the trabecular meshwork. Indeed early trials suggested the use of argon laser trabeculoplasty might be superior to medical therapy as a first line treatment for primary open angle glaucoma (The Glaucoma Laser Trial, 1995). The side effect profile of laser treatments has negated this change however. Argon laser trabeculoplasty (ALT) can cause IOP spikes, inflammation, peripheral anterior synechiae and a lack of efficacy in the longer term. Another form of laser, selective laser trabeculoplasty, allowed more specific treatment of the pigmented trabecular meshwork rather than the non-pigmented but post operative inflammation, although less than ALT, can still occur (Martinez-de-la-Casa et al., 2004). Conventional cyclodiode can cause inflammation and IOP spikes too, but has also been associated with sympathetic ophthalmia and suprachoroidal haemorrhage (Tay et al., 2006; Roberts et al., 2009). Recent promising developments in laser therapy are techniques that have fewer side effects including the use of anti-angiogenic adjuncts as a more effective means to tackle NVG.

1.3 Glaucoma Filtration Surgery

The 'gold standard' surgical procedure for glaucoma is still the trabeculectomy, devised in the late 1960s (Cairns, 1968) and subsequently modified by Watson

(Watson and Barnett, 1975). The basic concept involves creation of a guarded fistula in the eye, effectively a ‘trap door’ in the sclera. Held in place by sutures, the aqueous seeps out at a controlled rate, determined initially by the suture tension. The translucent mucosal lining of the eye, the conjunctiva, when replaced over the trap door, forms a blister or ‘bleb’. The aqueous fluid drains into the systemic circulation via the conjunctival and episcleral veins (Figure 1-3).

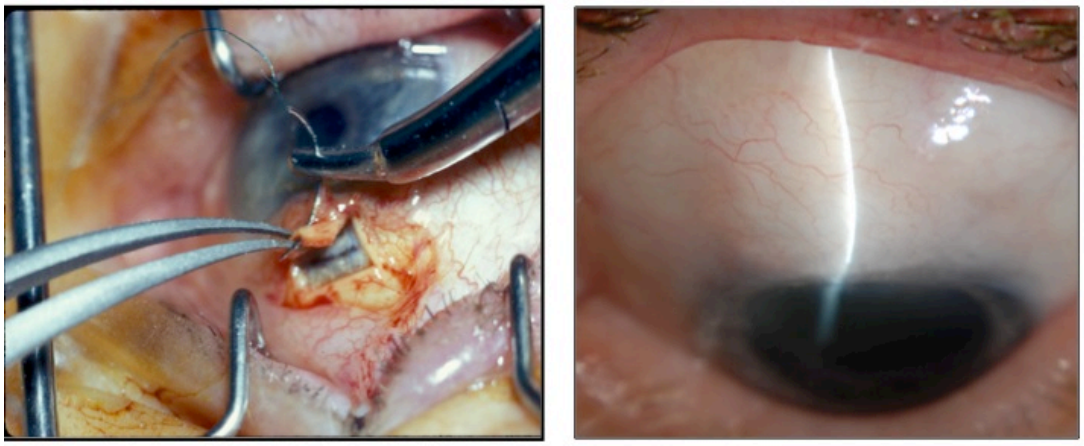

Figure 1-3. Guarded sclerostomy and resulting bleb.

After any surgical procedure of tissue trauma however, there is an intrinsic wound healing response that results in the deposition of scar tissue. This scarring process after a trabeculectomy can effectively close the ‘trap door’, which results in surgical failure (Figure 1-4) (Hitchings and Grierson, 1983).

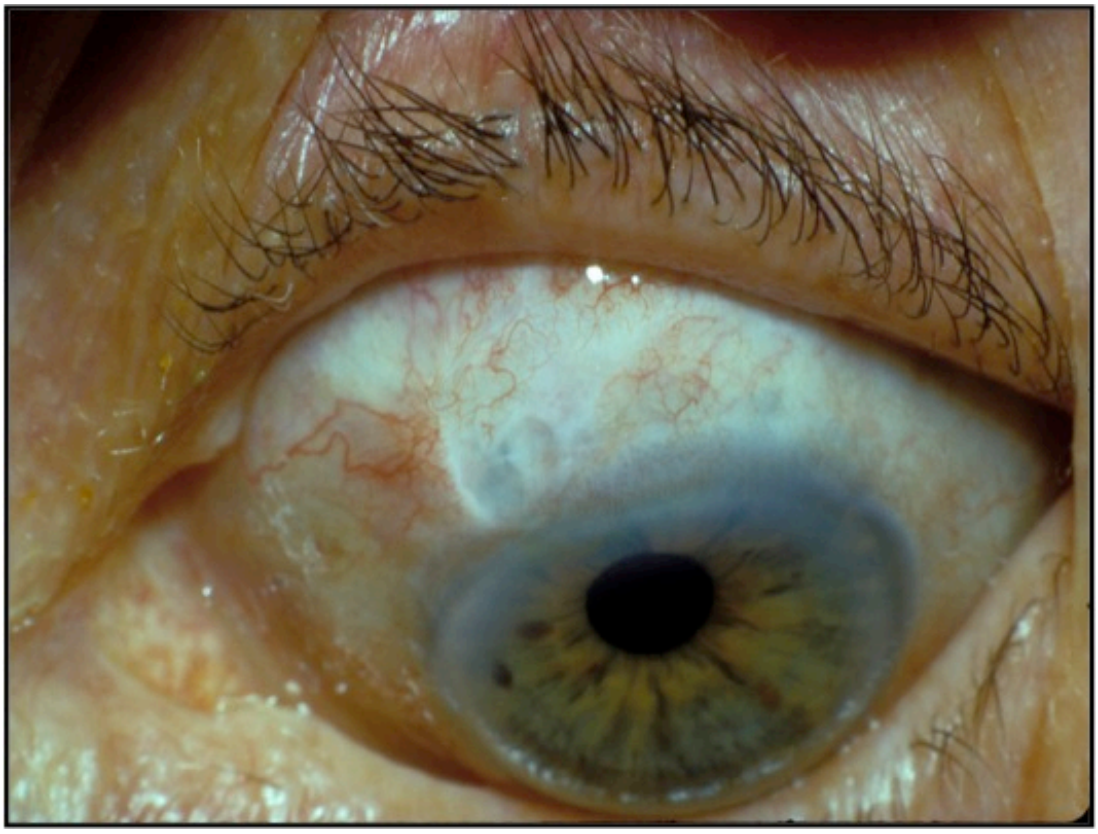

Figure 1-4 Failed bleb.

In the national trabeculectomy survey 1/3 of patients where surgery was performed, further ocular hypotensive treatment was required at the end of 1 year (Edmunds et al., 2001). Histological analysis of failed trabeculectomies as compared to functioning ones show increased collagen deposition and new capillary formation (Addicks et al., 1983) (Figure 1-5).

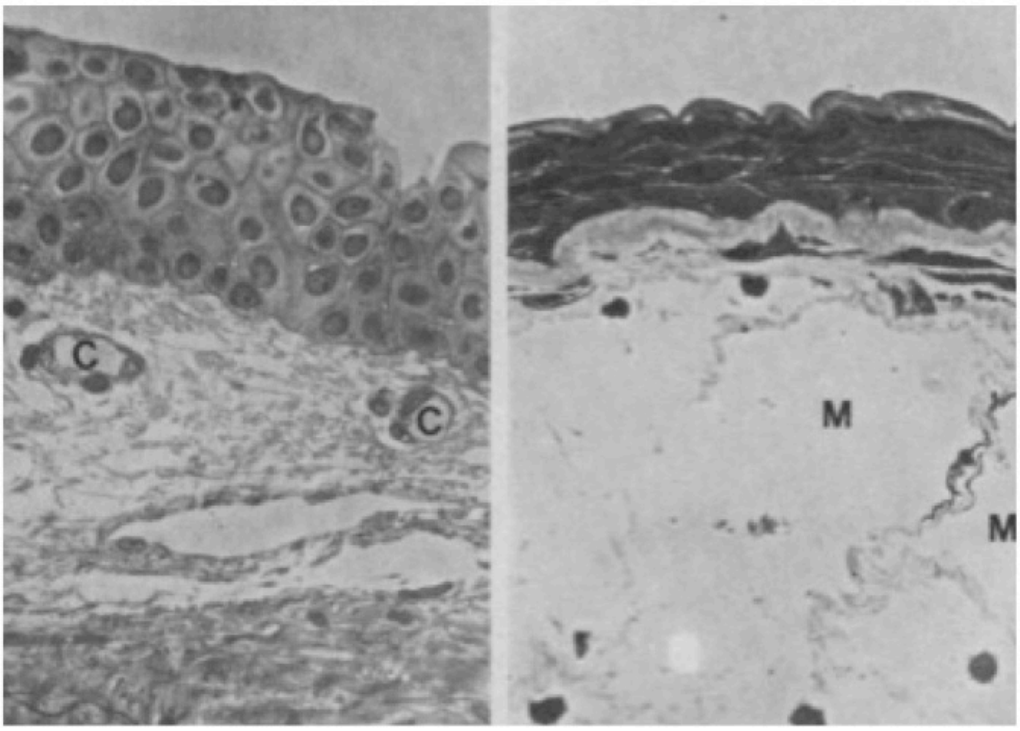

Figure 1-5 Histology of a failed bleb (left) and functioning bleb (right). Capillaries (C) seen in dense collagenous connective tissue. Microcystic spaces (M) seen in functioning bleb. Adapted from (Addicks et al., 1983).

1.4 Augmentation with Antimetabolites

Since the 1980s surgeons have attempted to prolong trabeculectomy survival through the use of antimetabolites (Chen et al., 1990; Rothman et al., 2000). Mitomycin C is a naturally occurring antibiotic-antineoplastic compound produced by Streptomyces caespitosus. It acts as an alkylating agent after enzyme activation resulting in DNA cross-linking. 5-fluorouracil (5FU), a pyrimidine analogue inhibits cellular proliferation by being converted to 5-fluoro-2'-deoxyuridine 5'-monophosphate. This interferes with DNA synthesis through its action on thymidylate synthetase. Both agents result in greater surgical success though at the cost of an increased rate of complications. This was particularly noticeable in early reports. Their application can result in tissue thinning and bleb leaks. In the 5FU trial 33% of cases treated with 5FU had bleb leaks as compared to 20% in the no augmentation group (Fluorouracil Filtering Surgery Study Group, 1989).

The resulting hypotony causes retinal swelling and disruption of visual function (Zacharia et al., 1993). Bindlish and colleagues reported an incidence of late hypotony (IOP < 6 mmHg) in 42% of eyes (including both leaking and non leaking trabeculectomies) at some point between six months and final follow-up at five years, in a series of 123 primary trabeculectomies with MMC (Bindlish et al., 2002). Worse still, bleb leaks act as a tract or infection, which can result in the loss of an eye (Wolner et al., 1991; DeBry et al., 2002). The incidence of bleb-related endophthalmitis in trabeculectomy without antimetabolite ranges from 0.2% to 1.5%. With intraoperative 5-FU and MMC, this incidence increases to 1.0 - 5.7% and 0.3 - 4.9%, respectively (Razeghinejad et al., 2012).

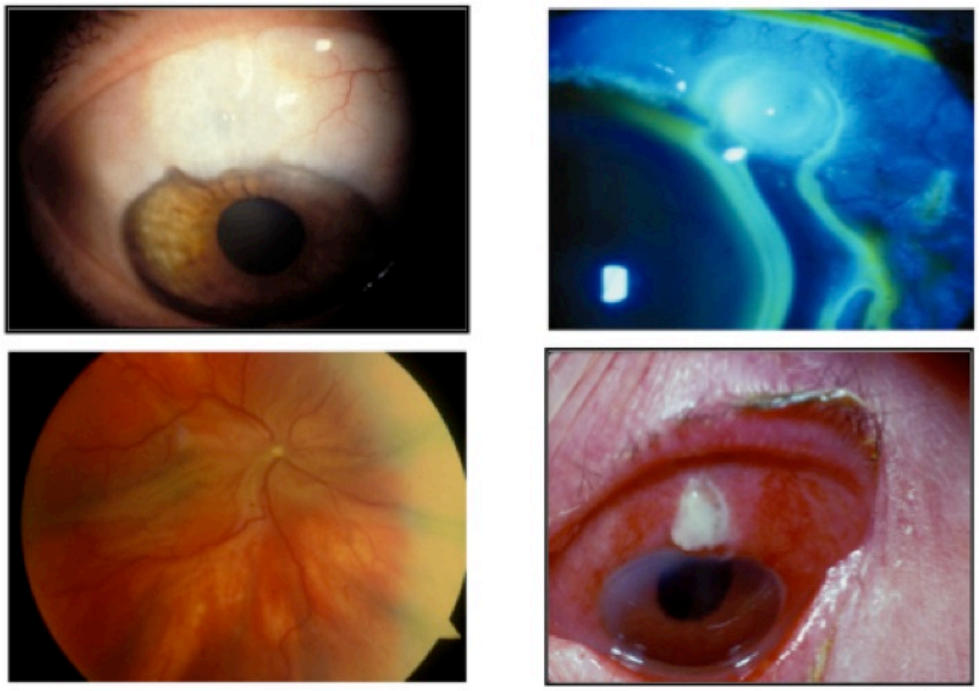

Figure 1-6. Clockwise from top left: bleb thinning, bleb leakage outlined by fluorescent dye, infection and hypotony with retinal swelling and retinal folds.

More recently changes in the surgical technique and anti-metabolite application have resulted in improved bleb morphology, good control of IOP with a significant reduction in complications. The 'Moorfields Safer Surgery System' involves a number of modifications such as use of antimetabolite where type, concentration and

exposure time are graded according to patient risk (usually at a lower concentration than in early studies) (Khaw et al.). There is a wide area of application under the conjunctival flap using polyvinyl alcohol sponges (methylcellulose sponges can fragment leaving remnants behind (Al-Shahwan and Edward, 2005)). Releaseable sutures with or without adjustable sutures are used routinely. Surgeons using this technique have reported a success rate of 96.7% (IOP < 21 mmHg) at 3 years in a complex case mix (Shah et al., 2011). Stalmans et al reported a success rate of 100% (IOP < 21 mmHg) in lower risk patients at 15.7 months mean follow up, with few complications (flat AC 1.8%; hypotony beyond 3 weeks 1.5%) (Stalmans et al., 2006).

Nonetheless, surgeons are in general agreement that using antimetabolites necessitates close monitoring and considerable work post surgery. Suture manipulation and postoperative antimetabolite injection require many visits sometimes to theatre: "completion of trabeculectomy surgery is just the beginning of a process that takes several months to complete" (King et al., 2007). An alternative to using an agent that is cytotoxic or antiproliferative would be to use an agent that inhibits the scarring mechanism more selectively. Much research has been performed to develop an effective anti-scarring agent without the toxic side effects. Part of the difficulty in establishing an agent that is both effective and non-toxic is understanding the complexity of the wound healing response, and the interplay between fibroblasts and other key cells involved (Bruno et al., 2007; Georgoulas et al., 2008).

1.5 Wound Repair

After surgical trauma to the skin, conjunctiva or other epithelial surface a sequence of events occurs that result in either restitution of tissue architecture or scarring (Figure 1-7). The process can be divided into 3 major phases:

1) haemostasis and inflammation

2) re-epithelisation and granulation tissue formation

3) tissue remodelling

These phases, although histologically and functionally different, overlap temporally and involve communication between numerous cell types and in different tissue layers (Park and Barbul, 2004; Toriseva and Kähäri, 2009; Eming et al., 2007).

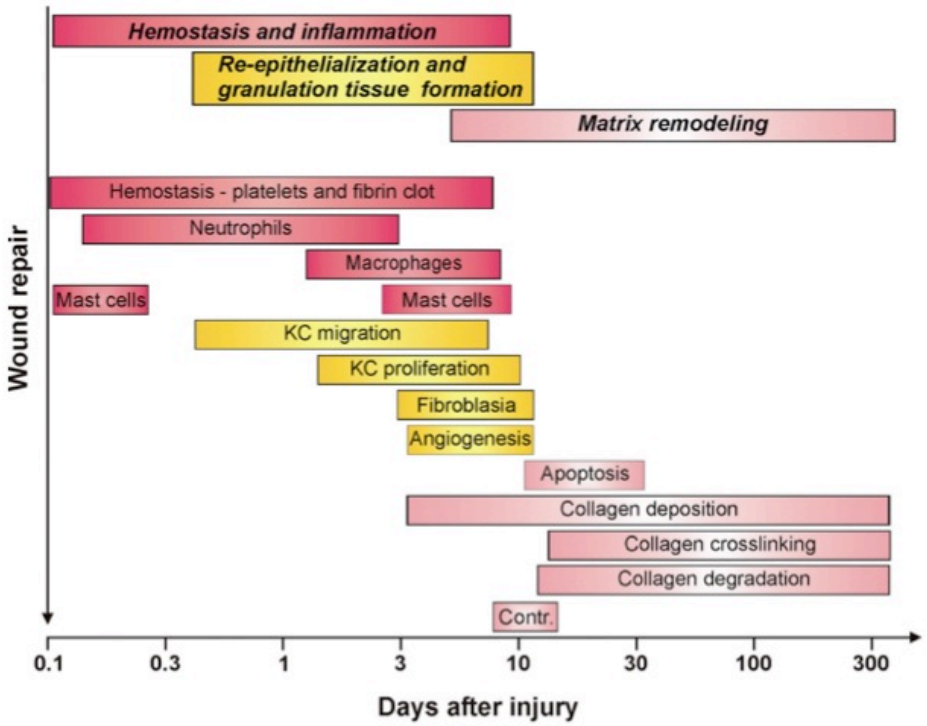

Figure 1-7. The phases of wound repair. Taken from (Toriseva and Kähäri, 2009).

1.5.1 Haemostasis and inflammation

A surgical or traumatic wound leads to the release of blood products including platelets from disrupted vessels. These activated platelets aggregate and release numerous factors that contribute to the coagulation cascade. As a consequence, a meshwork of fibrin binds to platelets and wound tissues, acting as a physical 'plug' to stop further bleeding.

The coagulation factors, cell fragments and other proteins act as attractants for inflammatory cells and fibroblasts (Eming et al., 2007). Neutrophils phagocytose infectious agents and necrotic tissue. Monocytes migrate to the wound site and become activated to become macrophages. These are not only able to phagocytose

but present antigen to other cells for recognition as 'foreign', thereby intitating the adaptive immune response. Furthermore macrophages release growth factors, such as transforming growth factors (TGF-B, TGF-a), platelet-derived growth factors (PDGF) and fibroblast growth factor (FGF), which contribute to wound healing regulation (Park and Barbul, 2004).

1.5.2 Re-epithelialisation and granulation tissue formation

In parallel to the inflammatory phase there is re-epithelialisation and granulation tissue formation. The epithelial cells at the wound edge proliferate, lose cell-cell contacts, change morphology and begin migration across the wound. Once the wound gap is closed, a basement membrane is reformed and the cells return to their original morphology.

The granulation tissue is made up of fibroblasts, endothelial cells and macrophages. The fibroblasts, which have either migrated to the wound site or become transformed from residential fibrocytes, deposit and remodel wound extracellular matrix (ECM). This initially consists of fibronectin and hyaluronan, both of which facilitate cell migration. The endothelial cells migrate to the area and are stimulated by hypoxia and growth factors to proliferate. These cells coalesce to form a network of primitive blood vessels (angiogenesis). It is through the proteolytic activity of plasmin and matrix metalloproteinases that ECM vascularisation is allowed.

1.5.3 Tissue remodelling and contracture

The final phase of wound maturation is the process of tissue remodeling, contracture and the formation of collagenous scar. This process may continue for months and during this time the ECM is synthesised, deposited and remodeled. It is the fibroblast that is the principal cell involved, depositing and degrading collagen molecules and arranging collagen fibres.

The fibroblasts themselves also differentiate into myofibroblasts, with the formation of intracellular actin bundles. Resembling smooth muscle cells, these cells have strong intercellular attachments. They contribute to wound contraction as a

coordinated group. With time as the ECM becomes stronger and takes more of the mechanical stress, the myofibroblasts undergo apoptosis (Hinz et al., 2007).

1.5.4 Matrix Metalloproteinases

Matrix metalloproteinases (MMPs) are key proteins involved in the wound healing process. Discovered by identifying the collagenolytic factor that enables tadpoles to lose their tales during metamorphosis (Gross and Lapiere, 1962), initially they were believed to be simply enzymes that remodeled ECM. However, subsequently they have been found to play roles in regulating the inflammatory process as cytokines and chemokines as well.

1.5.4.1 Matrix metalloproteinase structure

The general structure of MMPs involves 3 domains: the propeptide, the catalytic and a haemopexin-like C-terminal domain that is linked to the catalytic domain via a hinge region (Figure 1-8)(Yong et al., 2001).

Figure 1-8 MMP structure. Adapted from (Yong et al., 2001).

MMPs are initially expressed in an inactive state due to the cysteine "switch" residue of the prodomain region interacting with the zinc ion of the catalytic site. They are stored as granules within inflammatory cells or anchored to the cell surface and extracellular matrix (ECM). Proteolysis by other proteases or cell surface molecules can activate the switch and enzyme (Nagase, 1997).

There are 23 different types (at the time of writing) and are classified into families according to substrate specificity: collagenases, gelatinases, stromelysins,

matrilysins, membrane bound MMPs and 'other' MMPs (Yong et al., 2001). Collagenases degrade collagen, unwinding the triple helix to a denatured gelatin form. Gelatinases degrade basement membranes. Stromelysins are less specific and are able to degrade extracellular compounds such as fibronectin, laminin and proteoglycans. Matrilysins can degrade ECM components, but also cleave cell surface molecules such as Fas ligand and VE-cadherin to generate soluble forms, therefore acting as 'sheddases'(Ichikawa et al., 2006). The membrane bound MMPs are different from other MMPs in that they have a transmembrane domain and cytoplasmic tail of 25 amino acids. They contain a cleavage site for furin like proteases and are likely to be activated within the secretion pathway.

They are regulated at 3 levels:

1) Proteolytic activation (described above).

2) Biological inhibition - tissue inhibitors of metalloproteinases (TIMPS). There are 4 known types in mammals, which usually exist as soluble extracellular proteins.

3) Transcriptional control of genes - growth factors such as FGF can up-regulate MMP gene expression via the c-Fos and c-Jun proto-oncogenes. Glucocorticoids can down-regulate MMPs.

MMPs have numerous roles in physiological and pathological processes. These are linked to their capacity to digest selective proteins, latent growth factors, cytokines, inactivating binding proteins as well as pro-peptidases. The mechanisms involved continue to be elicited, however identifying substrates for MMPs is not without difficulty. Rarely do in vitro experiments where substrates are incubated with purified MMP and analysis of the protein products actually reflect what happens in vivo. An alternative method is to perform a proteomic experiment by the creation of tissue models without a specific MMP gene and comparing the protein products to the wild type (Overall et al., 1987). Traditionally proteins were identified on a 2 D SDS PAGE gel, but with the disadvantage of not being able to distinguish longer molecules. More recently the use of mass spectrometry has improved detection. Further analysis using in vivo models with targeted mutagenisis help to verify MMP

function (Parks et al., 2004). Although there is still much to learn it is clear that MMPs are involved in all 3 stages of wound healing:

1.5.5 MMPs in Inflammation and Healing

MMPs allow the passage of inflammatory cells such as neutrophils by altering the basement membrane permeability of both endothelial and epithelial cells. In endothelial cells MMP 7 'sheds' VE-cadherin, causing cell junction proteolysis (Ichikawa et al., 2006). MMP2 and MMP9 cleave occludin, the endothelial component of tight junctions (Reijerkerk et al., 2006). Thus areas that would normally be impermeable to plasma proteins and cells, such as the blood brain barrier and the blood retinal barrier can become leaky (Figure 1-9). This may be important in for example hypoxic brain injury, meningitis or in diabetic eye disease (Manicone and McGuire, 2008). Indeed dendritic cells infected with Dengue virus over produce MMP9 and MMP2, and are associated with decreased expression of the cellular adhesion molecules PECAM1 and VE Cadherin in vitro and in vivo (Luplertlop et al., 2006). Therefore MMP expression may contribute to the increased vascular permeability and haemorrhagic shock seen in Dengue fever and other haemorrhagic fevers, e.g. Ebola virus (Dolnik et al., 2004).

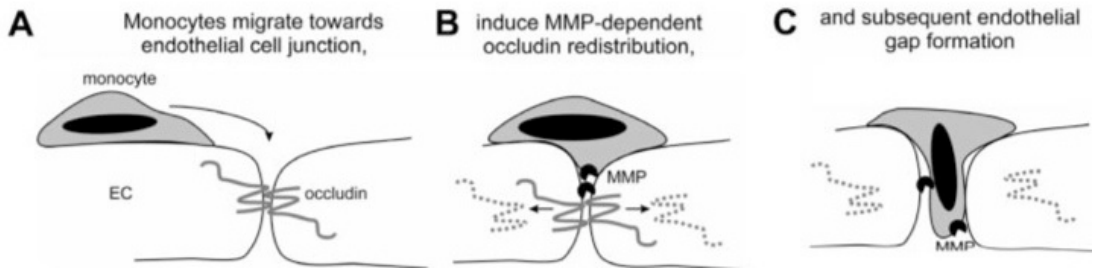

Figure 1-9 Monocyte migration across the blood brain barrier with A adhesion, B local redistribution of occludin, C formation of endothelial gap. Adapted from (Reijerkerk et al., 2006).

MMPs are also involved in proteolysis of epithelial cell junctions. An example is in the animal model of autoimmune bullous pemphigoid. MMP 9 contributes to skin blisters by cleaving hemidesmosome protein bp 180, through proteolytic inactivation of serpin α 1 proteinase inhibitor (Liu et al., 2000).

Further knowledge of MMP function comes from studies of cutaneous wounds. In intact skin MMP expression is minimal with only MMP-7 and MMP-19 expressed in sweat and sebaceous glands (Toriseva and Kähäri, 2009). When there is basement membrane disruption, however, there is a sharp rise (within hours) in MMP-1 expression in migrating epithelial cells. Type 1 collagen appears to be the primary stimulus for MMP-1 expression. Furthermore the MMP-1 expression appears to be essential for the migration by epithelial cells on collagen. After re-epithelisation the epidermal expression of MMP-1 is repressed by contact with basement membrane proteins such as laminin-111. The importance of MMP-1 control is illustrated by over expressing MMP-1 in mouse epidermis. After wound incision there is markedly delayed closure and hyper-proliferation of the epidermis. Its ability to break down collagen is also essential for normal function. In mice with collagenase resistant collagen, wound closure is impaired with slowed tissue contraction and wound re-epithelialisation.

1.5.6 MMPs as Chemoattractants and Modulators of Inflammation

MMP cleavage of proteins can result in the activation of cytokines or chemokines, or the MMP fragments themselves can act as chemoattractants. TNF α is a fundamental cytokine in inflammation that is expressed on T cells and macrophages. It exists in an inactive form and is switched on by TNF converting enzyme (TACE), a molecule identical in structure to ADAM (a disintegrin and metalloproteinase) 17 (Gooz, 2010). TNF α activation is seen in septic shock, Crohns and rheumatoid arthritis as well as many other inflammatory autoimmune diseases. Several other MMPs also have TACE activity *in vitro* including MMPs 1, 2, 3 ,9, 12, 14, 15, 17 (Manicone and McGuire, 2008). It is postulated that whilst TACE may be the main converter of pro TNF α in systemic disease, local response to wounds may be through MMP activation.

Chemokines are proteins that direct cell migration through concentration gradients. They exist in two forms CXC and CC according to the location of cysteine residues. The N-terminus end of CXC8 and Lix8 (the mouse model version) are processed by MMP 8 and 9, and render more active peptides. Evidence of the role MMP 8 can play in the pathogenesis of disease comes from the mouse model lacking MMP 8

(Lint et al., 2005). If these mice are made to develop lethal hepatitis, Lix fragment release is reduced. Compared to the wild type, the knock out mice had less neutrophil migration into the liver and lower mortality.

MMPs may also affect chemokine influence through chemokine release from tissue of cell compartments (Manicone and McGuire, 2008). Ordinarily chemokines are bound to the cell surface or ECM. MMPs such as MMP 7 are able to cleave the binding proteins, release the chemokine, and thereby set up a concentration gradient. MMP 7 'sheds' syndecan 1, an epithelial binding proteoglycan that restricts the chemokine CXCL1. MMP7 null mice are unable to release CXCL1 and therefore prevent neutrophil migration into the alveolar tissue after lung injury.

The MMP products themselves can function like chemokines and be involved in the pathogenesis of disease, and loss of function can lead to tissue protection. An example is illustrated by the activity of MMP 9 in mice after pulmonary infection of *Francesella tulerinis*. MMP 9 null mice have significantly less Pro-Gly-Pro, a chemotactic peptide released by that MMPs cleavage of collagen. As a consequence there is less neutrophil migration into tissue and less injury.

1.5.7 MMPs and Granulation Tissue Formation

During granulation tissue formation fibroblasts express MMP 1 and MMP 2 near the wound front. This allows the organisation of the newly synthesised ECM. MMP 1 may also regulate fibroblast survival by exposing binding sites in collagen for fibroblast integrins. MMPs expressed by stromal cells include MMP 1, 2, 3, 9, 11, and 12. In the remodelling phase, the stromal cells, including fibroblasts, keratinocytes, endothelial and inflammatory cells, populate the granulation tissue and are believed to continue their expression of MMP-1,-2,-3,-9,-11,-12 and -14 (Steffensen et al., 2001). As a new basal lamina is formed at the wound site, MMP-1 expression is reduced and the basement membrane-keratinocytes interactions through hemidesmosomes are stabilised (Sudbeck et al., 1997). Hemidesmosomes, formed within keratinocytes, bind them to anchoring fibrils of the subtending dermis. In conclusion, when the cells finish the process of wound healing, there is a decrease in MMP expression and MMP levels approach those of normal tissues.

1.5.8 MMPs and Remodelling

There is prolonged expression of MMP2 by fibroblasts in the dermal compartment of cutaneous tissue after injury (Karim et al., 2006). MMP 2 is a gelatinase whose expression may be important in ECM remodelling. Indeed it is believed that TGF β can activate MMP 2 via the NF-κB pathway leading to fibroblast migration and collagen remodelling (Wang et al., 2011).

The process of angiogenesis is also dependent on MMPs. The gelatinases MMP 2 and MMP 9 cannot only break down the vascular basement membrane (as discussed above) but also activate angiogenic cytokines. MMP 9 is upregulated in stromal cancer cells and can release vascular endothelial growth factor (VEGF) from ECM (Hawinkels et al., 2008). MMP 9 and MMP 13 have been shown to be more upregulated together with VEGF in rheumatoid arthritis (Kim et al., 2011). MT1 MMP has fibrinolytic and collagenolytic activity that allow vessel invasion through tissue stroma (Chun et al., 2004). *In vitro* MT1 MMP is associated αVβ3 integrins at the intercellular contacts in endothelial cells, indicating involvement in endothelial cell adhesion and migration (Gálvez et al., 2004).

1.5.9 MMPs and Conjunctival Injury

MMPs have been shown to exist in subconjunctival tissue and their expression varies with wound healing. Comparison between normal and healing conjunctiva specimens showed that MMP-1 and TIMP-1 were located only in the healing subconjunctival tissue and not in normal subconjunctival tissue or conjunctival epithelium. MMP-TIMP expression and activation alterations therefore may play an important role in the post-operative cell proliferation and subconjunctival scarring (Kawashima et al., 1998). Moreover, expression of other MMPs and TIMPs, including MMP-1, -2, -3, -9, -14 and TIMP-1 and -2 occur in cultured human Tenon's fibroblasts (Mietz et al., 2003). Postmortem examination of patients that had undergone glaucoma filtration surgery revealed an increased staining of MMPs near the surgery site. MMPs 1, 2, and 3 were found to be expressed in fibroblasts found in the bleb walls around Molteno plate implants (McCluskey et al., 2009). A summary illustrating the involvement of MMPs in conjunctival wound healing is shown in Figure 1-10.

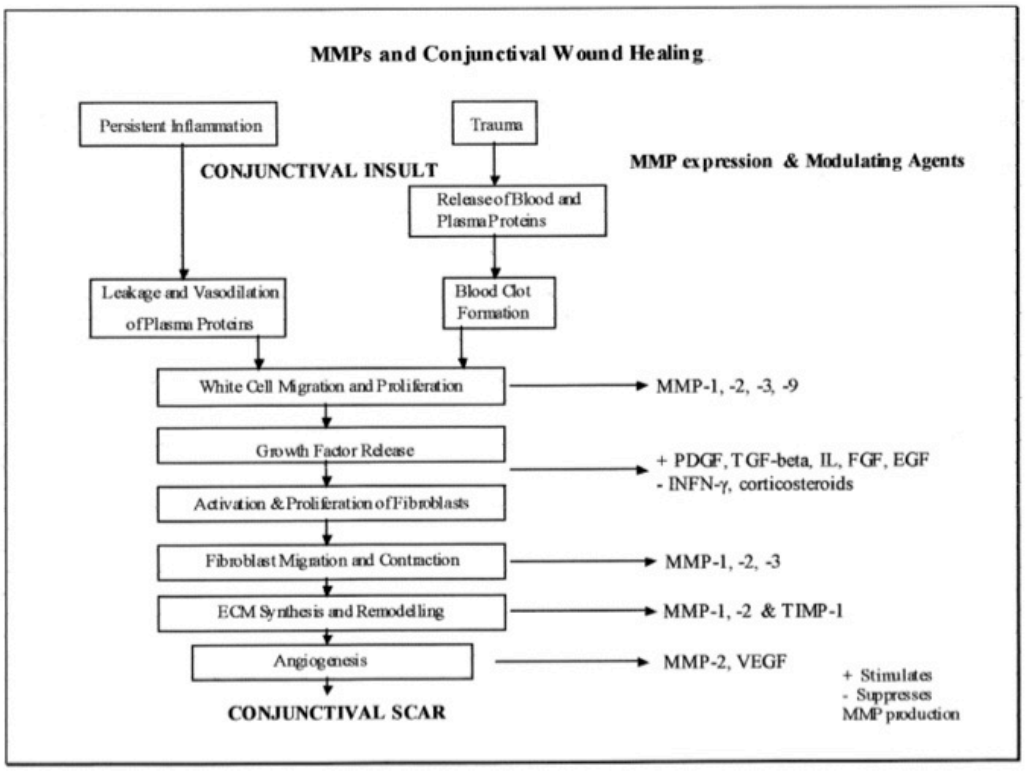

Figure 1-10 MMPs involved in subconjunctival wound healing adapted from (Wong et al., 2002).

1.6 MMP inhibition

As MMPs are key proteins in regulating inflammation and angiogenesis, much research has been performed into MMP inhibitors as possible therapeutic agents in disease. The greatest area of research and investment has been to use inhibitors as a potential treatment for cancer. Evidence for MMP involvement in cancer progression comes from work that illustrated that MMP expression was up-regulated in tumours at the time of spread and metastasis (Coussens et al., 2002). Furthermore if the natural MMP inhibitors such as TIMP 1 were over-expressed, the invasive ability of tumours was reduced. Indeed deletion of TIMPs in normal cells can lead to the production of cells that are tumourogenic. Although it was not possible to develop TIMPs into therapeutic drugs, early artificial smaller MMP inhibitors showed promise as therapeutic agents against cancers, for example the treatment of mice that human breast cancer xenografts with batimastat (a broad-spectrum hydroxamate inhibitor) lead to reduced metastasis and inhibition of local regrowth (Sledge et al., 1995).

That MMPs play a pivotal role not only in wound healing but in also in cancer progression is to be expected. Virchow identified chronic inflammation as an underlying cause of cancer in 1863. Since then a number of chronic inflammatory conditions or chronic inflammatory infectious diseases have been linked to the development of cancer: Helicobacter Pylori causes inflammation in the form of stomach ulcers and an increased risk of gastric carcinoma (Grivennikov et al., 2010). Crohn's disease causes bowel inflammation and is associated with an increased risk of colorectal carcinoma. Hepatitis B and Hepatitis C cause inflammation of the liver and are associated with an increased risk of hepatocellular carcinoma.

What are the mechanisms behind inflammation causing neoplastic change? Proliferating cells do not simply result in tumourogenisis. However a sustained proliferation of cells in an environment of DNA damaging agents, inflammatory mediators and growth factors can potentiate neoplastic change (Grivennikov et al., 2010). It is hypothesised that the cells damaged or 'initiated' by an agent are transformed to become somatically different. Promotion by chronic inflammation can lead to subversion of cell death and loss of growth control. There is further release of inflammatory mediators and angiogenic factors by cells such as tumour associated macrophages and in this way this leads to more inflammation. Therefore in effect tumours then become wounds that fail to heal.

Other directly mutagenic factors are released in chronic inflammation. Peroxynitrite is produced by leucocytes and is a highly toxic agent that can interact with the DNA of proliferating epithelium. Mutations in p53 are seen at similar rates in rheumatoid arthritis as they are in tumours of chronic inflammatory bowel disease.

The roles that MMPs play in tumour progression continue to be elicited. It is not just the cells that are part of the tumour per se that up-regulate their MMP expression, enabling the tumour to cause angiogenic stimulation and matrix breakdown. The surrounding stromal cells themselves also up-regulate their MMPs. Indeed the expression of MMPs can often be up-regulated before the basement membrane destruction and tumour metastasis. This suggests that they have more complex functions than just causing holes in the basement membrane and allowing malignant

cells to escape (Coussens et al., 2002). It also appears that several MMPs have the same role and some MMPs have multiple roles. Indeed MMPs are involved in the regulation of a number of different events in tumour progression such as cell death, cell proliferation, angiogenesis and malignant conversion.

Early trials involving MMP inhibitors were unsuccessful. The MMPis had poor bioavailability and were replaced by other orally active drugs. These second generation MMPis, however, had musculoskeletal side effects at high cumulative systemic doses that were alleviated with a drug holiday, but this still meant limited dosages could be given.

Later trials using MMPis that had fewer side effects were thwarted by the lack of consensus over endpoints for the trials. Previous cancer trials relied upon survival as an endpoint. MMPis target cancer cells at the point of spread or metastasis. Furthermore they are cytostatic, not cytotoxic. The patients enrolled for trials of MMPi mostly had advanced disease. Although tumour marker levels were found to decrease with treatment, there were few results where there was an impact on survival (Table 1-1)(Coussens et al., 2002). As a consequence there are no MMPi treatments that are licensed for use in humans.

Table 1-1 Phase III clinical trials with MMPis adapted from (Coussens et al., 2002).

MMP inhibitor	Cancer	Treatment	Result
Marimastat	Pancreatic	5, 10, 25 mg bd vs gemcitabine 1000 mg / m2	No significant difference in overall survival
Prinomastat	Non-small-cell lung cancer	Cisplatin + gemcitabine 1250 mg / m2 with prinomastat 15 mg bd or placebo	No survival benefit
Tanomastat	Small cell lung	Tanomastat vs placebo	Terminated prematurely because placebo patients had better survival rates
BMS-275291	Non small cell lung cancer	Carboplatin + paclitaxel with BMS – 2755291 1200 mg od or placebo	Musculoskeletal toxicity. Poor response

1.7 MMP Inhibition as a Therapeutic Intervention against Scarring

An exciting potential use for MMPi therapy is the modulation of wound healing after surgery to prevent scarring. Most research so far has focused on using MMPis in *in* vitro and in *in* vivo models. Ilomastat, a broad spectrum potent MMPi was designed as an inhibitor of human skin collagenase for the treatment of the invasive phase of rheumatoid arthritis (Grobelny et al., 1992). Later studies of this drug showed that it had potential to treat corneal ulcers by reducing the infiltration of inflammatory cells in alkali burned rabbit corneas (Galardy et al., 1994), however this did not translate to humans. Other MMPis, such as marimastat, have also been reported to have a reversible inhibitory effect on human dermal fibroblasts (Scott et al., 1998).

One significant property that ilomastat has, unlike a number of other MMPis, is poor solubility in water, yet being very effective at low concentrations (Table 1-2). This

makes ilomastat an attractive prospect as a potential slow release anti-scarring agent in an aqueous environment.

Figure 1-11 Ilomastat

Table 1-2 The minimal inhibitory concentrations of ilomastat necessary to inhibit enzyme activity by half (Ki values for ilomastat) (Galardy et al., 1994)

MMP	Ilomastat Ki Values
MMP 1 (Fibroblast collagenase)	0.4 nM
MMP2 (Gelatinase)	0.5 nM
MMP 3 (Stromelysin)	27 nM
MMP 8 (Neutrophil collagenase)	0.1 nM
MMP 9 (Gelatinase)	0.2 nM

1.7.1 *In vitro* Scarring Model

One *in vitro* model of wound healing developed to examine cellular function in the scarring process is the gel contraction model using a collagen lattice seeded with fibroblasts (Bell et al., 1979). Over time the fibroblasts cause contraction of the gel lattice. The effect of different drugs at different concentrations on fibroblastic function can be determined.

Using this model it has been shown that inhibition of MMPs induces inhibition of contraction of collagen I lattices populated by human Tenon's fibroblasts (Daniels et al., 2003). Comparison between three MMP inhibitors (MMPis) – Ilomastat, BB-94 and Cell Tech- revealed inhibition of gel contraction with the application of all the three MMPis in a dose-dependent manner, although ilomastat was found to be the most effective.

It also appeared that this inhibition was reversible and non-toxic to the cells. Removing ilomastat two days after application on cultured fibroblasts initiated further gel contraction. Furthermore there was no inhibitory effect of ilomastat on cell proliferation despite being incubated with an ilomastat concentration at a factor of 10 higher than that found to inhibit gel contraction.

1.7.2 Animal Model of Glaucoma Surgery

The use of rabbits as an animal model for glaucoma surgery is well established. The earliest experiments with trephination on rabbit eyes date back to 1913. Since the trabeculectomy was developed researchers have used the rabbit to characterise the healing response post surgery histologically. Initially the experimental technique performed on the animals mimicked the procedure performed on humans. However, due to the aggressive nature of healing and the anterior position of rabbit ciliary processes, conventional trabeculectomy results in bleeding and failure of blebs between 10 and 14 days (Skuta and Parrish, 1987). Modification of the technique

involving a thermosclerostomy rather than creation of a scleral flap to control haemorrhage led to less bleeding, however occlusion with scar tissue still occurred by the tenth postoperative day. Even so considerable information has been gained such as illustrating how the antimetabolites 5 FU and MMC can prolong bleb survival (Khaw et al., 1993; Doyle et al., 1993; Hyung et al., 1994).

More recently a technique from our group of experimental glaucoma fistulising surgery (GFS) in rabbits has been developed that results in longer bleb survival with less inter operative variability (Cordeiro et al., 1997). The key changes are:

1) The sclerostomy is created using an MVR blade (typically used by retinal surgeons) instead of a 'trapdoor' - the thickness of which can vary and considerably affect outcome.

2) A 22 gauge cannula is passed into the anterior chamber and sutured to the scleral surface. Iris bleeding is therefore negated by not needing to perform an iridectomy. The presence of the tube also prevents the formation of a scar tissue plug over the sclerostomy that often caused the failure of blebs in other experimental surgeries.

This method of GFS has conclusively shown how MMC should be applied to a greater surface area to promote bleb survival. (Cordeiro et al., 1997) Rabbits were assigned to having GFS with MMC application using a larger sponge soaked in MMC (8 X 10 mm) or a smaller sponge (4 X 2 mm). Those rabbits that received the larger sponge resulted in having blebs that survived longer with a more diffuse morphology.

There was less cellularity in the subconjunctival area over the drainage site in the eyes treated with the large sponge as opposed to the smaller sponge or control on histological analysis. Furthermore, there appeared to be more extracellular matrix deposition and elastic fibres in the eyes treated with the smaller sponge or control.

1.7.3 Ilomastat injections promote bleb survival

Two sequential studies have illustrated how ilomastat injections after GFS on the rabbit model can promote bleb survival with minimal scarring. (Wong et al., 2003; Wong et al., 2005). The first compared postoperative injections of ilomastat to phosphate-buffered saline (PBS). Forty rabbits underwent GFS and then received either 10 consecutive days of subconjunctival PBS (0.1 ml), or 10 consecutive days of subconjunctival ilomastat (0.1 mls of 100 μM).

The bleb appearance, height and vascularity were assessed over 30 days. Subsets of animals were terminated at weekly time points and their globes enucleated for histological analysis.

The blebs treated with post-operative ilomastat sub conjunctival injections survived significantly longer than those treated with the PBS sub conjunctival injections.

Histological analysis of the blebs found that extracellular matrix was present to a greater degree in the PBS treated eyes as opposed to the ilomastat treated eyes. Furthermore there was increased cellularity at the surgical site in the PBS treated eyes. Indeed the study found that the morphology of the conjunctiva of the operated eyes treated with ilomastat closely resembled virgin eyes with no surgical intervention or treatment.

The second study compared the postoperative course of rabbits that had undergone GFS treated with subconjunctival injections of ilomastat to those that received treatment with MMC at the time of surgery only and PBS subconjunctival injections (control).

The concentration of MMC used was 0.2 mg / ml and applied for 3 minutes at the drainage site. Ilomastat injections were applied daily for 10 consecutive days at the time of the surgery, and afterwards twice weekly for 2 weeks and weekly for 2 weeks. The concentration used was 100 μM, as above at a volume of 0.1 ml. The PBS injections were of the same volume and applied at the same intervals as ilomastat.

Overall the MMC and ilomastat treated groups all had blebs that survived compared to none of those treated with the PBS injections at day 30.

Histological examination of the ilomastat and PBS treated eyes revealed similar findings to the first study, namely that there was less scar tissue formation in the ilomastat treated blebs. The conjunctival tissue in the ilomastat treated eye more closely resembled unoperated eyes than either the MMC or control eyes. Ilomastat also reduced the population of cells expressing α-smooth muscle actin indicating fewer myofibroblasts. The MMC treated eyes, however, had conjunctiva with thickened disrupted epithelium with cells sloughing from the surface.

1.8 The Ilomastat "tablet" implant

Multiple postoperative injections of ilomastat inhibit scarring after GFS in the rabbit animal model, however to translate this to the clinical setting a slow release preparation would be desirable. Patients are unlikely to tolerate multiple ocular injections due to the discomfort and inconvenience caused. Furthermore, injections also result in 'spikes' of drug delivery with rapid clearance.

Georgoulas et al developed an implant consisting of pure ilomastat known as the "ilomastat tablet", which could be applied at the time of surgery resulting in drug release over the following weeks (Georgoulas, 2010). By using a drug where the solubility (Cmax) in aqueous fluid was similar to its therapeutic level the release is "set" or limited to this range. Ilomastat's low solubility should also mean that the drug persists in the subconjunctival space for a significant duration, and could be adjusted according to implant size. Furthermore, by only using pure drug without excipient to bind the drug together or enhance dissolution there should be no 'by product' remaining that might cause toxic or inflammatory side effects. In an in vivo experiment with 24 rabbits it was claimed that the ilomastat "tablet" implant prolonged bleb survival significantly longer than MMC with significantly less collagen deposition than either MMC or negative control (application of water in the same way as MMC at the time of surgery) (Georgoulas et al. 2010).

1.9 Aim and summary of experiments

Given the promise of this anti-scarring therapy the aim of this PhD was to investigate further its potential as a treatment for patients undergoing glaucoma surgery. The hypothesis was that MMPi therapy could inhibit fibrosis to the same extent as current treatments for glaucoma filtration surgery, but with fewer side effects than those seen with the antimetabolites 5-FU and MMC. By prolonging the antiscarring pharmacokinetic profile fewer postoperative interventions might be required than seen with Kirwan et al., 2013.

The research was funded by the Medical Research Council as part of a project whose aim was to develop the antiscarring MMPi tablet implant for clinical trials. The unique selling point of this implant and the basis of its international patent was that it was constructed without any excipient.

Because the experiments by Georgoulas et al., 2010 showed complete success in vivo with implants of 3 mm diameter the first experiments aimed to investigate the pharmacokinetic profile of different smaller sized implants in vitro and efficacy in vivo.

Implants were fabricated using a cylindrical punch and die apparatus that pressed crystalline drug into a compacted implant. Cylinders of different diameters produced drug implants of different sizes. In *in vitro* flow release studies these implants were placed in chambers with fluid flow passing over them designed to mimic the aqueous flow in a bleb environment. High performance liquid chromatography analysed the concentration of drug in solution sampled at different times, thus determining the dissolution behaviour of the implant.

Ilomastat implants of 1 mm, 2 mm, and 3 mm diameter released drug at a concentration of more than 10 μM (the concentration reported to inhibit fibroblast contraction (Daniels et al., 2003)) for between 12 and 26 days. Because theoretical therapeutic levels were attained with even the smallest implants the 1st in vivo experiment investigated the anti-scarring efficacy of implants of a smaller size than previously examined by Georgoulas et al., 2010. Twenty-eight New Zealand White

Rabbits were divided into 4 different perioperative antiscarring treatments for modified glaucoma filtration surgery: 1 mm ilomastat implant, 2 mm ilomastat implant, MMC (0.2 mg / ml applied for 3 minutes), and 2 mm ethylcellulose implant (an implant with similar dimensions to the 2 mm ilomastat implant but with no presumed active anti-scarring component).

Contrary to expectation although the ilomastat implants appeared to prolong the bleb survival of glaucoma surgery in rabbits, a significant foreign body reaction was seen at a histological level conflicting with the findings of the previous in vivo data and raising questions about therapeutic efficacy. The 2nd in vivo experiment therefore aimed to confirm whether ilomastat implants of the same diameter as the original pilot studies (3 mm) had a similar response, and the same foreign body reaction was seen. The effect of increasing drug dissolution on surgical survival was investigated by using ilomastat implants combined with hyaluronic acid, excess aqueous fluid at the time of implant placement, and using more water soluble MMPi implants (AZ8955 and AZ 6731). The implants that dissolved faster had less scar tissue, but failed earlier.

Implants of the highly water soluble broad spectrum MMPi marimastat were found to dissolve completely within 48 hours and showed little foreign body reaction in a pilot 3rd in vivo study. In a 4 arm efficacy in vivo experiment (4th in vivo experiment) the anti-scarring efficacy of marimastat implants were compared to a combination implant made of the dexamethasone and ilomastat. The positive control was MMC sponge application (0.2 mg / ml applied perioperatively for 3 minutes) and negative control water applied in the same way as MMC. The hypothesis for using dexamethasone was that a potent steroid anti-inflammatory would dampen the foreign body response, leading to less foreign body encapsulation, greater MMPi dissolution and enhanced anti-scarring efficacy.

The combined implant of the steroid dexamethasone and ilomastat appeared to prolong survival with a less, but still significant tissue reaction but those blebs treated with marimastat failed shortly after the negative control. It was therefore postulated that reducing the dose size of the combined implant might tip the balance

in favour of the active soluble moiety away from the aggravating antagonistic effect of the non-solubilised drug. Combination implants of a smaller size were not physically possible to create due to incomplete mixing and fragmentation, and therefore individual 1 mm dexamethasone and ilomastat implants were fabricated and applied together. These were investigated in a pilot 5th in vivo together with polymers to create a less abrasive tissue implant interface. Different types of hyaluronic acid polymer were examined. The aim was either to dissolve the drug or shield the drug in a hyaluronic acid / drug / hyaluronic acid "sandwich" implant. Another hydrophobic polymer (used by Alex Sefalian's group for the development of artificial tracheas) was also piloted to see whether these could coat pure drug implants.

The hyaluronic acid ilomastat implants and individual dexamethasone / ilomastat implants still had considerable tissue reaction, but the polymer coated pure drugs had less. Pockets of inflammation were seen instead, associated with presumed defects in the implants. Further work with the hydrophobic polymer however found that the challenge of coating pure drug uniformly without defects, and allowing drug elution was too great.

A more hydrophilic polymer was insvestigated in the 6th in vivo efficacy experiment compared to MMC positive control and sterile water negative control. Here too there was less reaction than seen with naked implants, though with significant macrophage infiltration.

From all of the experiments involving space occupying implants it was apparent that bleb appearance did not necessarily correlate with histological scarring. Thus the notion of 'bleb survival' as an outcome was questioned and other outcomes tested. Indocyanine Green dye to trace aqueous movement by injection into the anterior chamber after glaucoma filtration surgery was too slow, and fluorescence from the dye was found in the blood vessels within the bleb tissue, shortly after application, suggestive of egress into the systemic circulation via traditional aqueous outflow mechanisms.

Induction of ocular hypertension was examined as a potential means to using IOP as an alternative outcome of success for experimental glaucoma surgery. Injection of magnetic beads or cross linked hyaluronic acid into the rabbit anterior chamber to block aqueous outflow caused only a temporary, unpredictable pressure rise, and buphthalmos. Pooling IOP data from larger numbers after standard surgery appeared to be a more accurate method.

Chapter 2 Materials and Methods

2.1 Implant formulation

The implants were formulated without excipient using custom-made punch and die sets (Holland, Nottingham, UK). Three different punch and dies created implants of of 1 mm, 2 mm and 3 mm in diameter. A diagram illustrating the apparatus for a 1 mm punch and die set is in Figure 2-1. To lubricate the parts, micrograde Poloxamer 188 (Lutrol F68, BASF, Germany) 0.1% in acetone was applied and solvent allowed to evaporate before tablet compression. The FDA has approved the use of Poloxamer 188 in ophthalmic drops.

The implants were pressed using a Specac IR press. Powdered drug was poured into the die. The punch was placed with the pin inside the die and compression applied. Various compression forces were used according to the tablet size and drug pressed. The implant heights were measured with a micrometer screw gauge.

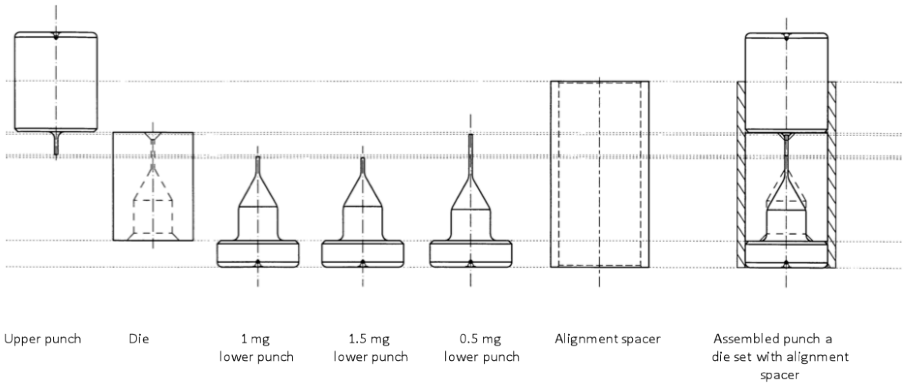

Figure 2-1 The different components of the punch and die set. To fabricate an implant the lower punch was inserted into the die of corresponding size and pre-weighed drug poured into the die funnel. The upper punch was then placed on top of the die and alignment spacer used to keep the apparatus stable during pressing. The implant was ejected with a punch and then reweighed.

2.2 Flow Release Studies using an in vitro model of a bleb

Artificial ‘blebs’ or ‘flow rigs’ were constructed to allow examination of drug release from the implant (Figure 2-2). These consisted of watertight containers of 200 μl volume that have an inflow and outflow. Tubes were connected to a peristaltic pump

(ISMATEC, Switzerland) and allowed media to pass into the rig at a constant rate. By being placed in a heated oil bath (Grant) the rigs were maintained at a constant temperature. For the purpose of these studies the temperature was maintained at 35.5 °C, an estimate of the sub-conjunctival temperature (Kawasaki et al., 2009). The effluent was collected at time points and High Pressure Liquid Chromotography (HPLC) used to analyse drug concentrations. Using the flow rate, quantity of drug release was determined.

Initial experiments examined the drug release profile from implants at a flow rate of 2 μl / minute, a putative rate of aqueous production in the normal eye (McLaren, 2009). PBS at pH 6.5 was used as the solvent to mimic the aqueous. A slower flow rate was also used, a setting that might occur after surgery when the eye is recovering. The flow rig apparatus was calibrated and checked using by collecting and weighing effluent over a set period of time. Calibration took place at the start and the end of the experiment. A temperature of 35.5 °C (estimated temperature of conjunctiva (Kawasaki et al., 2009)) was maintained for the duration of the experiments. An attempt was made to use sterilised 'balanced salt solution', a solution that is used to irrigate the eye during ocular surgery and whose constituents closely resemble those of the aqueous humour, however this led to microbial overgrowth that thwarted HPLC analysis.

The media used for the majority of flow rig experiments was phosphate buffer saline (PBS). The pH of the media was maintained at 7.4. HPLC analysis took place according to the methods below:

2.2.1 HPLC method for Ilomastat

The detection of ilomastat in the first set of drug release experiments was through the use of an isocratic HPLC with a reverse phase C18 Superlco Discovery column 88913-05. The detection wavelength was 280 nM. The following settings were used: flow rate 1 ml / min, running time 12 minutes and injection volume of 10 μl. The mobile phase consisted of 25% acetonitrile and 75% buffer (0.0135 M ammonium acetate, 0.6% triethylamine adjusted to pH 5.0 ± 0.1 with acetic acid). An integrated HP 1050 series HPLC system comprising an HP1050 autosampler, HP 1050 pump

and HP 1050 multiple wavelength UV-vis spectrophotometric detector was employed. The detector was interfaced with a pc with PC/Crhom + Software (H & A Scientific Inc., Greenville, NC).

2.2.2 HPLC method for Marimastat and Ilomastat / Dexamethasone

The detection of marimastat, ilomastat and dexamethasone in later experiments used a gradient HPLC method with a reverse phase Synergi Polar-RP Phenomenex 4 μm, 15 cm column. The detection wavelengths for marimastat, ilomastat and dexamethasone were 210 nm, 280 nm and 241 nm respectively. There was a flow rate of 1 ml/min, a running time of 24 minutes and an injection volume of 10 μl. The mobile phases 0.1 % Trifluoroacetic acid (TFA) in water and acetonitrile were used in a gradient where TFA:acetonitrile started at 4:1 and ended at 3:7. The time between start and end point was 17 minutes. The Agilent 1200 series HPLC system (Agilent, USA) was employed with Chemstation software (Agilent, USA).

2.2.3 Sterilisation of implants

The implants were sterilised using gamma irradiation at a level of 25 KGy (Isotron, Swindon, U.K.). USP regulations stipulate a 25 KGy dose and 5 KGy has been proven to achieve a sterility assurance level of SAL=10^{-6}. Irradiation has been shown in previous work not to affect the ability of ilomastat to inhibit HTF gel contraction (Georgoulas, 2010).

Figure 2-2 Flow rig chamber illustrating inflow and outflow tubes, 'O' ring seal and implant within the chamber.

2.3 First in vivo experiment implant fabrication

All rabbits were acclimatised for 5 days in the Biological Research unit (BRU) of the UCL Institute of Ophthalmology before the start of the experiments. The experiments conformed to the ARVO statement for the Use of Animals in Ophthalmic and Vision Research as well as the Animal Scientific Procedures Act (1986). The Animals were observed for a period of 30 days. The experiments were performed as a randomised, controlled study with an observer who was as masked as possible (the MMC treated arm had no implant and therefore an implant's absence at follow up may indicate this treatment). This observer assessed the clinical data from 28 males New Zealand White Rabbits (Harlan LK Ltd. C. 2.0-2.5 kg, 12-14 weeks old)

2.3.1 Modified glaucoma filtration surgery

Rabbits were anaesthetised with Ketamine (50 mg / kg) and Xylazine (10 mg / kg). All rabbits underwent surgery to the left eye only. Povidone iodine 5 % was instilled into the left eye. The nictitating membrane was excised. A partial thickness 8-O silk corneal traction suture (Ethicon) was placed superiorly and the eye infraducted. A fornix-based conjunctival flap was then raised and blunt dissection exposed sclera to approximately 15 mm behind the limbus. An MVR blade was passed through the sclera at a shallow angle to enter the anterior chamber tangentally to the iris and then withdrawn. A 22 gauge / 25 mm cannula was then passed along the tract created by the blade and sutured to the scleral surface with a single 10-O nylon suture. The cannula was trimmed and beveled so that it would extend 1 mm above the scleral

surface. The conjunctival incision was closed laterally with two purse string sutures. Chloramphenicol ointment was instilled at the end of surgery. The surgical steps are illustrated in Figure 2-3.

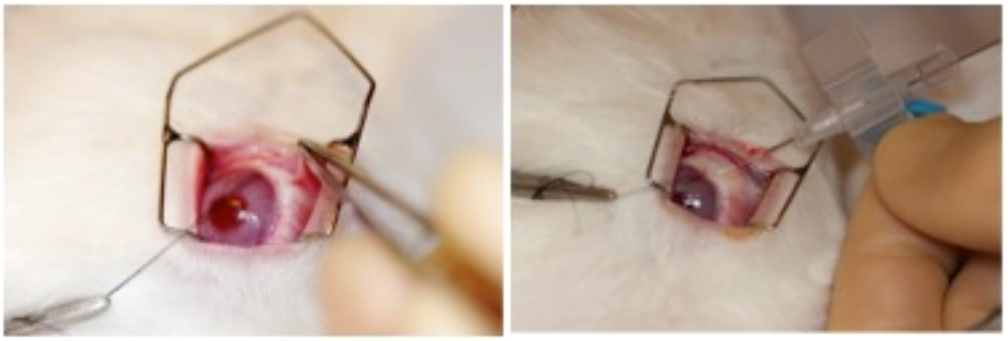

A B

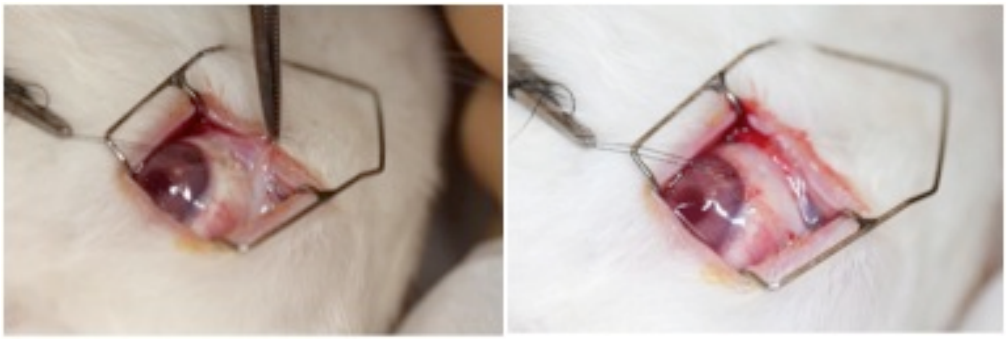

C D

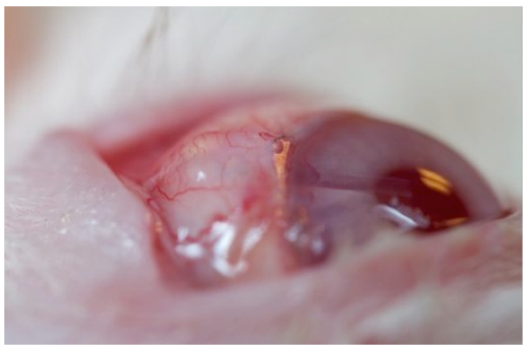

E

Figure 2-3 Surgical steps. [A] conjunctival flap, [B] cannula insertion, [C] implant placement if applicable, [D] conjunctival closure, [E] bleb filled at the end of surgery.

2.3.2 Treatment Regimen

The 28 Rabbits were randomly assigned into 4 groups (7 rabbits in each group) with a Latin square crossover design (Table 2-1). Ethylcellulose, an excipient that does not swell, is poorly soluble in water, is not pharmacologically active, and was therefore used as a negative control. Mitomycin C was applied prior to cannula insertion using PVA sponges, and washed off with sterile water.

Table 2-1 Treatment arms for 1st in vivo experiment. (For left eyes, during GFS; Right eyes are untreated and unoperated)

Treatment Group	Pharmaceutical Treatment
A	Ethylcellulose implant (2 mm, 1 mg) (Negative Control)
B	One ilomastat implant (1mm, 0.5 mg)
C	One ilomastat implant (2 mm 1 mg)
D	Mitomycin C (0.2mg/ml) 3 minute application (positive control)

2.3.3 Clinical Assessment

Clinical examinations by a masked observer were performed preoperatively and at set time points after surgery. The following parameters were recorded using a portable slit lamp (Keeler SL-14 Portable Slit Lamp)(Figure 2-4):

Figure 2-4 Use portable slit lamp.

- Intraocular pressure. Measurement of both eyes was performed using a 'Tonovet'. Readings were taken until 3 consecutive readings were within 2 mm Hg of each other and the mean calculated.
- Bleb surface area. Length and width measurements with calipers enabled surface area calculation.
- Bleb height. Height was graded semi-quantitatively by slit lamp examination (0, flat; 1, shallow/formed < 1 mm; 2, elevated < 2 mm; 3, high > 2 mm)
- AC depth (determined as flat, shallow or deep)
- Bleb vascularity (graded as: 0 = vascular, 1 = normal, 2 = hyperaemic, 3 = very hyperaemic)
- Anterior chamber inflammation (graded as: 0 = no inflammation, 1 = cells present, 2 = fibrin, 3 = hypopyon).

2.3.4 Termination of the study

All animals were terminated after experiment completion with a lethal injection of intravenous pentobarbitone (4 mls) according to schedule 1. After termination eyes were enucleated and placed in formaldehyde.

2.3.5 Histology

Eyes were fixed in 10% neutral buffered formalin. In the first study the globe was divided into two: a transverse anterior to posterior section was made to divide the globe into superior and inferior halves. The filtration tube was not removed from the operated rabbit eyes. The section was placed in a cassette and loaded into the tissue processor for 48 hours. To dehydrate the eyes, they were immersed in gradually increasing alcohol concentration (70 % methyl alcohol, 80 % methyl alcohol, 95 % methyl alcohol, 100 % methyl alcohol) and finally washed with xylene.

The specimens were then embedded in molten paraffin wax in a mold of approximately 4 cm x 2 cm x 3 cm. Orientation was such that the eyes were lying on their sides with cornea and posterior pole at the front and rear of the cassette respectively. The molds were kept in the cold storage area until they became solid. The paraffin blocks were then secured to a microtome and sagittal sections were cut with a blade at 15°. Ribbons of tissue embedded in wax 5 μm thick were obtained and placed on the surface of warm distilled water to allow the ribbons to straighten. The paraffin sections were collected on microscope slides and briefly exposed to temperatures of 65^{o}C, the melting point of paraffin wax, to encourage adhesion.

Prior to staining the specimens were dewaxed and rehydrated with immersion in xylene for 5 minutes, followed by two further xylene washes for three minutes each. They were then washed with descending concentrations of methylated spirit, and finally with water. Histological stains used for the purposes of this experiment include haematoxylin and eosin (to assess the inflammatory reaction and cellularity of the bleb), and Picrosirius red (to evaluate collagen deposition).

2.3.6 Haematoxylin and Eosin staining

The sections were hydrated incrementally. Immersion began with xylene and then decreasing concentrations of methyl alcohol: 100 %, 90 %, 80 %, and 70 %.

After rinsing they were then stained with Harris's haematoxylin for 3 minutes, and rinsed again. For differentiation purposes, the slides were placed in 1% acid alcohol (1%HCl and 70% alcohol) for 5-10 seconds. They were then washed with tap water

for 5 minutes or until sections were blue. The sections were then stained with 1% Eosin Y for 10 minutes, and washed in tap water for 1-5 minutes. The specimens were dehydrated with ascending concentrations of methylated spirit and finally xylene. A drop of Digital Picture Exchange mounting media was placed in the centre of a coverslip, which was pressed gently onto each slide and left to dry.

Using this method, nuclei are stained blue or black, cytoplasm is presented as varying shades of pink, muscle fibres show as dark pink-red, red blood cells are orange or red in colour, and fibrin are deep pink.

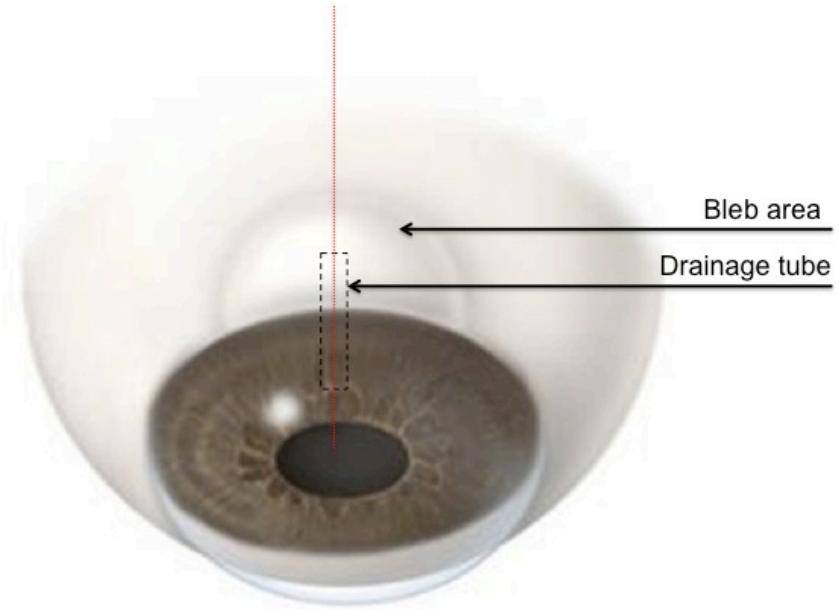

Figure 2-5 Orientation of globe for histology. Thin red line indicates sagittal plane of sections through the drainage tube.

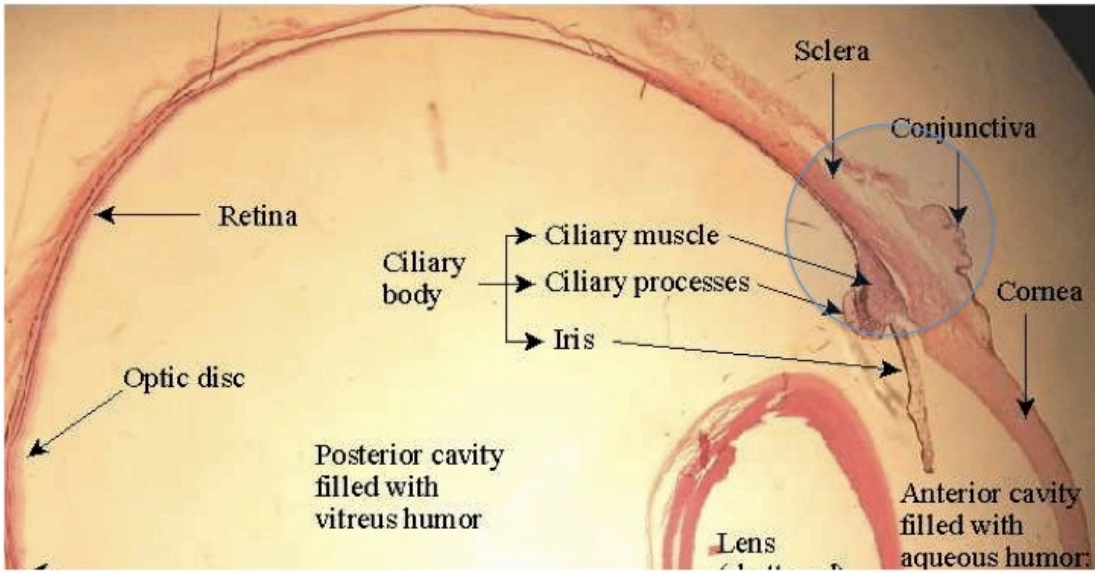

Figure 2-6 Sagittal section through a globe in a plane similar to that of the drainage tube illustrating anatomy. Blue circle indicates bleb area.

2.3.7 Picrosirius Red staining

The Picrosirius Red staining was done with 100ml of a saturated picric acid solution mixed with 0.1 g Sirius red powder.

The sections were hydrated incrementally. Immersion began with xylene and then decreasing concentrations of methyl alcohol:100 %, 90 %, 80 %, and 70 %. Once hydrated, the sections were placed in distilled water for 10 minutes, then dehydrated as before with ascending concentrations of methylated spirit and finally xylene. For each slide, a drop of Digital Picture Exchange was placed in the centre of a coverslip and pressed gently to the slide, then left to dry.

Using polarizing microscopy, collagen type I is stained yellow, orange or red, collagen type II is stained blue or pale yellow depending upon orientation, and collagen III is stained green (Junqueira et al., 1979).

2.4 Second in vivo experiment implant fabrication

Excipientless ilomastat and AstraZeneca 8955 and 6357 implants were formulated as above in the first experiment using a punch and die set. Unfortunately there was error in calculating the mass of the some of the implants. Preparation was rushed. The overall dimensions of diameter were the same, however weights of the pre-pressed drug were confused with implant weights, furthermore weighing took place on scales that were less accurate (+/- 0.5 mg error) and therefore it was not possible to be sure of the masses of 5 of the implants.

Those implants where there was doubt over the accuracy have been labelled as unknown in the table below (Table 2-2)

Ilomastat / hyaluronic acid (Visiol) implants were produced by dissolving 2.5 mg of ilomastat in 1.5 ml of ethanol 96% (v/v) and 2 ml of demineralised water. Visiol (1.5 ml) was added to this solution. The mixture was then freeze-dried. The homogenate weighed 45 mg after freeze-drying and was compressed into five tablets of approximately 9 mg each (diameter 3 mm, height 1 mm). A compression of 0.4 bar for 10 seconds was used. The compaction was kept constant during the preparation of all tablets. The drug was assumed to be dispersed evenly thoughout the homogenate and therefore each tablet to contain approximately 0.5 mg of ilomastat. The tablets were stored at 4°C in an eppendorf tube (1.5 ml). Four tablets were placed in one eppendorf tube (1.5 ml) and transported at room temperature to Moorfields Eye Hospital for beta-irradiation using Strontium 90 (215 Gy) for 6 h. Sterilisation was not confirmed. The weights at the time of surgery were determined by subtracting the weight after each tablet removal.

2.4.1 Treatment regimen

Eighteen rabbits were assigned into 7 groups. Three rabbits were assigned to each of groups A, B, C, D and 2 rabbits to each of groups E, F, and G (Table 2-1). The rabbits were randomised in a Latin square crossover design.

Table 2-2 Treatment regimen 2nd in vivo. Treatment groups A and B aimed to determine whether excess aqueous fluid (phosphate buffer solution) applied perioperatively enhanced dissolution. The implants in arms A and B were supposed to be approximately 2 mg, however due to errors in fabrication were variable. Where denoted unknown* there was doubt over the exact mass of the implant (Right eyes are untreated and unoperated).

Treatment Group	Pharmaceutical Treatment
A n=3	3 mm (2.1mg, 3.5 mg and one unknown* mg) ilomastat implant dry
B n=3	3 mm (3.4 mg, 3.4 mg and 3.6 mg) ilomastat implant hydrated.
C n=3	1 mm (0.4 mg and two unknown* mg) ilomastat implant hydrated
D n=2	1 mm (0.4 mg and two unknown* mg) ilomastat implant surrounded by Healon 5
E n=2	Hyaluronic acid (Visiol) / ilomastat tablet freeze dried 3 mm; weight of the tablets 9.3 mg and 8.3 mg (0.52 and 0.46 mg Ilomastat);
F n=2	1 mm (0.4 mg and 0.2 mg) AZ 6357 tablet hydrated
G n=2	1 mm (0.5 mg and 0.4 mg) AZ 8955 tablet hydrated

2.4.2 Additional Surgical Technique

Modified glaucoma filtration surgery was performed as in the first *in vivo* experiment. For each arm where applicable the additional surgical techniques were followed:

2.4.2.1 Hydration of the 3 mm and 1 mm excipient free implants

The conjunctiva and Tenon's tissue were hydrated with sterile Phosphate Buffer Saline solution (PBS) using a syringe and a pressure similar to that used for hydrodissection in cataract surgery. The implant was placed behind the tube and then further saline droplets applied to ensure complete wetting. The conjunctiva was then sutured and then further hydrated underneath to facilitate bleb formation.

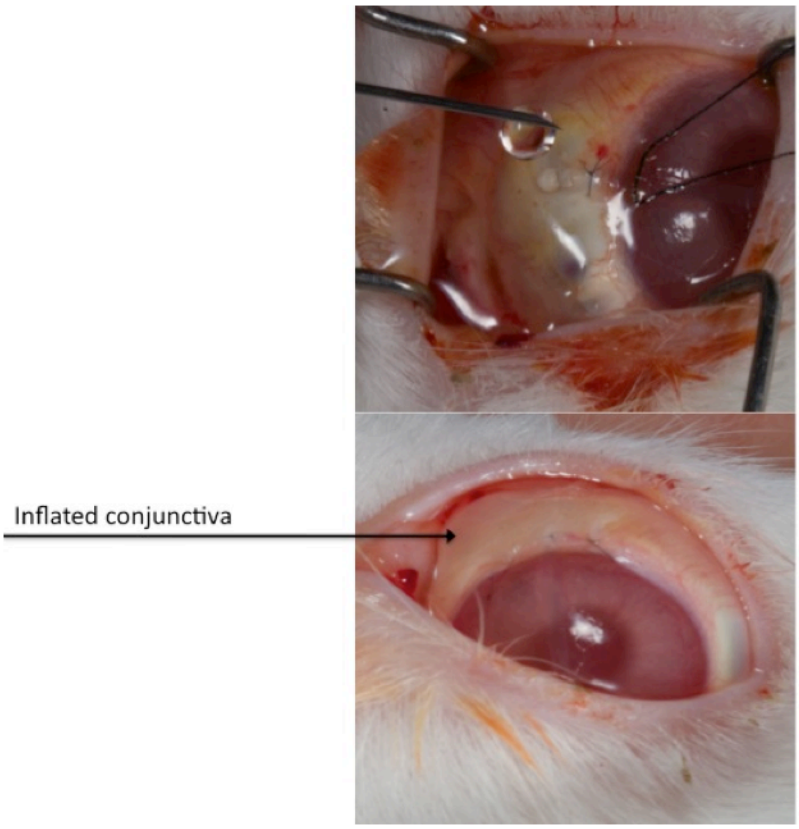

Figure 2-7 Implant hydration and conjunctival inflation at the time of surgery.

2.4.2.2 Implant surrounded by hyaluronic acid gel cushion

A small drop of Healon 5, approximately 0.1 ml was applied to the sclera behind the tube and an implant placed on top. A drop of phosphate buffered saline solution was then applied, followed by further Healon 5 to completely surround the implant.

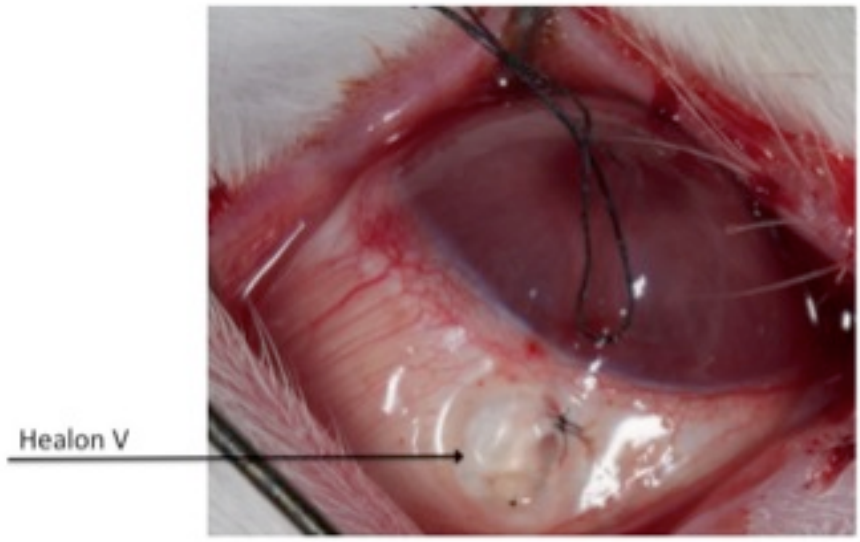

Figure 2-8 Healon V application to sclera before implant placement.

2.4.3 Outcomes

Clinical evaluation and termination were performed in a similar manner to the first in vivo experiment. All operated eyes and one unoperated eye from each treatment group (26 eyes total) were used for histology. The whole globe was used for processing and analysis. This enabled conjunctiva and sclera on the operated side of the eye to be examined and compared to the unoperated side on the same slide. From the first experiment it became clear that anatomical localisation of the bleb area within a millimetre or two was of crucial importance. To enable more accurate location of the surgical site during microtoming, a marker 7-0 silk suture was used, placed 2 mm adjacent to the drainage tube.

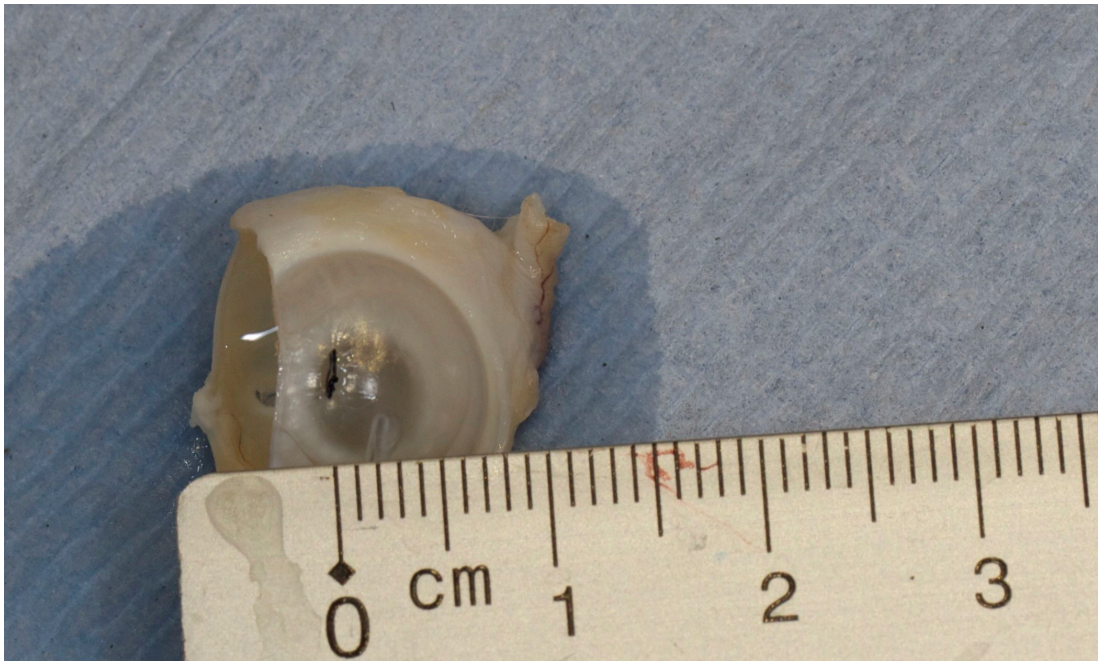

Figure 2-9 Suture position 2 mm adjacent to the drainage tube. Visualising suture through the opaque paraffin wax enables the location of sectioning to be determined.

2.5 Third in vivo experiment implant fabrication

Excipient free marimastat tablets were fabricated using a punch and die set; a lubricant (0.1 % polaxamer 188 in acetone) was applied to the punch and die after each tablet fabrication. Marimastat powder was weighed out, and poured through a hopper into the 2 mm punch and die, and compressed at 4.5 bars for 10 seconds. The tablets were weighed and placed individually into tared eppendorf tubes (1.5 ml), and stored at 4°C. For the in vivo experiment they were then transported at room temperature to Isotron and sterilised by exposure to gamma irradiation (~25 kGy). To confirm the final weight of the tablets used, individual eppendorfs with individual tablets are weighed pre and post surgery.

2.5.1 Treatment regimen

Four rabbits each received a 2 mm marimastat implant (2.2 – 2.4 mg). Application of the implant and modified glaucoma surgery was performed was as per the 1st experiment.

2.5.2 Termination

Animals were terminated as in the previous in vivo experiments. The termination day for 2 rabbits was day 7 and for the other 2 rabbits was day 14. All operated eyes and 1 unoperated eye for each time point were harvested for histology.

2.6 Fourth in vivo experiment implant fabrication

Marimastat implants were fabricated as in the last *in vivo* experiment. To create dexamethasone / ilomastat implants twenty percent of the end implant weight was assumed to be lost during fabrication: for dexamethasone 1mg / ilomastat 1 mg implants approximately 1.2 mg of dexamethasone and 1.2 mg of ilomastat were weighed out and placed in an eppendorf lid and mixed using a spatula. Once fully mixed the mixture was poured using a hopper into the 2 mm punch and die, and compressed at 2 bars for 10 seconds. The implants were weighed and placed individually into tared eppendorf tubes (1.5 ml) and stored at 4°C. They were then transported at room temperature to Isotron and sterilised by exposure to gamma irradiation (~25 kGy). To confirm the final weight of the implants used, individual eppendorfs with individual tablets are weighed pre and post surgery

2.6.1 Treatment regimen

Twenty-four rabbits received treatments (Table 2-1) following a Latin Square design. Modified glaucoma surgery was performed on the rabbits as per the 1st experiment.

Table 2-3. Treatment arms. (For left eyes, during GFS; Right eyes are untreated and unoperated). The marimastat implants dimensions and weight were chosen because these were the most stable and least likely to fragment. Two implants were used to maximise dose within the physical limitations of the surgical site.

Treatment Group	Pharmaceutical Treatment
A	Two 2 mm marimastat implants (2.9 – 3.1 mg) Overall drug mass 6 mg.
B	2 mm ilomastat / dexamethasone tablet (total drug 2 mg made up of 1 mg ilomastat and 1 mg dexamethasone)
C	Mitomycin C (0.2 mg/ml) 3 minute application (positive control)
D	Sterile water group (negative control)

2.6.2 Examinations

Examinations were performed as in the previous experiments, however the additional procedures were performed:

- Photographs of the bleb were taken with a Canon EOS 7D SLR at each time point looking down on the bleb from above and a view anterior to posterior to gauge bleb height. A macro lens was used. The settings were AV mode for the camera and flash with diffusers applied. The focus was set as close as possible to enhance detail and consistency. Multiple photographs were taken at each time point to enable selection of similar views at the various time points for comparison.

- Anterior segment optical coherence tomography (SL-OCT, Heidelberg Engineering, Berlin, Germany) was used as an adjunct to visualise the implants. The OCT consists of a 1310 nm Superluminescent Diode to produce cans of 15 mm in width and 7 mm in depth. Rabbits were restrained by an assistant and encouraged to look down.

2.6.3 Histology

Twenty-six eyes *(*22 operated and 4 unoperated controls*)* were harvested and fixed with 10% neutral formaldehyde buffer for approximately one week. The whole of the eye was used without removing the filtration tube. A 6 'O' suture was used to mark the position 2 mm lateral from the tube. The tissue was processed and embedded as before. Sections were cut from the globe with a microtome (in a sagittal plane) so the bleb area is at the top of the ribbon. Five μm cut sections are placed in warm distilled water and then collected on a microscope slide. The slides were subsequently stained with haematoxylin and eosin.

2.7 Fifth in vivo experiment implant fabrication

2.7.1.1 Ilomastat and dexamethasone implants

The excipient-free ilomastat and dexamethasone implants were fabricated using a 1mm punch and die set. Approximately 0.6 mg of ilomastat powder was weighed out, and poured into the 1 mm punch and die, and compressed at 0.4 bars for 10 seconds. The implants were weighed and placed individually into tared eppendorf tubes (1.5 ml) and stored at 4°C. They were then transported at ambient temperature to Isotron and sterilised by exposure to gamma irradiation (~25 kGy). To confirm the final weight of the implants and the amount of ilomastat and dexamethasone used, individual eppendorfs with individual implants were weighed pre- and post-surgery.

2.7.1.2 Polymer coated ilomastat implants

Excipient-free ilomastat tablets were fabricated using a 2 mm punch and die. Approximately 1.2 mg of ilomastat powder was weighed out, and poured into the 2 mm punch and die, and compressed at 2 bars for 10 seconds. The implants were weighed and placed individually into tared eppendorf tubes (2 ml) and stored at 4°C. They were then transported at room temperature to UCL Business (contact Jaspal Kaur-Griffin) for coating with polymer in the laboratory of Alex Seifalian (UCL/Royal Free Hospital). The coating process involved spraying a dimethylacetamide solution of the polymer onto the tablet; other details are not known due to the Seifalian group wishing to keep this knowledge to themselves. The coated implants were then reweighed in individual eppendorfs before being transferred to Isotron and sterilised by exposure to gamma irradiation (~25 kGy). To confirm the final weight of the tablets used, individual eppendorfs with individual tablets are weighed pre- and post-surgery. The proportion of polymer to ilomastat was not accurately known.

2.7.1.3 Ilomastat-Hyaluronic acid implants

The following mixing processes were conducted in a biological flow hood to maintain aseptic conditions. Ilomastat powder (32.0 mg) was dissolved in tert-butanol (40% aqueous solution) (32.0 ml), then sterilised by filtration using a syringe

filter (0.22 μm). Healon GV® (14.0 mg/ml) or Healaflow® (22.5 mg/ml) was transferred into a 1.0 ml syringe slowly to avoid entrapment of air bubbles inside the syringe. An amount of Healon® or Healaflow® equivalent to 3.0 mg hyaluronic acid (133.3 μl of Healon or 214.3 μl of Healaflow) was aliquoted into a glass vial (14.0 ml). The polymer solution was diluted by addition of sterile water (1.0 ml) then vortexed to produce a homogenous solution. The ilomastat solution (1.0 mg/ml) (1.0 ml) was added into the polymer solution in the glass vial and vortexed to produce a homogenous solution. The mixture was then frozen quickly using dry ice. An empty syringe (50.0 ml) was capped with a sterile filter (0.22 μm). Air was removed from the filter by pulling the syringe plunger slowly. The glass vial containing the frozen mixture of ilomastat and the polymer was sprayed with ethanol (70% in water) and then placed inside the syringe (50.0 ml). The syringe (50 ml) was then placed into dry ice and transferred quickly into the freeze drier after being sprayed with aqueous ethanol (70%). The formulation was freeze-dried for 4 days. The freeze-dried powder was pressed using a clean tablet press (3 mm punch and die), which had been placed in an aseptic flow hood. The punch and die were sterilised by dry autoclave and the tablet press machine was sterilised by spraying with aqueous ethanol (70 %). Empty eppendorf tubes (1.5 ml) were weighed and then sterilised by autoclaving. The fabricated tablets were then transferred under sterile conditions into the autoclaved eppendorf and then weighed. The implants were stored at 4°C under argon to eliminate moisture.

2.7.1.4 Sandwich implant

These tablets involved prefabrication and sterilisation of an excipient-less ilomastat implant as was done in arm A. The ilomastat tablet was then pressed with solid hyaluronic acid as a process to coat the ilomastat with hyaluronic acid. This process can be termed “a solid tablet coating process.” Since these tablets are fabricated by a process involving the pressing of a tablet within solid hyaluronic acid, these implants are named sandwich implants to distinguish them from traditionally coated implants (i.e. tablets coated for arm B).

i. Preparation of ilomastat implants

The excipient-less ilomastat implants were fabricated using a punch and die (2 mm diameter) with no lubricant being used. Ilomastat (1.2 mg) was weighed and placed into the die and compressed (2 bar) for 10 seconds. The implant was ejected from the die and its weight was recorded. The ilomastat implant was placed individually into tared eppendorf tubes (1.5 ml) and stored at 4°C. They were transported at ambient temperature to Isotron and sterilized by exposure to gamma irradiation (~25 kGy).

ii. Preparation freeze-dried hyaluronic acid using Healon GV : Revanesse Ultra (cross-linked hyaluronic acid) (1:3 by weight)

A total of approximately 3.0 mg of solid hyaluronic acid was used to press around each ilomastat implant. To prepare the hyaluronic acid for freeze-drying, Healon GV (30 µl; 14 mg/ml) and Revanesse Ultra (50 µl; 25 mg/ml) were transferred to an autoclaved 7 ml glass vial in an aseptic hood. Sterile water (1.0 ml) was added to the hyaluronic acid solution in the glass vial and this solution was then vortexed till a homogeneous mixture was obtained. After freezing the hyaluronic acid mixture in the vial with dry ice, the vial was transferred to a 50 ml syringe that was capped with a sterile filter (0.22 µm) and the solid mixture in the vial was freeze-dried for a period of 3 days following the same procedures as described for arms C and D.

iii. Preparation of sandwich implants

The following mixing and pressing processes were conducted in a biological flow hood to maintain aseptic conditions. The freeze-dried hyaluronic acid powder and pre-formed ilomastat implant was pressed using a clean and sterilised press (3 mm punch and die) as described in arms C/D. The punch and die were sterilised by dry autoclave and the press was sterilised by spraying with aqueous ethanol (70 %). The freeze-dried hyaluronic acid contents from a vial (1.5 mg) were emptied into the 3 mm die. The ilomastat implant was carefully centred in the middle of the 3 mm die on top of the freeze-dried hyaluronic acid. To this was added freeze-dried hyaluronic acid from a second vial (1.5 mg). Fitting the punch into the die, this combination of solids was compressed (2 bars) for 15 seconds to yield a hyaluronic acid coated

ilomastat tablet that was ejected from the punch. The implants were then transferred under sterile conditions to empty eppendorf tubes (1.5 ml) that had been tared and previously sterilised (autoclaved). The tablets were stored at 4°C under argon to eliminate moisture.

2.7.2 Treatment Regimen 5th in vivo

Twenty-four New Zealand White rabbits underwent modified glaucoma filtration surgery (as per 1st in vivo experiment) with six groups of four animals each receiving treatments according to Table 2-4 and following a Latin Square randomisation.

Table 2-4. Treatment Groups. For left eyes, during GFS; Right eyes are untreated and unoperated.

Treatment Group	Pharmaceutical Treatment
A	One ilomastat implant (1 mm, 0.5 mg) and one dexamethasone implant (1 mm, 0.5 mg)
B	One ilomastat implant (2 mm, 1 mg) coated with polymer provided by Alex Seifalian, UCL/Royal Free Hospital.
C	Ilomastat (1 mg) / hyaluronic acid (3 mg) (Healon GV) combination freeze dried and fabricated into a 3 mm implant.
D	Ilomastat (1 mg) cross-linked hyaluronic acid (3 mg) (Healaflow) combination freeze-dried and fabricated into a 3 mm implant.
E	Healon GV: Cross linked HA (1:3) (3mg) combination freeze dried and fabricated as base and top (3 mm) for ilomastat implant 2 mm (1 mg).
F	Sterile water treated group (negative control)

2.7.3 Examinations

A single masked observer undertook examinations pre-operatively, and on days 3, 7, 10 and 14. Each examination is within 24 hours of the time point. Both eyes were examined in every rabbit with a portable slit lamp. Evaluations were performed as in the previous in vivo experiments.

2.7.4 ICG dye evaluation of bleb functionality

One rabbit from each treatment arm of the 5th in vivo experiment was chosen at random and prior to termination on day 14 before terminal anaesthesia. This particular in vivo was chosen for this type of test following extensive discussions regarding whether clinical observation of a bleb indicated functionality. Furthermore due to it being only 14 days long dye flow would be more likely to be seen. It was also a pilot study and not an efficacy study when intervention should be kept to a minimum. The animal was positioned in front of the Heidelberg Retinogram digital camera. A butterfly needle (27Fr) connected to a transducer to measure intracameral IOP was inserted into the anterior chamber. The IOP was measured every 2 minutes. Using an insulin needle inserted inferiorly at an angle parallel to the iris into the anterior chamber, 0.1 mls of aqueous was drawn off and 0.1 mls of 0.5 % ICG injected. Using a digital camera several sequenced images were recorded.

2.7.5 Termination

All animals are killed under Schedule 1 with a lethal injection of intravenous pentobarbitone (1ml/kg) via ear marginal vein. The termination was at day 14. All of the eyes were exenterated for histology and placed in formalin.

2.7.6 Histology

All eyes were harvested and fixed with 10% neutral formaldehyde buffer for approximately 2 weeks. The whole of the eye was processed without removing the filtration tube and stained as in the previous experiment.

2.8 Sixth in vivo experiment implant fabrication

Excipient-free ilomastat implants were fabricated using a 2 mm punch and die set. Approximately 1.2 mg of powder was weighed out, and poured into the 2 mm punch and die, and compressed at 2 bars for 10 seconds. The tablets were weighed and placed individually into tared eppendorf tubes (2 ml) and stored at 4°C. They were then transported at room temperature to Vertellus (Basingstoke) for coating with polymer in the laboratory of Mike Driver (Vertellus). If being used for the *in vivo* experiment the coated tablets were then reweighed in individual eppendorfs before being transferred to Isotron and sterilised by exposure to gamma irradiation (~25 kGy). To confirm the final weight of the tablets used, individual eppendorfs with individual tablets are weighed pre- and post-surgery.

The design of experiment was chosen after considering the advantages / disadvantages of possible treatment arms (Table 2-5)

Tissue sampling

Blood was sampled at two time points: days 3 and 30 for systemic levels.

Six globes treated with polymer coated ilomastat tablets were used to determine tissue drug levels. The globes were dissected to yield tissue from the bleb conjunctiva, remaining implant, cornea, aqueous and vitreous. The concentrations of drug were analysed by Dr Ahmed using liquid chromatography mass spectrometry. The unoperated eyes from the sterile water group were used as controls.

Table 2-5 Advantages and disadvantages of different in vivo designs.

Experimental design	For	Against
MMC, Ethylcellulose spacer, drug, sterile water, 30 day outcome.	Sterile water provides baseline Ethylcellulose qualifies spacer effect / isolates drug effect MMC gold standard	Earlier time points missing, which may miss changes in the inflammatory process, i.e. sterile water may show greater inflammation at an earlier time point, and tissue remodeling likely to be significant by day 30. Conversely, if implant disappears before day 30 any particulate effect may be missed
MMC, Ethylcellulose spacer, drug, sterile water, histology at multiple time points	Sterile water provides baseline Ethylcellulose qualifies spacer effect / isolates drug effect MMC gold standard Multiple time points evaluates wound healing process and effect on the wound healing process comprehensively. Less likely to miss earlier peaks in inflammatory activity.	Numbers of animals required significant. Harvesting at multiple time points requires minimum of n of 3 at each time point. If 6 in each arm, only 2 time points allowed!
MMC, drug, sterile water, 30 day outcome	Sterile water provides baseline MMC gold standard More n numbers	Earlier time points missing, which may miss changes in the inflammatory process. i.e. sterile water may show greater inflammation at an earlier time point, as tissue remodeling likely to be significant by day 30. Conversely if implant disappears before day 30 any particulate effect may be missed. Remodeling in the sterile water group will most likely result in significantly less inflammation than around implant at 30 day time point. Difficult to make comparison therefore. Bleb survival interpretation affected by spacer.
MMC, drug, sterile water, histology at multiple time points	More n numbers Sterile water a useful gauge for the effect of surgery	No spacer comparison for bleb survival or to show anti-scarring effect of drug compared to spacer.
MMC, Ethylcellulose spacer, drug, 30 day outcome	More n numbers particulate effect of ethylcellulose useful comparison for histology	No baseline comparison – therefore any early scarring in the wound healing process related purely to surgical intervention missed
MMC, Ethylcellulose spacer, drug, multiple time points	More n numbers particulate effect of ethylcellulose useful comparison for histology	No baseline comparison – therefore any early scarring in the wound healing process related purely to surgical intervention missed

Table 2-6 Treatment groups (for left eyes, during glaucoma filtration surgery; right eyes are untreated and unoperated)

Treatment Group	Pharmaceutical Treatment
A n = 16	One 2 mm (1 mg presumed) pure ilomastat tablet coated with polymer provided by Mike Driver (Vertellus)
B n = 10	MMC (0.2 mg / mL) applied perioperatively for 3 minutes
C n = 10	Water sponge (sterile water applied in the same way as MMC in 'C')

2.8.1 Histology 6th in vivo

Thirty-six eyes (30 operated and 6 un-operated controls) were harvested and fixed with 10% neutral formaldehyde. The whole of the eye was processed without removing the filtration tube. The processing and embedding were planned to be the same as in previous experiments, however due to breakdown of the processor this was not possible (please see start of 6th *in vivo* results section).

2.9 Investigation into inducing raised intraocular pressure to be used a measure of success in vivo

Six rabbits were used (n = 3) in each arm to investigate the potential to induce ocular hypertension (Table 2-7). All treatments were applied to the left eye. The right eye did not receive any treatment during the study and serves as the un-operated control.

Magnetic beads, approximately 100 mcg (Bangs laboratories) were washed in 70% ethanol and resuspended in 0.5 mls sterile PBS, then aliquoted into an eppendorf.

Table 2-7 Experimental arms to investigate induction of ocular hypertension.

A	Magnetic bead injection into the anterior chamber (sterilisation prior to injection by washing in 50% aqueous ethanol and rinsing with sterile PBS)
B	Cross linked hyaluronic acid injection into the anterior chamber

2.9.1 Surgical technique

An MVR blade was used to create a paracentesis and an insulin needle (30 gauge) attached to an empty 1 ml syringe advanced into the anterior chamber. Approximately 100 ul of aqueous was drawn off. A second syringe and needle containing either suspended beads or Healaflow® was advanced into the anterior chamber and 100 ul of contents injected into the angle. If magnetic beads were injected a ring magnet of 16 mm diameter (Supermagnete, Germany) was used to pull the beads into the angle. Chloramphenicol ointment was instilled at the end of surgery.

2.10 Appendix

2.10.1 Equipment and Materials

2.10.2 Tablet fabrication

- Punch and die set designed and supplied by Holland Ltd, Nottingham, UK.
- Ilomastat obtained from Ryss Inc, Union City, California,
- Dexamethasone obtained from Sigma, UK,
- Healaflow purchased from Vision Matrix, Harrogate, UK.
- Revanesse Ultra, source of cross-linked hyaluronic acid was purchased from Boston Medical Group Limited, London, UK.
- Polymer from Alex Seifalian (UCL/Royal Free), London, UK.
- Sterilization of tablets by Isotron UK, 25 KGY, Swindon, UK.
- Micrometer screw gauge produced by Mituoto, Japan.

Medication

- Ketamine (Ketaset) 35mg/kg
- EMLA Cream
- Xylazine (Rompun) 5mg/kg
- Povidone iodine
- Chloramphenicol
- Viscotears
- Sterile water

Surgical Instruments

- 7-0 silk corneal traction suture (Johnson and Johnson Ethicon W817)
- Microvitreoretinal Blade (20 Gauge) (Beckton Dickinson, Oxford, UK)

- 22-gauge, 25-mm IV cannula (Venflon 2: Beckton Dickinson, Oxford, UK)

- 10-O Nylon suture attached to needle (B/V 100-4; ethicon) Alcon 8065 198001, Camberley, Surrey.
- Orange needles (25 gauge)
- Syringes (5ml)
- PVA surgical Spears (Altomed Spears)
- Needle holder
- Heavy scissors
- Speculum
- Toothed forceps
- Artery forceps
- Non- toothed forceps
- Spring scissors/Wescotts
- Vannas scissors
- Suture tiers
- Corneal light shield
- Tonovet, Finland

Termination Medication (Schedule 1)

- Thiopenthal Sodium (pentothal)

Histology

- 4% Formaldehyde
- Insulin 1ml syringes
- Vials 2ml
- Histology Slides

Beads

-magnetic polymer coated beads 8 um COMPEL™ Magnetic COOH modified (Bang's laboratory, Indiana)

Randomisation – using random number generator (http://www.randomizer.org)

Chapter 3 Results

3.1 Excipientless pure ilomastat tissue-tablet implant studies

3.1.1 Ilomastat implant in vitro experiments

Cells that are instrumental in the process of scarring can be inhibited reversibly by using the MMPi ilomastat. As ilomastat has a low aqueous solubility (Parkinson et al., 2012) and a low concentration of therapeutic efficacy (Daniels et al., 2003) it was hypothesised that an excipientless implant of appropriate size and mass would release drug at a therapeutic concentration over the wound-healing period after glaucoma surgery. The aim of these experiments was to see whether it was possible to formulate and determine release kinetics from 1, 2 and 3 mm implants in vitro and the duration a therapeutic concentration that could be maintained. The range of sizes was chosen according to what seemed reasonable to insert into the sub conjunctival space. Investigations also examined the pharmacokinetics of two implants together to see if the therapeutic concentration could be prolonged. Furthermore the rate of dissolution was looked at to discover whether drug concentration in the surrounding fluid was sufficient to limit the rate of release of drug from the implant. The compression pressure for implant formulation needed to be great enough to create a stable implant that would not fragment, but not so high as to impair release significantly (as found in pressure experiments performed by S Georgoulas).

3.1.1.1 Implant fabrication

Compression forces of 0.4, 2 and 4 bars were required for stable implants of 1, 2 and 3 mm diameter respectively. The source of ilomastat used (Ryss) consisted of particles that poured easily into the press and resulted in less than 10% loss between weighing the powder and the resulting implant. After fabrication, a number of implants were then re-weighed and those that were greater than 10% either side of the target weight were discarded. The approximate yield was 60%. To ensure fabrication was as consistent as possible one supplier was chosen. Batch numbers were recorded and tried to be kept as constant as feasible.

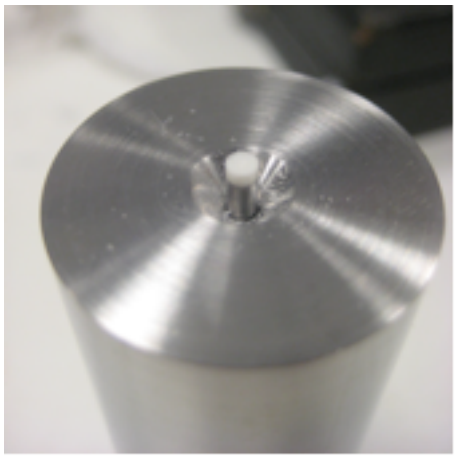

Figure 3-1 A 2 mm ilomastat implant after fabrication of 2 mg mass

Table 3-1 Ilomastat tissue-tablet implant dimensions. A range of 10% either side of the target was chosen as acceptable

Implant diameter (mm)	Implant height (mm)	Implant mass (mg)	Tablet surface area (mm2)	Tablet volume (mm3)
1	0.55	0.5	3.3	0.43
2	0.35	1	8.5	1.09
3	0.35	2	17.4	2.47

3.1.1.2 Release profile of implants

3.1.1.2.1 Release from a 3 mm implant

Single 3 mm implants released ilomastat at concentration above 10 μM (14.3+/- 25 μM to 170 +/- 44 μM) for 23 days (Figure 3-2 and Figure 3-3). The mean maximum concentration (Cmax) released was 170 μM with a cumulative release of 81%.

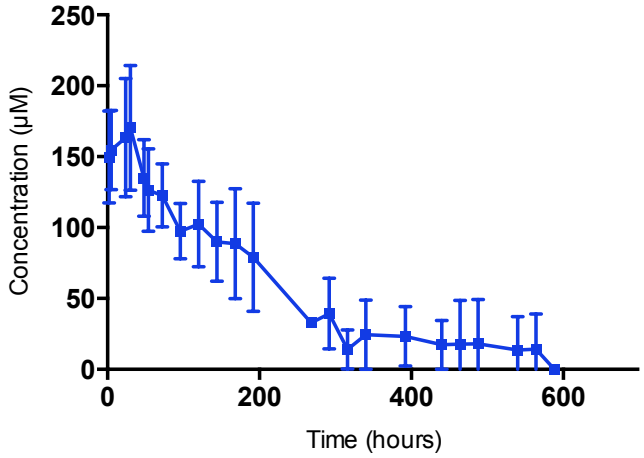

Figure 3-2 Ilomastat concentration of elutent from single 3 mm ilomastat implants over time. A concentration of ilomastat of > 10 μM was maintained for 23 days. Number of implants n = 3. Implant masses were 1.7, 1.4, and 1.9 mg (mean 1.7 mg). PBS flow rate was 2 μl / minute. The data displays mean +/- standard deviation.

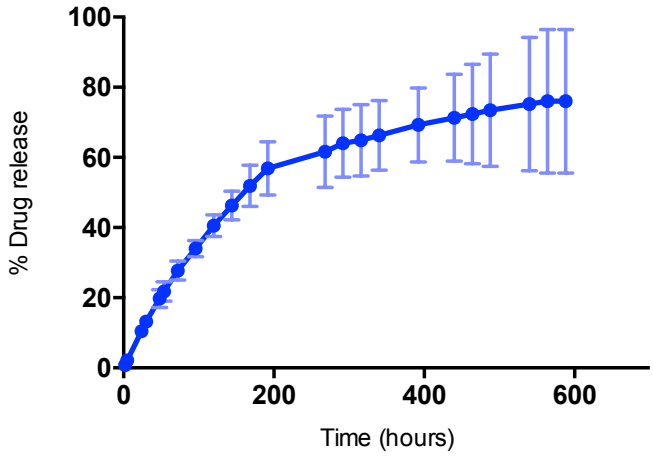

Figure 3-3 Cumulative mean percentage release of the 3 mm implant. The release was determined by calculating the quantity of drug present in the elutent at each time point. The data displays mean +/- standard deviation.

3.1.1.2.2 Release from a 2 mm implant

Single 2 mm implants of ilomastat released drug at a concentration that was maintained above 10 μM for 12 days (Figure 3-4 Figure 3-5). The mean Cmax released was found to be 100 μM.

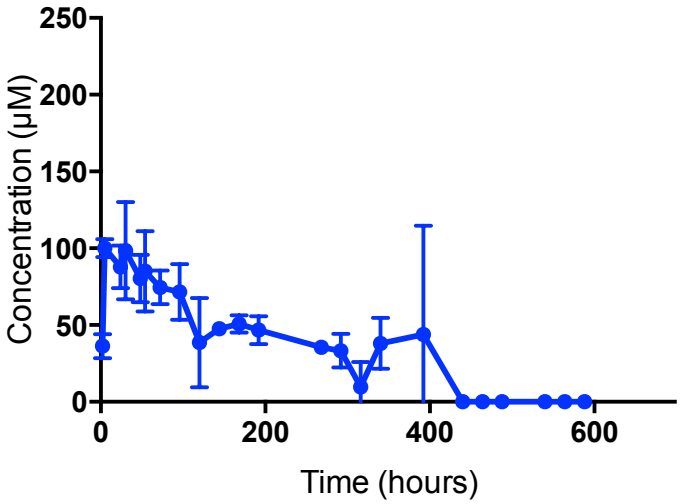

Figure 3-4. Ilomastat concentration of elutent from single 2 mm ilomastat implants with time. A mean concentration of ilomastat of > 10 μM was maintained for over 12 days. Number of implants n = 3. Implant masses were 1.1, 1.1 and 1.29 mg (mean 1.16 mg). Error bars indicate standard deviation.

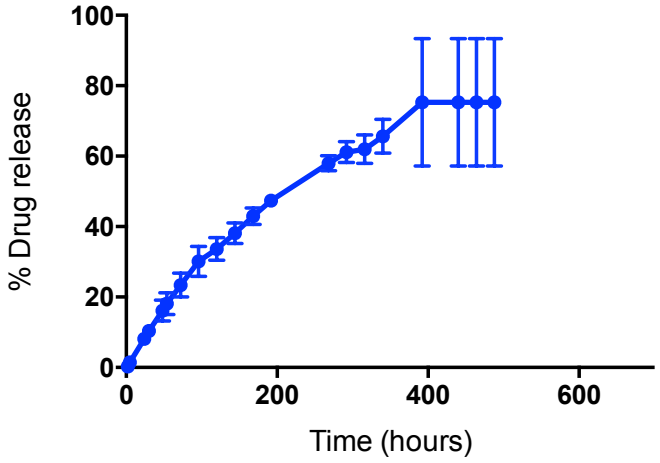

Figure 3-5 Cumulative mean percentage release of the 2 mm ilomastat implants with time. The release was determined by calculating the quantity of drug present in the elutent at each time point. Error bars indicate standard deviation.

3.1.1.2.3 Release from a 1 mm implant

The release of ilomastat from 1 mm implants maintained a drug concentration of > 10 μM for 19 days. The mean Cmax of drug released was 68 μM. One rig released a much higher concentration of drug for the time-points between 22 and 43 hours.

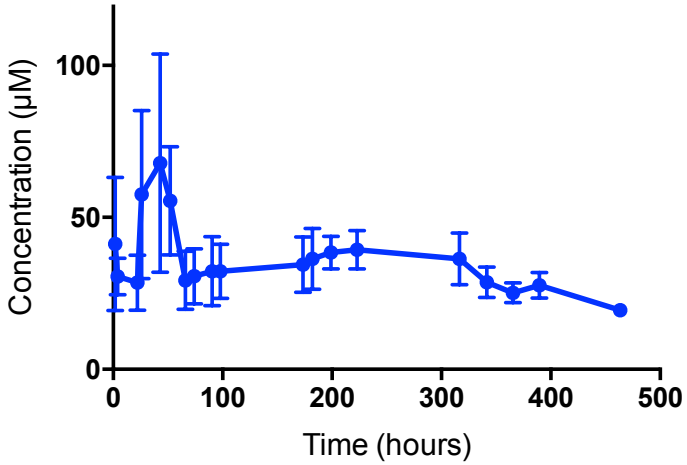

Figure 3-6 . Ilomastat concentration of elutent from single 1 mm ilomastat implants with time. A concentration of ilomastat of > 10 μM was maintained for over 19 days. Number of implants n = 3. Implant masses were 0.45, 0.65 and 0.50 mg (mean 0.53 mg). Error bars indicate standard deviation.

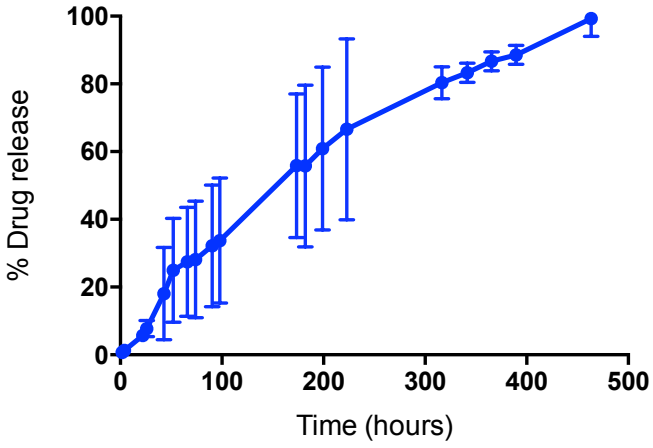

Figure 3-7 Cumulative mean percentage release of the 1 mm ilomastat implants with time. The release was determined by calculating the quantity of drug present in the elutent at each time point. The rate of release was slower than the larger implants.

3.1.1.3 Two 2 mm implant release

A concentration of > 10 µM was maintained for 11 days when the rigs contained 2 implants implants (Figure 3-8 and

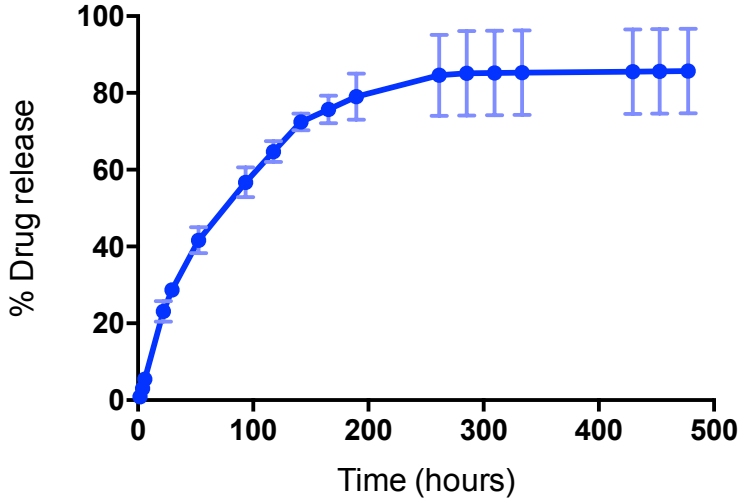

Figure 3-9). The total masses of implants in each rig were 1.52 mg, 1.5 mg and 1.53 mg. The Cmax was 288 µM.

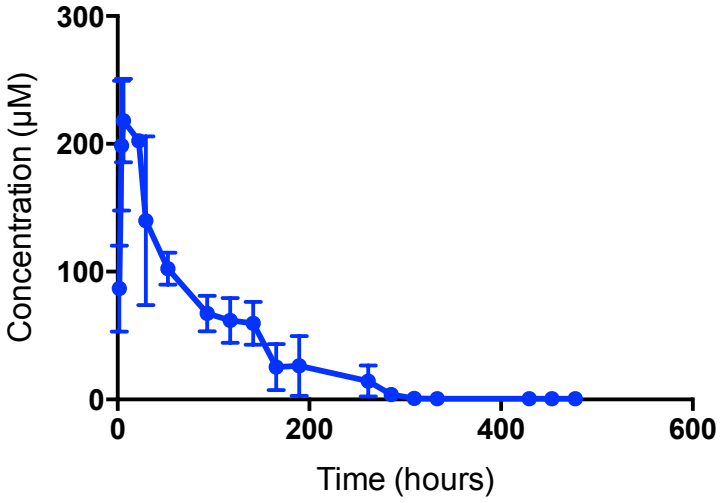

Figure 3-8 Ilomastat concentration of elutent from two 2 mm ilomastat implants with time. A concentration of ilomastat of > 10 µM was maintained for over 12 days. Number of implants n = 6. Implant masses in each rig were: 0.76 and 0.77 mg, 0.73 and 0.77 mg, 0.7 and 0.82 mg (mean total 1.52 mg). Error bars indicate standard deviation.

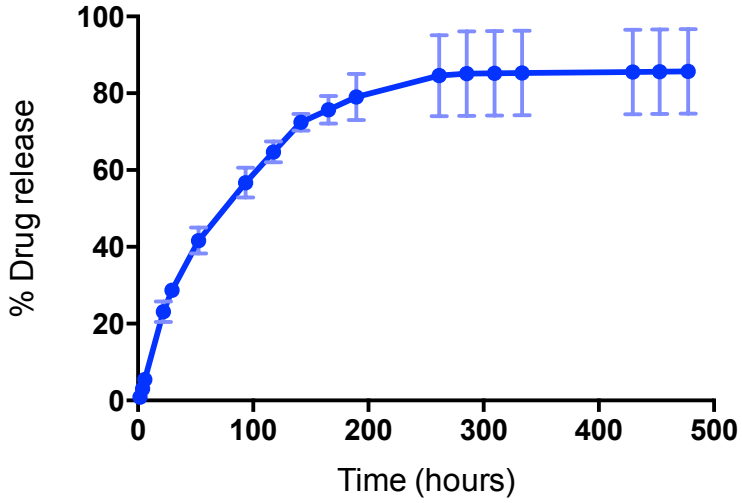

Figure 3-9 Cumulative mean percentage release of two 2 mm ilomastat implants with time. Rig n = 3. The release was determined by calculating the quantity of drug present in the elutent at each time point. Approximately 80% of calculated drug was released, attributable to loss during handling and systematic error in weighing.

3.1.1.4 Determining release of drug from at a slower flow rate

Aqueous production can be impaired after ocular surgery or in certain pathological states, and therefore the kinetics of release at a lower flow rate was investigated. Implants of 2 mm diameter were exposed to PBS flow rates of 1 μl / minute (Figure 3-10 and Figure 3-11). The mean maximum concentration reached was 206 μM. A concentration of > 10 μM was maintained for 22 days. All implants had dissolved by 40 days at the 1μl / minute flow rate.

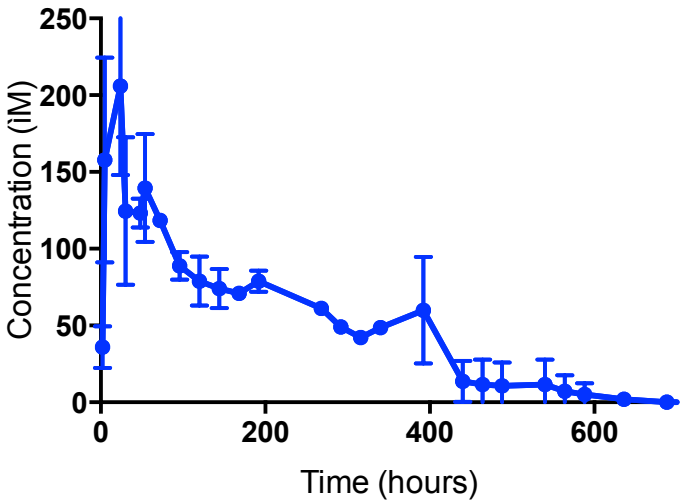

Figure 3-10 Concentration of ilomastat released over time with a flow rate of 1 µl / minute. Single 2 mm implants of 1.1 mg, 1.15 mg and 1.3 mg (mean 1.18 mg) were exposed to a flow rate of 1 µl / minute PBS.

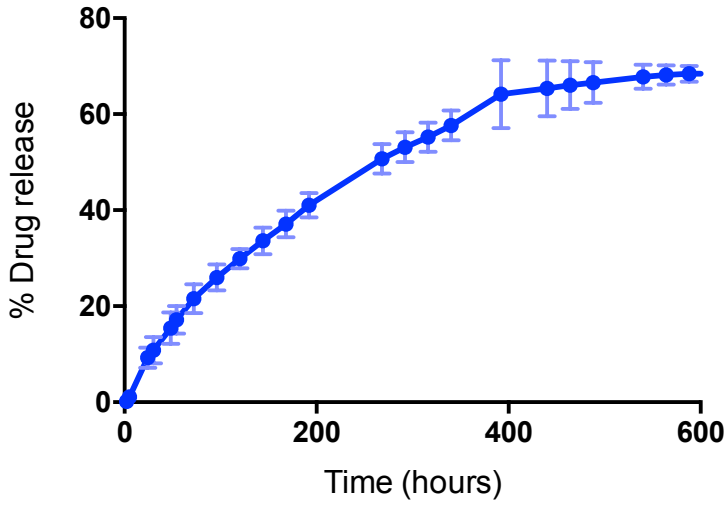

Figure 3-11 Mean cumulative percentage release profile of 2 mm ilomastat implants exposed to a flow rate of 1 µl / minute PBS. Drug loss during handling may be the cause of release not reaching 100%. Alternatively the speed of flow at lower flow rates may be less accurately controlled.

3.1.1.5 Discussion

Single implants in this *in vitro* rig model exposed to a fluid flow rate similar to aqueous production have the potential to maintain a therapeutic concentration of ilomastat (> 10 μM) for a range of between 12 to 26 days. The low solubility of the drug means that toxicity is unlikely. At lower flow rates the duration of drug release is extended and the concentration of drug increased. This in theory would be of benefit, as reduced aqueous production and flow occurs commonly in situations where there is heightened inflammation.

The results can be related to the Noyes Whitney equation (1897), which determines the factors involved in the drug dissolution from a single spherical drug particle:

$dm/dt = k^{-}{}_1A*(Cs-Ct)/h$

where the mass transfer (dm/dt) of a substance is a function of the surface area (A) available for dissolution, the diffusion coefficient of the compound in the dissolution media (k_1), the boundary layer thickness of surrounding fluid (h), and the difference between the concentration of the drug's saturated solubility, (Cs) and its concentration in the bulk of the dissolution media at time t (Ct).

It is therefore unsurprising that in the single implant experiments the larger the individual implant surface area, the greater the mass transfer and the greater the peak concentration seen in solution. That two 2 mm implants increased the mass transfer by two fold and did not increase the duration of the drug release indicates that Ct is not increasing significantly to affect release for the 2 mm implant, and that dissolution is operating in "sink" conditions. Conversely at the lower flow rate the duration of drug release is extended approximately two fold indicating "non-sink" conditions are occurring and the presence of drug in solution is limiting release. In this situation the surrounding solubilised drug has a greater effect on the mass transfer of the drug into solution than the solubility. This effect may be illustrated by using a dialysis membrane to determine drug release from colloidal formulations (Washington, 2009).

The kinetics of drug release for the 1 mm implants are of interest. According to the above equation, as the surface area is less, the mass transfer should be correspondingly less than the larger implants. This is presuming that the implant is a solid piece of drug and does not fragment into particulates. For example, the 1 mm implant has a surface area that is 0.39 of the 2 mm implant (if the surface area of the implant bases are excluded, as these are in contact with the rig surface, the factor then is 0.47). The peak concentration seen with the 1 mm implant was 69 μM, whereas with the 2 mm implant it was 100 μM. However if the time-points between minutes 22 and 43 are excluded due to the spurious results from one rig – which may have been caused by an air bubble in the apparatus affecting flow or particulate release from the implant - the concentration released for the 1 mm implant is between 30 and 40 μM, which correlates well with what is expected from the equation.

That the release duration for the 1 mm implant is at least 1.6 times than that of the 2 mm is contrary to initial expectations; the release duration of the 2 mm implant was less than the 3 mm. However the surface area to mass ratio for the 1 mm implant is less (6.6 mm^2 / mg) than the surface area to mass ratio of the 2 mm implant (8.5 mm^2 / mg) or the 3 mm implant (8.5 mm^2 / mg). It is likely that this ratio will also change as the implants dissolve with time, and that the disparity between ratios will increase as more dissolution occurs from the superior surface of the larger diameter discs. Furthermore, the larger discs are more fragile and over time were more likely to develop cracks, which would also contribute to an increased surface area.

The boundary layer is another factor in the equation that is difficult to determine in this model. Velocity of fluid flow will affect the pattern of flow as will the diameter of the implant (Sumer and Fredsøe, 2006). These variables combined with the kinematic viscosity of water (viscosity / density) enable a ‘Reynolds’ number to be determined. At the slow flow rate in this experiment it is unlikely that eddies will form, however to be sure a detailed examination using dye and flow in a more easily visualised environment, is required.

$$Re = DU/v$$

Figure 3-12 The Reynolds number for fluid flow behaviour around a cylinder. This factor is determined by the diameter of the cylinder (D), flow velocity (U), and kinematic viscosity (v). For a cylinder of diameter 3 mm (3 x 10^{-3} m) and a chamber where the fluid flow is presumed to be 2 ul min-1 through a cross sectional area of approximately 25 mm^2 gives 0.8 $mmmin^{-1}$ (1.3 x 10^{-5} m/s) Presuming water has a kinematic viscosity of 0.7 x 10^{-6} m^2/s at 35 ^{0}C, the Reynolds number is 3.9 x 10^{-2}.

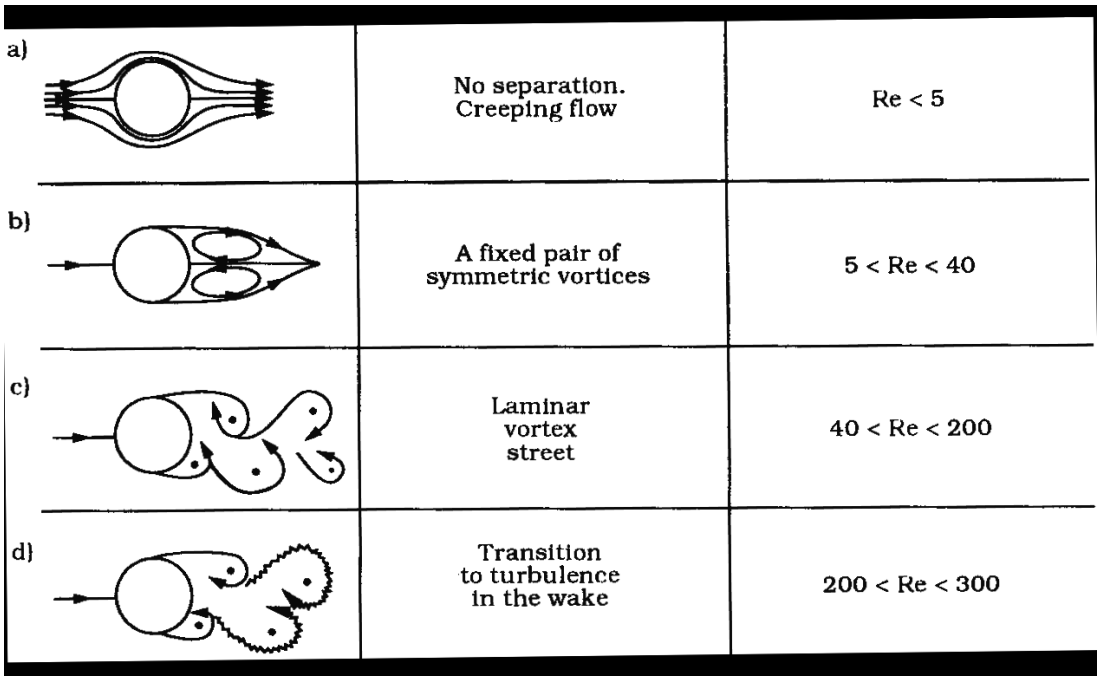

Figure 3-13. The pattern of fluid flow for different Reynolds numbers. Adapted from (Sumer and Fredsøe, 2006). With a Reynolds number of 3.9 x 10^{-2} turbulent flow is unlikely.

Intrinsic and proportional to the size of the implants are the systematic errors in their formulation and measurement of release. The mass balance used, although one of the most accurate in the School of Pharmacy, still has an error of +/- 0.25 mg (personal communication Dr Simon Gaisford). Thus smaller implants have a greater error in measurement than larger ones. This is not just related to the capability of the balance itself, but also to the effect of air currents – just having the air-conditioning on can increase the mass of an implant by 0.2 mg! (Shown by repeating measurements in different environments) Efforts were made to limit airflow and even perform the measurements in a closed environment. Nonetheless this error and loss of drug in

handling is the most likely reason for the release not reaching 100%. Further repeat experiments would be able to determine the variability of error, but some idea of the variability is indicated by the error bars. That residual drug did not remain in the rig at the end of experiments was shown by opening the chambers and finding no visible pellets.

The measurement of low concentrations of drug using HPLC is also susceptible to increased error. As measurements approach the baseline the variability increases. This is reflected in the graphs of concentration vs time for the implant release, and is one reason for the error bars increasing as the drug concentration falls.

The rig provides valuable information regarding drug dissolution in an open flow system. It shows that theoretically an implant could release drug at a therapeutic concentration in a sustained manner, without the spikes and troughs that might be seen with an injection. It does, however have limitations as a model of the bleb. The chamber is 200 mm^3 whereas a functioning bleb has been estimated to have a fluid volume as small as 6.3 mm^3 using optical coherence tomography (Kawana et al., 2009). The aqueous fluid drains through one exit point as opposed to diffusely through episcleral veins. However key factors involved in the pharmacokinetics of release are the interplay of cells and tissue around the implant, and to be able to test this an experimental animal model is required.

3.1.2 *In vivo* results of pure ilomastat 2 mm and 1 mm implants

As the results of the previous drug release experiments found that therapeutic concentrations of ilomastat could be maintained for 12 to 23 days, it was postulated that 1 mm and 2 mm implants would prolong the success of glaucoma filtration surgery in the in vivo model, and that the lower dose implant might be sufficient. The details of the procedure are outlined in the methods. In brief however, a fornix based conjunctival flap is raised and a 23 gauge cannula (blue) is inserted into the anterior chamber. The tube is trimmed and fixed with nylon, an implant placed if appropriate for the treatment arm, and the conjunctiva replaced and sutured with nylon. The visible presence of a bleb is taken as the main observational outcome measure of success, because unlike patients with glaucoma, rabbits have a low intraocular pressure before surgery.

The four treatment arms in a 28 rabbit experiment (n = 7 in each arm) were:

1) Ilomastat implant1 mm (0.5 mg)

2) Ilomastat implant 2 mm (1 mg)

3) Mitomycin C 0.2 mg/ml for 3 minutes perioperatively

4) Ethylcellulose implant 2 mm (1 mg) negative control

The rabbits treated with ilomastat 1 mm (0.5 mg) tablets all had blebs that survived to day 30. The ilomastat 2 mm (1 mg) tablet group all survived until day 27, and 6 (86%) survived to day 30. Of the MMC treated group, 2 (29%) had successful blebs at day 30. Three (43%) of the ethylcellulose tablet treated group had successful blebs at day 30. The differences in bleb survival between the ilomastat 1mm and ethylcellulose groups, and the ilomastat 1 mm and MMC groups, were statistically significant (log rank $P = 0.0221$ and 0.0078 respectively). Representative images at different time points are shown in Figure 3-12 and Figure 3-13. The Kaplan Meier curve in Figure 3-14 illustrates bleb survival.

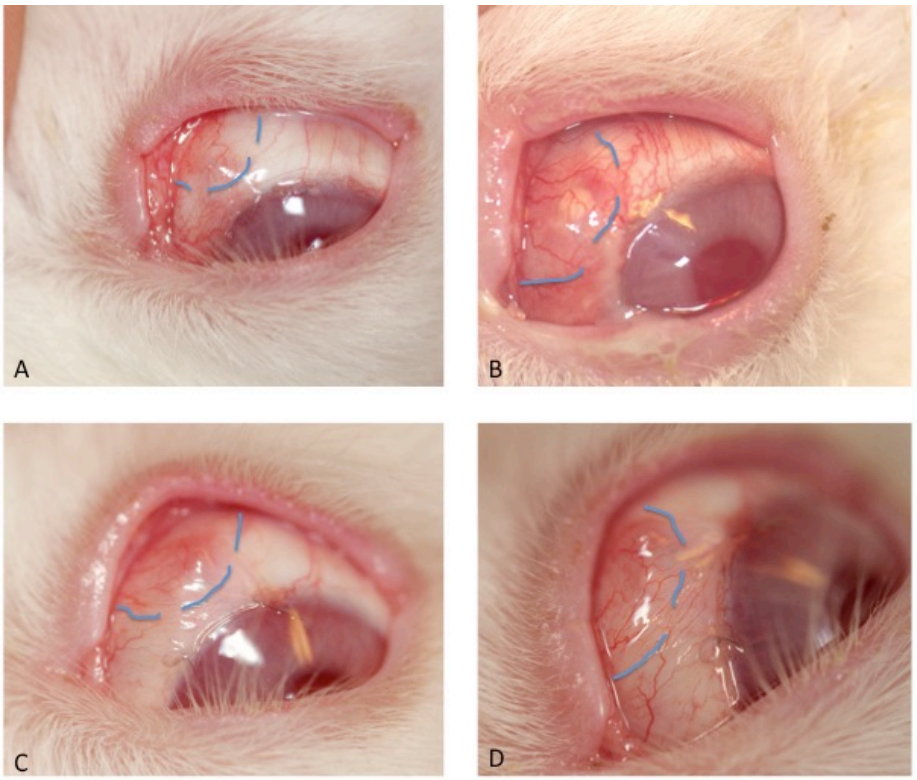

Figure 3-14 Representative photos of blebs at day 15 for each of the treatments: ilomastat 1 mm (A), ilomastat 2 mm (B), ethylcellulose 2 mm (C), and mitomycin C (D). All eyes have the appearance of a functional bleb at this stage. Blue line indicates bleb margins.

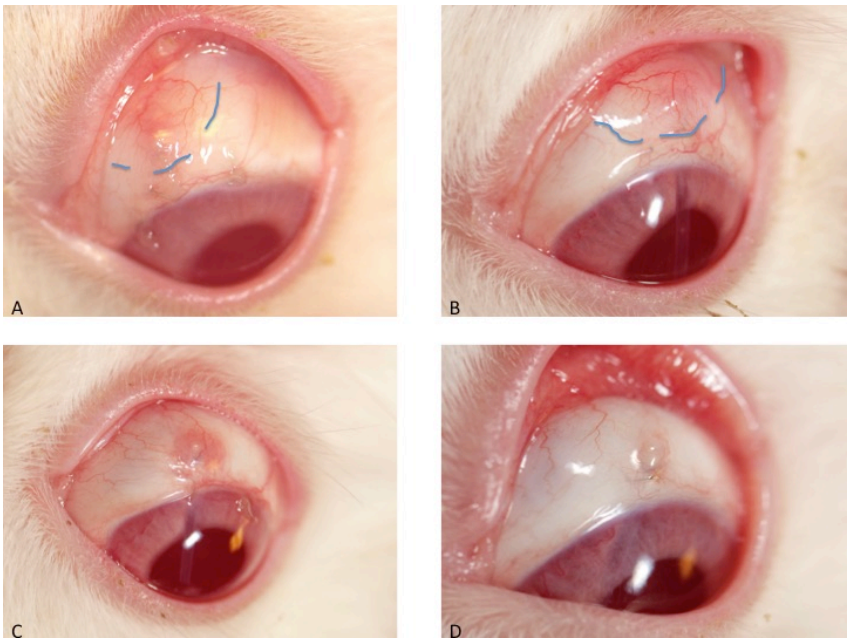

Figure 3-15 Representative photos of blebs at day 30 for each of the treatments: ilomastat 1 mm (A), ilomastat 2 mm (B), ethylcellulose 2 mm (C), and mitomycin C (D). The appearance of blebs A and B indicate functionality and those of C and D as failures. Blue line indicates bleb margins.

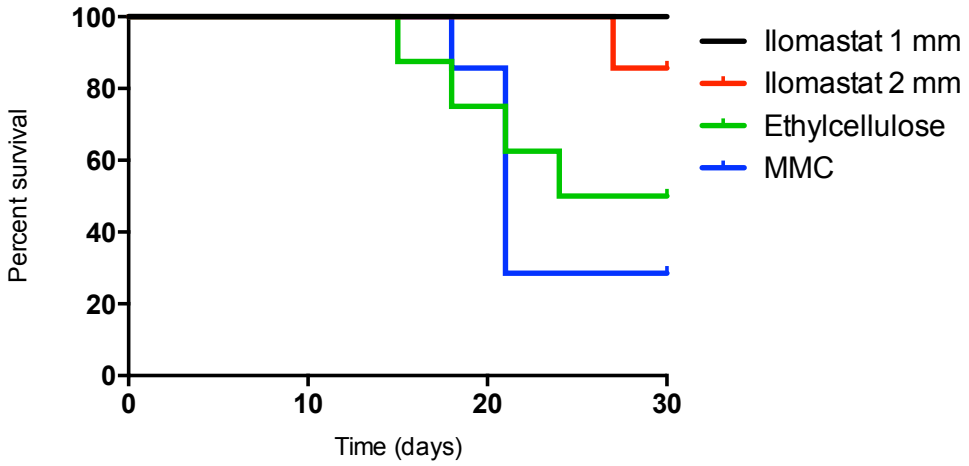

Figure 3-16 Bleb survival of the four groups. The ilomastat 1 mm and ilomastat 2 mm implants survived significantly longer than the ethylcellulose and MMC groups (log rank $P = 0.0221$ and 0.0078 respectively).

The bleb surface area of all four groups decreased with time (Figure 3-17). Those blebs with the ilomastat 1 mm and ilomastat 2 mm implants maintained blebs of greater surface area than those of either MMC or ethylcellulose after day 9 to day 30.

A Kruskal-Wallis test showed that there was a significant difference between bleb surface areas at day 30 ($H(3) = 10.2$, $P = 0.017$). Compared to ethylcellulose using Dunn's multiple comparison test there was no significant difference for individual treatments.

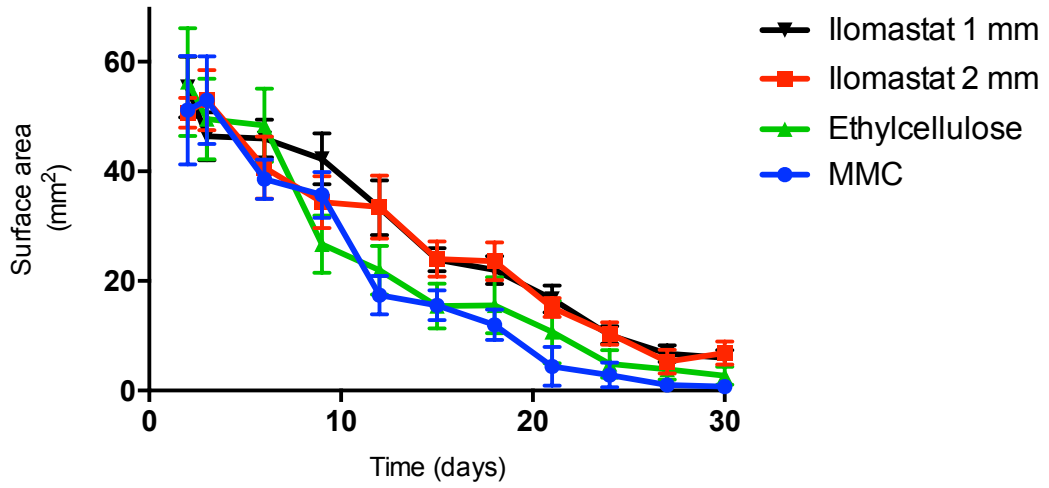

Figure 3-17 Mean bleb surface area over time for the four groups. The ilomastat 1 mm and 2 mm maintained a greater mean bleb surface area than MMC and ethylcellulose from day 12. Error bars indicate standard error.

A Kruskal-Wallis test revealed that there was a significant difference between bleb heights at day 30 (H (3) = 10.2, P = 0.017). Inspection of the group means using Dunn's multiple comparison test showed no significant difference, however, compared to the ethylcellulose treated group.

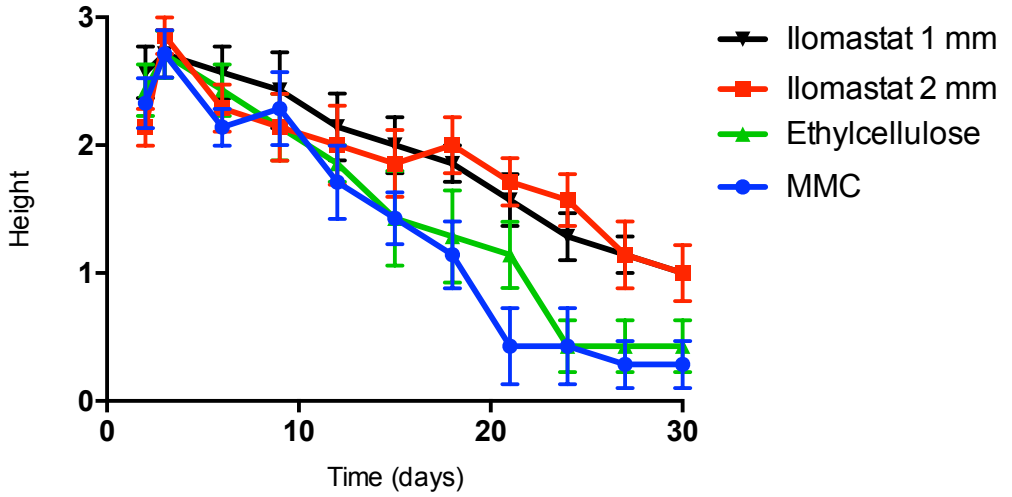

Figure 3-18 Mean bleb height of the 4 groups over time. Bleb height was graded as 0, flat; 1, shallow/formed; 2, elevated < 2 mm and 3, high > 2 mm. From day 12 the ilomastat 1 mm and ilomastat 2 mm treated animals maintained higher blebs than the ethylcellulose or MMC treated animals. Error bars indicate standard error.

There was a fall in mean IOP early after surgery. This was followed by a post-operative return to base line for all groups (Figure 3-19). There was no significant difference between treatment groups. An attempt was made to reduce variability in IOP between rabbits that might be unrelated to the surgery by subtracting the IOP of the operated eye from the IOP of the unoperated eye. No increased discernible difference was found. n

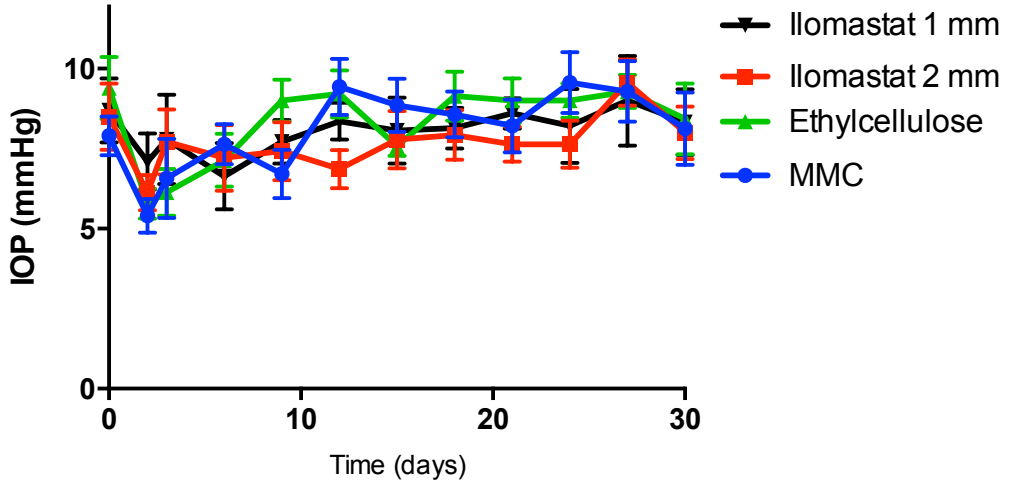

Figure 3-19 Mean IOP of operated eye with time. There was an initial fall in IOP followed by a return to baseline for all groups. Error bars indicate standard error.

The vascularity of the blebs in the initial stages of the experiment showed no difference between the four groups. After 15 days the ilomastat 1 mm and 2 mm blebs appeared to have comparatively greater vascularity than the ethylcellulose or MMC blebs (Figure 3-20). A Kruskal-Wallis test showed that there was a significant difference between vascularity at day 30 (H (3) = 9.1, P = 0.028). Compared to ethylcellulose using Dunn's multiple comparison test there was no significant difference for other treatment arms.

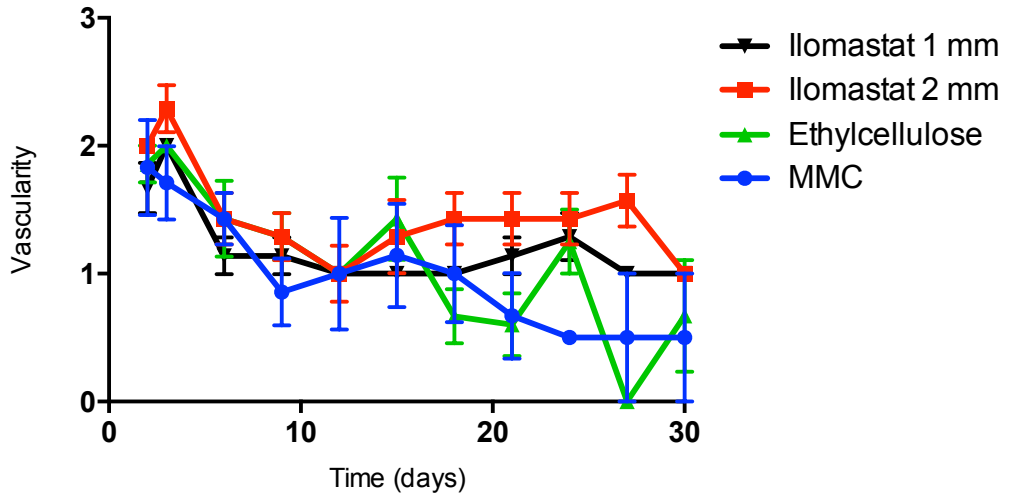

Figure 3-20 Bleb vascularity post surgery. The vascularity was graded as 0 = avascular, 1 = normal, 2 = hyperaemic, 3 = very hyperaemic. Data displays blebs at each time point as mean and standard error of the mean.

There was no significant inflammation in any of the four treatment groups.

3.1.2.1 Bleb dissection

After termination 3 blebs from each group (chosen at random) were dissected to investigate implant presence and obtain a macroscopic view. Implants were found in all ethylcellulose, ilomastat 1mm and ilomastat 2 mm treated blebs. The surrounding tissue was found to have bands of adhesions to the implants, and dissection led to their fragmentation.

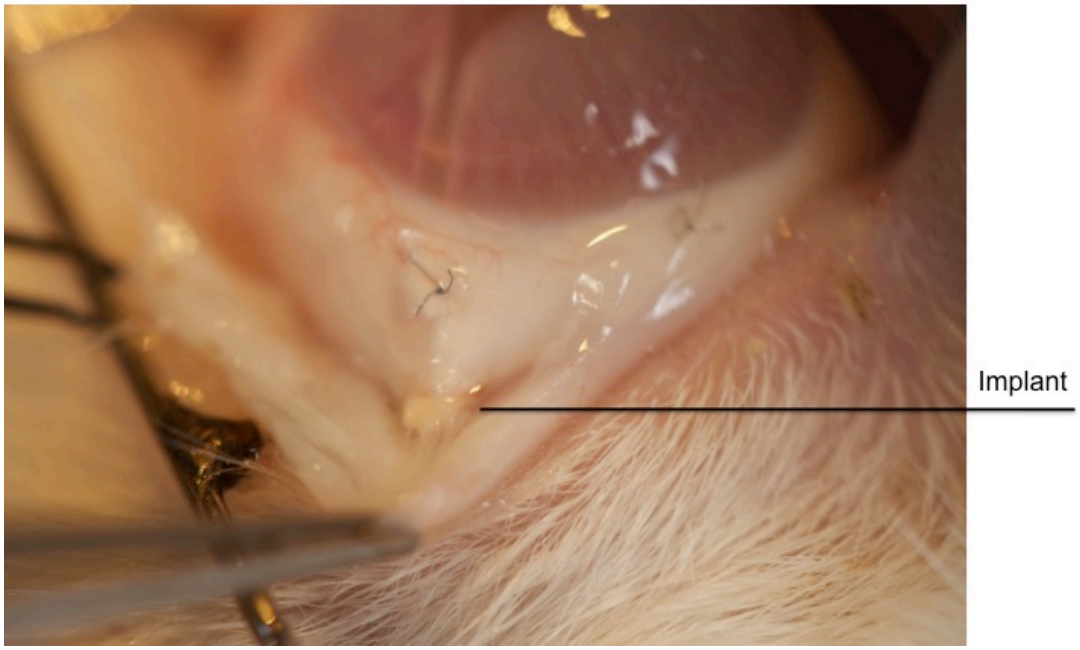

Figure 3-21 Bleb dissection of an ilomastat 1 mm treated bleb. Adhesive bands can be seen between the implant and the reflected conjunctiva.

3.1.2.2 Histology

Ethylcellulose treated blebs showed some thickening of the conjunctiva with a mild increase in cellularity in comparison to the unoperated conjunctiva (Figure 3-20, Figure 3-21). Posterior to the tube site revealed implant remnants in three of four blebs. Infiltrating the remnants was a network of inflammatory cells, and surrounding the remnants were closely compacted fibroblasts.

The MMC blebs showed some evidence of increased cellularity and conjunctival thickening with some epithelial disruption (Figure 3-24). Increased inflammation was seen associated with the tube site and suture material in a similar way to the other three experimental arms.

Figure 3-22 Haematoxylin and Eosin of an Unoperated eye. Legends: Co: cornea, T: drainage tube, S: sclera. Scale bar 1 mm. A loosely packed conjunctiva was seen.

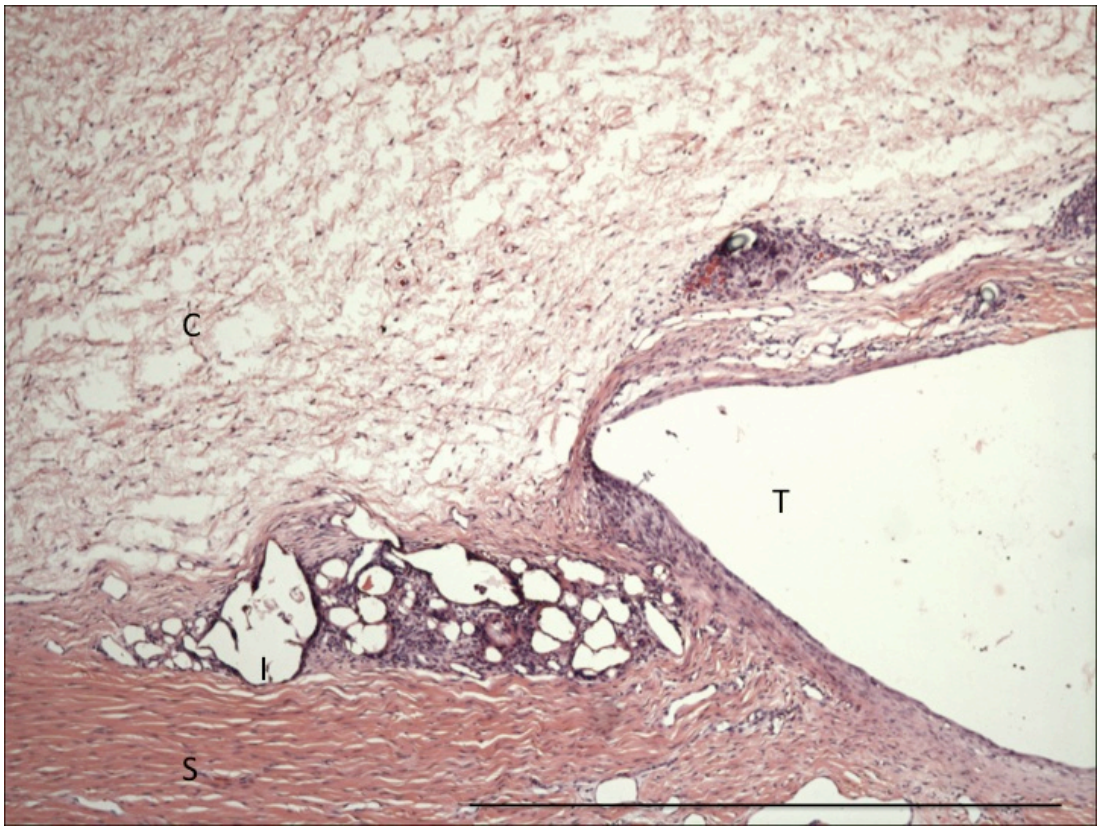

Figure 3-23 Ethylcellulose treated bleb. Legends: C: conjunctiva, T: drainage tube, S: sclera, I: implant remnants. Scale bar 1 mm. A mildly thickened conjunctiva with increased cellularity was seen with Haematoxylin and Eosin stain. Where implant remnants were seen they were interlaced with inflammatory cells. Surrounding the remnants were fibroblasts.

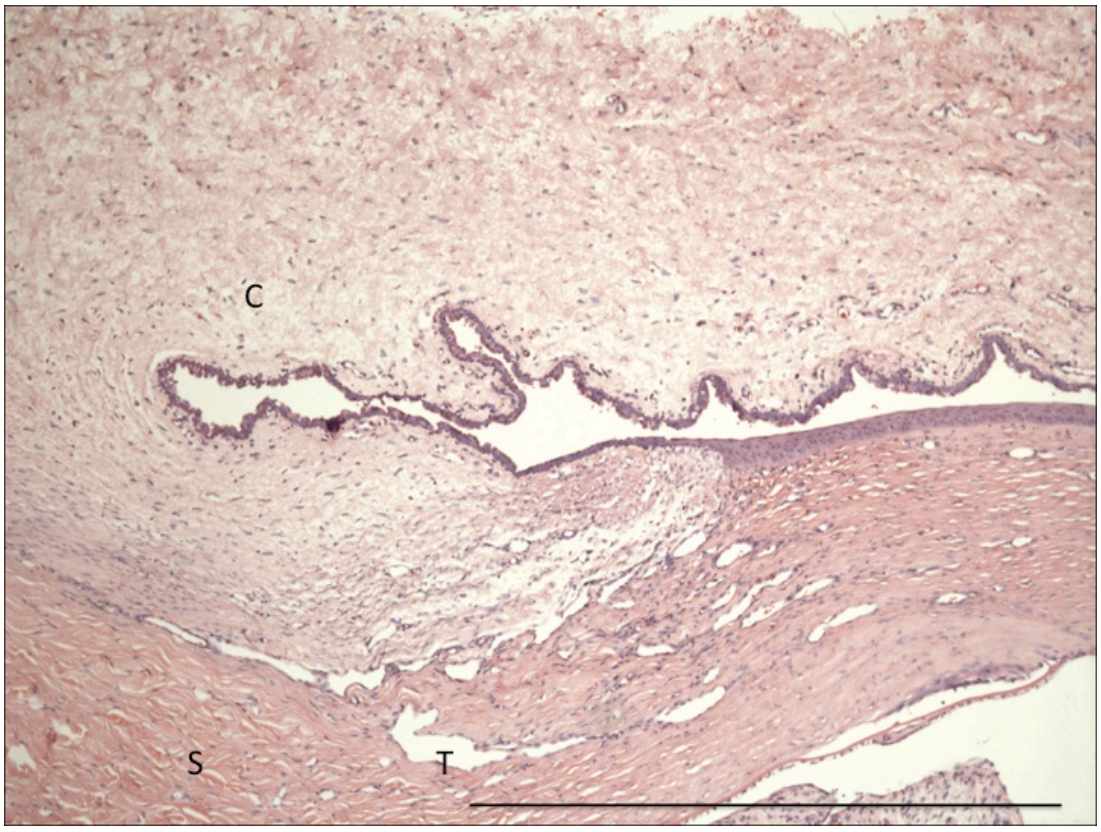

Figure 3-24 MMC treated bleb. Legends: C; Conjunctiva, T: drainage tube, S: sclera. Scale bar 1 mm. Increased cellularity and thickening of the conjunctiva was seen with Haematoxylin and Eosin staining. Increased inflammation was seen associated with the tube location.

The ilomastat 1 mm and 2 mm blebs showed evidence of immune cell infiltration and greater conjunctival thickening around the surgical site with more protein deposition. In the 2 mm treatment arm refractile pink implant remnants were seen in two of the four blebs and the edge of an inflammatory capsule in the remaining 2 blebs. In the 1 mm treatment arm an implant remnant was seen in one of four blebs and the edge of an inflammatory capsule in one other bleb. Where implant remnants were seen there was an associated dense halo of surrounding inflammatory cells (Figure 3-25, Figure 3-26). Adjacent to the remnant were seen neutrophils, and macrophages with eosinophilic granular cytoplasm. More peripherally the predominant cells appeared to be smaller, with densely staining nuclei and little cytoplasm, consistent with lymphocytes. More peripheral still were closely compacted fibroblasts.

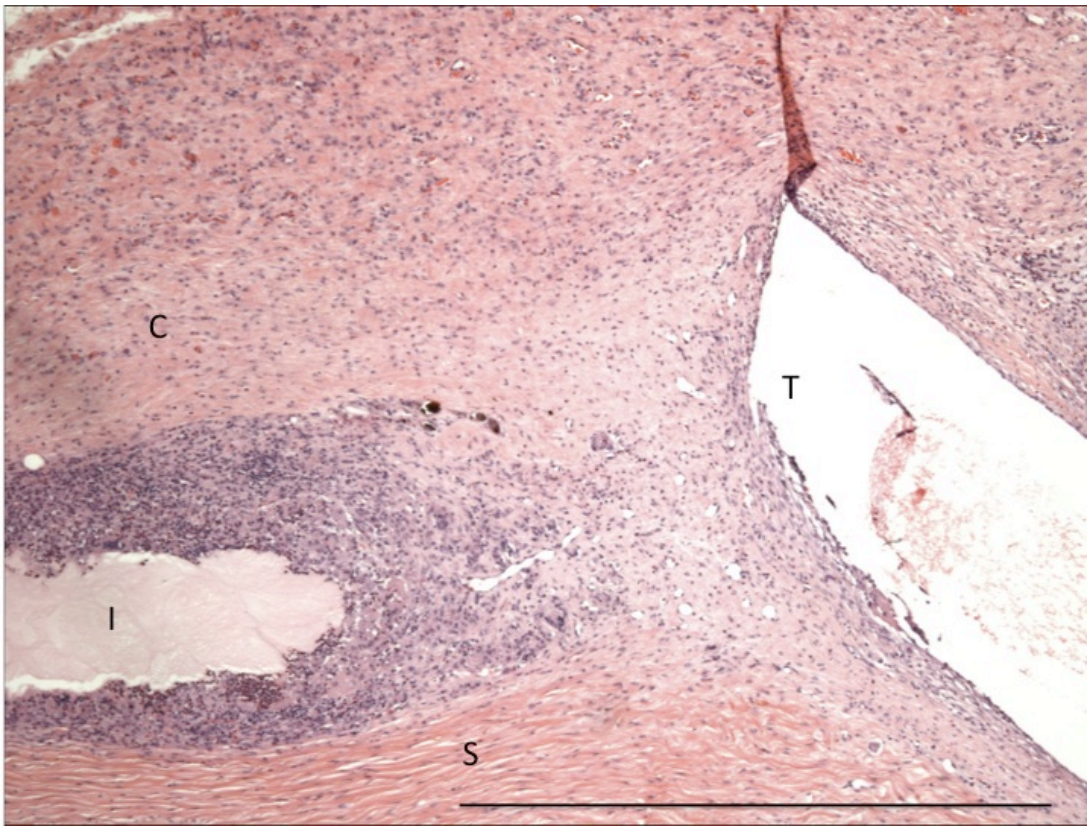

Figure 3-25 Ilomastat 2 mm treated bleb. Legends: C: conjunctiva, T: drainage tube, S: sclera, I: implant remnants. Scale bar 1 mm. A purple halo of immune cells was seen surrounding the implant with Haematoxylin and Eosin staining. Amongst those cells seen were neutrophils, macrophages and a smaller number of eosinophils

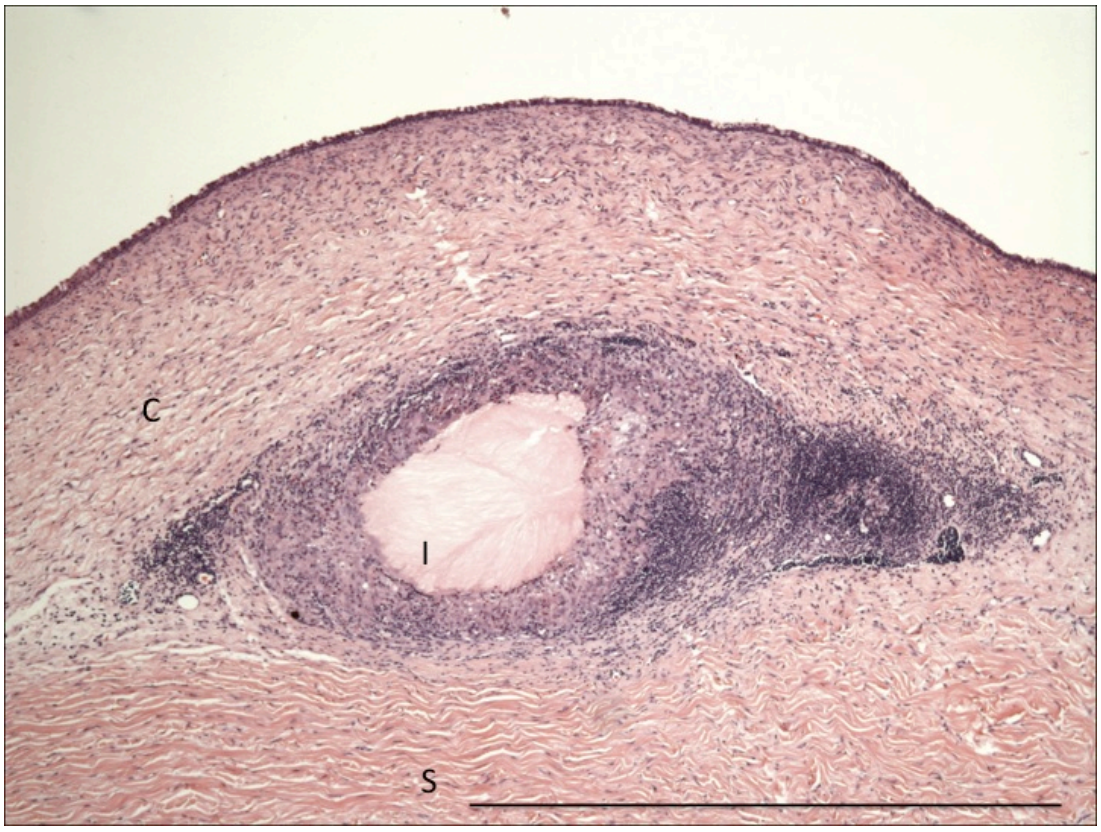

Figure 3-26 Ilomastat 1 mm treated bleb. Legends: C: conjunctiva, S: sclera, I: implant remnants. Scale bar 1 mm. A purple halo of immune cells was seen surrounding the implant with Haematoxylin and Eosin staining.

Picrosirius red staining for collagen revealed increased collagen deposition in the ilomastat 2 mm, ilomastat 1 mm, and ethylcellulose arms associated with the implant remnants (Figure 3-27).

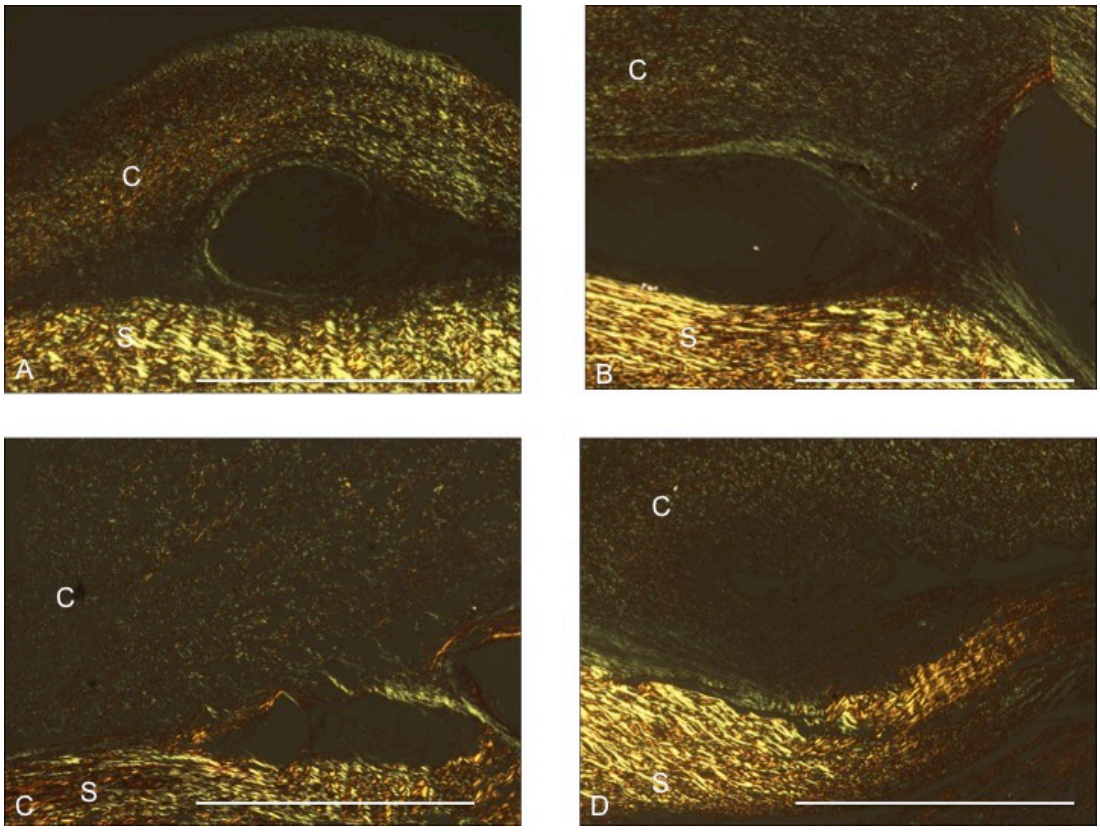

Figure 3-27 Picrosirius red staining of the four treatment arms: ilomastat 1 mm (A), ilomastat 2 mm (B), ethylcellulose (C) and MMC (D). Legends: S: sclera, C: conjunctiva. Scale bar 1 mm. A greater density of staining in the conjunctiva was seen associated with the ilomastat 1 mm and ilomastat 2 mm treatment arms with most concentration associated with implant remnants.

3.1.3 Discussion

The results of this in vivo study lead to conflicting conclusions. Both the ilomastat 1 mm and 2 mm implants appear to prolong the clinical observational parameter of bleb survival, a parameter used in other studies (Cordeiro et al., 1997; Wong et al., 2003; Wong et al., 2005), compared to either ethylcellulose or MMC. However there was a relative increase in inflammation and scarring seen in the ilomastat implant treated blebs. Indeed the ilomastat implants themselves were associated with the greatest amount of inflammatory infiltrate, with many macrophages, lymphocytes and eosinophils.

Ilomastat has been proven to inhibit fibroblast mediated contraction in collagen gels (Daniels et al., 2003). Multiple postoperative injections have promoted bleb survival

in the same animal model as used in this experiment accompanied by a significant reduction in scarring and inflammation (Wong et al., 2003; Wong et al., 2005). Ilomastat also showed promise as an anti-inflammatory drug for corneal ulcers following experiments that proved that it would inhibit inflammatory cell infiltration in rabbit corneas after alkali exposure (Galardy et al., 1994).

A drug is only active, however, if it is in solution form. In solution it is able to occupy the binding sites of its target enzyme or other molecule, and exert its effect. The above examples used ilomastat in solution form either as an injection using the solvent dimethyl sulphoxide (DMSO) (Wong et al., 2003; Wong et al., 2005) or as a topical droplet (Galardy et al., 1994).

Two deductions can be made from this experiment's histological observations:

1) The inactive solid state ilomastat is stimulatory to the immune system.

2) Any active solubilised ilomastat is insufficient to dampen this immune response.

Solid particulate matter is well known to cause an immune response. In the acute inflammation stages this response consists predominantly of neutrophil recruitment and infiltration. These cells are limited in their ability to reconstitute the proteases needed to eliminate pathogens, and if a foreign material persists, recruitment of macrophages in great numbers occurs during the stages of chronic inflammation. Although the macrophage has a much greater appetite for ingestion – it is capable of ingesting particles of more than its own size (Cannon and Swanson, 1992) – larger particles cause the macrophages to "wall off" the stimulus and contain it in a foreign body granuloma. For example, fragments of cotton retained from gauze used in surgery can cause a significant foreign body reaction, similar to seen in this experiment (Parmar and Sharr, 1999). In the conjunctiva this has been explicitly demonstrated by the retention of particles of methylcellulose sponge, and is the reason why most surgeons now use polyvinyl alcohol sponges (Al-Shahwan and Edward, 2005).

It may not simply be the presence of a solid that excites a foreign body reaction. Examining crystalline ilomastat under the scanning electron microscope also reveals a spiky appearance with multiple rods of up to 200 μM long and compression into an implant does not eliminate this appearance. It is possible that micro movements of the implant could lead to adjacent tissue trauma stimulating the immune response. It is believed that failure of glaucoma drainage devices due to scarring is enhanced by micromovements (Jacob et al., 1998). How smooth or how rough a surface is will also determine the overall surface area, fluid flow behaviour and drug dissolution (Jimenez, 2004). A completely smooth surface will not necessarily yield the least friction for fluid passing over it however, as demonstrated by the America's cup yacht 'Stars and Stripes', whose hull was coated in fine grooves to ease passage of water. In 1987 she beat Kookaburra III to regain the America's cup (Demeis, 1988).

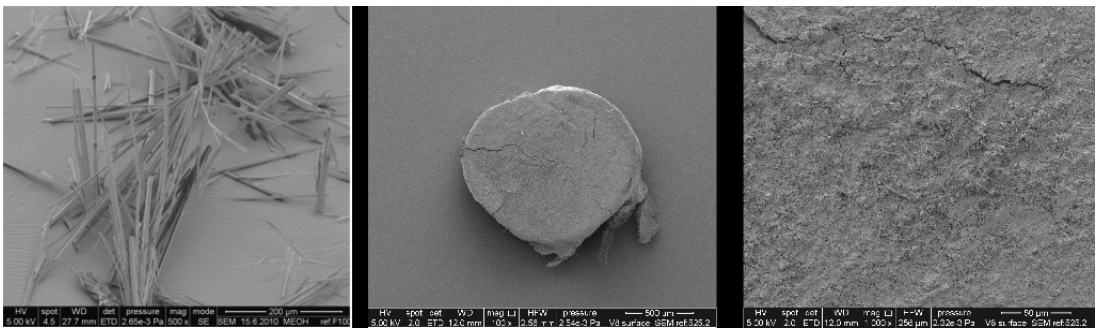

Figure 3-28 Scanning electron micrograph of crystalline ilomastat and ilomastat implant. The crystals in the compressed drug are shorter, but the surface remains irregular. Magnifications left to right 500 x, 100 x, 1000 x.

An example of where spiky material causes "frustrated phagocytosis" is seen in asbestosis (Kamp and Weitzman, 1999; Shin and Firminger, 1973). Particles of insoluble crystalline hydrated silicates, particularly if in an amphibole form (straight, brittle fibres), are able to penetrate deep into the lungs. Too small to be impacted in the upper airways and removed by the mucociliary elevator, the fibres enter and lodge themselves in the alveoli. Macrophages fail to ingest the fibres and cause continuing inflammation through the release of reactive oxygen species.

Figure 3-29 Macrophage attempting to ingest an asbestos fibre. Adapted from (Environmental, 2011)

Tackling host tissue response is a major challenge in the development of implantable drug delivery devices throughout the body (Zhang et al., 2013). Inevitably cell – implant surface interaction results in the adhesion of non-specific proteins that coat the implant. These too could encourage macrophage activation (Ratner, 2002). The same frustrated phagocytosis then occurs and a key result is the sealing off of the implant in a collagenous bag preventing drug release (Figure 3-30), destroying any correlation seen with the in vitro results.

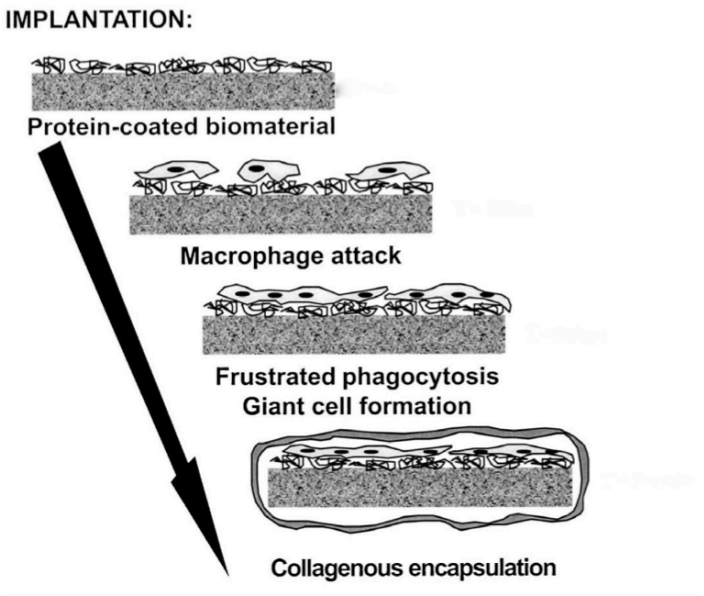

Figure 3-30 Foreign body encapsulation of an implant. Adapted from (Ratner, 2002).

Evidence for a collagenous capsule surrounding the ilomastat implants not only comes from the histology but also from the macroscopic appearance of the dissected blebs. If the ilomastat implants had been walled off effectively, so no drug was available to diffuse out, this would explain the second deduction: that "there was insufficient free ilomastat to provide an anti-inflammatory or anti-scarring effect." Removing samples of bleb fluid throughout the experiment would have provided an indication of the free ilomastat concentration, but would have necessitated a surgical intervention and possible interference in the wound healing response.

Bleb survival was found not only to be greater in the ilomastat treatment arms than the MMC arm but also in the ethylcellulose arm. Although there was no significant difference between them, that both the positive and negative control achieved a similar success rate is of interest. Bleb survival is an outcome based on the observation of the "presence" of a bleb. Ethylcellulose implants were chosen as a negative control: the implants were of a similar dimension to the ilomastat 2 mm arm and had supposedly no biological activity, thereby attempting to account for a "spacer" effect that the physical presence of an implant might have. Assuming that ethylcellulose does indeed have no biological activity, this leads to the conclusion that this spacer effect can promote bleb survival in this model to the same degree as MMC. A further negative control to examine the spacer effect would be to use water

instead of MMC. When the experiment was designed however it was believed that there would be little implant at the end, that the ilomastat implant was efficacious and that the question to be asked was whether size was important.

These findings therefore also raise the question of how much bleb survival reflects drug efficacy as an anti-scarring treatment. The surface area and bleb height followed the pattern of bleb survival, however there was almost an exponential decay. This would suggest that there is more than just the physical presence of an implant playing a role in outcome, or else one would see more of an initial fall in bleb surface area and height, followed by a plateau.

Three factors would each seem to be able to play an independent role in contributing to the appearance of a bleb in this rabbit model: 1) the presence of aqueous, 2) the spacer effect of the implant, 3) the conjunctival thickening associated with inflammation and scarring, i.e. a more fibrotic response to the implant could increase "bleb size" and prolong "bleb survival". It is not possible to quantify the contribution of each in this experiment, but in the MMC treatment arm one can be sure that there is no contribution from a spacer effect. In the ilomastat arms there is clearly a contribution from the spacer effect and from conjunctival thickening from fibrosis – seen in histology, the macroscopic appearance of bleb dissection, and the level of vascularity.

Is there another possible end point that could be used? In clinical trials of patients with glaucoma, the endpoint most commonly used for evaluating surgical or medical efficacy is intraocular pressure. With humans it is a measurement that is easy to perform, is reproducible and takes minimal time, as compared to visual field testing which is frequently unreliable, and optic nerve head appearance, which is dependant on subjective interpretation. The rabbits in this experiment however do not have glaucoma, and their baseline intraocular pressure is low. There is considerable variability not only between animals, but also between measurements taken at different times in the same animal. Easily startled, a tense rabbit was found to increase its IOP. The exact mechanism is not known, however an analogy is that of a patient squeezing in anticipation of having tonometry performed or a weight lifter who increases his IOP through a valsalva manoeuvre (Vieira et al., 2006). Previous

studies have found difficulty in using IOP as an outcome measure in rabbits (Miller et al., 1989).

These results show that the ilomastat implants are able to promote the longevity of the appearance of a bleb, but encapsulation with a foreign body reaction occurs around the implants that will distort the interpretation of a functional bleb. This is the first time to our knowledge that encapsulation with a foreign body reaction around a pure drug anti-inflammatory / anti-scarring implant has been described at a histological level. Other reports of implants are also not without a foreign body reaction, however they use carriers such as the Ozurdex implant (SooHoo et al., 2012). It is likely that in the blebs where implant remnants were not seen, this was due to the section being in a different plane, rather than complete dissolution in that bleb due to the strength of foreign body response in those blebs where remnants were seen.

If the foreign body reaction we are seeing is associated with negligible drug release after surgery, would enhanced dissolution with drug in solution negate this effect? From the Noyes Whitney equation and the previous in vitro experiment this might be achieved by increasing the implant surface area. Using a 3 mm diameter implant would increase the surface area by more than two times that of the 2 mm implant. Another method of increasing drug release would be to expose the implant to more aqueous fluid at the time of surgery. By ensuring adequate hydration there would be a greater solvent volume, and in theory more active drug in solution. A third way to increase MMPi in solution would be to use a more soluble MMPi. Perhaps by making the implant less abrasive there would be less physical stimulation of surrounding tissue. This might be achieved by surrounding the implant in a cushion of polymer such as hyaluronic acid, or indeed combining the drug with hyaluronic acid to create a rapidly hydrating gel: this would also have the added bonus of enhancing surface area and drug release.

In the next experiment these hypotheses were tested. An excipient would enable the drug material to be more easily distributed, and alter its dissolution characteristics. It also allows the implant to have a greater cohesiveness. Unfortunately, however this project had a patent attached that stipulated that the implant should be excipientless.

The lines of investigation UCL partners who were directing this MRC funded project were keen to retain this “intellectual property”. Therefore lines of investigation that satisfied this were the avenues of first choice.

3.2 Optimisation of MMPi release to reduce inflammatory response: a second *in vivo* study

As pure 1 mm and 2 mm ilomastat implants resulted in a significant foreign body reaction to the undissolved material and questionable drug release, it was postulated that increasing dissolution or altering implant tissue surface interaction might reduce this significantly.

A pilot in vivo study of 7 arms was constructed to examine the effect on histology after GFS of increasing the amount of active drug in solution, whilst reducing the antagonistic particulate effect:

1) The effect of increasing the surface area for dissolution was examined using a larger 3 mm ilomastat implant (n = 3). This diameter was chosen because it was the same as the diameter of implants in the pilot study (Georgoulas, 2010).

2) In the second arm 3 mm implants were used as in '1' but excess PBS was also applied to irrigate the implant at the time of surgery to see whether hyper-hydration would encourage dissolution and reduce the foreign body response (n = 3).

3) Smaller (1 mm) implants with excess PBS applied at the time of surgery were used in the 3rd treatment arm (n = 3). The hypothesis was that reducing the aggravating particulate might, with hyper-hydration, result in less foreign body reaction.

4) It was postulated that cushioning the implant might reduce tissue abrasion and inflammation: The ilomastat implant (1 mm) was placed within a soft cushion of high molecular weight gel hyaluronic acid (Healon 5)(n = 2). Healon 5 is a high molecular weight hyaluronic acid gel suspension commonly used for providing temporary structural support to the globe during ocular surgery. The advantage of this approach is that in theory there would be less abrasion from the implant sides to the surrounding conjunctival tissues, however the duration of this effect is unknown and the Healon 5 may dissipate relatively quickly.

5) An ilomastat hyaluronic acid combination implant was also created. Although outside the patent, this line of investigation combined both a method of increasing dissolution (*in vitro* release see below), and potentially reducing the abrasiveness of the implant. Visiol was selected for the in vivo, as it appeared easy to combine with an aqueous ethanol (10%) solution of ilomastat (n = 2).

6) MMPis that have a similar inhibitory profile as ilomastat but were more soluble were also investigated. Two compounds (AZ 8955 and AZ 6357) in previous *in vitro* studies had shown potential to be developed into effective anti-scarring slow-release implants (PhD thesis S. Dhingra). The compound AZ 8955 had a water solubility of more than 3 fold that of ilomastat (140 μg ml^{-1}) and was formulated into 1 mm implants (n = 2)

7) AZ 6357 has a water solubility of more than 16 fold that of ilomastat (624 μg ml^{-1}). Implants (1 mm) were formulated for the *in vivo* (n = 2).

3.2.1 *In vitro* release of ilomastat hyaluronic acid (visiol) implants

Combination implants of ilomastat and hyaluronic acid (visiol) (0.75 mg ilomastat overall mass 8.0 mg) released ilomastat over the period of 8 days (Figure 3-32). They were created by mixing a solution of aqueous ethanol containing ilomastat, and then freeze dried (see methods). The mean maximum concentration was found to be 146 μM. A sustained early release of ilomastat maintained a mean concentration ≥ 10 μM for 4 days.

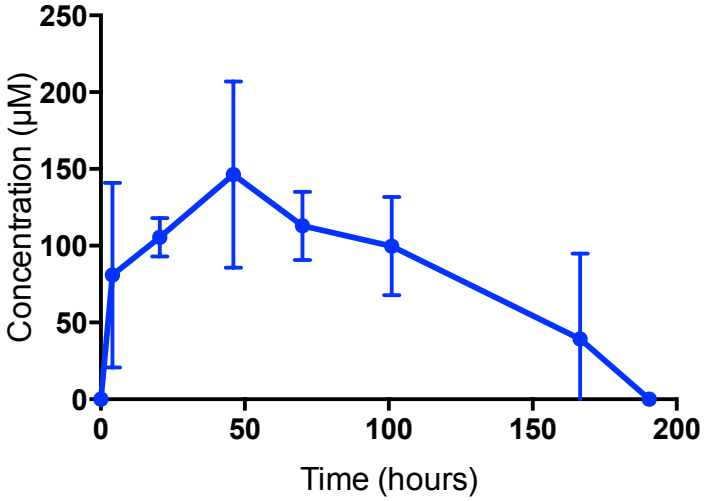

Figure 3-31 Ilomastat released from combination implants of hyaluronic acid (visiol) and ilomastat over time. A concentration of ilomastat of > 10 µM was maintained for 4 days in one rig and 7 days in the other rig.

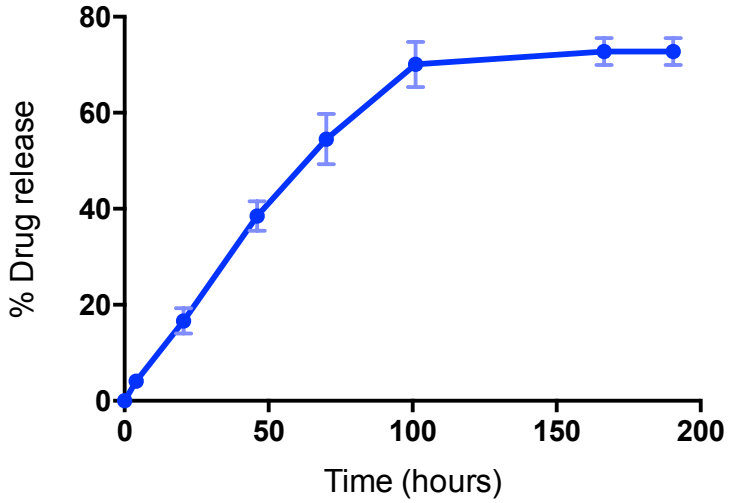

Figure 3-32 Cumulative mean percentage release of ilomastat combined with hyaluronic acid over time. The release was determined by calculating the quantity of drug present in the elutent at each time point. Again there was approximately 80% of calculated drug released, attributable to loss of drug during handling.

3.2.2 Experiment to optimise MMPi release *in vivo* results

The seven arms for the in vivo pilot study are summarised in the table below. During the formulation of the implants in this second in vivo study error occurred in the measurement of the implant masses. The overall dimensions of diameter were the same, however weights of the pre-pressed drug were confused with implant weights, and therefore it was not possible to be sure of the masses of 5 of the implants. The range of masses was between 2.1 to 3.6 mg for 3 mm implants and 0.5 to 1 mg for 1 mm implants (see methods).

Table 3-2 Treatment regimen 2nd *in vivo*. Where denoted unknown* there was doubt over the exact mass of the implant (range 2.1 – 3.6 mg for 3 mm implants and 0.5 to 1 mg for 1 mm implants).

Treatment Group	Pharmaceutical Treatment
A	3 mm (2.1mg, 3.5 mg and one unknown* mg) ilomastat implant dry
B	3 mm (3.4 mg, 3.4 mg and 3.6 mg) ilomastat implant hydrated.
C	1 mm (0.4 mg and two unknown* mg) ilomastat implant hydrated
D	1 mm (0.4 mg and two unknown* mg) ilomastat implant surrounded by approximately 0.1 mL Healon 5
E	Hyaluronic acid (Visiol) / ilomastat tablet freeze dried 3 mm; weight of the tablets 9.3 mg and 8.3 mg (0.52 and 0.46 mg Ilomastat);
F	1 mm (0.4 mg and 0.2 mg) AZ 6357 tablet hydrated
G	1 mm (0.5 mg and 0.4 mg) AZ 8955 tablet hydrated

3.2.2.1 Survival and bleb surface area

All blebs treated with pure ilomastat implants appeared to be raised until day 30 (Figure 3-33, Figure 3-34). The group of animals with 3 mm ilomastat implants that received hydration (n = 3) had a greater bleb surface area than those that received dry 3 mm implants in the initial stages of the experiment, though after day 12 there was minimal difference between the two. The animals treated with 1 mm hydrated ilomastat and 1 mm Healon 5 cushion implants retained similar surface area blebs throughout the experiment. Both of the blebs treated with an AZ 8955 implants failed at day 27. One of the blebs treated with AZ 6357 failed at day 21 and the other failed at day 27. Both of the blebs treated with the combination implant of ilomastat and Visiol failed at day 24. The surface area of the blebs treated with the AZ 8955 were consistently greater than those treated with AZ 6357 or ilomastat / Visiol. A Kruskal-Wallis test showed that there was a significant difference between bleb surface areas at day 30 (H (6) = 16.34, P = 0.012). There was no significant difference between the individual means, however, using Dunn's multiple comparison test.

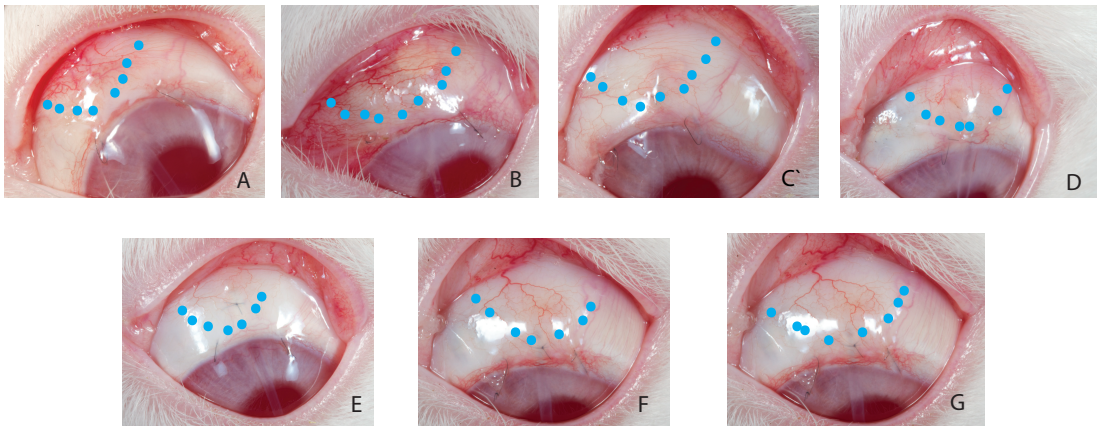

Figure 3-33 Representative photos of blebs at day 15 for each of the treatments: ilomastat 3 mm dry (A); ilomastat 3 mm hydrated (B); ilomastat 1 mm hydrated (C); ilomastat 1 mm enveloped in hyaluronic acid gel (Healon 5) (D); ilomastat in combination with hyaluronic acid (Visiol) formulated as a freeze dried implant 3 mm (E); AZ 6357 1 mm hydrated (F); AZ 8955 1 mm hydrated (G). All blebs were classed as surviving at this stage. Blue dotted line indicates bleb margins.

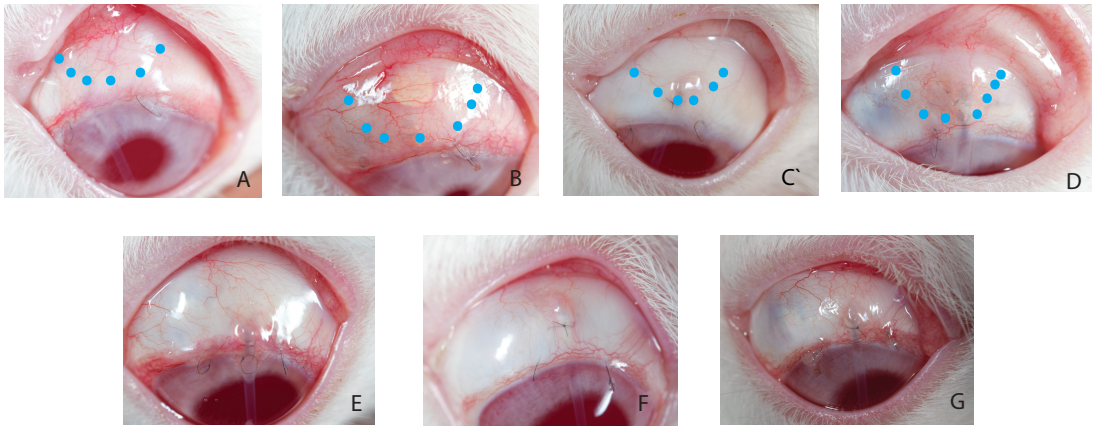

Figure 3-34 Representative photos of blebs at day 30 for each of the treatments: ilomastat 3 mm dry (A); ilomastat 3 mm hydrated (B); ilomastat 1 mm hydrated (C); ilomastat 1 mm enveloped in hyaluronic acid gel (Healon 5) (D); ilomastat in combination with hyaluronic acid (Visiol) formulated as a freeze dried implant 3 mm (E); AZ 6357 1 mm hydrated (F); AZ 8955 1 mm hydrated (G). The pure ilomastat implant treated blebs (A, B, C, D) were classed as surviving (blue dotted line indicates bleb margins) and the remainder had failed.

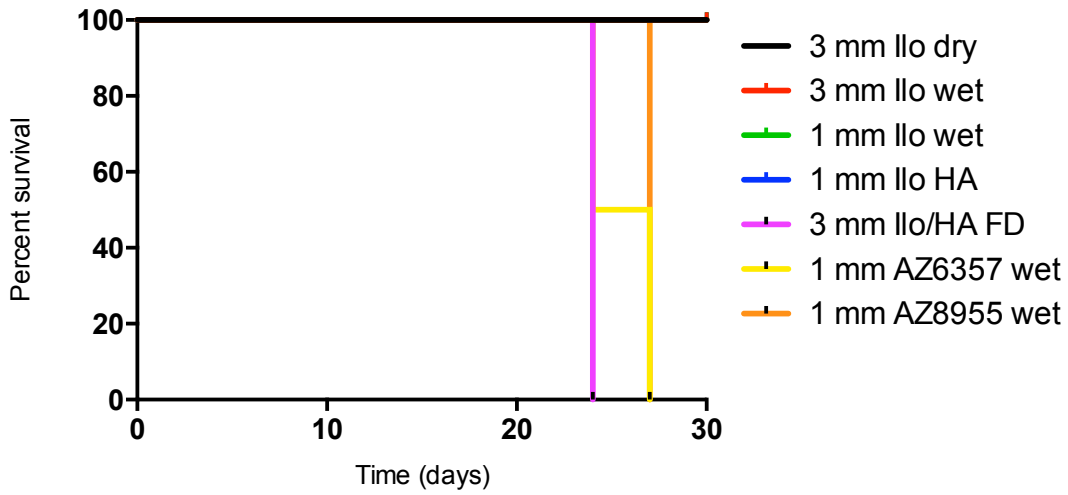

Figure 3-35 Bleb survival of the 7 different groups: ilomastat 3 mm hydrated (n = 3); ilomastat 3 mm dry (n = 3); ilomastat 1 mm hydrated (n = 3); ilomastat 1 mm enveloped in hyaluronic acid gel (Healon 5) (n = 2); ilomastat in combination with hyaluronic acid (Visiol) formulated as a freeze dried implant 3 mm (n = 2); AZ 6357 1 mm hydrated (n = 2); AZ 8955 1 mm hydrated (n = 2).

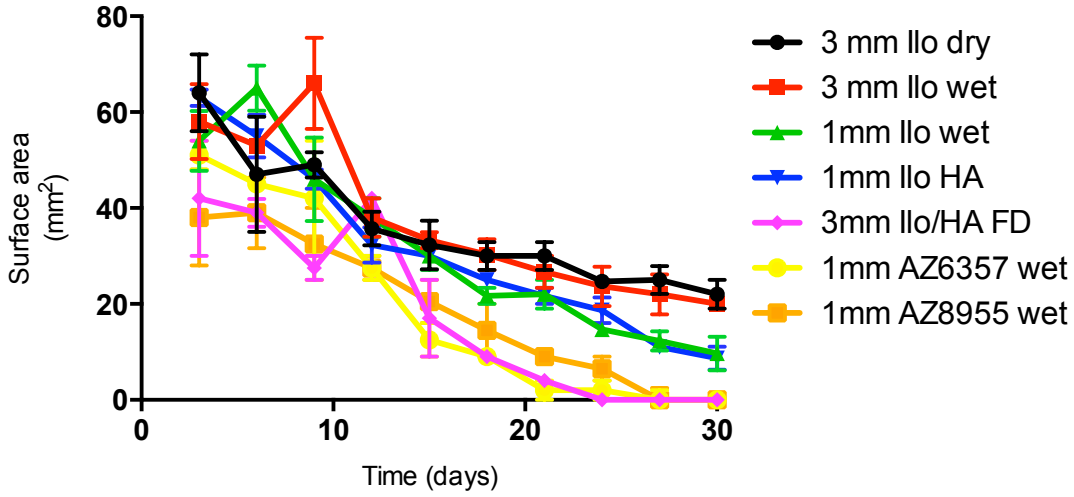

Figure 3-36 Bleb surface area for the 7 groups over time. After day 12 similar bleb surface areas were seen for rabbits treated with the hydrated 3 mm and non hydrated 3 mm pure ilomastat implants, and the hydrated 1 mm ilomastat and 1 mm ilomastat enveloped in hyaluronic acid gel (Healon 5). Error bars indicate standard error.

3.2.2.2 Bleb height

The results of the bleb height correlated with those of the surface area (Figure 3-37).

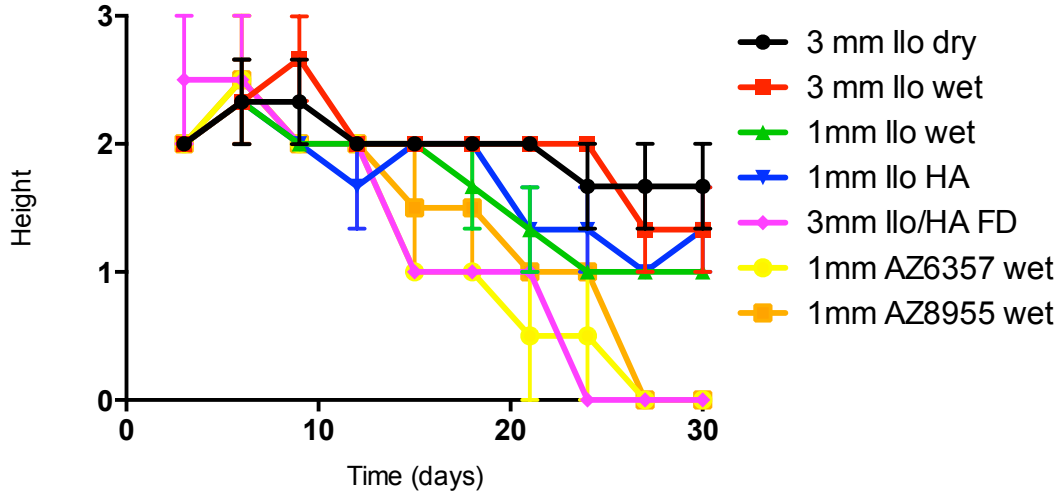

Figure 3-37 Bleb height for the 7 groups over time. Bleb height was graded as 0, flat; 1, shallow/formed; 2, elevated < 2 mm and 3, high > 2 mm. Error bars indicate standard error.

3.2.2.3 Intraocular pressure 2nd in vivo

Little difference was seen between the seven treatment arms with the exception of the ilomastat 3 mm non-hydrated arm. These rabbits maintained a lower IOP for days 12 and 15 (Figure 3-38).

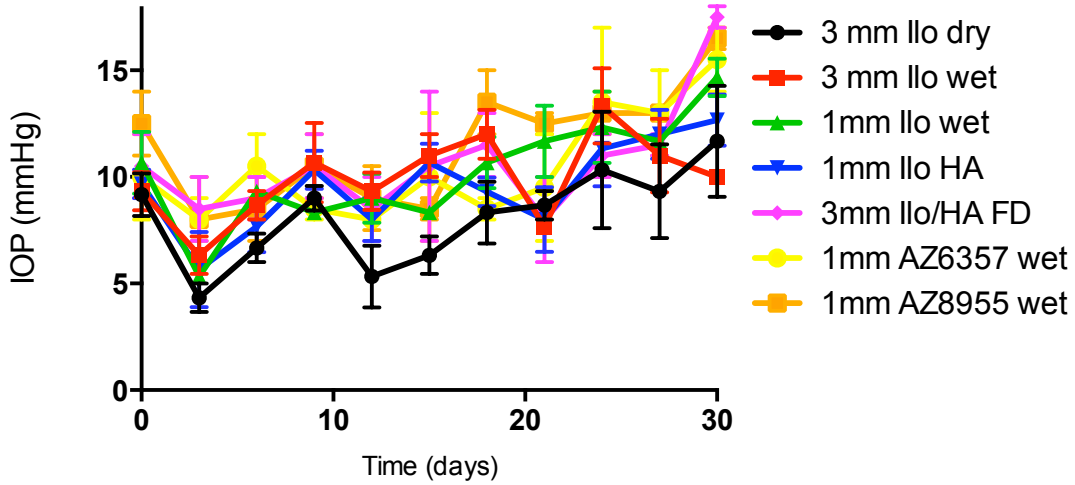

Figure 3-38 IOP for all 7 groups over time. The eyes that received the non-hydrated 3 mm ilomastat implant maintained a lower IOP for day 12 and 15 though no significant trend could be seen otherwise. Error bars indicate standard error.

3.2.2.4 Bleb vascularity

The larger implants showed greater vascularity than the smaller implants. Little difference could be distinguished between the 1 mm implant treatment arms (Figure 3-39).

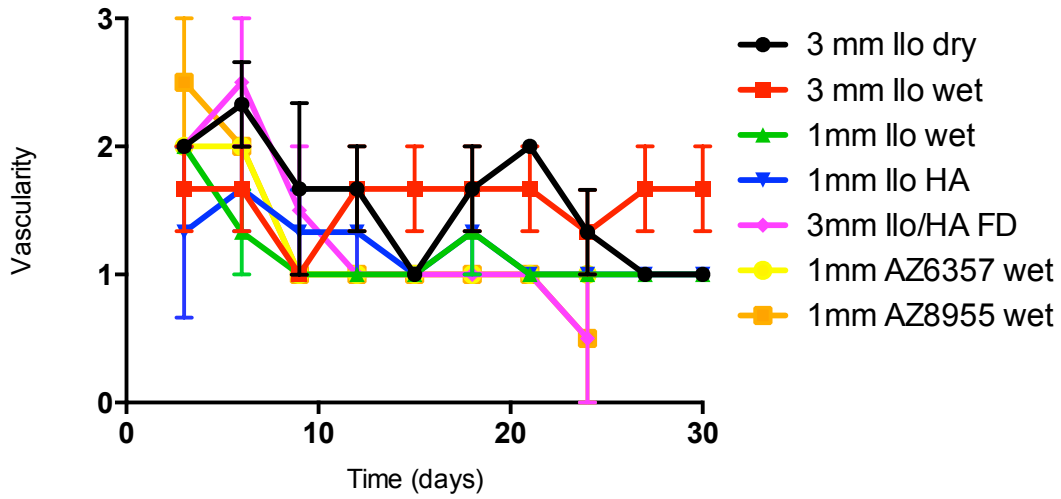

Figure 3-39 Bleb vascularity. The vascularity was graded as 0 = avascular, 1 = normal, 2 = hyperaemic, 3 = very hyperaemic. Data displays functional blebs at each time point as mean and standard error of the mean.

3.2.2.5 Other events

One of the 3 mm implants was found to extrude during the 30 day period. It is not clear exactly when this took place, however it became apparent that the leading edge of the conjunctiva retracted after day 18 with the implant migrating towards the limbal edge.

3.2.2.6 Histology

A cuff of inflammatory cells was seen surrounding the 3 mm ilomastat implants. Amongst those cells seen were neutrophils, macrophages and Langhans' giant cells. There was no appreciable difference in immune cell infiltration between the hydrated and non-hydrated implants. There was also no appreciable difference between the immune reaction around the hydrated ilomastat 1 mm implants and the hydrated AZ 8955 1 mm implants (Figure 3-40).

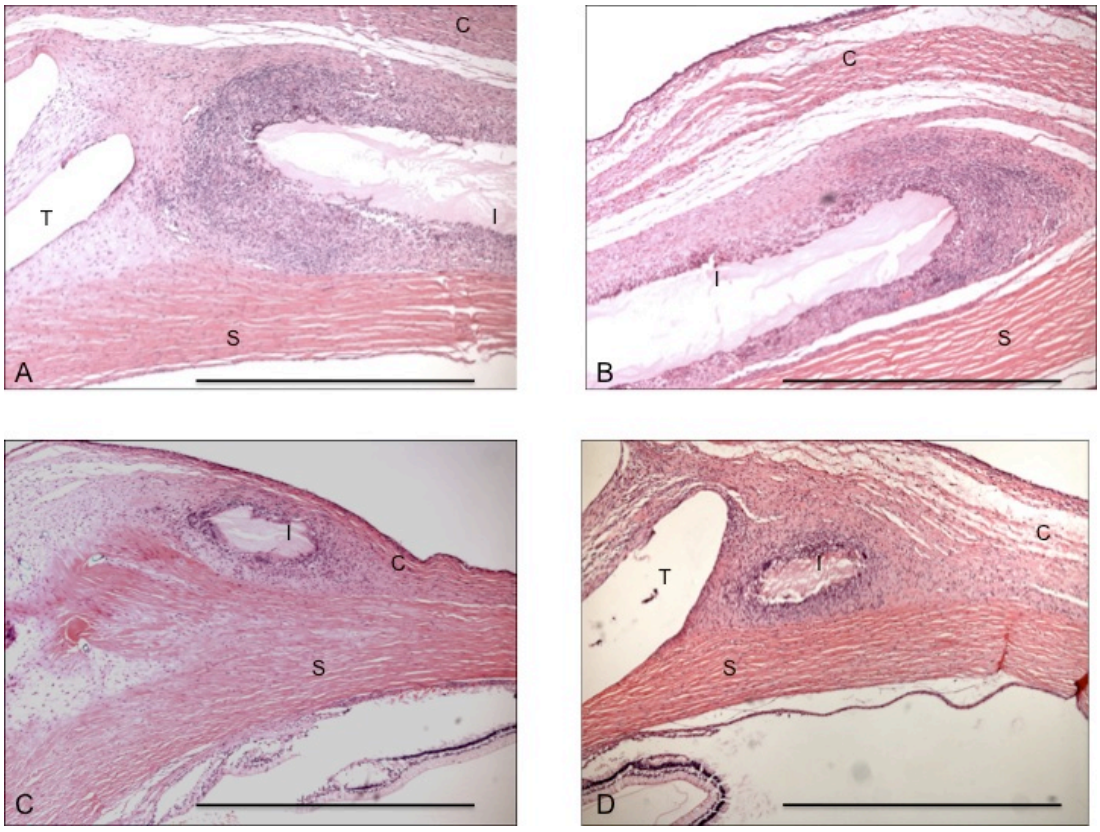

Figure 3-40 Hamatoxylin and Eosin staining of pure ilomastat implants. Legends: C: conjunctiva, T: drainage tube, S: sclera, I: implant remnants. Scale bars 1 mm. No appreciable difference was seen in quantity of immune cell infiltration or conjunctival thickening between the hydrated (A) and non-hydrated (B) 3 mm implants. There was also no appreciable difference in the quantity of immune cell infiltration between the 1 mm hydrated ilomastat implant (C) and the 1 mm hydrated AZ 8955 implant (D).

There appeared to be less immune reaction around the ilomastat implants enveloped in Healon 5 although the morphology of the conjunctiva was similar to the previous arms discussed, namely that there was thickening with closely packed fibroblasts (Figure 3-41).

There was no evidence seen of any refractile substance consistent with drug remnant seen in the blebs that received the 3 mm ilomastat / Visiol combination or the hydrated 1 mm AZ 6357 implant. The subconjunctival area had some inflammatory cells, but these were not distributed in a structured manner (Figure 3-41).

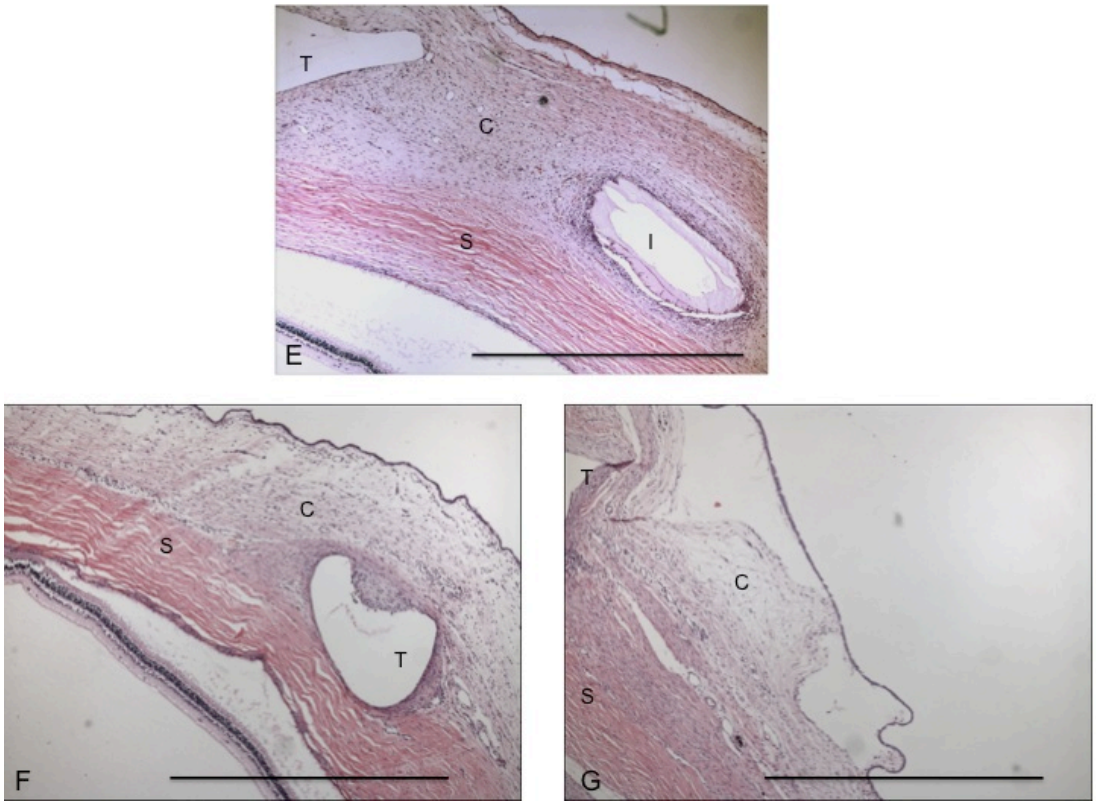

Figure 3-41 Haematoxylin and Eosin stain of blebs treated with ilomastat 1 mm enveloped in Healon 5 (E), AZ 6357 1 mm hydrated (F), ilomastat / Visiol 3 mm (G). Legends: C: conjunctiva, T: drainage tube, S: sclera, I: implant remnants. Scale bars 1 mm. Remnants were not detected in the blebs that received either AZ 6357 1 mm or the ilomastat / Visiol 3 mm implants.

3.2.3 Discussion

Increasing the amount of active drug available will increase the effect that it has, providing that this increase occurs within the therapeutic range, and that the counter stimulatory factors of foreign body reaction are minimised or at least maintained as constant. The results presented here demonstrate that hydration has no effect on the foreign body reaction and increasing the surface area of implants appears to increase it. Conversely, combining the ilomastat with Visiol, and using the much more soluble MMPi AZ 6357, did lead to significantly less foreign body response than previously seen at day 30.

It was hypothesised that hydration of the implant prior to implantation would encourage dissolution by reducing Ct – the concentration of fluid surrounding the implant and may create a boundary dissolution layer. The hydrated blebs certainly retained more fluid, signified by the greater bleb surface area in the initial stages of

the experiment. As the stimulatory effect of insoluble drug remained constant it would seem that any increased amount of free drug had no extra potency as an anti-inflammatory or anti scarring agent, reflected in the correlation of bleb surface area later in the experiment as well as the histology. This is most likely due to the quantity of extra free drug being negligible (due to the poor solubility of the compound). However, it could also be that the drug has already reached its maximum therapeutic effect: ilomastat has an inhibitory constant (Ki) of 0.4 nM for MMP1 in fibroblasts (Grobelny et al., 1992).

That the 3 mm implants caused no less (and possibly more) inflammation than the smaller 1 mm implants, supports the principle that the antagonistic effect caused by the insoluble drug was greater than the increased available free drug. Indeed if the concentration in the bleb was approaching C_s for the 1 mm implant, the only factor playing a role would be the antagonistic undissolved drug. The vascularity in this experiment again concurred with the foreign body response. In humans severe vascularity has been shown to represent risk of bleb failure (CATT study Group, 2007).

The inconsistencies between the results of the first in vivo and those of Geourgolas et al 2010 led to this second in vivo. It is clear that the application of an ilomastat implant perioperatively for experimental GFS resulting in a reduction of conjunctival scarring cannot be repeated. What is not clear is why this should be. The results of those experiments showed the presence of implants in photos at day 30. One explanation put forward for the lack of implant seen was that it dissolved between harvesting of the eyes, and histological processing. Pure implants inserted into formaldehyde fluid did not dissolve however after two months. In other *in vivo* experiments, despite globes having too much exposure or too little exposure to processing fluids than planned, if an implant was seen with the naked eye at the end of an experiment there was an implant found in histology. This was true for the 1 mm implants as well as 2 or 3 mm implants.

There was concern that the ilomastat being used for these experiments did not have the same structural properties as the ilomastat used for previous experiments by Georgoulas et al 2010. This might account for the foreign body reaction. We (Dr H

Fadda, Dr A Vetter and myself) performed pharmaceutical analysis including HPLC, mass spectrometry and found minimal differences for results in characterisation between different batches however (Parkinson et al., 2012). That the AZ 8955 implants gave a similar reaction to the ilomastat implants provides evidence that the response was due to particulate material or solid MMPi in general, and not just to the ilomastat per se.

It appeared that there were fewer inflammatory cells seen in the blebs that were treated with the ilomastat implants surrounded with Healon 5. However, with an n of 2 it is not possible to be sure that this appearance is significant, and more evaluation would be required. Apart from the ability of a gel to provide some reduction in the abrasiveness of the implant, the hyaluronic acid in the gel may also have an anti-inflammatory effect. Hyaluronic acid has been shown to reduce binding by macrophages to surfaces, believed to be due in part to its negative charge, and therefore may reduce inflammation (Tsai et al., 2011).

The AZ 6357 1 mm implants are the first excipientless implants in this project to show no evidence of a foreign body reaction at day 30. AZ 6357 has a similar inhibitory profile to ilomastat but is somewhat less potent, particularly with respect to MMP1 (Table 3-3). At 16 times the solubility of ilomastat though, far greater drug will be in solution, and the duration of antagonistic effect of insoluble drug will be far less: AZ 6357 2 mm implants took eight days to achieve complete dissolution (thesis S. Dhingra). That the blebs for the rabbits treated with AZ 6357 maintained ‘normal’ vascularity for the duration of the experiment after day 9 indicates that inflammation during this time is less.

Table 3-3. The inhibitory profile of the ilomastat as compared to AZ 6367 or AZ 8955. The values given indicate Ki for ilomastat and IC_{50} for AZ 6357 and AZ 8955.

MMP inhibited	Ilomastat	AZ 6357	AZ 8955
MMP 1	0.4	6858	378
MMP 2	0.57	0.3	0.1
MMP 3	27	19	26
MMP 7		>10000	966
MMP 8	0.18	5	0.8
MMP 9	0.2	1	1
MMP 12		4	1
MMP 13		0.6	0.8
MMP 14		1533	28

There are a number of reasons why the combination ilomastat / Visiol implant also resulted in no evidence of a foreign body reaction at day 30. Hyaluronic acid is one of the most hygroscopic polymers, and by having drug dispersed evenly throughout a combination implant, with exposure to aqueous fluid there would be enhanced dissolution through the greatly increased surface area. As a consequence there would also be reduced duration of exposure to undissolved particulate material as well as a maintenance of maximal solubilised drug. Other factors that could contribute to the dampening of inflammation are the less abrasive preparation, and the direct inhibitory effect of hyaluronic acid (Tsai et al., 2011). Challenges that arise when developing this as an implant include optimisation of the preparation, and characterisation. Visiol was chosen because, while it appeared to mix easily with aqueous ilomastat, it is a pre-prepared substance made up of a multitude of buffers and salts as well as the hyaluronic acid.

Another challenge raised by the use of implants constructed with hyaluronic acid is sterilisation. The most convenient and effective method of sterilisation is √

irradiation. Due to the constraints of time it was not possible to sterilise these implants in the conventional way, and instead β irradiation from a Strontium 90 probe was used (itself an antiscarring device used in the ophthalmological theatres). That no endophthalmitis was seen in this treatment arm supports the concept that some sterilisation has taken place, but sterilisation by this method has not been confirmed and would not be accepted for translation into man without further optimisation and validation. Indeed when samples of hyaluronic acid gel were sent for irradiation sterilisation there was considerable denaturation consistent with the literature (Srinivas and Ramamurthi, 2007). Other methods such as micro filtration would need to be investigated.

That the least soluble implants with the most foreign body reaction had the greatest bleb survival again shows how little bleb survival reflects the anti-scarring effect of the drug. It is not possible to determine the quantity of each of the possible contributory factors: presence of aqueous, physical implant and inflammatory response leading to conjunctival thickening.

One 3 mm implant that extruded during the experimental process could be due to surgical error in the closure of the conjunctiva at the leading edge, although no wound leak was detected. An alternative possibility is that contraction of the conjunctival tissue posterior to the implant pulled the conjunctiva at the leading edge away.

It is important to remember that this study is a pilot and consisted of 7 treatment arms, of which there were 4 groups of 3 animals, and 3 groups of 2 animals, with no positive or negative controls. Furthermore there was error in the formulation of the implants and therefore conclusions should be drawn with these factors in mind. It would appear, however, that a more soluble MMPi showed promise as a potential anti-scarring agent implant. Research in the following experiments was focussed on examining the efficacy of a more soluble MMPi formulated as a pure implant. By remaining pure the intellectual property for an excipientless implant was satisfied.

3.3 Investigation into the anti-scarring efficacy of a more water soluble MMPi

The pilot in vivo study just described found that an implant formulated from either an MMPi with a greater water solubility than ilomastat, for example AZ 6357 or ilomastat combined with hyaluronic acid thereby enhancing dissolution, might increase success whilst avoiding a foreign body response. As implants formulated from AZ 6357 remained within the intellectual property and did not require the characterisation of the ilomastat / hyaluronic combination, further investigation was performed by S. Dhingra. Although in another study no foreign body response was seen at day 30, harvesting eyes at days 7 and 14 revealed significant inflammation around the implants (thesis S. Dhingra). Research was then focussed on MMPis with the same spectrum of activity but with an even greater water solubility.

Marimastat was identified as a possible candidate. It is a broad spectrum MMPi that has been taken to human trials as an oral anti cancer chemotherapeutic (Wojtowicz-Praga et al., 1998; Bramhall et al., 2001). It too has a similarly broad inhibitory spectrum of MMPs to ilomastat but is over 100 times as soluble in water (aqueous solubility of 3.38 mg / ml). Marimastat has also been shown to inhibit the gel mediated contraction of dermal fibroblasts. In the presence of marimastat (10 μM) dermal fibroblast contraction was completely inhibited (Scott et al., 1998).

It was hypothesised that marimastat might be able to be formulated into an excipientless implant and used as an anti scarring treatment.

3.3.1 Fabrication of marimastat implants

The fabrication of marimastat implants was more technically difficult than either the ilomastat or AZ implants, as the powder was far less cohesive. Only 2 mm implants of more than 1 mg could be produced because upon removal the tablets frequently broke on punch and dye pressing. Even coating the die using the lubricant (polaxamer) between each implant fabrication, approximately 60 % of implants disintegrated. Using a 2 mm punch and die implants of 1 to 3 mg could be pressed. . The sterilisation process was by gamma irradiation, and approximately half of the implants fractured on passage to and from the site of sterilisation. Analysis of the drug post irradiation by mass spectrometry and HPLC showed no change, however.

3.3.2 In vitro release of marimastat implants

Marimastat implants of a mean of 1.56 mg completely dissolved in the rig by day 2 (46 hours)(Figure 3-42 and Figure 3-43). The mean maximum concentration in the elutent was 2.5 mM.

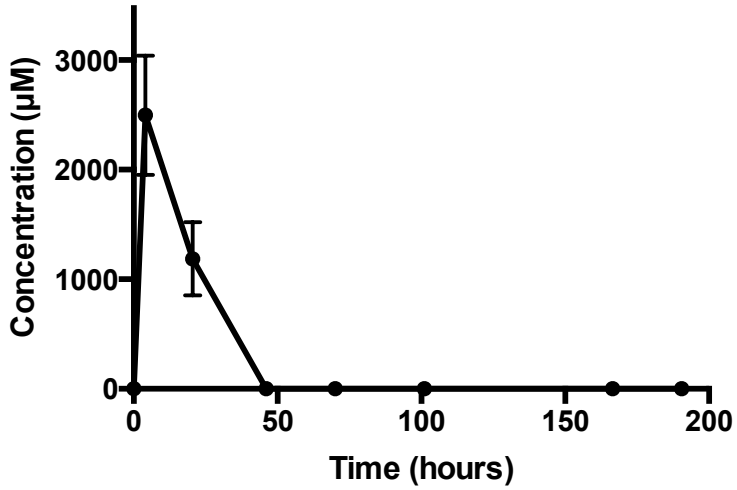

Figure 3-42 The concentration of marimastat released over time in the rig from 2 mm implants (mean 1.56 mg). At 46 hours there was no drug detectable in the elutent. Implants n = 3 (1.18 mg, 1.9 mg, 1.6 mg). The flow rate was 2 µl minute^{-1}. Error bars indicate SD**.**

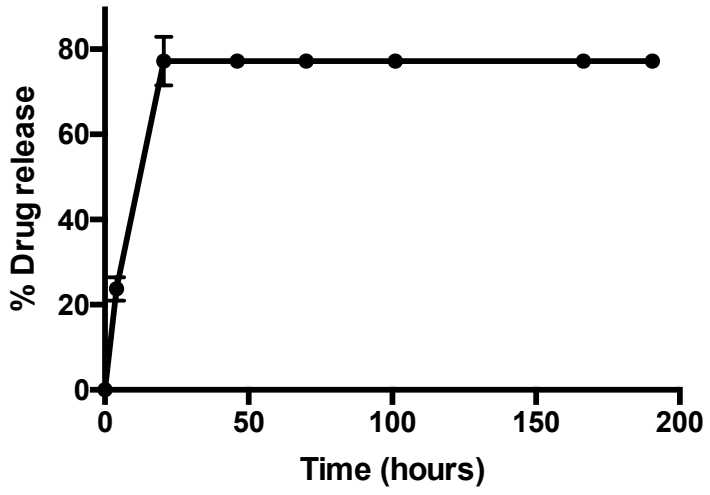

Figure 3-43 Cumulative release of the 2 mm marimastat implants (n = 3). Error bars indicate SD**.**

3.3.3 Pilot study using pure marimastat implants harvesting eyes at 14 days

To determine whether there would be implant remnant remaining at day 7 or day 14 and gain a better understanding of the wound healing process at an earlier time point, a pilot in vivo of 4 rabbits was performed. Each rabbit received a 2 mm marimastat implant (2.2 – 2.4 mg). Unfortunately one rabbit died under anaesthesia and a second developed endophthalmitis a few days after surgery. It was decided to terminate and harvest the eyes of the remaining two animals at day 14, and discard the day 7 time point (Figure 3-44). Histological analysis of the drainage area revealed a collection of inflammatory cells at the site of tablet placement but no implant remnant (Figure 3-44). As no remnants were seen it was concluded that marimastat might be a potential candidate as an antiscarring implant. An efficacy study was planned to compare marimastat with positive and negative controls. The discussion of marimastat results is incorporated into the discussion after this study.

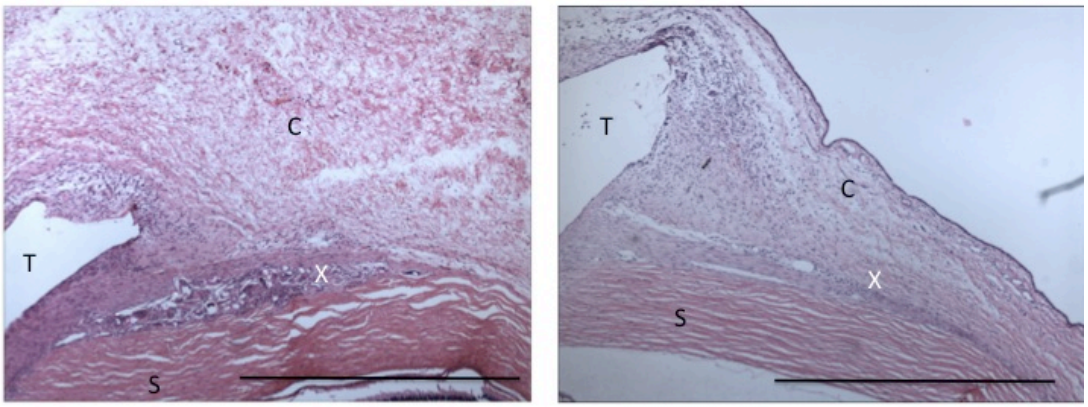

Figure 3-44 Haematoxylin and Eosin staining of the two rabbits treated with marimastat 2 mm implants. Legends: C: conjunctiva, T: drainage tube, S: sclera. Scale bars 1 mm. No implant remnants were seen at the site of implant placement (X), only collections of inflammatory cells.

3.4 Investigation into the efficacy of dexamethasone in combination with ilomastat as a slow release antiscarring agent

An additional line of investigation to develop an effective anti scarring MMP implant was to consider another class of anti-inflammatory in combination with an MMPi. Dexamethasone is one of the most potent of steroids. Dexamethasone is also poorly soluble (physicochemical attributes). It is routinely used after almost every surgical ocular procedure to reduce inflammation, therefore if a combination were to be successful this preparation would be comparatively easy to translate into the clinic. Fixed dose combinations are frequently used to treat infectious diseases such as TB and HIV, or chemotherapeutic cancer regimens.

It was hypothesised that an implant consisting of both dexamethasone and ilomastat in combination might provide the inhibition of inflammation necessary in the early postoperative period to prevent foreign body encapsulation, whilst allowing the MMPi to be freely available in solution.

In order to figure out the dose for the formulation vitro experimentation investigation determined the feasibility of formulating combination implants, and determining the release profile.

3.4.1 Fabrication of dexamethasone / ilomastat implants

The fabrication of implants using crystalline solid dexamethasone and ilomastat was achieved through mixing powder in eppendorf lids for each individual implant. Poorly soluble in water (Galardy et al., 1994), attempts were made to improve uniformity by dissolving the mixture in a solution of *tert*-butanol 40 % and then freeze drying, however the amorphous product had minimal cohesiveness and fragmented constantly. Amorphous material also crystallizes with moisture exposure, making physicochemical analysis more challenging. Due to time constraints it was not possible to pursue this further.

Investigations were performed into the optimum size of implant and ratio of dexamethasone to ilomastat. Two mm diameter combination implants were found to

be the optimum size to press without fragmentation however the crystalline dexamethasone had far less cohesiveness than the ilomastat. The minimum proportion of ilomastat in an ilomastat / dexamethasone combination that could be pressed without fragmentation was 0.5:1.

3.4.2 *In vitro* release data from Dexamethasone ilomastat implants

The concentration and release profiles over time for different combinations of ilomastat / dexamethasone are illustrated in Figure 3-45 to Figure 3-50. The length of time a drug concentration of > 10 μM was maintained is shown in Table 3-4. Sustained release of dexamethasone and ilomastat was achieved with all combinations of implants. The decay was not smooth however, which may be related to the implant developing fracture lines that abruptly increased implant surface area. An alternative explanation might be temperature change in the laboratory, although efforts were made to maintain this as constant. The level of 10 μM for dexamethasone was taken as previously found to be inhibitory for inflammation, in particular macrophage activation by lipopolysaccharide (Jarvis and Qureshi, 1997).

Table 3-4 Duration of release where > 10 μM was maintained for the combination implants.

Ilomastat : Dexamethasone	Duration > 10 μM ilomastat maintained	Duration > 10 μM dexamethasone maintained
1 mg : 1 mg	25 days	29 days
1 mg : 0.5 mg	22 days	16 days
0.5 mg : 1 mg	15 days	29 days

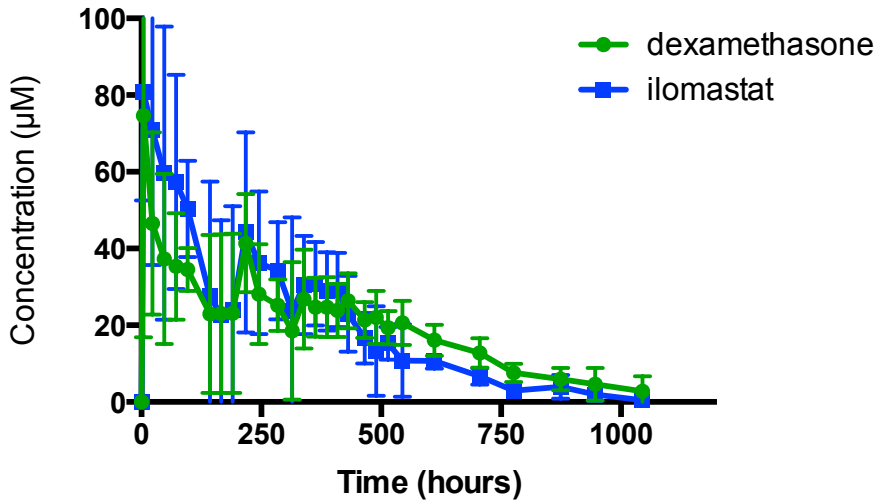

Figure 3-45 Mean concentration released from ilomastat and dexamethasone (1 mg : 1 mg) implants over time. Ilomastat was released at a concentration of > 10 µM for 25 days. Dexamethasone was released at a concentration of > 10 µM for 29 days.

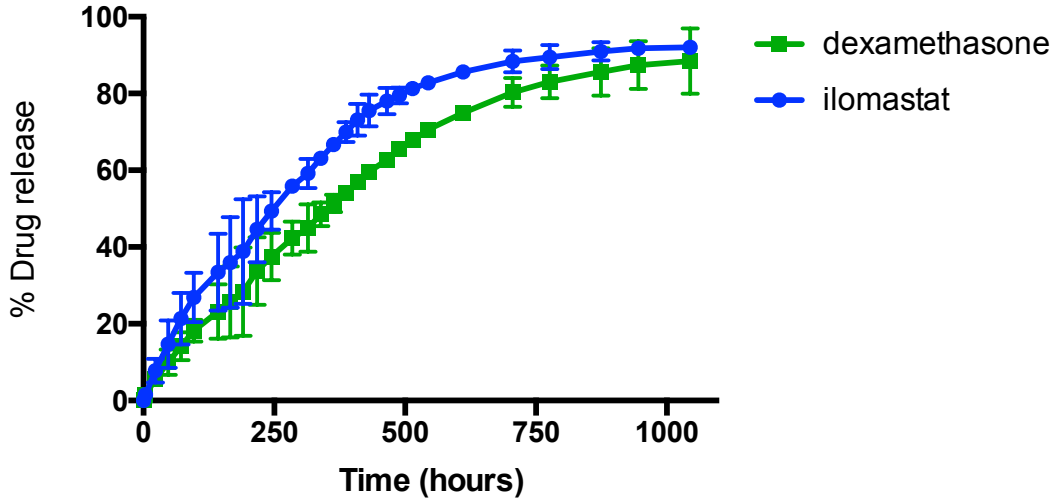

Figure 3-46 Cumulative release of ilomastat and dexamethasone (1 mg : 1 mg) implants over time. Error bars indicate SD.

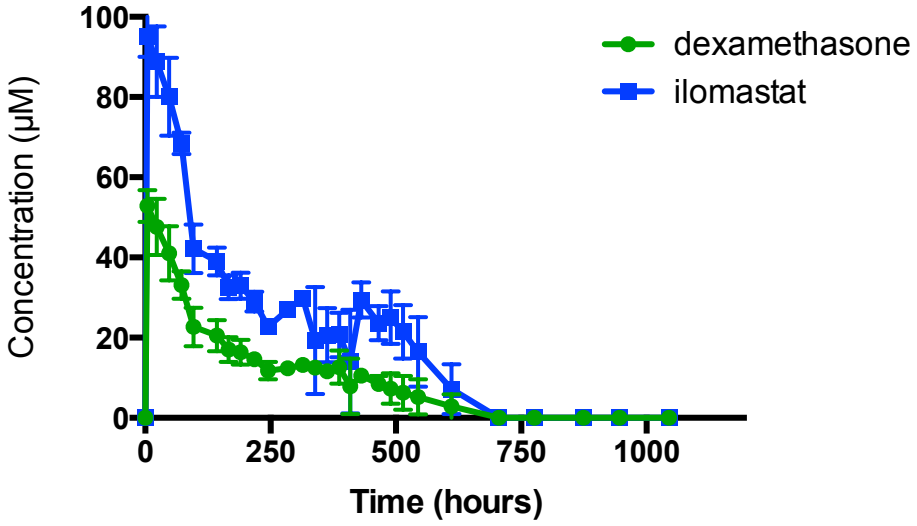

Figure 3-47 Mean concentration released from ilomastat and dexamethasone (1 mg : 0.5 mg) implants over time. A concentration of > 10 µM ilomastat was maintained for 22 days and a concentration of > 10 µM dexamethasone was maintained for 16 days.

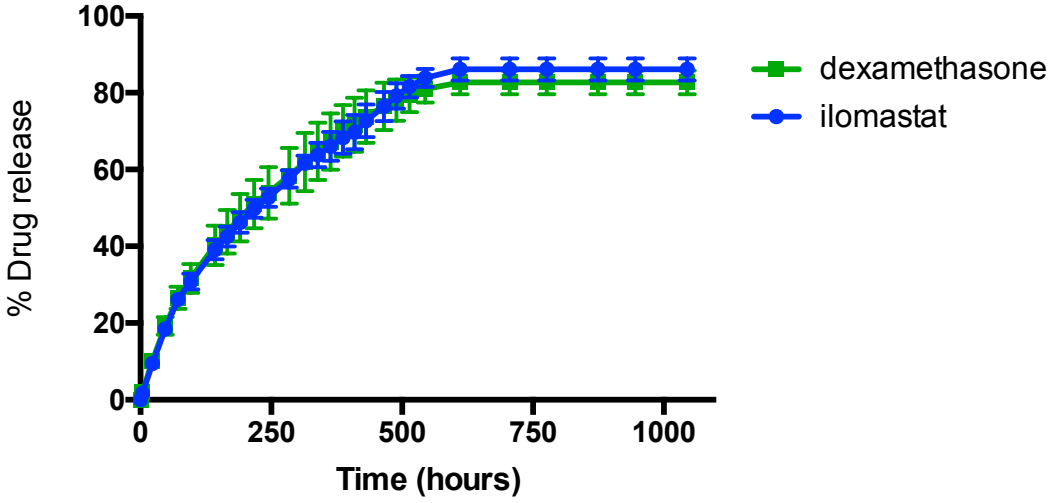

Figure 3-48 Cumulative release of ilomastat and dexamethasone (1 mg : 0.5 mg) implants over time. Error bars indicate SD.

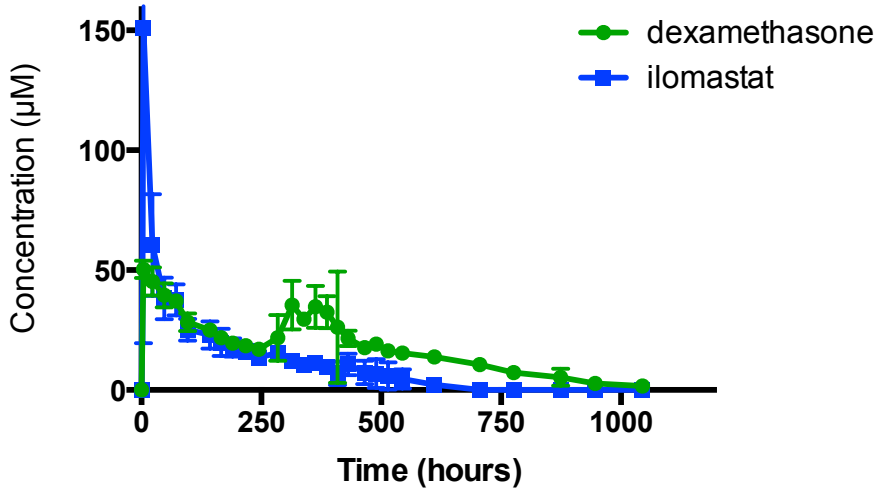

Figure 3-49 Mean concentration released from ilomastat and dexamethasone (0.5 mg : 1 mg) implants over time. A concentration of > 10 µM ilomastat was maintained for 15 days and a concentration of > 10 µM dexamethasone was maintained for 29 days.

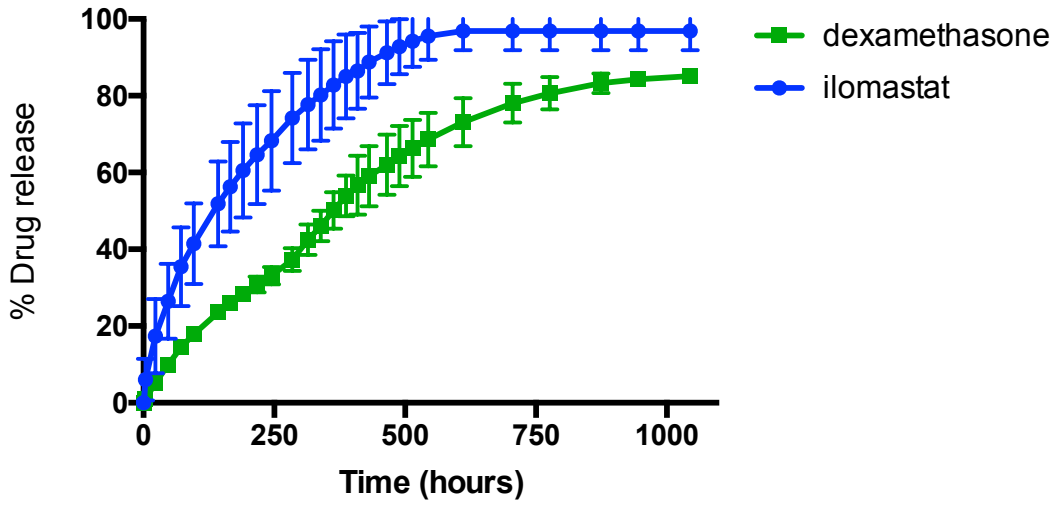

Figure 3-50 Cumulative release of ilomastat and dexamethasone (1 mg : 0.5 mg) implants over time. Error bars indicate SD.

3.4.3 I*n vivo* results of dexamethasone / ilomastat combination implants and pure marimastat implants as anti-scarring agents

An in vivo experiment to test the anti-scarring efficacy of marimastat and dexamethasone / ilomastat combinations was designed.

As the greatest release for both of the drugs ilomastat and dexamethasone were with the 1 mg : 1 mg implants, it was decided that this ratio should be tested in the animal model of aggressive scarring. To achieve the greatest likelihood of success the greatest dose of marimastat that could be made into an implant without fragmentation was chosen.

The four experimental treatment arms investigated on 6 rabbits each were:

1) Ilomastat / dexamethasone 2 mm implant (1 mg : 1 mg) (height 0.6 mm)

2) Marimastat 6 mg (two 2 mm 3 mg implants) (height 0.8 mm)

3) Mitomycin C applied at a concentration of 0.2 mg/ml for 3 minutes perioperatively (positive control)

4) Sterile water applied in the same way as MMC (negative control)

Four of the six rabbits treated with ilomastat / dexamethasone combination maintained the appearance of a functional bleb until day 30. Of those that did not, one developed an endophthalmitis in the first week post surgery and the other failed on day 27. If the animal with endophthalmitis is excluded then 80% (4/5) had the appearance of a functional bleb at day 30. The marimastat treated rabbits had blebs that failed at a median of 24 days (range 21 - 24). The sterile water treated group failed at a median of 18 days (range 12 -21). Of the MMC treated group one animal had a bleb that failed at day 27 and the other 5 survived until day 30 (Figure 3-51).

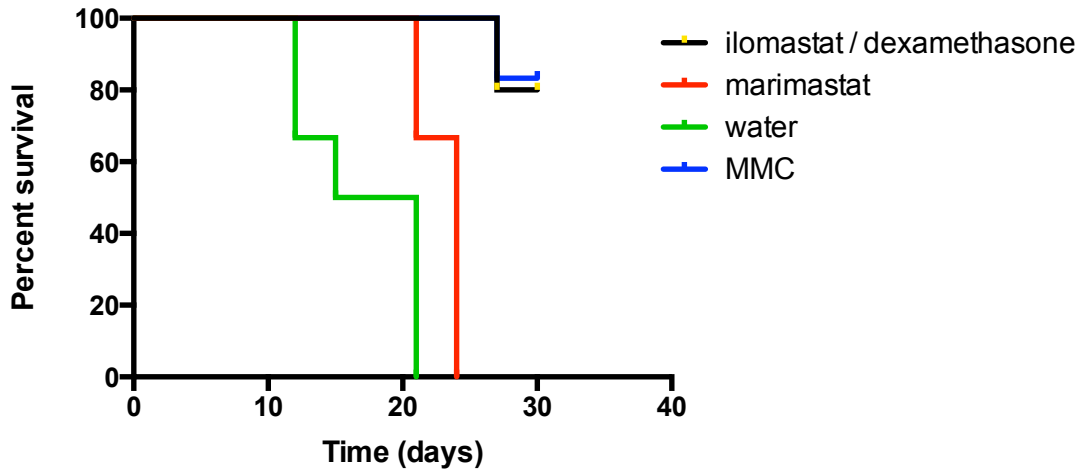

Figure 3-51 Bleb survival of the four groups. The MMC and ilomastat / dexamethasone groups survived significantly longer than the marimastat and the sterile water groups (log rank P < 0.005). The marimastat group survived significantly longer than the sterile water group (long rank P < 0.01).

3.4.3.1 Bleb Surface area

The bleb surface areas of the MMC and the ilomastat group were greater than the marimastat or sterile water groups from day 6 (Figure 3-52). A Kruskal-Wallis test revealed that there was a significant difference between bleb heights at day 30 (H (3) = 14.37, P = 0.024). Inspection of the group means using Dunn's multiple comparison test showed that there was a significant difference between ilomastat dexamethasone group and sterile water group, and sterile water group and MMC group

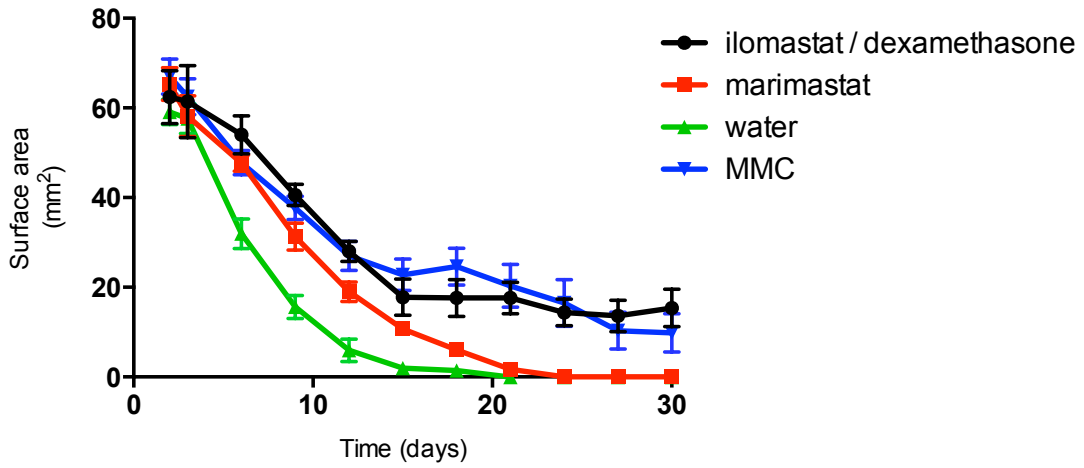

Figure 3-52 Mean bleb surface area over time for the four groups. The ilomastat / dexamethasone implants consistently maintained a greater mean bleb surface area than marimastat and the sterile water group from day 9. Error bars indicate standard error.

3.4.3.2 Bleb Height

The bleb heights of the MMC and ilomastat / dexamethasone groups were constantly greater than marimastat or sterile water group. Initially the bleb height of the ilomastat dexamethasone group was greater than the MMC group however the two maintained similar heights after day 15 (Figure 3-53). A Kruskal-Wallis test revealed that there was a significant difference between bleb heights at day 30 (H (3) = 15.44, P = 0.015). Inspection of the group means using Dunn's multiple comparison test showed that there was a significant difference between ilomastat dexamethasone group and sterile water group, and sterile water group and MMC group.

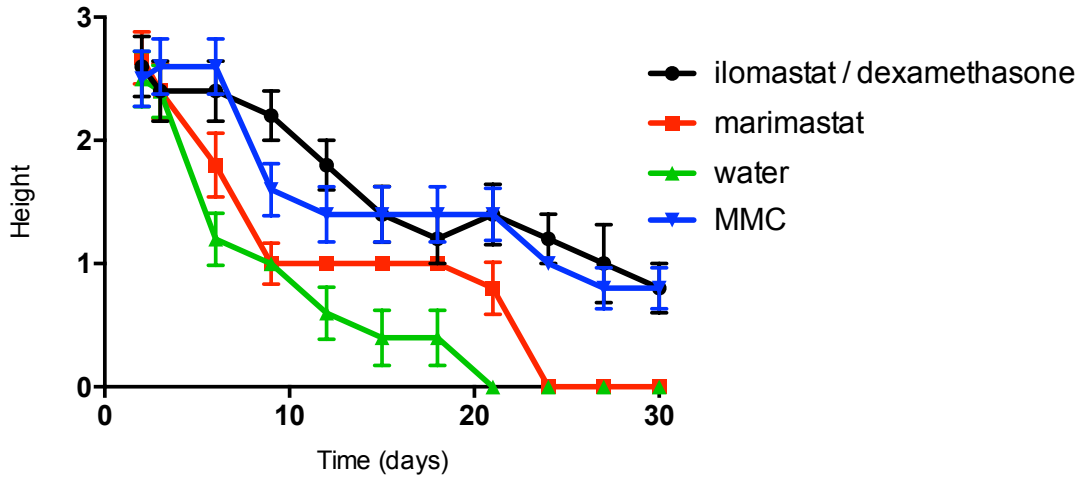

Figure 3-53 Bleb height of the 4 groups over time. Bleb height was graded as 0, flat; 1, shallow/formed; 2, elevated < 2 mm and 3, high > 2 mm. From day 6 the ilomastat / dexamethasone and MMC groups maintained higher blebs than the marimastat or sterile water groups. Error bars indicate standard error.

3.4.3.3 Intraocular pressure

There was an initial fall in IOP for all four groups, as expected. This was followed by a return to baseline, of which the sterile water and marimastat groups returned most quickly, followed by the ilomastat / dexamethasone group, and then the MMC group. After day 18 the IOP of the ilomastat / dexamethasone group became consistently greater than the other three groups and the initial baseline pressure. Although not significant at day 30, on day 27 there was a significant difference between the groups (Kruskall-Wallis: (H (3) = 12.2, P = 0.067). Between day 18 and the end of the experiment the MMC group maintained a lower IOP than the other 3 groups, however this was not less than the baseline preoperative IOP (Figure 3-54).

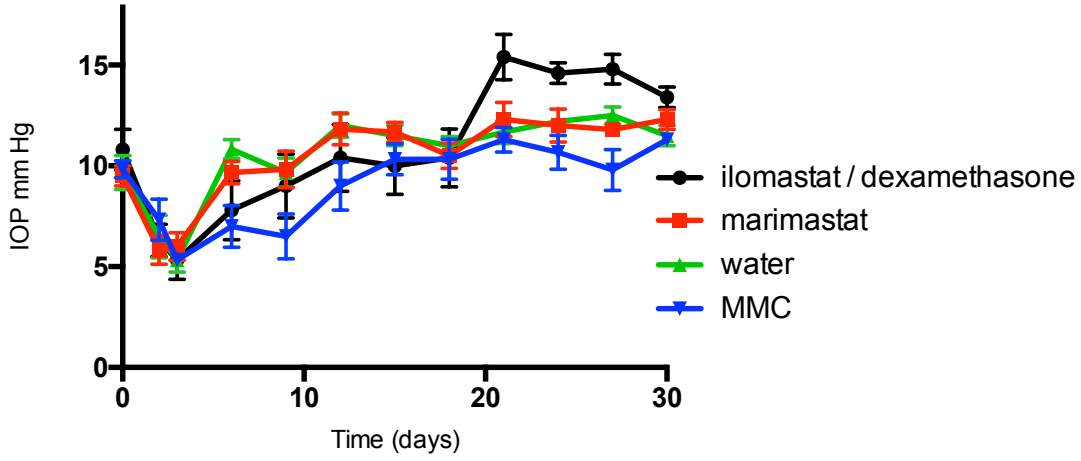

Figure 3-54 Mean IOP of operated eye with time. There was an initial fall in IOP. Between days 6 and 18 the ilomastat / dexamethasone and MMC treated animals maintained a lower IOP than the other groups. Between day 18 and day 30 the ilomastat / dexamethasone group maintained a higher IOP than preoperative baseline. Error bars indicate standard error.

3.4.3.4 Bleb Vascularity

There was similar bleb vascularity for all groups from day 9 until day 30 (Figure 3-55).

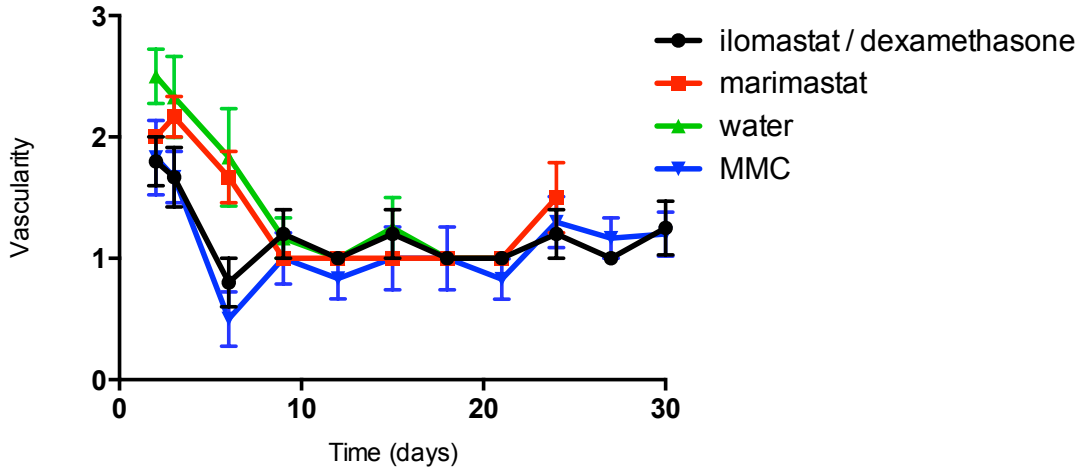

Figure 3-55 Bleb vascularity post surgery. The vascularity was graded as 0 = avascular, 1 = normal, 2 = hyperaemic, 3 = very hyperaemic. Data displays blebs at each time point as mean and standard error of the mean.

3.4.4 Bleb morphology

High resolution photographs revealed detailed morphology of the blebs at different time points. Information about the contours of the blebs was obtained by high magnification from the side.

Photographs of examples of blebs at day 15 are illustrated below (Figure 3-56). At this stage three of the sterile water group had failed (the example illustrated failed at day 21).

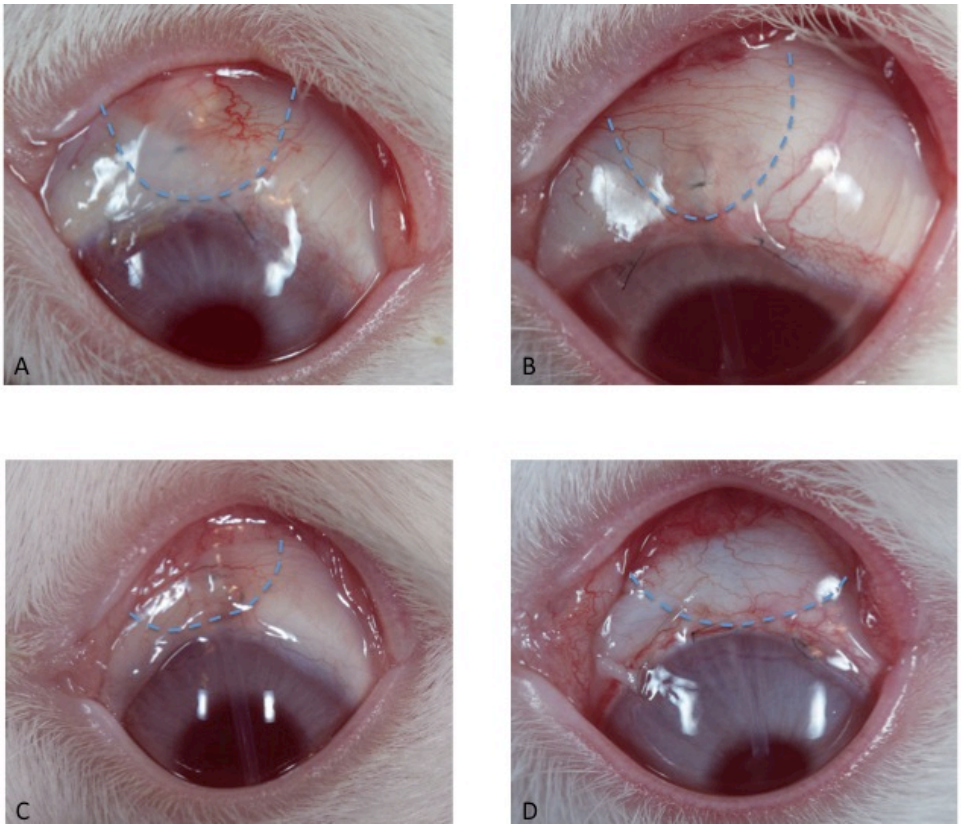

Figure 3-56 Representative photos of blebs at day 15 for each of treatments ilomastat / dexamethasone 2 mm (A), marimastat 2 mm (B), sterile water (C), and mitomycin C (D). Blue dashed line indicates location of bleb edge. The blebs illustrated have the appearance of functionality at this stage.

Implants in the dexamethasone / ilomastat treatment arm became clearly visible in four of the blebs from day 12. Once visible they remained so until termination (Figure 3-57). The one implant that was not visible was discovered to have migrated posteriorly out of the bleb area on histology. It was this bleb in the dexamethasone / ilomastat treatment arm that failed on day 27. None of the marimastat implants were

visible during the observational period. The contours of three of the blebs of the dexamethasone / ilomastat implants outlined the shape of the implant from day 18. The bleb morphology of the fourth visible dexamethasone / ilomastat implant (number 14) became temporarily conical, and the implant inside became smaller with time. The bleb morphology of this particular rabbit also became conical in appearance when viewed from the side (Figure 3-59). Optical coherence tomography (OCT) revealed evidence of implant fragmentation. Later in the experiment the conical shape diminished with the implant appearing to become smaller on OCT examination and visually. One of the MMC blebs became cystic in appearance.

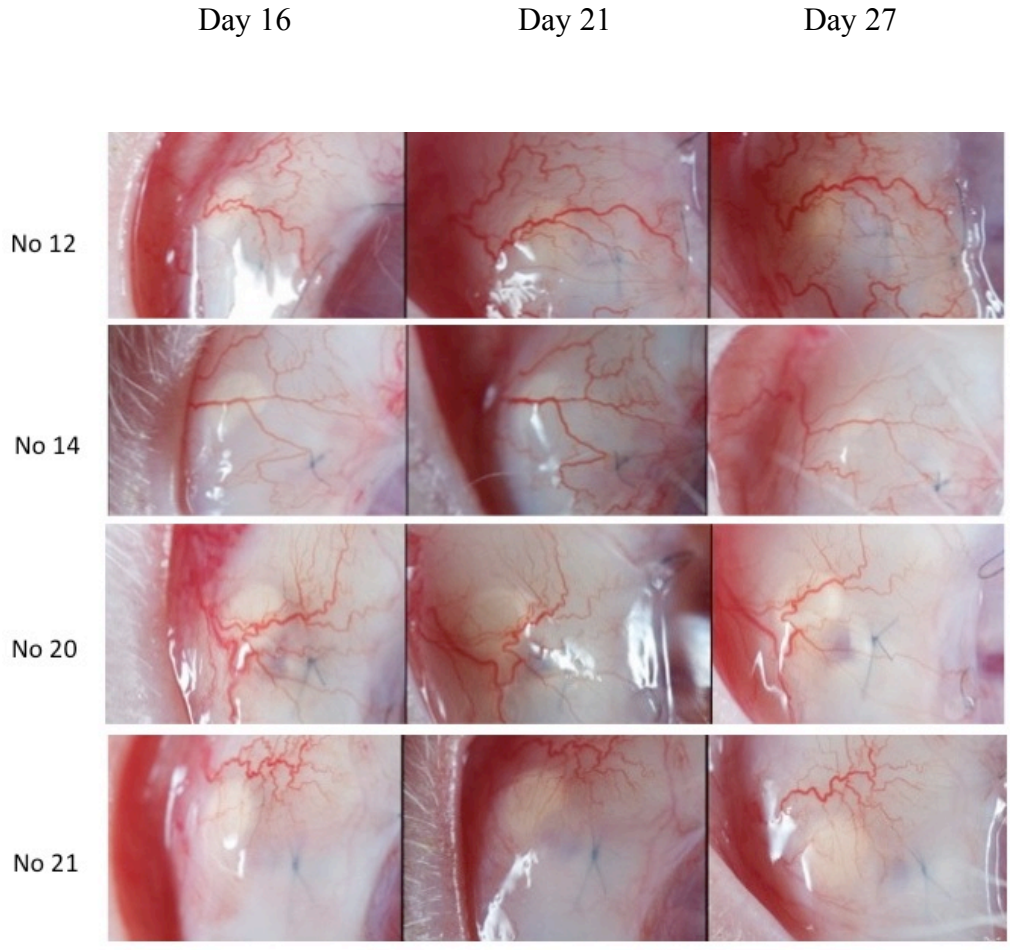

Figure 3-57 Sequential photos of dexamethasone / ilomastat treated blebs where the implants were seen using the extension tube. The implant within the bleb of rabbit no 14 appeared to be diminishing in size with time. Vascularity is also increased. Photos courtesy of A. Khalili.

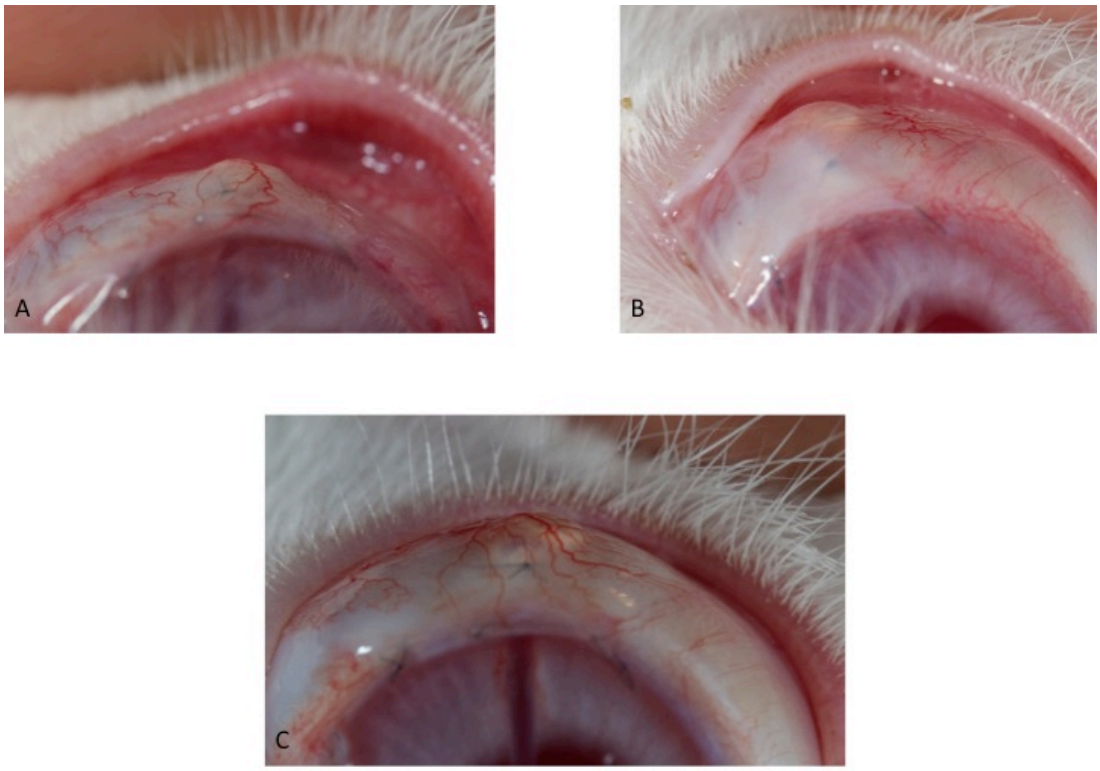

Figure 3-58 Outlines of three blebs of the ilomastat / dexamethasone implant rabbits at day 18. The bleb morphology follows the contours of the implant. Photos display rabbits 12 (A), 20 (B) and 21 (C). Here the conjunctiva appears to be closely apposed to the implant. The mean intraocular pressure at this time-point was raised in comparison to baseline.

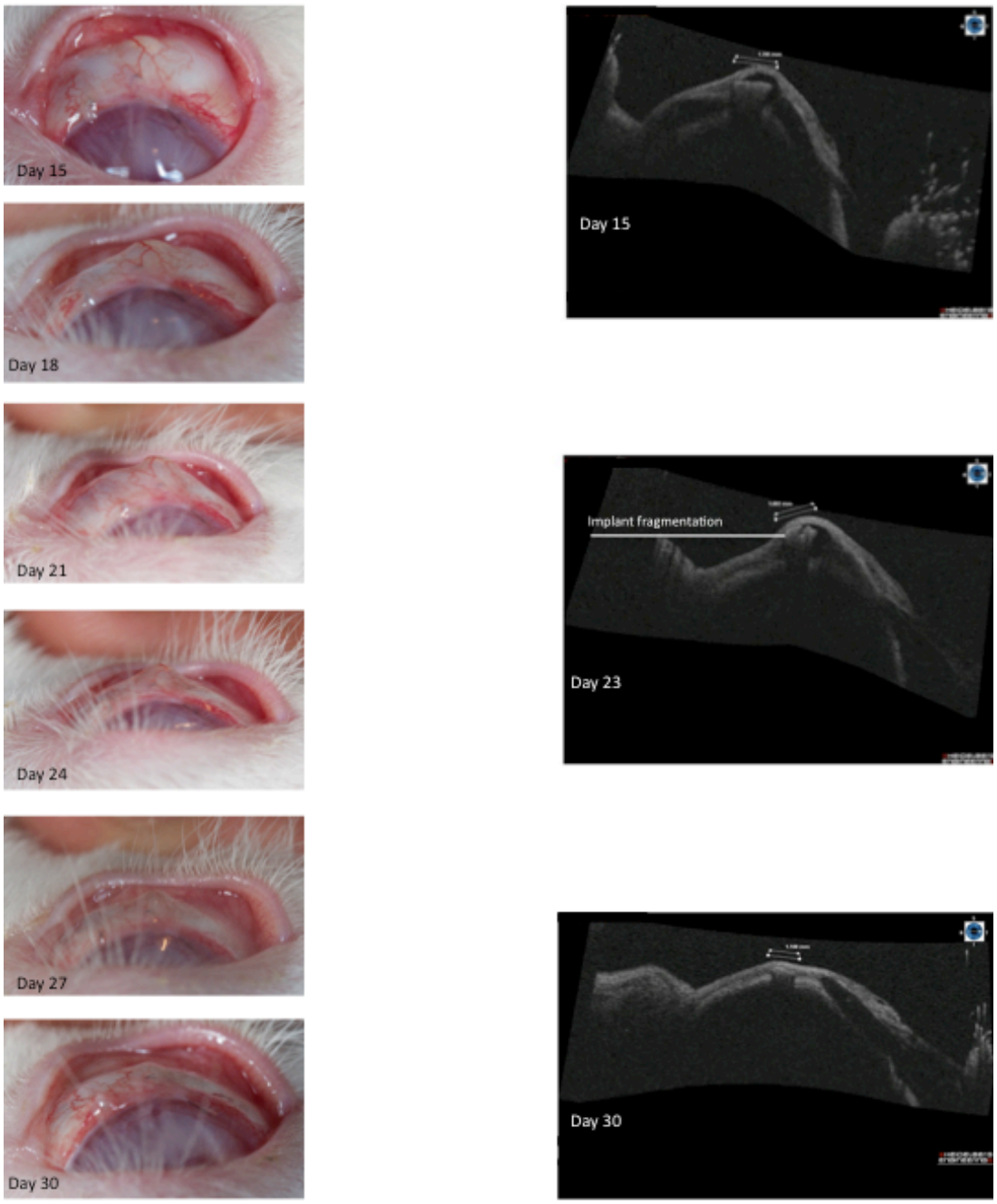

Figure 3-59 Sequential images of the bleb of R14 dexamethasone / ilomastat. The OCT views the bleb in a sagittal section with cornea to the right of the picture. Implant fragmentation can be seen at day 23.

3.4.5 Histology

There was a paucity of nuclear staining of cells posterior to the drainage site in the MMC treated group using the Haematoxylin and Eosin stain (Figure 3-60). This was seen in the section bisecting the drainage tube and at parallel sections 1 mm and 2 mm away. Extra sections were taken to ensure that the histological response was the similar throughout the bleb. Lining the inside of the cystic bleb of number 1 (MMC) was evidence of necrotic and apoptotic tissue.

The marimastat treated blebs revealed no evidence of encapsulated drug material, however there were considerable numbers of inflammatory cells localised around where the implant had been placed. On higher magnification refractile deposits were seen amongst the inflammatory cells. Overlying this area and more posterior there was evidence of eosinophilic staining of collagen deposition.

Blebs of the dexamethasone / ilomastat combinations revealed refractile drug material located in close proximity to the tube in four of the five blebs (Figure 3-61). If not found in the tube section evidence of the implant was seen in the 1 mm or 2 mm parallel sections away from the tube. Associated with the implants were a number of inflammatory cells in the conjunctiva, though far fewer than seen associated with ilomastat implants in the previous experiments. There were a number of inflammatory cells also seen in the sclera. The conjunctiva overlying the implants showed denser eosinophilic staining consistent with collagen deposition. There were a number of large blood vessels found in this tissue that were sectioned.

The sections of the sterile water treated group revealed an infiltration of inflammatory cells around the tube implant, however posterior to this and in parallel sections not including the tube the numbers were fewer and distributed more evenly. The morphology of the conjunctiva had the appearance of being loosely packed with less eosinophilic staining, similar to an unoperated eye.

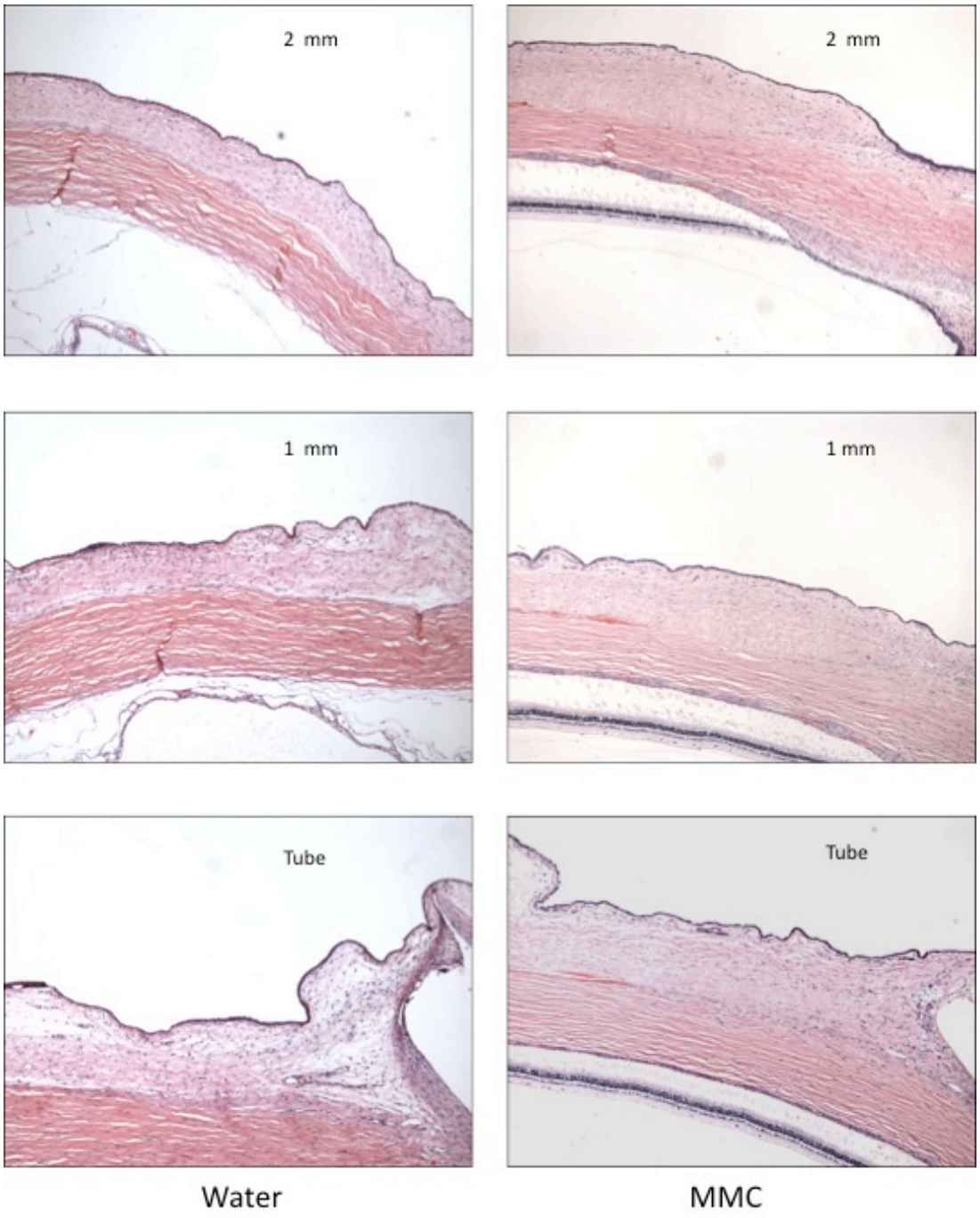

Figure 3-60 Sections of representative blebs of the MMC and sterile water groups. Scale bar 1 mm. The planes of section were: sagittal, bisecting the tube, 1 mm parallel and 2 mm parallel. The sections of blebs treated with MMC showed cellular paucity in the region of the bleb. Sterile water treated group had a diffuse inflammatory infiltrate that was less than either marimastat implant treated blebs or dexamethasone treated blebs (see below).

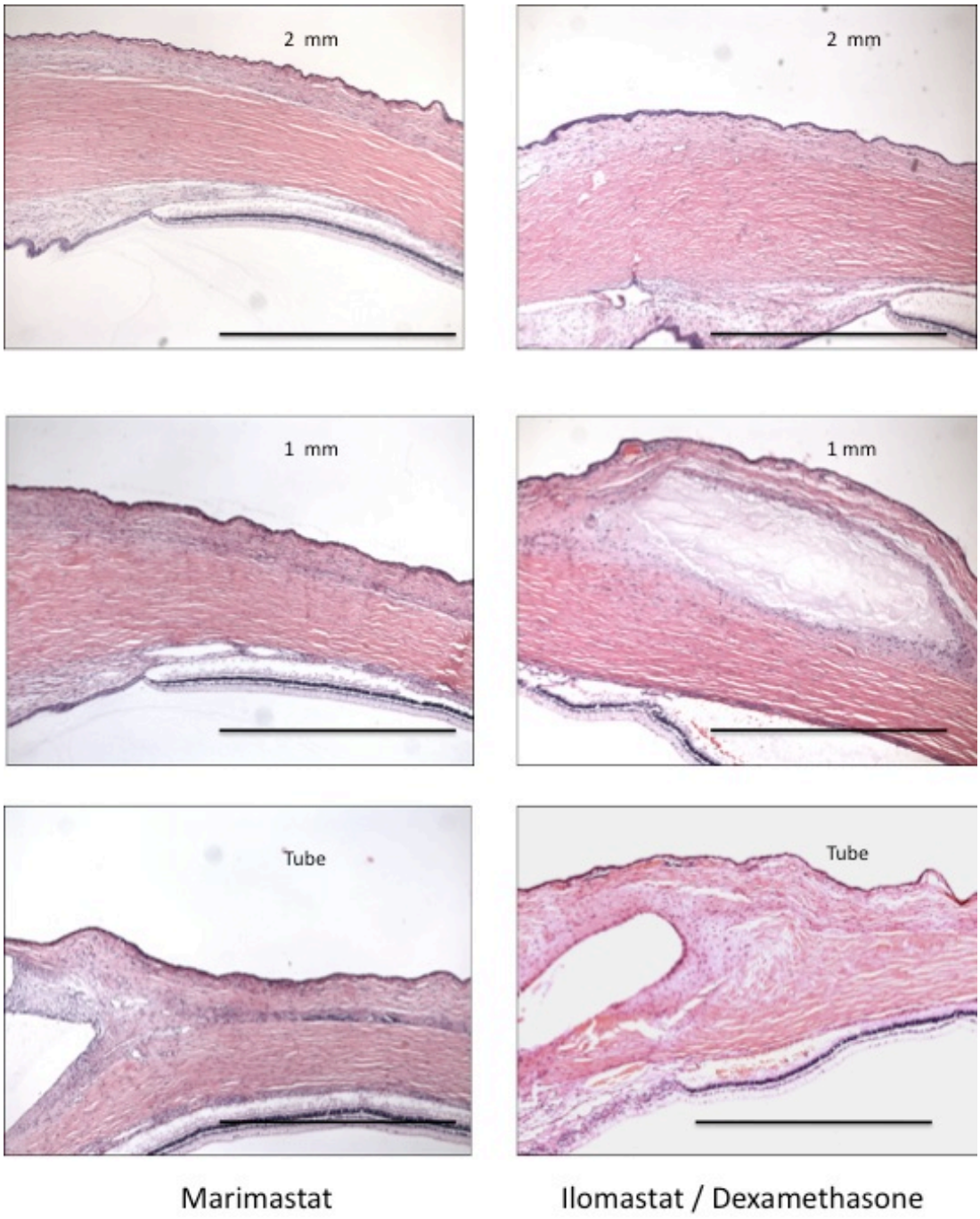

Figure 3-61 Sections of representative blebs of the marimastat and ilomastat / dexamethasone groups. Scale bar 1 mm. The planes of section were sagittal: bisecting the tube, 1 mm parallel and 2 mm parallel. The blebs treated with implants of ilomastat / dexamethasone exhibited significant inflammatory infiltrate and fibrosis, although less than the pure ilomastat implants in the first *in vivo* experiment.

3.4.6 Discussion

This *in vivo* experiment revealed results that require careful consideration. On the face of it the ilomastat / dexamethasone implants appeared to prolong the survival of the bleb. However, again there was more collagen deposition in the overlying conjunctiva in the implant treated groups than in the controls. It was increasingly clear from halfway through the experiment that the physical presence of an implant was contributing to the bleb outline (Figure 3-59). Furthermore from day 18 the intraocular pressure became greater than the baseline, and than in the other treatment groups; something that is counter intuitive to what would be expected in a functioning bleb, with dexamethasone believed to induce ocular hypertension due changes in the cytoskeletal structure of the trabecular meshwork. The marimastat treated group had the greatest MMPi dose with the greatest amount of MMPi in solution in the first 48 hours (assuming correlation with the *in vitro* data), yet although there was a significant difference in survival between the two groups, a third of the blebs failed on the same day as half of the sterile water treated group, and the remainder failed at the next time point suggesting little difference in efficacy. In the sterile water treated group (the negative control where no antiscarring treatment was given other than the standard postoperative dexamethasone injection), there was the least amount of eosinophilic staining consistent with collagen deposition.

Steroids are commonly used as therapy to reduce inflammation and prevent pathological consequences in disease processes. They are the mainstay of treatment in acute asthma, reducing the inflammation and oedema in the walls of bronchi (Dziedziczko and Banach-Wawrzeńczyk, 1997). In rheumatoid arthritis, an autoimmune disease where the immune system targets connective tissue resulting in joint destruction, steroids can reduce inflammation and symptoms (Bijlsma, 1999). In Crohn's disease, a chronic inflammatory disease of the gastrointestinal tract where scar formation can result in obstruction of the tract, steroids are often the first line of treatment in an exacerbation (Cottone et al., 2011). They are also the first line of treatment for a multitude of ocular inflammatory diseases including uveitis and thyroid eye disease (Saraiya and Goldstein, 2011) (Meyer, 2006).

Steroids are believed to interact directly with immune cells and have a myriad of effects (Weller et al., 1998). There is a reduction in circulating monocytes with steroid therapy: if humans are given a dose of 40 mg / kg of glucocorticoid the number of circulating lymphocytes drops from 2000 mm^{-3} to 500 mm^{-3} 6 hours after administration. IL1 production by monocytes in general is inhibited, which then results in an inhibition of T cell activation and less IL2 production. Indeed there is a generalised inhibition of the synthesis of inflammatory cytokines Il1, Il2, Il4, Il6, Il10 and TNFα. The mechanisms involved include the acceleration of IL1 mRNA breakdown and direct inhibition of the promoter regions for IL4, IL6 and Il10.

In comparison to the ilomastat implants in previous in vivo experiments, there was far less of an immune cell infiltrate around the dexamethasone / ilomastat combination implants on staining with haematoxylin and eosin. No dense "halo" was seen. This would indicate that having the addition of the steroid does reduce the inflammation, whether or not there was a significant contribution from the postoperative injection of dexamethasone (the only other difference in surgical technique for this *in vivo* compared to previous experiments).

Why then did the dexamethasone / ilomastat combination not lead to less collagen deposition than either the negative or positive control? Why too were the blebs not enlarged, diffuse and full of aqueous fluid? Basal cortisol levels in the blood in humans have been recorded as 351 nM and can increase by 300 nM (Zarković et al., 2008). Dexamethasone has a potency that is 25 to 30 times that of hydrocortisone (Cantrill et al., 1975). A study on the binding of dexamethasone to intact fibroblasts found a dissociation constant (K_D) of 3.47 ± 0.38 nM (Nakada et al., 1987), and can cause an inhibition of TNFα induced VEGF expression by 30 % at levels of 10^{-12} M (Raidl et al., 2007). The concentration of dexamethasone in this experiment should therefore have been at least at a therapeutic level even if the rig data was a gross overestimate of bleb dexamethasone concentration (Figure 3-45). Less foreign body encapsulation should also have readily allowed more MMPi dissolution. Again it would appear that the antagonistic effect of inactive solid drug is playing a significant role. Despite the presence of a highly potent, slowly dissolving steroid and a highly potent MMPi, the particulate effect is overriding. Interestingly the vascularity of all of the blebs throughout the experiment was relatively similar. It

may be that the injection of dexamethasone at the end of surgery was sufficient to cause this similarity.

Other possible mechanisms at play that may impair antiscarring efficacy are redundancy and resistance. MMPs can perform a number of functions and a particular function can be performed by a number of different MMPs (Hu et al., 2007). If the immune system is activated yet enzymes or other signalling molecules are inhibited, other ones can be upregulated to compensate (Nish and Medzhitov, 2011). Steroid resistance is well documented (Sibley and Tomkins, 1974) and may develop directly through glucocorticoid mediated inhibition of glucocorticoid receptor mRNA transcription. The half-life for this down regulation in human lymphocytes can be as fast as 120 minutes (Rosewicz et al., 1988). Inflammatory cytokines may also contribute to resistance. In asthma, a disease where the mechanism of steroid resistance is one of the most studied, IL1β and IL6 can form protein complexes with the glucocorticoid receptor preventing activation (Barnes and Adcock, 1995).

The mean bleb heights for the ilomastat / dexamethasone arms in this experiment were less than the recordings for the 2 mm ilomastat implants in the first in vivo experiment at comparable time points, particularly after day 15, even though the initial heights of the implants were greater. This is most likely due to the difference in inflammation between the two groups. A caveat must be made when comparing the experiments, for example the two groups of animals are different; the first experiment used males whilst the others used females. Little is known about the differences in scarring between rabbits, however in humans women are believed to scar less following myocardial infarction, and therefore may benefit from cardiac resynchronisation therapy more than men (Kwon et al., 2014).

Bleb height estimation is difficult and highly subjective. On the whole lower blebs led to clearer outlines of implants within the conjunctiva, and it could be determined that the spacer effect was contributing to the appearance of a bleb from day 18. As in the previous experiment it is not clear how much the spacer effect contributes to functionality. Furthermore if the bleb were not functional in the presence of an implant, would the appearance of the bleb be any different? The area of conjunctival

elevation would be significant. The conjunctiva has a thickness of approximately 0.4 mm judged on OCT. Even discounting any extra elevation caused by inflammation, an implant of 2 mm diameter and 0.6 mm height could raise the conjunctiva an area whose diameter is almost 1.5 x the implant diameter (2 + 0.4 + 0.4), and therefore mislead the observer into thinking a bleb was present (Figure 3-62).

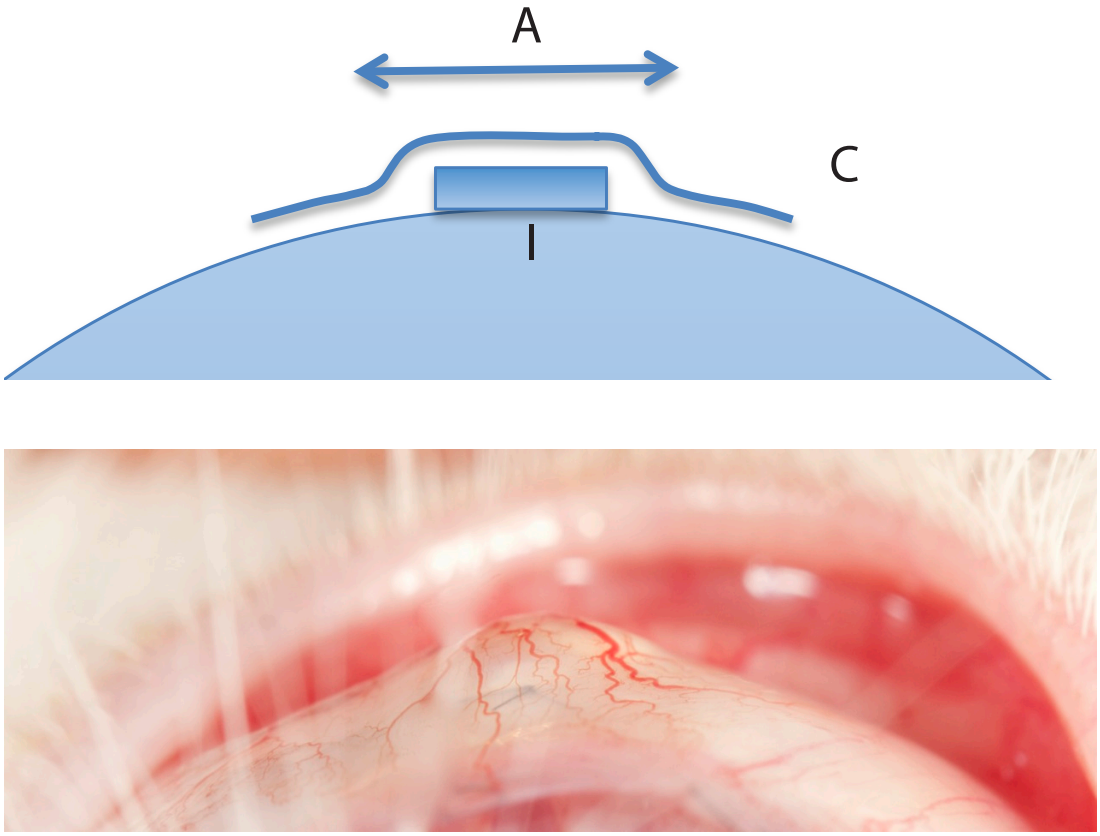

Figure 3-62 Diagram illustrating conjunctival elevation caused by an implant and representative photograph of dexamethasone / ilomastat implant at day 30. Legends: Implant (I); conjunctiva (C), length of conjunctival elevation (A).

The spacer effect may be in itself an advantage in developing an antiscarring agent. A number of studies have reported on their use in trabeculectomy surgery with variable success (Takeuchi et al., 2009). Where the principal of a spacer is most commonly used, however, is by glaucoma drainage devices such as the Ahmed, the Baerveldt and Molteno tubes. They structurally consist of a flexible plate attached to a tube, and rely on foreign body encapsulation around the plate to create a lake of aqueous in a Tenon's cyst (Rao et al., 2009; Filho and Sit, 2009). A randomised trial performed in the USA indicated that a device might even have a better success rate

than augmented trabeculectomy for patients that required repeat glaucoma surgery (Gedde et al., 2007a; Gedde et al., 2007b; Gedde et al., 2009). Little is understood about the foreign body reaction around implants, although some data from rabbits suggests that there are relatively few giant cells (Jung et al., 2013). Globes with Molteno implants have been studied histologically after patients' death (Molteno et al., 2009) The time an implant had been present varied widely (2 months to 20 years) but older capsules appeared to have newer cells with fibroblasts and other inflammatory cell types on the periphery and degenerate cells on the inside, suggestive of a continuous cell turnover.

The bleb of rabbit 14 (dexamethasone / ilomastat) had an unusual morphology of almost conical shape at day 15 that is not solely explained by the spacer effect. OCT revealed some fluid located around the implant at 14 days (Figure 3-59). However the edges of the base of this conjunctival cone appeared to be contracting in a similar way to the 'ring of steel' that is most often seen in the scarring process of limbal based trabeculectomies (Wells et al., 2003). Towards the end of the experiment this conical shape resolved. Histological analysis did not reveal any gross differences between this bleb and others of the same group other than the presence of less implant remnant. The changes in morphology of this bleb over time indicate how dynamic the process of wound healing is, and histological analysis at an earlier time point may have yielded differences between these blebs.

The rise in IOP in the ilomastat / dexamethasone treated group after day 18 indicates that drainage of aqueous is impaired. A rise in IOP in patients treated with topical steroids is not uncommon and can occur in up to 90% of primary open angle glaucoma patients due to changes in the trabecular meshwork. Mechanisms believed to be in play are the increased expression of glycosaminoglycans and the altered phagocytic activity of trabecular meshwork endothelial cells (Jones and Rhee, 2006). Topical dexamethasone can also cause a significant rise in the IOP of rabbits, particularly if they are young (Qin et al., 2010). The Ozurdex implant was found to cause a rise of more than 10 mm Hg in 17% of patients (Lobo et al., 2010). The findings raise the question as to whether there was drainage of aqueous into the blebs at this stage, i.e. that they were functional or whether the drainage of aqueous from the blebs is being impaired.

The blebs treated with marimastat failed to survive beyond day 24, although this treatment group had the highest dose of solubilised MMPi. It was hoped that the high dose of MMPi in solution would tip the balance in favour of dampening of inflammation and scarring away from the undissolved aggravating solid drug. However, MMPis are cytostatic and not cytotoxic, and it is likely that there was rapid clearance of the drug and the process of healing continued undeterred. As MMPs have wide reaching effects during the wound healing process, it is likely that an MMPi presence is required for the duration of increased activity of the cells involved.

A paradoxical finding in this experiment was that the negative control (sterile water treated group) exhibited minimal evidence of scarring, for example compared to the negative (ethylcellulose) control in the first experiment. This may have been due in part to the postoperative dexamethasone injection, but may also have been due to the remodelling behaviour of the animal. The rabbit is an aggressive model of scarring, however it is likely to be able to remodel extremely efficiently as well. Furthermore the animals are young, and younger animals heal more quickly. If histology is examined at day 30 only, a considerable proportion of the wound healing response may be missed (Bruno et al., 2007). In a diagram adapted from an analysis of cutaneous wound healing in humans it can be seen that sectioning at day 30 would be in the middle of the remodelling phase (Figure 3-63). In rabbits the wound healing process will be more rapid, and sectioning at day 30 may be after resolution of tissue architecture as found with the AZ 6357 implants. Of pivotal importance therefore in the evaluation of an antiscarring therapy is histological examination at multiple time points post surgery. Interestingly the MMC bleb of number 1 showed signs of toxicity, with tissue necrosis in the conjunctiva. The surgery for this animal was planned to be no different, however may represent a longer operation, this being the first rabbit to undergo the procedure. Similar blebs were seen in earlier and later studies

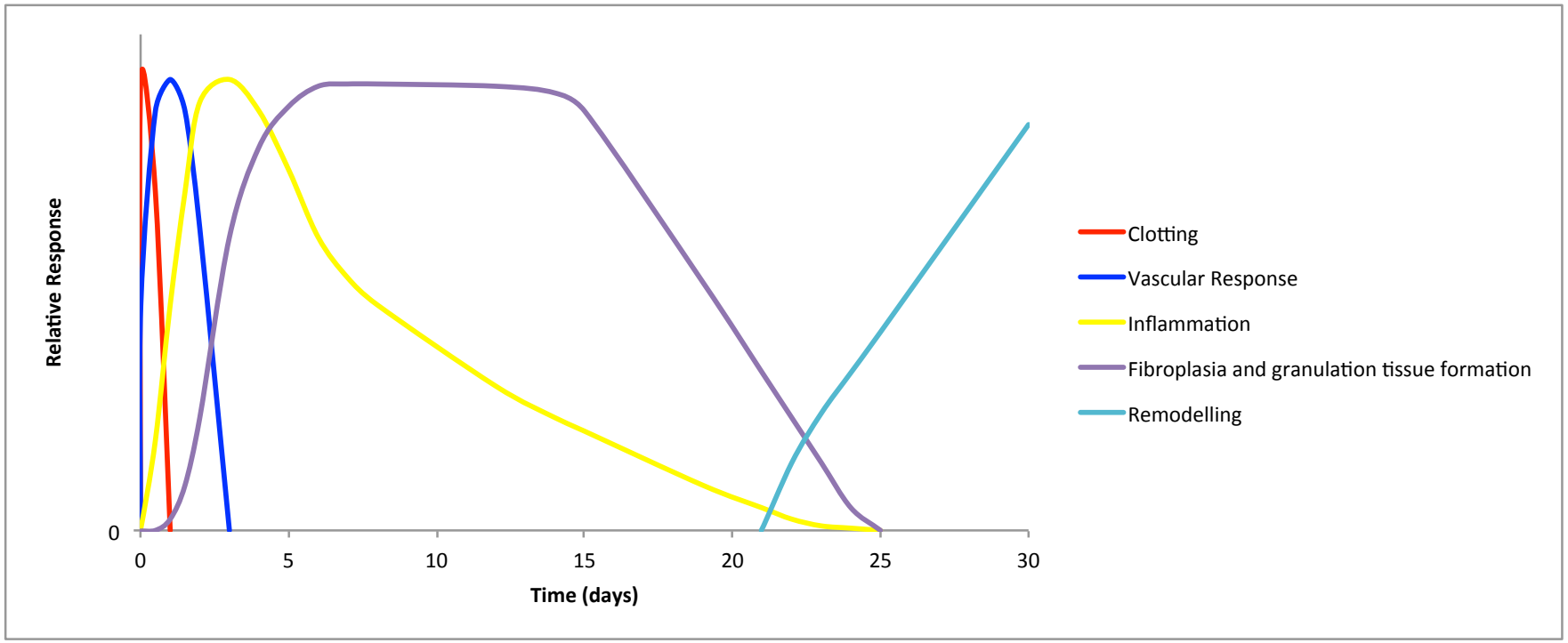

Figure 3-63 The stages of cutaneous wound healing in humans.

The dose of 1 mg dexamethasone was chosen for the *in vivo* study; the implants constituted with this dose released the greatest amount of drug and were therefore likely to be the most efficacious. High dose dexamethasone can cause toxicity however, and this also needed to be taken into account when considering the dose. Most ocular data is related to intravitreal injection (Nabih et al., 1991). One study found that up to 4.8 mg could be injected intravitreally without deleterious effect (Nabih et al., 1991). Kwak et al injected dexamethasone phosphate, in Dutch pigmented rabbits. Eyes enucleated after injection found that there were minimal changes at 800 mcg, but there was distinct vacuolation in between the outer plexiform layers and outer nuclear layers of the retina and photoreceptor degeneration at 1.2 mg dose (Kwak and D'Amico, 1992). They suggest that vacuolation might be related to impaired glucose transport. A number of studies have reported on the use of intravitreal sustained release devices that release dexamethasone (Chang-Lin et al., 2011; Cheng et al., 1995; Hainsworth et al., 1996; London et al., 2011). Ozurdex has recently been licenced for use in humans in the treatment of non-infectious uveitis and macular oedema associated with retinal vein occlusion (London et al., 2011). The dose of dexamethasone used is 0.7 mg. Minimal evidence of toxicity was seen in monkeys treated Ozurdex implants over the period of nine months (Chang-Lin et al., 2011). In this experiment there appeared to be some vacuolation of the goblet cells in the conjunctiva overlying the implants, and possibly some scattering of inflammatory cells in the sclera. It is not possible to be sure of whether the vacuolation of the goblet cells is related to that seen in the Muller cells of the retina after high dose dexamethasone exposure (Kwak and D'Amico, 1992).

Unlike pure ilomastat implants the dexamethasone / ilomastat combination implants were more fragile due to the less cohesive nature of dexamethasone. This is likely to have contributed to the variable release seen in the *in vitro* experiments and also to the fragmentation seen in rabbit number 14. In the formulation process one of the key challenges identified was to establish a method of mixing that resulted in the implants having consistent quantities of each drug, and for that ratio to be evenly dispersed throughout the implant. Freeze-drying a solution of ilomastat and dexamethasone using 40 % tert butanol was attempted: this would provide an

amorphous uniform mixture. However pressing the product was analogous to pressing powder snow and no implants could be formulated. Furthermore this state quickly changes with exposure to water, with crystallisation. Adding an excipient would have been necessary as a binding material, however this would have been outside our patent and the grant funding this research (for legal purposes dexamethasone was considered an active and not an excipient). Another method attempted was to use a fine sieve however this led to increased drug loss. It is not possible to be sure from these experiments of the uniformity of the implants and whether the powdered drug lost during pressing was consistently of the same proportions of drug. Further work would be required if this line of preparation was developed.

In the release experiments there was considerable variability in release not just between implants (as shown by the considerable size of the error bars) but also with time, with not just a steady decay. It is likely that the implants were not uniformly mixed with islands of pure ilomastat and dexamethasone, fracture lines could open up within the implant which would lead to greater surface area exposed to fluid, and greater drug dissolution dissolution. Although attempts were made to maintain the temperature of the rigs at a constant level there was still variability with the thermostatically controlled oil bath that may have affected drug release (temperature varied +/ 5 degrees in this experiment). Dexamethasone solubility is particularly affected by temperature and varies by a factor of 10 between 20 and 37 degrees centigrade (Yalkowsky and He, 2003).

The findings of these experiments indicate the challenges faced in developing a solid form of antiscarring agent, not only in terms of tissue response to the particulate microstructure of the tablet surface, but also in being able to determine what defines success in the in vivo model. Further work is required to determine functionality of the bleb, either through following a tracer injected into the anterior chamber or by modifying the model to make it hypertensive as has been done in the mouse in models to test treatments of optic nerve regeneration (Sappington et al., 2010). In an ocular hypertensive model IOP could then be used as an outcome measure. For a sustainable release antiscarring agent to be developed further work is required to make it non-particulate, either encased in a device or in liquid form.

3.5 Investigation into the release and efficacy of ilomastat in conjunction with dexamethasone, ilomastat / hyaluronic acid combinations and polymer coated ilomastat implants

In the previous experiment it was shown that using dexamethasone in combination with ilomastat the inflammatory response surrounding the implant was considerably less than ilomastat alone, however there was still the significant aggravating antagonistic effect of the non solubilised drug. It was postulated that reducing the dose size might tip the balance in favour of the active soluble moiety so long as a therapeutic level could be maintained. Mixing smaller drug doses to produce implants that were consistent in mass, uniform and unlikely to fragment was too great a challenge. It was possible, however, to formulate ilomastat and dexamethasone as individual 0.5 mg implants, which could be inserted together.

The combination of ilomastat with hyaluronic acid in an implant had shown potential as a candidate for formulation as an antiscarring implant in the 2nd in vivo experiment, with minimal evidence of foreign body reaction at day 30 and promotion of bleb survival. It was hypothesised that dissolving ilomastat in solution and combining with hyaluronic acid (HA) would enable the drug to be dispersed evenly throughout an implant. This approach is common in pharmaceutical science (Aulton and Taylor, 2013). After freeze drying and pressing, exposure to aqueous fluid would lead to rapid hydration and the implant becoming a gel. There would been less abrasion between implant and surrounding tissues, and enhanced drug dispersion. Both linear and cross-linked HA were investigated that might release drug at different rates. Cross-linked HA will become hydrated in the same way as non-cross-linked HA, but due to it being cross-linked, its dissolution from the subconjunctival space would, in theory, take more time.

Surrounding the pure ilomastat implant in the second *in vivo* study possibly showed less inflammation than the implant alone. It was postulated that surrounding a pure ilomastat implant with a freeze dried hyaluronic acid preparation would enable a reduction in inflammation, and this effect might be prolonged by using a preparation of hyaluronic acid that would be more likely to persist in the bleb. Based on previous experiments dried hyaluronic acid appeared to remain present for longer.

Masking the non-solubilised drug from cells that trigger an immune response whilst allowing drug dissolution may also reduce a foreign body reaction. A polymer known as POSS PCU developed by Alex Seifalian (UCL/Royal Free Hospital) has shown promise in humans when used as a cardiovascular stent (Tan et al., 2013). Other work has shown that it may also be used to make an artificial trachea as a replacement for one invaded by tumour that is able to integrate well into host tissue (Jungebluth et al., 2011)(Crowley et al., 2014). The polymer may also be coated in a substance such as an antibody to allow for enhanced efficacy after implantation (Tan et al., 2013). It was postulated that an ilomastat implant, coated in this low immunogenic polymer might allow drug dissolution, but without dendritic or immune cell access. As a drug-eluting device ideally the polymer would be degradable and resorb following dissolution. The Seifailian group were in the process of developing a biodegradable version, however this was at a concept stage. Non-degradable material is not necessarily contraindicated in the sub conjunctival space, as shown by the use of glaucoma drainage devices such as the Ahmed or Baerveldt tubes.

The outcome of "success" when expressed as Kaplan Meier curve or "bleb survival" in previous *in vivo* experiments is ambiguous. Treatment arms with a persisting implant have shown promotion of bleb survival where the interpretation of "bleb survival" may have been significantly affected by the implant's physical presence: this spacer effect will contribute to bleb appearance and may contribute to bleb functionality. Furthermore it was apparent that the deposition of scar tissue or inflammation did not correlate with bleb survival in the implant treatment arms. Considerable conjunctival re modelling may have occurred in the negative control that resulted in the little collagen deposition seen. A shorter study was therefore planned examining the blebs at the earlier time point of 14 days.

To attempt to determine a method of testing bleb functionality that did not rely simply on the appearance of a bleb the use of a tracer was investigated. Indocyanine green (ICG)(Cardiogreen) is a negatively charged polymethine dye that forms noncovalent fluorescent complexes with proteins. This fluorescent dye is commonly used in the clinic to image the choroidal vasculature, and delineate structures during ocular surgery such as the inner limiting membrane in macular hole repair, corneal

tissue in keratoplasty, and the lens capsule during cataract extraction (Rodrigues et al., 2009). It was hypothesised that an injection of ICG into the anterior chamber under terminal anaesthetic would result in ICG being carried through the drainage tube, and diffuse throughout the bleb. This would enable the dimensions to be determined, and bleb volume.

3.5.1 Scanning electron microscope analysis

Coating the implants was not trivial. The polymer is only soluble in dimethylacetamide (DMAC), which has the potential to be significantly hepatotoxic (Kennedy and Sherman, 1986). The implants were spray coated using an applicator. The implants were then washed three times in water to remove the DMAC after they had been spray coated (Seifailian group personal communication). The polymer coated implant exhibited a smooth surface covering the crystalline drug beneath (Figure 3-64). There were a number of holes / pits however up to 20 micrometres in diameter (Figure 3-65).

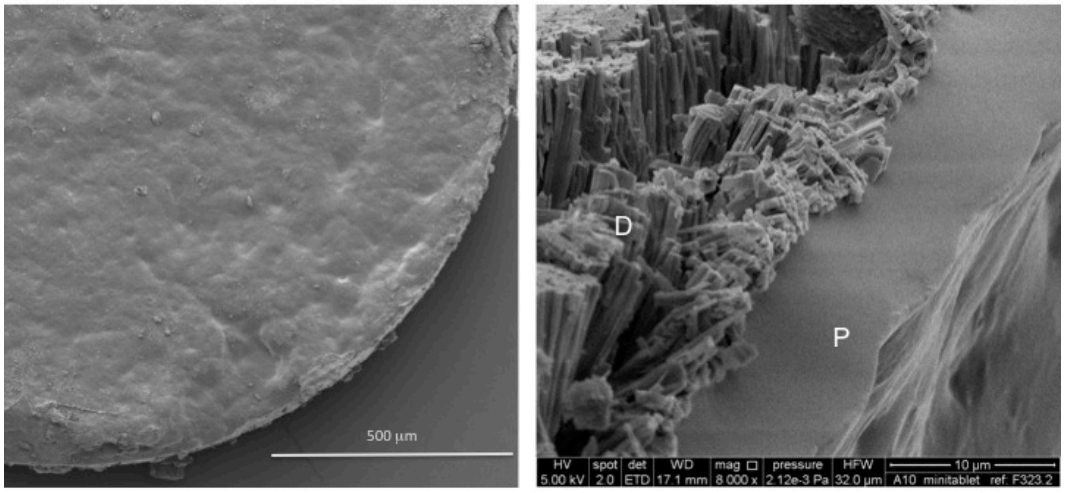

Figure 3-64 Scanning electron micrograph of polymer coated implant. A cut edge revealed smooth coating (P) over the crystalline drug (D). The pictures show a polymer spray-coated 2 mm implant. The cut edge shows how the polymer might be able to mask the particulate crystalline nature of the drug.

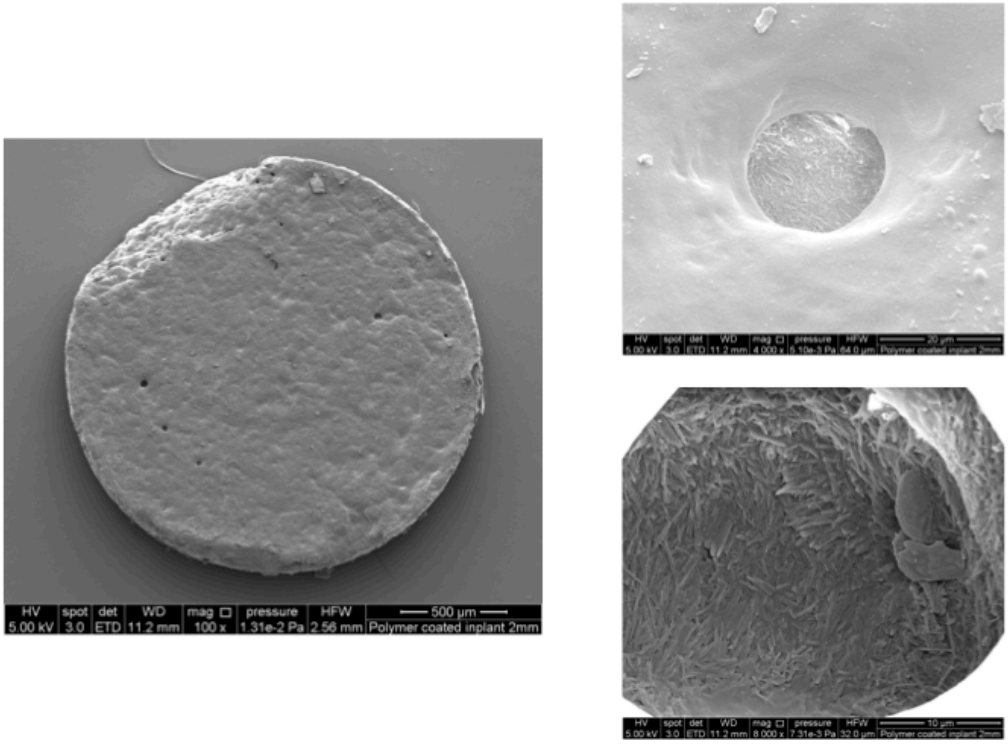

Figure 3-65 Images of increasing magnification of the implant surface clockwise from left, illustrating pits and crystalline drug beneath. Defects although useful to allow drug dissolution, if as large as shown (20 µm) would allow immune cell access.

3.5.2 In vitro release

3.5.2.1 Release from ilomastat 1 mm and dexamethasone 1 mm implants

The release of ilomastat from the rigs containing individual 1 mm ilomastat and 1mm dexamethasone implants side by side resulted in the maintenance of a drug concentration of > 10 mM for 15 days for ilomastat and 16 days for dexamethasone (Figure 3-62). The peaks concentration of ilomastat and dexamethasone were 49 mM and 34 mM respectively. The appearance of the cumulative release for the ilomastat appeared similar to that of the 1 mm implants examined without the dexamethasone in previous experiments (Figure 3-66).

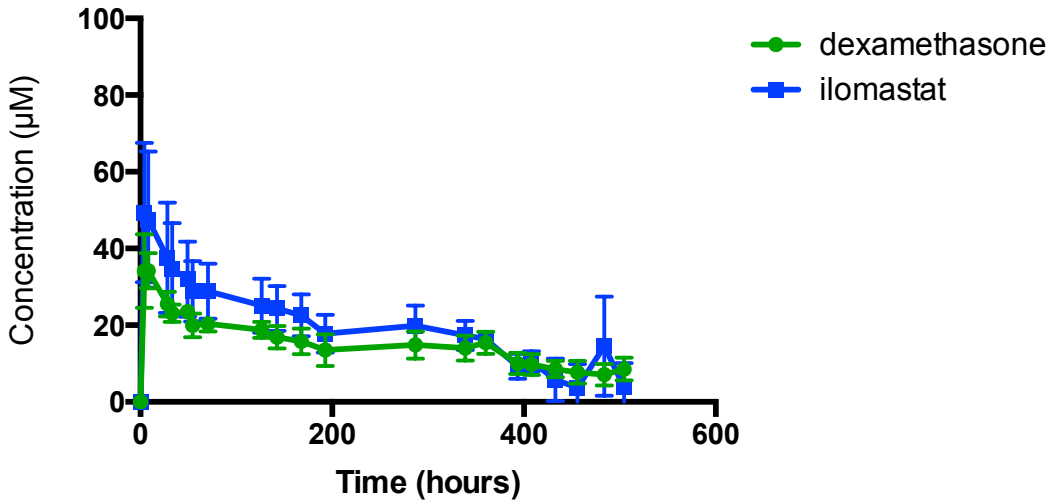

Figure 3-66 Ilomastat and dexamethasone released from implants of ilomastat (1 mm, 0.46 mg) and dexamethasone (1 mm, 0.5 mg) over time (n = 3). A mean concentration of ilomastat of > 10 µM was maintained for 15 days and a mean concentration of dexamethasone of > 10 µM was maintained for 16 days. Flow rate 2 ul/min.

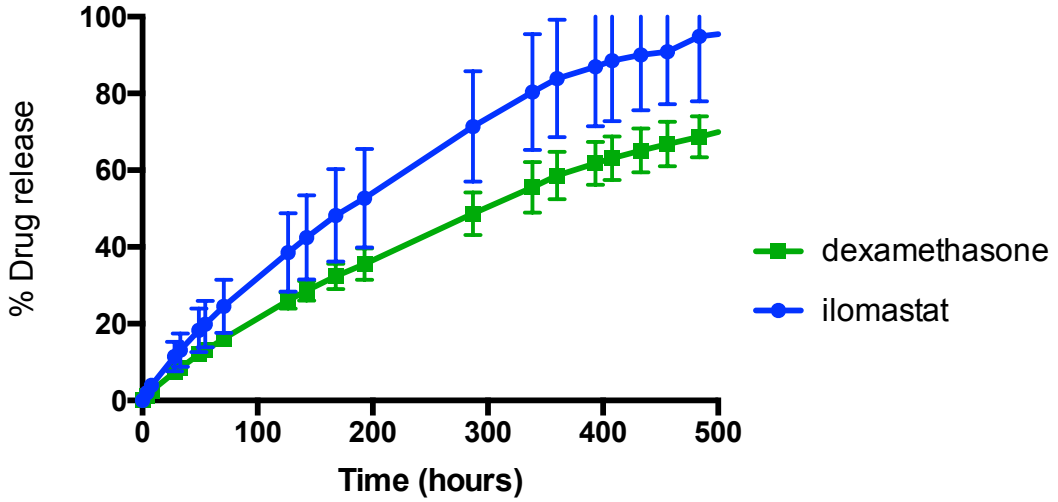

Figure 3-67 Cumulative mean percentage release of ilomastat 1 mm and dexamethasone 1 mm implants over time.

3.5.2.2 Ilomastat release from polymer coated 2 mm implants

Ilomastat release from the POSS PCU polymer coated implants was at a slower rate than for previous experiments using 2 mm implants. It was not possible to determine the exact quantity of drug present after coating by the polymer, however given that overall mass of the implants was similar it is likely that some of the drug dissolved in the solvent (DMAC) used in the coating process. Further drug will have dissolved in the washing process. A concentration of > 10 μM was maintained for over 34 days (Figure 3-68, Figure 3-69). The peak concentration of ilomastat was 38 μM. At this point a small shell of polymer could be seen on the base of the rig chamber (Figure 3-70). No defects were seen macroscopically, however any manipulation caused damage to the thin and fragile shell.

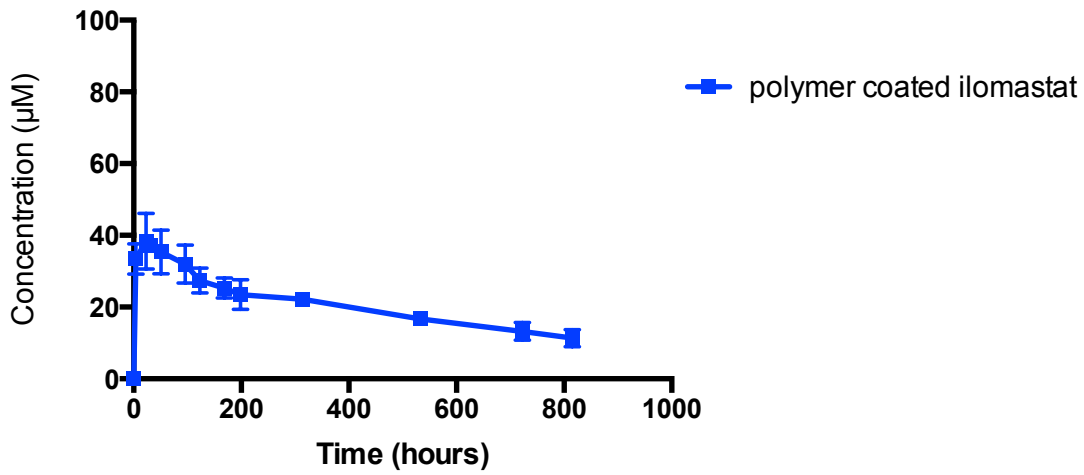

Figure 3-68 Mean concentration of ilomastat released from polymer coated 2 mm ilomastat implants (n = 3). Presumed mean mass of drug = 1 mg rigs (n = 3) with time. A concentration of > 10 μM was maintained for 34 days.

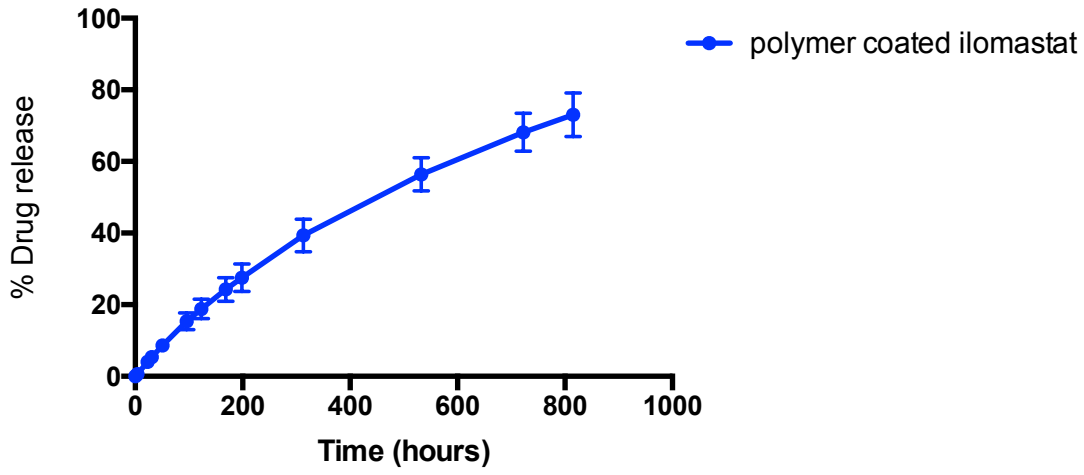

Figure 3-69 Cumulative release of ilomastat over time from polymer coated implants.

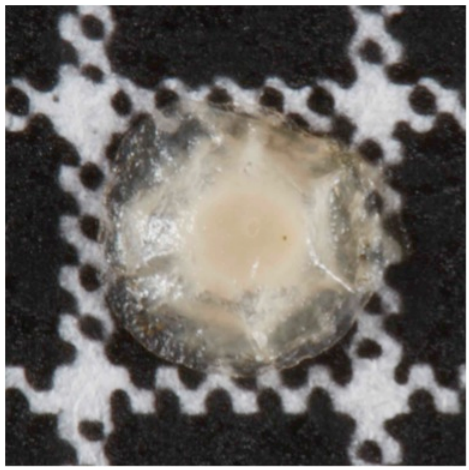

Figure 3-70 Polymer shell around implant remnant after 34 days of release experiment. Distance between lines is 2 mm. Macroscopically no defects could be seen before removal, however the casing was delicate and any manipulation resulted in the casing crumpling.

3.5.2.3 Ilomastat release from Healon GV / ilomastat combination

The release of ilomastat from combination implants of Healon GV (3 mg) and ilomastat (1 mg) took a little over 10 days (Figure 3-71, Figure 3-72). A concentration of > 10 μM was maintained for 9 days. The maximum concentration achieved was 210 μM.

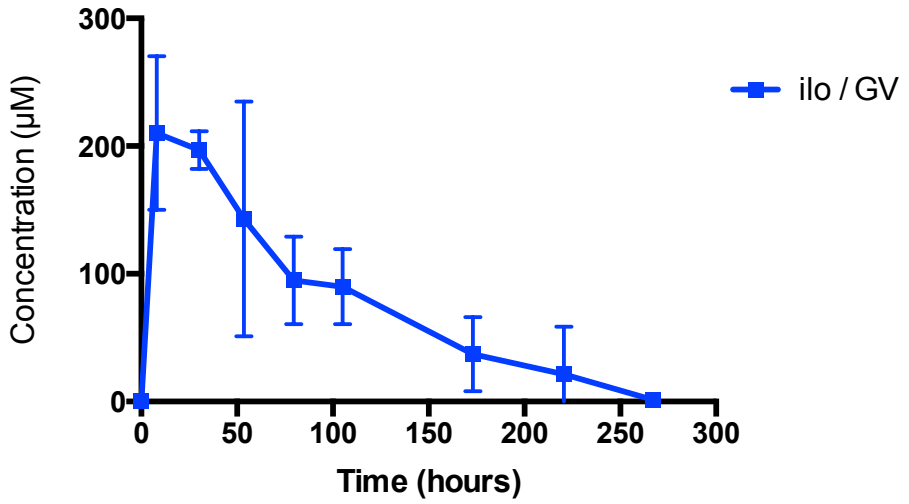

Figure 3-71 Ilomastat release from the combination implants ilomastat / Healon GV. Combination implants consisted of 1 mg ilomastat and 3 mg of hyaluronic acid (Healon GV), mixed as a solution, freeze dried and pressed into an implant (n = 3). A concentration of > 10 µM was maintained for 9 days.

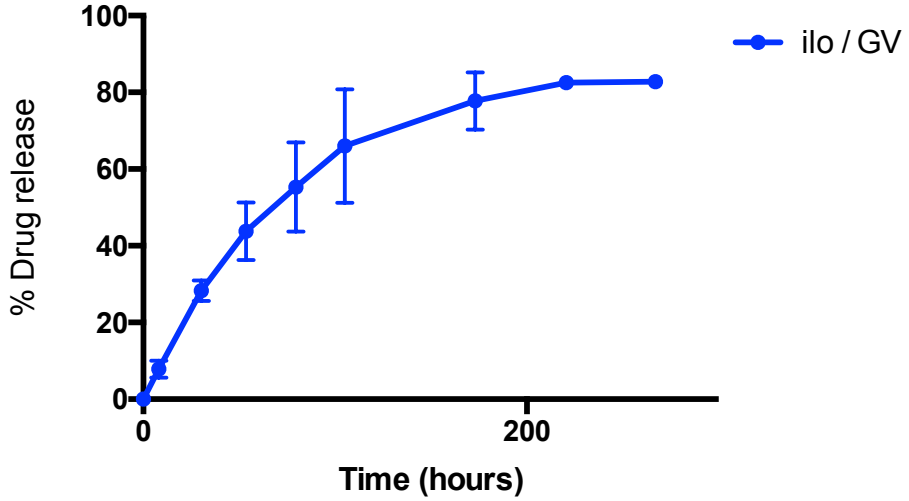

Figure 3-72 Cumulative release of ilomastat from Healon GV / ilomastat combination implants.

3.5.2.4 Ilomastat release from Healaflow / ilomastat combination implants

The release of ilomastat from combination implants of Healaflow (3 mg) and ilomastat (1 mg) lasted 32 days (Figure -3-73, Figure 3-74). A concentration of > 10 µM was maintained for 27 days. The maximum concentration reached was 212 µM.

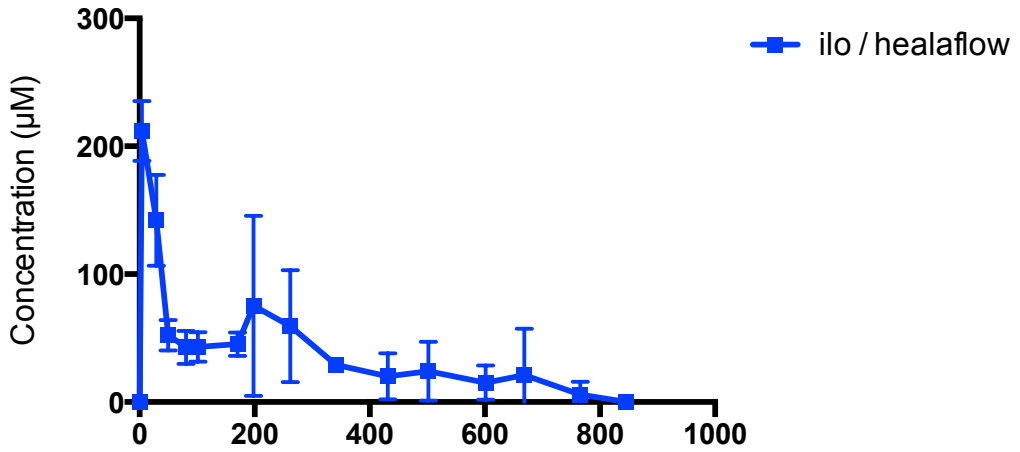

Figure -3-73. Ilomastat release from the combination implants Healaflow / ilomastat. Combination implants consisted of 1 mg ilomastat and 3 mg of cross-linked hyaluronic acid (Healaflow), mixed as a solution, freeze dried and pressed into an implant (n = 3). A concentration of > 10 µM was maintained for 27 days.

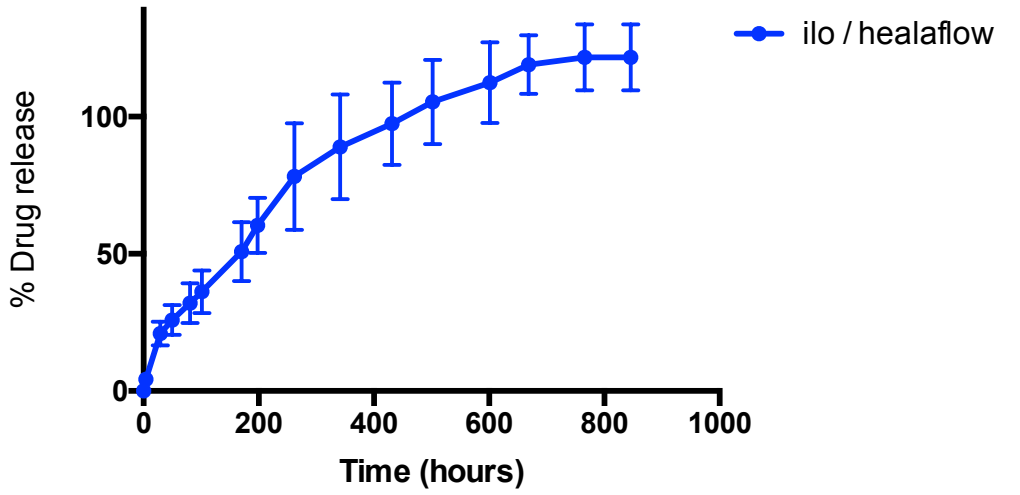

Figure 3-74 Cumulative release of ilomastat from Healaflow / ilomastat combination implants. Error bars indicate SD.

3.5.2.5 Ilomastat release from sandwich implants

The drug release results of ilomastat from 2 mm implants constructed from pure drug that had a mixture of freeze-dried hyaluronic acid pressed on either side, so called

'sandwich implants' are illustrated in Figure 3-75. Fabrication and collection of samples for in vitro analysis were performed by S Awwad and G Sharma. An ilomastat concentration of > 10 μM was maintained for 14 days. The mean maximum concentration achieved was 97 μM.

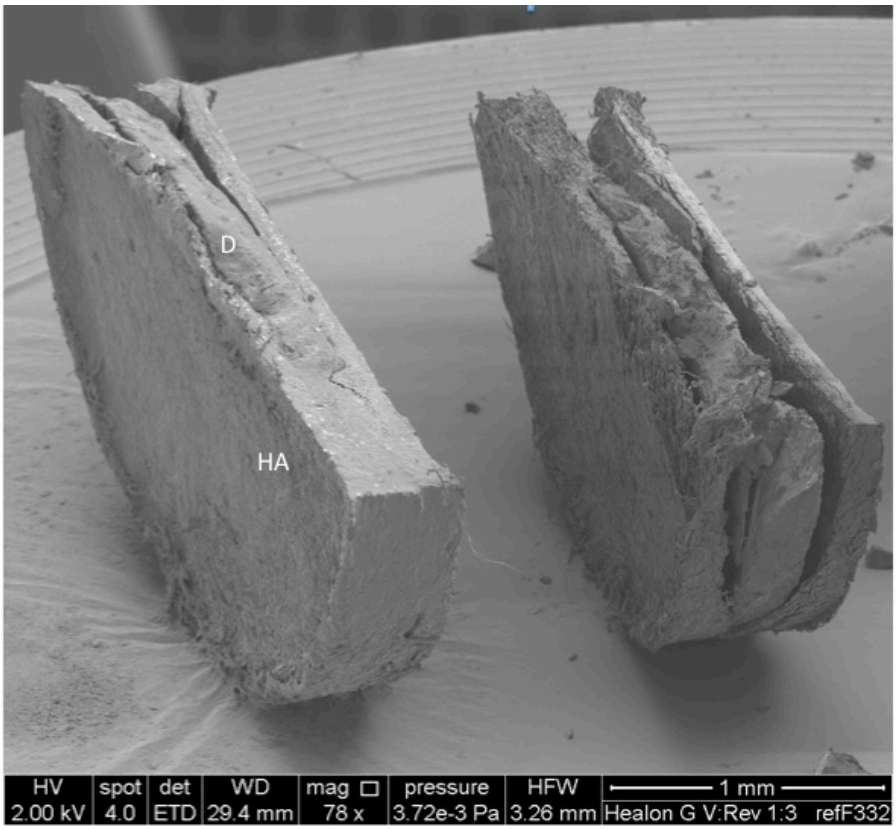

Figure 3-75 Scanning electron micrograph of a sandwich implant. Picture displays implants cut in half with 2 mm diameter drug implant (D) and 3 mm diameter freeze dried cross-linked / non cross-linked hyaluronic acid mixture (1:3 Revanesse: Healon GV) on either side (HA). Mean mass of drug = 1 mg. Mean mass of hyaluronic acid = 3 mg.

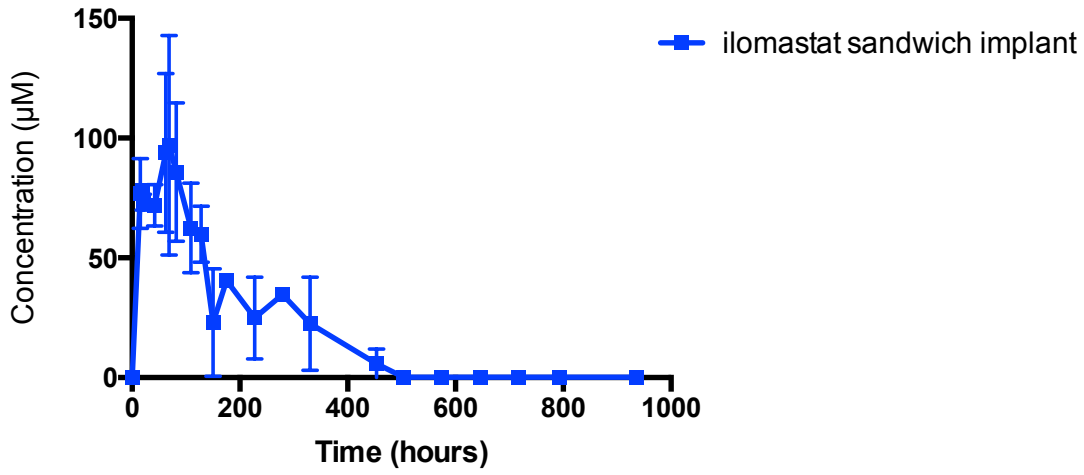

Figure 3-76 Concentration of ilomastat released with time from sandwich implants (n=3). Sandwich implants consisted of 2 mm 1 mg pure ilomastat implants (D) with 3 mm diameter freeze dried cross-linked / non cross-linked hyaluronic acid mixture (1:3 Revanesse: Healon GV) pressed on either side (HA). A concentration of > 10 mM was maintained for at least 13 days.

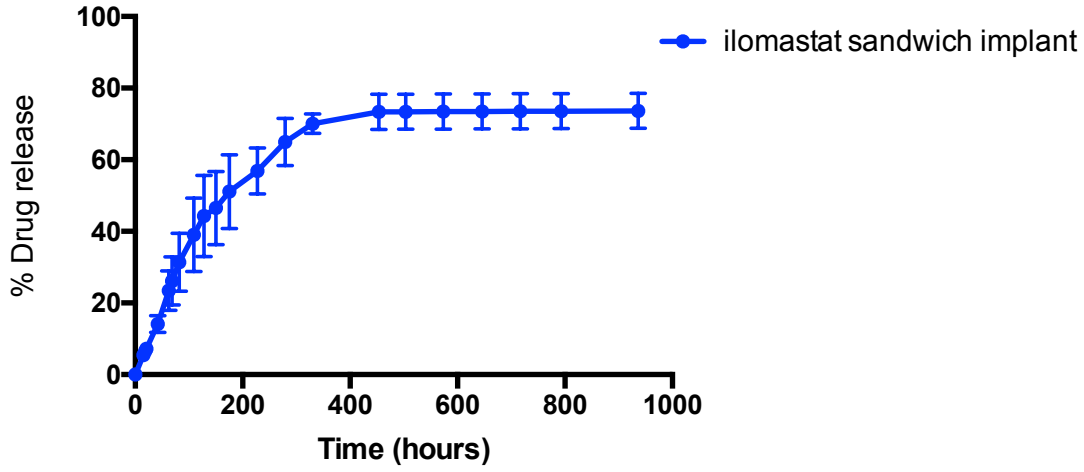

Figure 3-77 Mean cumulative ilomastat release from the sandwich implants (n = 3). Error bars indicate SD.

3.5.3 In vivo experiment

The six arms that were investigated in a 24 rabbit experiment (n = 4 each arm) for a 15 day study (as this was a pilot a time point was chosen that would hope to achieve significant differences in histology and reduce expense and time):

1) An ilomastat 1 mm 0.5 mg implant and a dexamethasone 1 mm 0.5 mg implant

2) An ilomastat 2 mm 1mg (presumed) implant coated with POSS PCU polymer provided by Alex Seifalian, UCL/Royal Free Hospital.

3) A combination of ilomastat 1 mg and hyaluronic acid 3 mg (Healon GV), which was freeze dried and pressed into a 3 mm implant.

4) A combination of ilomastat 1 mg and cross-linked hyaluronic acid 3 mg (Healaflow), which was freeze dried and pressed into a 3 mm implant.

5) An ilomastat 2 mm 1 mg implant with freeze dried hyaluronic acid mixture - hyaluronic acid / cross linked hyaluronic acid ratio 1:3 (Healon GV / Revanesse) – pressed on either side of the implant in a 3 mm punch and die. This arm would be referred to as the sandwich implant arm. The ratio of hyaluronic acids and their ratio were chosen according to most uniform appearing implants with the most consistent release characteristics (performed and communicated by S. Awwad).

6) Sterile water group (negative control).

3.5.3.1 Survival and bleb surface area

All blebs survived until day 14 with the exception of one bleb in the sterile water group, which failed at that time point. One animal in the ilomastat / Healon GV group developed an endophthalmitis at day 3 and was terminated. The mean bleb surface area was greater for the sandwich implants than the other groups from day 10 (Figure 3-78).

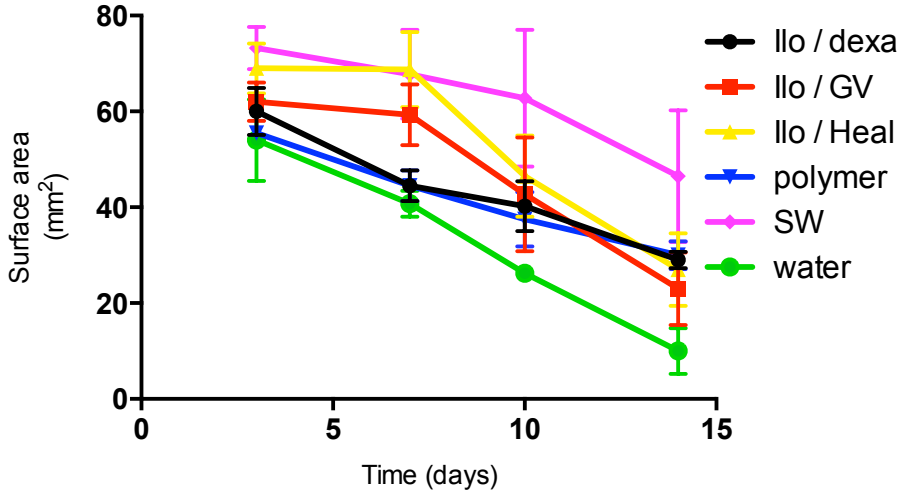

Figure 3-78 Bleb surface area of the six groups. Legends: ilo / dexa, individual implants of ilomastat 1 mm 0.5 mg and dexamethasone 1 mm 0.5 mg; ilo / GV, ilomastat 1 mg combined with Healon GV 3 mg (3 mm); ilo / Heal, ilomastat 1 mg combined with Healaflow 3 mg (3 mm); polymer, ilomastat 2 mm 1mg coated in polymer provided by Alex Seifalian; SW, sandwich implant consisting of ilomastat 2 mm 1 mg with hyaluronic acid combination (3 mg) pressed on either side (3 mm); Water, sterile water applied in the same way as MMC (negative control). The sandwich (SW) implants maintained a greater mean bleb surface area than the other groups from day 10. Error bars indicate standard error. Total number of rabbits = 24, n = 4 each arm.

3.5.3.2 Bleb Height

The heights of the blebs in the ilomastat / Healaflow arms and sandwich implants were consistently greater than the other arms for the duration of the second half of the experiment (Figure 3-79).

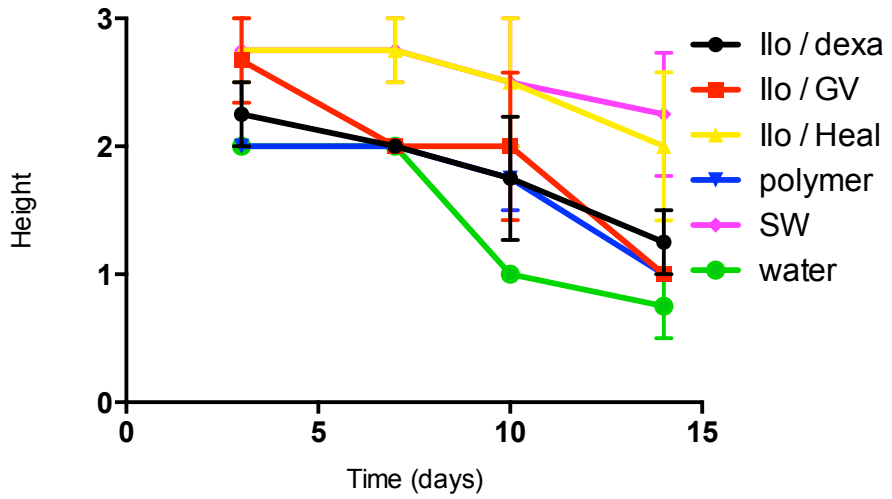

Figure 3-79 Bleb height of the six groups over time. Bleb height was graded as 0, flat; 1, shallow/formed; 2, elevated < 2 mm and 3, high > 2 mm. From day 7 the sandwich and ilomastat / Healaflow groups maintained higher blebs. Error bars indicate standard error.

3.5.3.3 Intraocular pressure

There was an initial fall in IOP in all groups and a return to baseline in five of the groups. The IOP of the sandwich implant group appeared to be consistently lower (Figure 3-80).

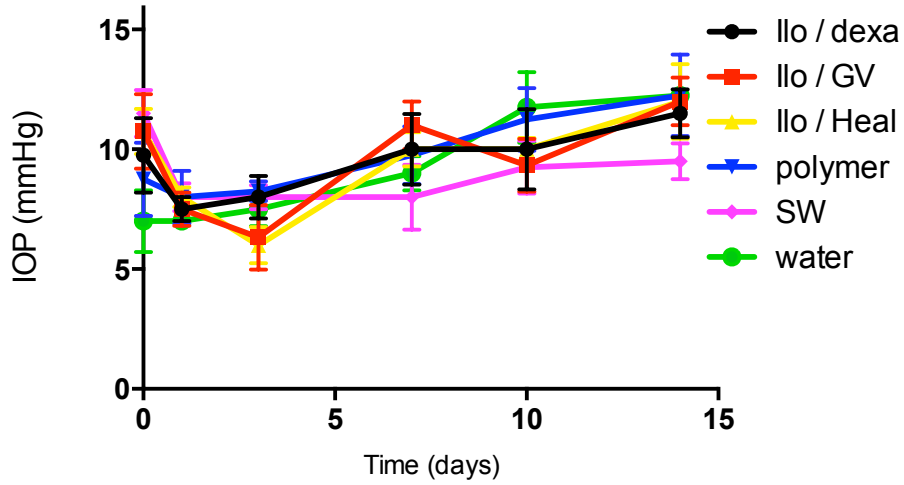

Figure 3-80 Intraocular pressure for all six groups. The sandwich implants appeared to maintain a lower IOP after day 7 of the experiment compared to the other treatment arms.

3.5.4 Bleb vascularity

There was considerable variation in vascularity across the six arms. Those blebs of the sandwich implant treated arm were the most hyperaemic and those of the sterile water treated group the least hyperaemic (Figure 3-81).

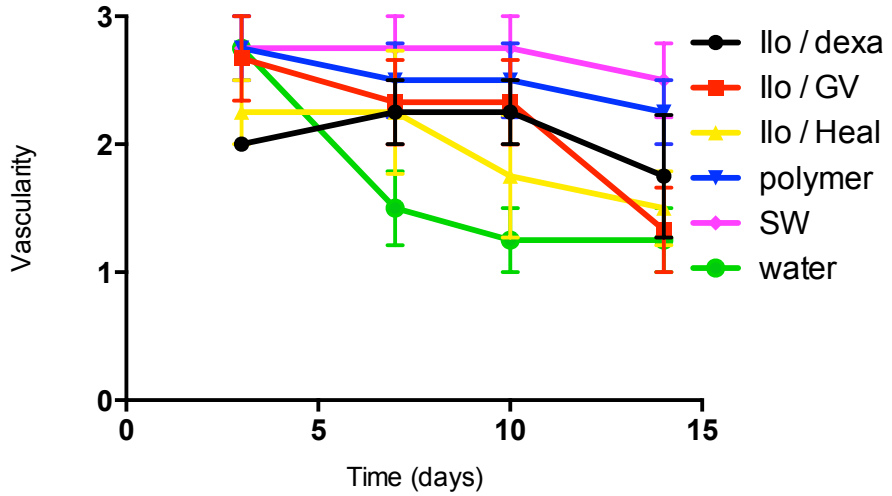

Figure 3-81 Bleb vascularity for the six groups. The vascularity was graded as 0 = avascular, 1 = normal, 2 = hyperaemic, 3 = very hyperaemic. The blebs with the greatest hyperaemia were those of the sandwich treated group and those with the least hyperaemia were those of the sterile water treated group.

3.5.5 Bleb morphology

The ilomastat / dexamethasone treated blebs had conspicuous implants in three of four animals at day 10. At this stage the contours of the bleb surface outlined the shape of the implants, indicating little adjacent tissue or fluid. In a similar way the polymer coated implants were conspicuous from day 10 in all four animals, and their physical presence appeared to contribute to the bleb shape from this point (Figure 3-82). The bleb morphology in the sandwich, Healaflow / ilomastat, and Healon GV / ilomastat treatment arms also appeared to be affected by the compounds within, with the surface contours of some blebs resembling more of a "bell shape." Furthermore some of the contents appeared to precipitate down the tube into the anterior chamber (Figure 3-84). Those of the Healon GV / ilomastat implant treated blebs had the least disturbance (Figure 3-83).

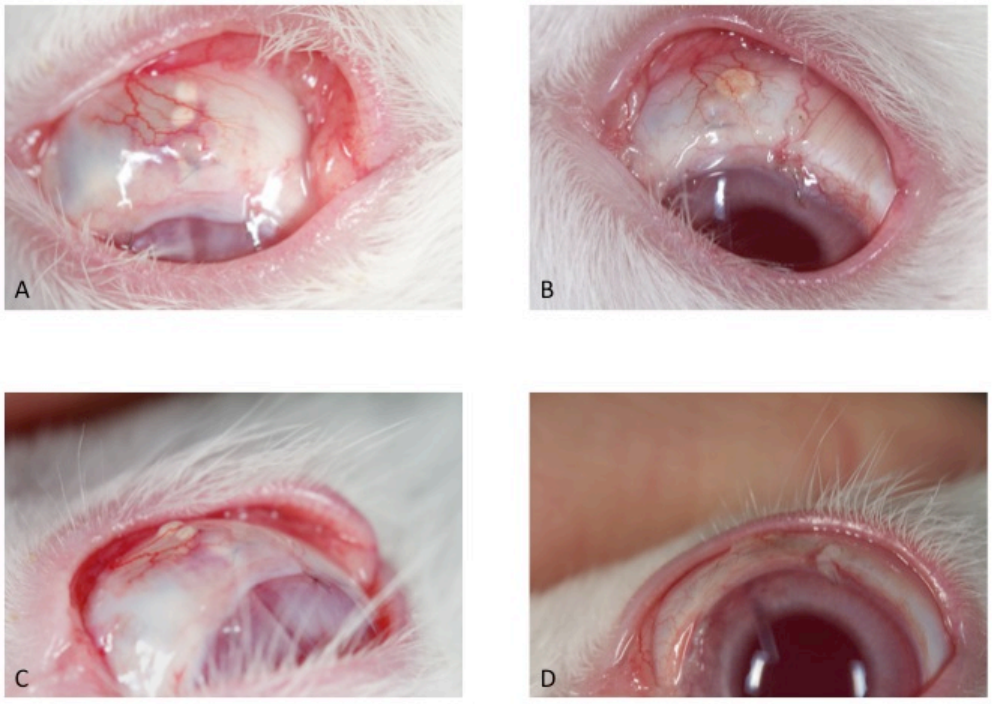

Figure 3-82 Representative photographs of blebs of the dexamethasone / ilomastat and polymer coated implants. Both the dexamethasone and ilomastat blebs were conspicuous by day 10. (A). A side view illustrates how both implants affect the surface bleb contour (C). The polymer coated implants were conspicuous at day 10 (B) and affected the bleb surface contour in a similar way (D).

Figure 3-83 Photographs of the bleb morphology of the hyaluronic acid / ilomastat combinations and the sterile water treated group. Three of the sandwich implant group had the most hyperaemic, raised blebs (E). The Healaflow / ilomastat blebs appeared less vascular, however were just as "bell shaped" in three of them (F). In this group the blebs appeared to have an opaque substance within. In one animal there were white clumps of material that passed down the tube and were found to precipitate in the anterior chamber in a similar way to the pseudohypopyon seen in phacolytic glaucoma though no anterior uveitis or fibrin in the anterior chamber was seen (see below). The ilomastat / Healon GV treated blebs were lower and less bell shaped (G). The blebs of the sterile water treated group were the lowest and had the least vascularity (H).

Figure 3-84 Precipitation of Healaflow / ilomastat in the anterior chamber. This can be seen at the end of the tube.

3.5.6 Testing of Bleb functionality using Indocyanine Green

Under terminal anaesthesia one animal from each treatment group arm, chosen at random, and 0.05 mls of ICG was injected into the anterior chamber. To be sure there was no artificial IOP rise that might significantly alter the progress of dye into the bleb a pressure transducer was inserted into the anterior chamber to monitor intracameral IOP and 0.05 mls of aqueous was withdrawn prior to ICG injection (Figure 3-85, Figure 3-86).

ICG injection resulted in the anterior chamber being filled with fluorescent dye. However, despite attempts to keep the globe surface dry using tissue and injecting the dye from an inferior position, dye was found to contaminate the surface of the conjunctiva resulting in a 'false fluorescence' from the bleb (Figure 3-87, panel within). After 30 minutes no dye was found to have entered the bleb area via the tube. Instead a number of blebs exhibited hyperfluorescence related to the dye entering the venous system, systemic circulation and bleb vasculature (Figure 3-88).

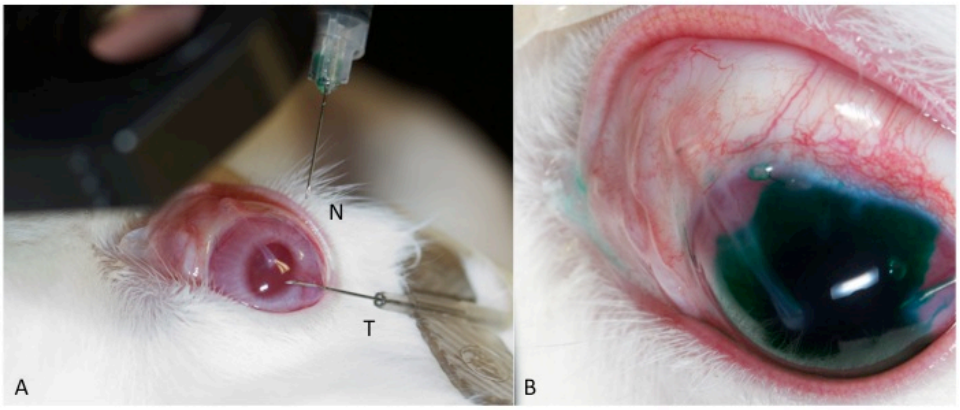

Figure 3-85(A) Transducer (T) and ICG needle (N) insertion into the anterior chamber. (B) anterior chamber filled with ICG.

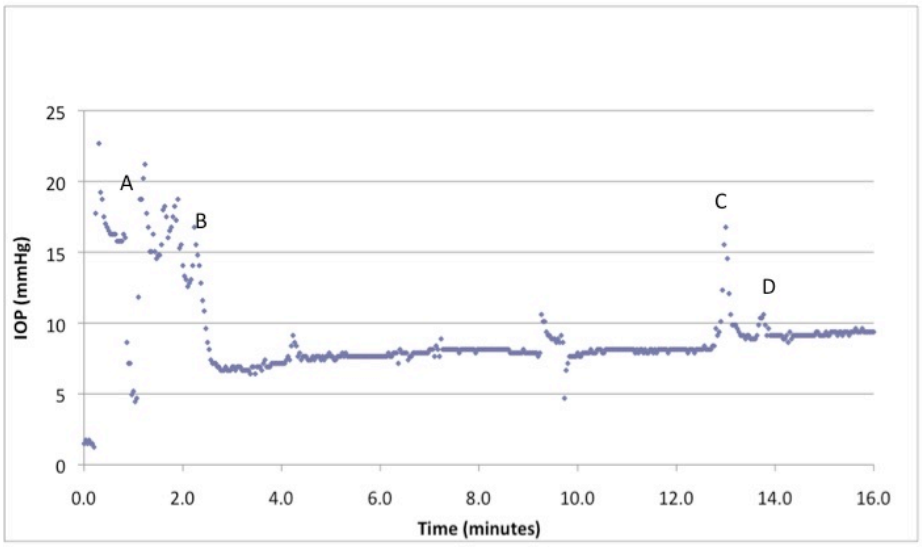

Figure 3-86 Changes in IOP with ICG insertion into the anterior chamber. Data displays intracameral IOP measured every 2 seconds and illustrates how IOP changes with transducer needle insertion (A), removal of 0.1 mls of aqueous by insulin syringe (B), insertion of syringe containing ICG (C) and injection of ICG (0.1mls)(D).

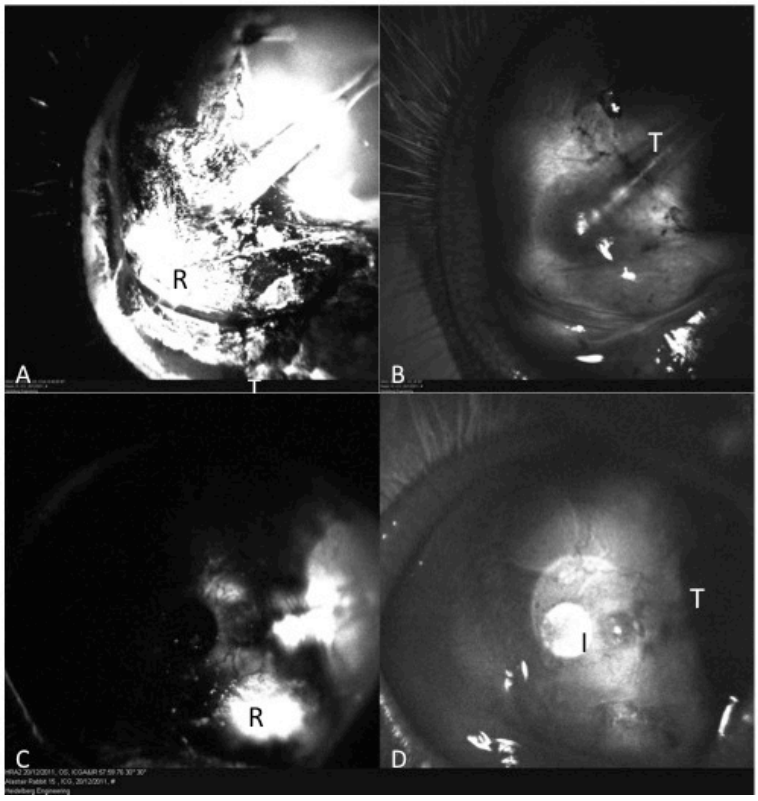

Figure 3-87 Fluorescence from ICG dye injected blebs illustrating hyperfluorescence from dye leakage onto the conjunctival surface. Pictures display dye and red-free (without dye) from sterile water treated group (A and B respectively) and polymer coated implant (C and D respectively). Legends: R; hyperfluorescence from ICG dye leakage onto the conjunctival surface, T; tube, I; implant.

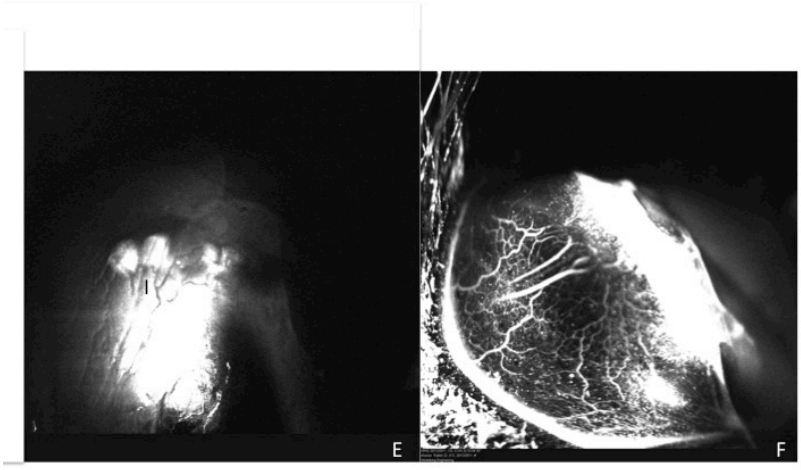

Figure 3-88 ICG hyperfluorescence in the bleb blood vessels. Pictures display red-free (E) and dye fluorescence (F) from the bleb area of a rabbit treated with dexamethasone / ilomastat implants. The implants can be seen in the red-free photograph and the dye hyperfluorescence outlines the vasculature, not the bleb interior as anticipated.

3.5.7 Histology

Implants were located in all of the ilomastat and dexamethasone treated groups. Where implants were not found at the level of the drainage tube they were found in adjacent sections.. In the rabbits treated with the dexamethasone and ilomastat 1 mm implants there were a scattering of inflammatory cells and adjacent fibroblasts. There were no apparent differences in inflammatory cell distribution between the two implants in any single rabbit (Figure 3-89).

All four of the polymer coated implants were located in the sections either in the same plane as the drainage tube or in adjacent sections. Around the pink refractile drug remnant there were also associated elongated pieces of clear snake-like substance consistent with the polymer. Above and below the polymer coated implant there were few inflammatory cells. There were however clusters of inflammatory cells at either end of most of the implants associated with gaps in the polymer coat, and in one particular section of (1 mm away from the drainage tube of rabbit 21) the cluster of inflammatory cells were associated with conjunctival vessel development.

All three of the Healon GV / ilomastat implant treated blebs had varying degrees of inflammatory cell infiltrate located in the region where the implant was placed. Numerous polymorphs, macrophages and lymphocytes were seen distributed throughout the subconjunctival area. Associated with these were small pink refractile islands that had cells including Langhans' cells associated with them.

A significant inflammatory infiltrate was seen in three of four of the Healaflow / ilomastat treated blebs. In one of the Healaflow / ilomastat treated blebs the histology was less clear with the repeated fracturing of the tissue during sectioning.

The sandwich implant treated blebs had significant inflammatory cell infiltrate in three of the four animals. Spaces were found between the significant foci of infiltrate. Surrounding the inflammation was an encapsulating band of fibroblasts.

Sections of blebs in the sterile water group exhibited an inflammatory response around the drainage tube. Behind the tube however the conjunctiva had a more open morphology.

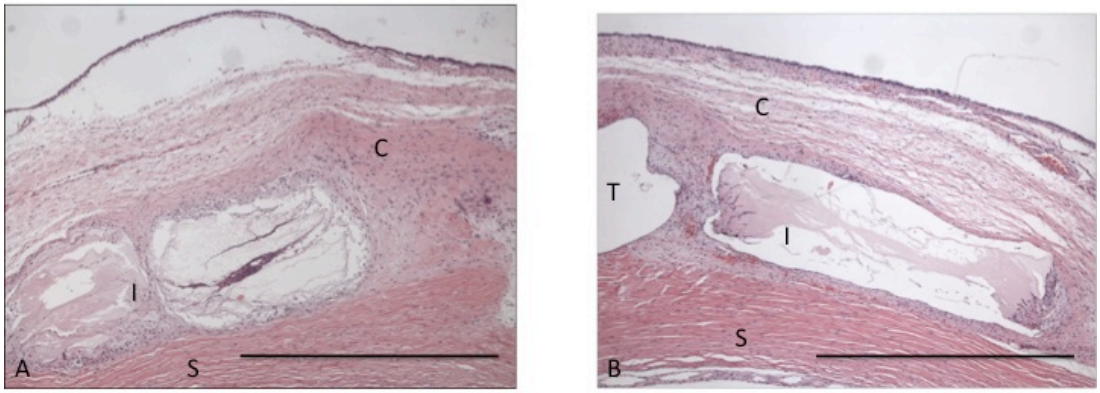

Figure 3-89. Sections of the representative blebs of the ilomastat / dexamethasone (A) and polymer coated implant groups (B). Legends: C, conjunctiva; S, sclera; I, implant; T, tube. Scale bars 1 mm. A scattering of inflammatory cells was noted around the surface of the polymer coated implants. An increased density was seen at either end, most notable in one rabbit 1 mm away (see below)

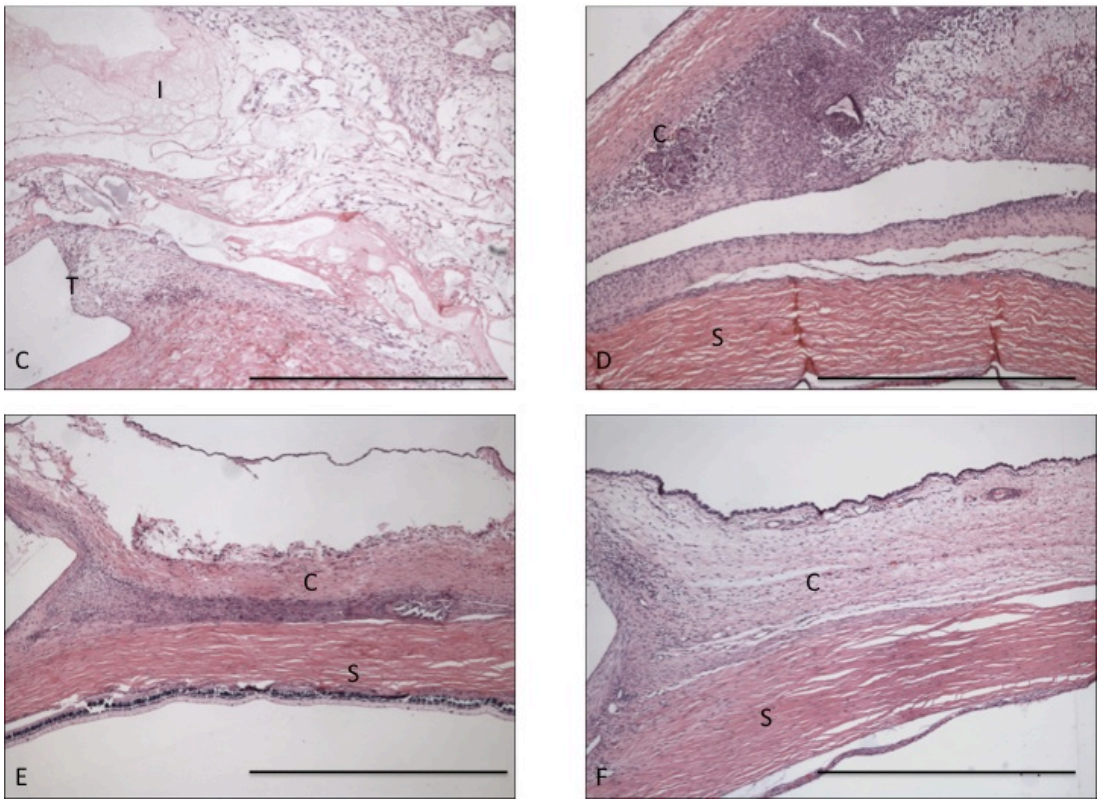

Figure 3-90. Representative histological sections of the sandwich implant (C), healaflow / ilomastat (D), healon GV / ilomastat (E), sterile water group (F). Scale bar 1 mm. A significant inflammatory response was seen in the bleb areas of all hyaluronic acid / ilomastat combinations. The sterile water treated group exhibited some inflammation in the proximity of the drainage tube but less posteriorly.

3.5.8 Discussion

The results from this experiment found that all combinations of hyaluronic acid / ilomastat led to histology demonstrating a significant amount of inflammation at day 14. The dysmorphic nature of the blebs concurred with the histology. Why should this contrast so greatly with the hyaluronic acid /ilomastat combination in the second experiment? Is it simply that the time point is earlier, and if a snapshot of histology in the previous experiment were taken a similar result would be seen? Apart from sectioning at day 30, the other differences between the previous experiment and the present one are the type of hyaluronic acid, the method of sterilisation, and the proportions of drug and hyaluronic acid used. If we examine each of these in turn:

Visiol has a lower molecular weight than Healon GV, Healaflow or Revanesse. It is possible that the Visiol was cleared more quickly and hence any inflammatory reaction to this hyaluronic acid resolved more quickly. However, Healon GV and Healaflow are both used in humans without ill effect (inflammation), albeit as a buffered gel / solution and not as a freeze-dried preparation. Hydrating freeze-dried hyaluronic acid does not revert it to the same physical state as the original preparation. An important comparative control would be to use the hyaluronic acid preparation but without the drug. Unfortunately due to limitations in animal number, and the nature of the experiment being a pilot, a large number of controls was not possible.

The method of sterilisation in this experiment was by ultrafiltration of the drug solution, one that has been used successfully by A. Khalili for the sterilisation of bevacizumab implants (PhD thesis A Khalili). The sterilisation of the Visiol / ilomastat implants in the previous experiments was by exposure to radiation from a strontium – 90 probe, typically used as an anti-scarring device in glaucoma surgery (Kirwan et al., 2006), and not in any way as intense as that used as a standard for sterilisation of medical equipment. Indeed, it would be less surprising if the animals in the previous experiment developed an endophthalmitis.

One factor likely to contribute to the inflammatory difference is the proportion of drug to hyaluronic acid, which was far less in the earlier experiment, or indeed that

whether the hyaluronic acid was cross-linked and with greater longevity. The quantity of ilomastat estimated in the Visiol experiment was 0.5 mg and, although the exact mass of hyaluronic acid was unknown, the overall implant had an estimated weight of between 8 and 9 mg. In the above experiment the quantities of ilomastat and hyaluronic acid were 1 mg and 3 mg respectively for all three arms. A lower quantity of hyaluronic acid was used so that not too great a volume of gel would be formed on hydration. A higher quantity of drug was used to prolong release. It would appear, however, that there was a greater proportion of crystalline drug in an undissolved state, despite being dispersed in a hyaluronic acid gel. Immune cells recognised the solid crystalline material and mounted a response. That islands of crystalline drug are seen in these combinations surrounded by foci of immune cells provides support for this. Furthermore, in the sandwich implant where drug was not dispersed throughout the hyaluronic acid ilomastat combination, there were open spaces not associated with drug in between foci of inflammation.

The dexamethasone and ilomastat implants exhibited less inflammation than the hyaluronic acid combinations at day 14. Indeed the intensity of inflammation seen around the implants was similar to that seen around the combination dexamethasone ilomastat implants in the previous in vivo experiment. Interestingly there was no propensity for more immune cells to be co localised with one implant rather than the other, indicating that the anti inflammatory effect of the drug from one implant was maintained beyond its own position, or that the antagonistic particulate effect of one implant versus the other was not significantly different. Not withstanding these findings, however, again the blebs seen in this group were low in comparison to the previous experiments and other blebs, and both implants from early on in the experiment affected the contour of the conjunctiva of the bleb. Again, interpretation of how functional the bleb is at this point is difficult, since spacer effects could influence interpretation of the bleb appearance.

The results of the polymer (provided by Alex Seifalian) coated implants are of interest. There was considerably less reactive inflammation in most of the sections than that seen in the uncoated pure ilomastat implants in the previous experiments. This implies that the foreign body response can be minimised. Islands of inflammation, however, were found most often at either end of the implants. In one

section the inflammatory reaction was considerable with evidence of a large blood vessel. It is likely that in these areas there were defects in the polymer allowing access to dendritic or other immune cells. Corroborating these findings were those of the detailed SEM images that showed small pits in the polymer coat and crystalline material underneath (Figure 3-65).

What is less clear, however, is how much drug is eluting from these polymer coated implants. *In vitro* release data suggested that polymer coated 2 mm implants are able to release drug at a similar rate to uncoated 1 mm implants. Whether the drug released is eluted through the coating or through defects such as those seen on the SEM is not possible to determine with the samples in this experiment. Analysis of the polymer remnants was attempted, however removal of the polymer casings from the rigs caused damage to the surface.

Determining the efficacy of the polymer coated implants, and indeed the other implants, in prolonging bleb survival in the animal model remains a challenge. As in the dexamethasone / ilomastat implant treated arm, the contours of the blebs in the polymer coated arms were affected by the implants within the subconjunctival space. An attempt was made to evaluate drainage of aqueous into the bleb using ICG injected into the anterior chamber at the time of termination. There was no conclusive proof of dye entering the bleb from the tube however. Instead it was apparent that the fluorescence seen in blood vessels within the bleb and this was due to the dye entering the circulation presumably via the trabecular meshwork. It may be that the flow of aqueous through the tube is too slow in the scenario of a functioning bleb, or alternatively the bleb has failed. Unfortunately we did not have a positive control to compare to such as an MMC treated bleb.

Further work is required to determine the polymer properties and its behaviour in the subconjunctival space. This was the first time this polymer was used for drug delivery and much of the previous work was on tracheal stents (Jungebluth et al., 2011)(Crowley et al., 2014). It is important to compare the tissue response that this polymer has to other polymers previously used in this location, for example in devices such as the Ahmed or Baerveldt tubes. It may be that there is significantly less tissue reaction, but this data needs to be obtained. Of note is that although the

polymer is ‘tissue biocompatible’ it is not biodegradable and remnants will remain in the subconjunctival space. Is this a benefit or an impediment? The Olagen implant uses the spacer effect as its underlying principle to prolong trabeculectomy survival (Rao et al., 2009). Longer-term data though is still required to be able to evaluate its efficacy. An unknown risk factor is extrusion. Extrusion of the metal Ex-PRESS tube, an implant not sutured into place, has been reported (Tavolato et al., 2006), although this is of a different material, size and shape.

A key aim in future experiments will be to develop a uniform coating without defects that has a porosity of sufficient size to allow drug dissolution but less than will allow immune cell access. It has been shown that membranes with pores of 3 μm diameter allow lymphocyte migration, but not those of 0.45 μm (Haston et al., 1982). It will be of interest to examine the release of drug in polymer coats of different pore sizes.

Where a polymer of low immunogenicity has significant promise is in the development of a glaucoma drainage device. Currently these are used in the setting of patients with failed trabeculectomy or those at high risk of failure. A recent randomised trial has suggested that the success rate for the Baerveldt tube in this type of patient is significantly greater than trabeculectomy with MMC (Gedde et al., 2007b; Gedde et al., 2007a; Gedde et al., 2009). Unlike trabeculectomy the Baerveldt, Molteno and Ahmed drainage devices rely on the development of a fibrous capsule with a lake of aqueous around the drainage plate, or so called Tenon’s cyst, to prevent hypotony, yet excessive scarring is still the main cause of failure (Rao et al., 2009). Developing a drainage device that has significant advantages in tissue biocompatibility, which may entail the integration of an antiscarring agent, would fulfil an unmet need.

The findings of the experiments described in this section indicate that coating a pure ilomastat implant with a polymer significantly reduces the inflammatory response seen to the naked implant. Hyaluronic acid ilomastat combinations exhibit a foreign body response that is considerable and most likely due to the presence of undissolved drug. Future work is required to develop a model of testing bleb functionality.

3.6 Investigation into the use of different polymer coated implants for antiscarring therapy

In the previous experiment ilomastat implants coated with polymer provided by Alex Seifalian (UCL/Royal Free Hospital) were found to release drug in the rigs within the therapeutic range, however a number of defects were noted on the surface of the implants when analysed by SEM. Thus it was not clear whether drug was being eluted through the polymer or via defects. Furthermore, although less inflammatory response was seen around these implants in the *in vivo* experiment compared to previously seen with uncoated implants, pockets of inflammation were noted, particularly at either end of the implants. It was therefore necessary to optimise the coating of the implants and verify drug release.

Work performed by Yasmin Rafieim, under the supervision of Professor Seifalian, aimed to improve coating a spray coating process, however despite multiple attempts using different coating times, and strategies (dip coating vs spraying), defects remained in the coated implants. Further experiments performed by myself aimed to use pre-fabricated polymer to make a shell before implant insertion. Even using polymers made with different porogens to enhance water permeation as used for example in gastric drug delivery (Mastropietro et al., 2012), no drug release was detected in standard rig experiments (2 mm, 1 mg implants). Further technical difficulties also became apparent. Attempts to seal the edges of the pocket using heat at 200 ^{0}C (the temperature of polymer denaturation) led to inconsistent results, with the polymer having variable cohesiveness and would not readily seal. Using cyanoacrylate glue was also found not to work (Figure 3-91).

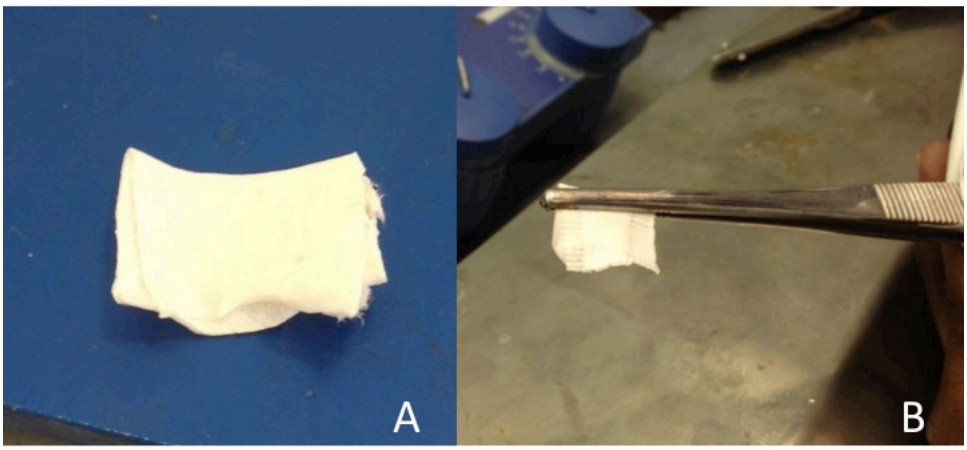

Figure 3-91. Attempts to seal a polymer pouch using cyanoacrylate glue (A) and forceps heated to 200 ^{0}C (B).

3.7 Investigation into the use of a hydrophilic polymer coated implants

An alternative more hydrophilic biocompatible polymer was sought. Vertellus is a company that has developed several different phosphorylcholine (PC) polymers for use in humans. Their polymers are used in contact lenses and coating of cardiac stents. Unlike the polymers used in the previous experiments, they swell on contact with water, becoming hydrated. Thus in theory water imbibition will allow drug dissolution. In the light of the work performed so far there were two main initial questions:

1) Would it be feasible to coat an ilomastat tablet with a PC polymer uniformly, without defects?
2) If so, would ilomastat elution occur at a therapeutic concentration?

Vertellus performed the coating process at their laboratory in Basingstoke. The polymer solution was prepared using ethanol as a solvent. They optimised the polymer concentration in preliminary experiments to establish a consistency that would give a smooth coat to the implant surface. Using a dip coating method with a polypropylene mesh basket, ilomastat implants were immersed and then allowed to dry. Two polymer types were potential candidates for the coating process: “PC 1059” and “PC1036”. Both polymers are made up of phophorylcholine groups, molecules which exhibit bipolar charge, but overall are neutral, similar to the non thrombogenic outer membrane of erythrocytes and have been used in clinical products. PC 1059 is synthesised without cross linking between polymer chains, whilst PC 1036 polymer chains become cross linked after curing at 50 ^{0}C. In theory the polymer that is more cross-linked should hinder flow of solution more. Implants of 2 mm diameter and 1 mg in mass were fabricated at the School of Pharmacy and sent to Vertellus for coating.

3.7.1 In vitro analysis of Phosphoryl polymer coatings

3.7.1.1 Appearance of ilomastat implants coated in PC 1036 and PC 1059

Using a dip coating procedure, initial experiments involved coating ilomastat tablet with a single coat of either PC 1036 and 1059. The implants appeared to have polymer of variable thickness on the surface. The periphery of the flat surfaces revealed greater coating than the edges or centre. Drug crystal shapes were also seen in outline.

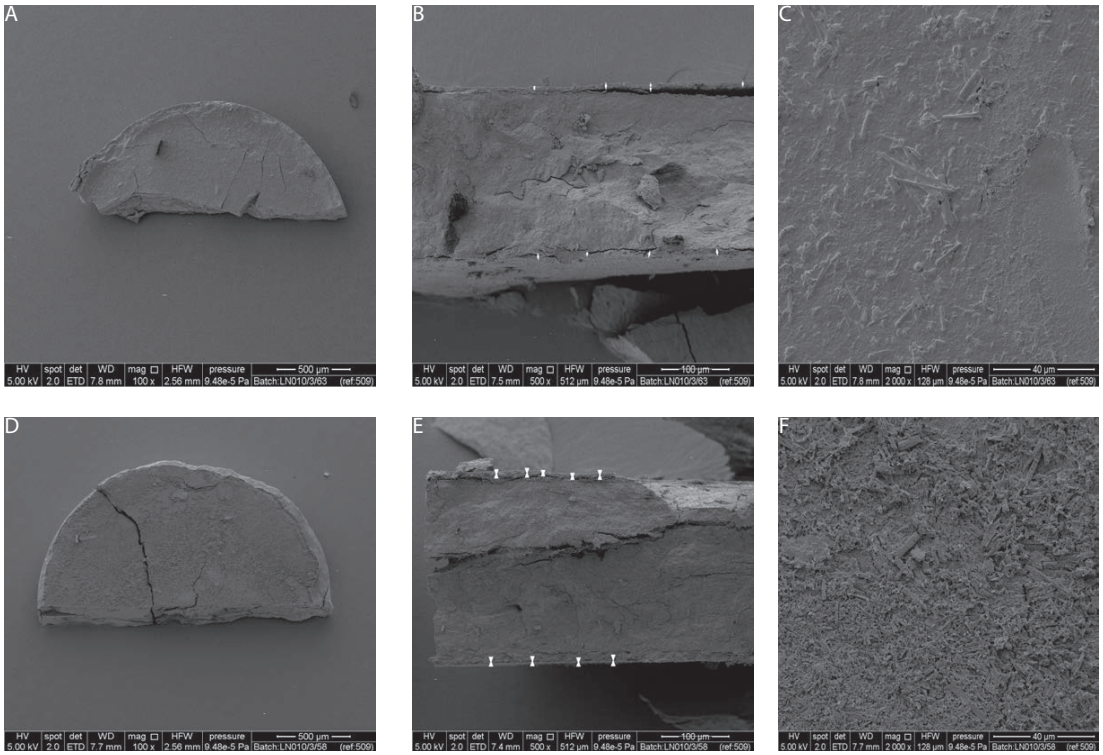

Figure 3-92. SEMs of implants coated with the polymers PC 1059 (A, B, C) and PC 1036 (D, E, F). Implants showed polymer coating with greater thickness at the periphery of the flat edge. Polymer PC 1059 thickness was found to be 8.2 +/- 1.8µm (mean +-SD). Polymer PC 1036 coating thickness was 6 +/- 2.25 (mean+-SD). The crystalline drug was seen in outline underneath the polymer skin in both types of implant.

3.7.1.2 Release studies for 1036 vs 1059

Both implants coated in PC 1036 (cross-linked) and PC 1059 (non cross-linked) released ilomastat at a concentration between 10 and 100 μM for 21 days, with a greater rate of release from the implants coated in PC 1059 (Figure 3-93, Figure 3-94). It was not possible to determine the exact quantity of drug present after coating by the polymer, however given that the overall mass of the implants was similar it is likely that some of the drug dissolved in the solvent used in the coating process. The mean peak concentration of ilomastat was 45 μM for implants coated in PC 1059 and 21 μM for implants coated in PC 1036.

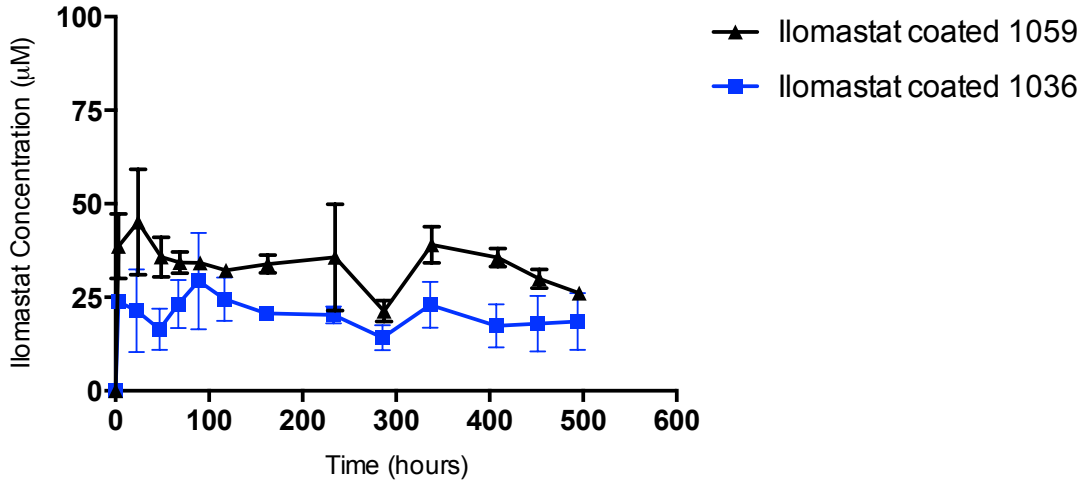

Figure 3-93. Mean concentration of ilomastat released from single coated PC 1059 (non cross-linked, n = 2) and PC 1036 (cross-linked, n = 2) polymer 2 mm ilomastat implants. Presumed mean mass of drug = 1 mg. A higher level of drug concentration was seen with the implants coated in the non cross-linked PC 1059. Error bars indicate SD.

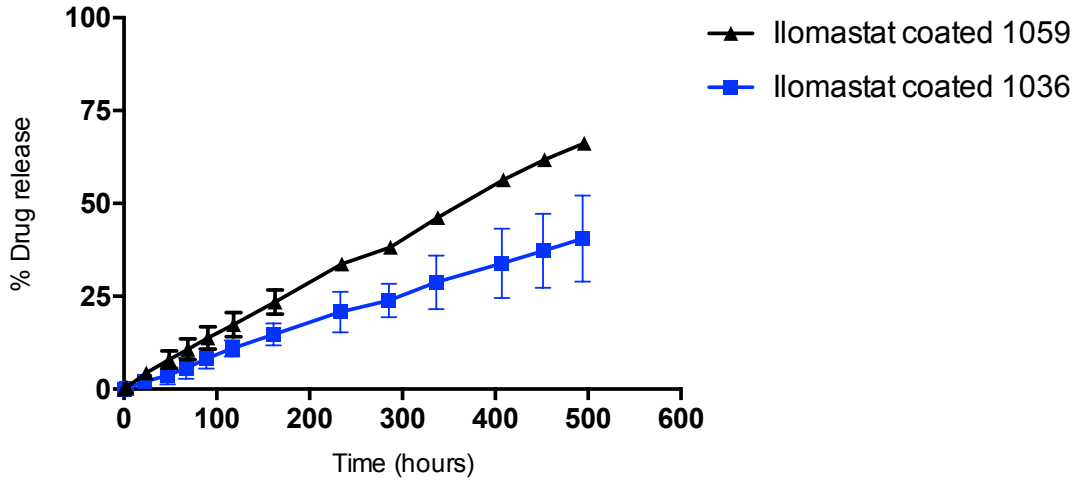

Figure 3-94. Cumulative release of ilomastat over time from PC 1059 and PC 1036 polymer coated implants. A faster release was seen with the implants coated in the non cross-inked polymer PC 1059.

3.7.1.3 Appearance and release characteristics of ilomastat implants with multiple coatings of PC1059 (3, 5, 7)

As the rate of drug dissolution was greatest with implants coated in PC 1059, yet appeared to have a thicker more even coating, this polymer became the coating of choice. Drug dissolution was also likely to be more efficient from this non-cross linked polymer. Subsequent experiments aimed to determine whether application of multiple coats yielded a smoother surface without drug exposure.

3.7.1.3.1 Appearance of ilomastat implants coated 3, 5, and 7 times in PC 1059

Implants exposed to 5 and 7 coating procedures had a greater polymer thickness than the implants coated 3 times (Table 3-5, Figure 3-95). The surface of implants coated 7 times appeared more smooth than those coated 3 or 5 times and with less variation in thickness.

Table 3-5. Mean coating thickness as determined by SEM for n = 9 measurements.

Number of coats	Mean thickness (µm) (n = 9)	Standard deviation	Range (µm)
3	24.4	26.9	3.5 - 87
5	40.7	30.5	1.1 - 83
7	37.5	19.3	4.8 - 66

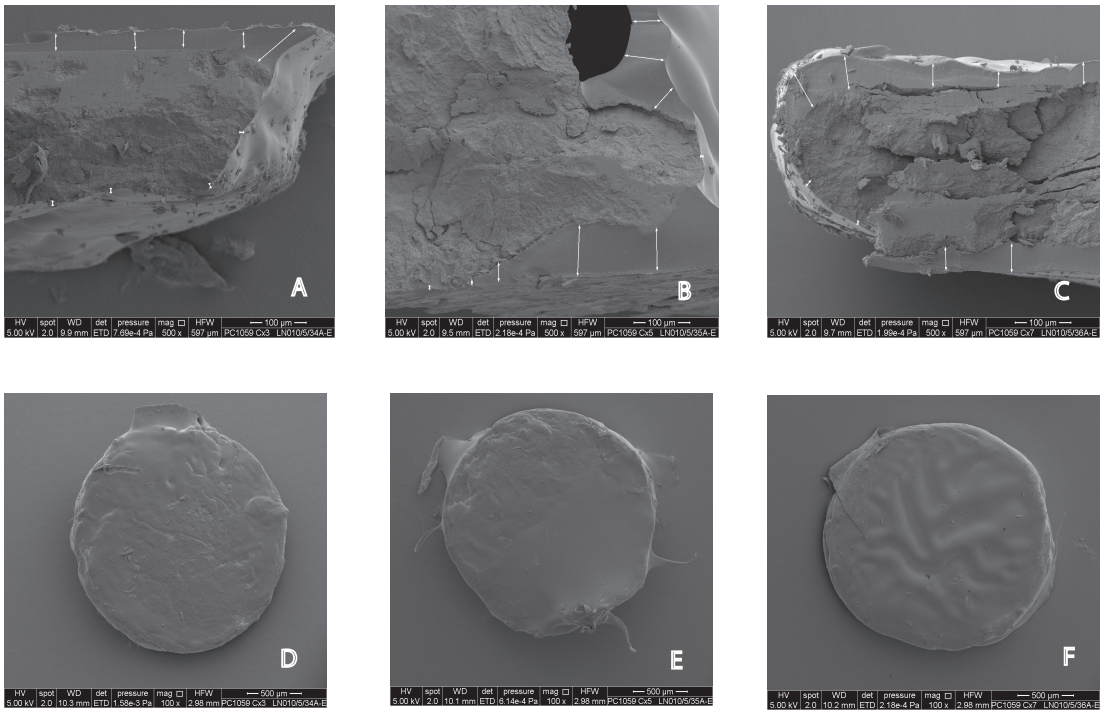

Figure 3-95. Appearance of implants with 3, 5 and 7 coats of polymer PC 1059. Images A and C are SEMs of an implant coated 3 times. Images B and E are of an implant coated 5 times. Images D and F are of an implant coated 7 times. White arrows represent measurements taken to determine polymer thickness.

3.7.1.4 Appearance of hydrated polymer PC1059 coated implants

Pure polymer PC1059 was delicate and fragmented easily on handling. As a consequence the manipulation required for SEM resulted in some indents in the surface. Coated tablets had greater uniformity. Of note however were small pores beneath the surface with the polymer having a spongy appearance (Figure 3-96).

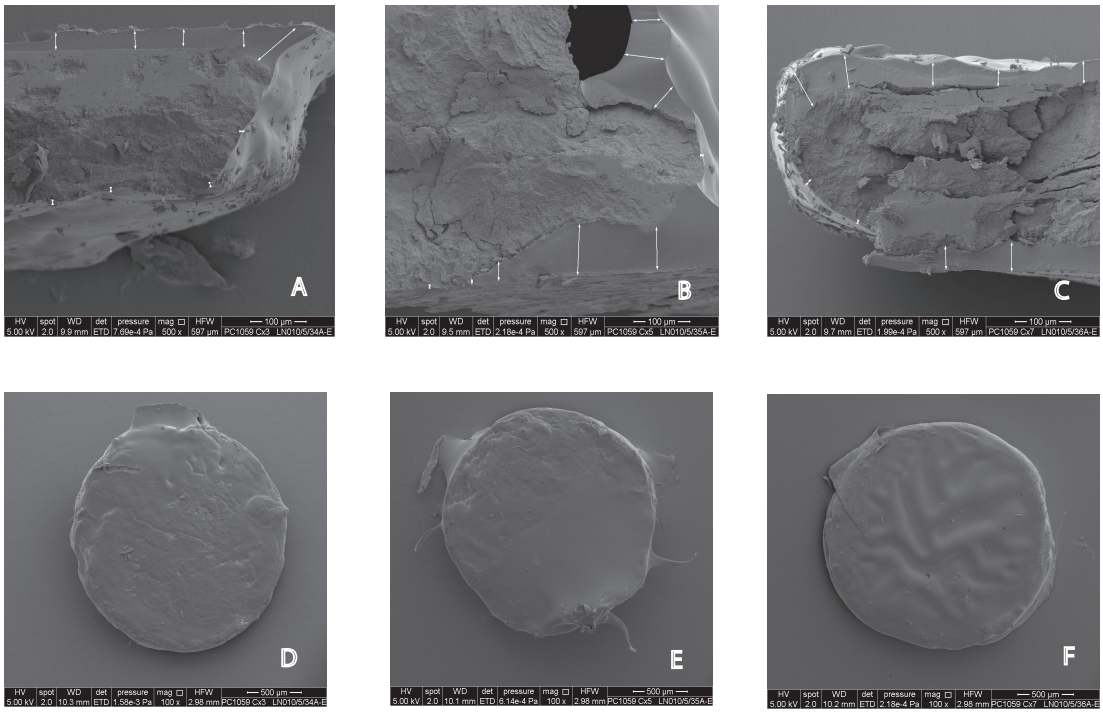

Figure 3-96 Hydrated polymer PC1059. A smooth surface may be seen with spongy appearance beneath.

3.7.1.5 Release studies for implants coated multiple times of PC 1059

A therapeutic concentration of ilomastat (between 10 and 100 μM) was maintained for the duration of the release study (Figure 3-97, Figure 3-98). Implants coated 5 and 7 times appeared to release ilomastat at a similar rate, and the greatest rate of release was from implants coated 3 times.

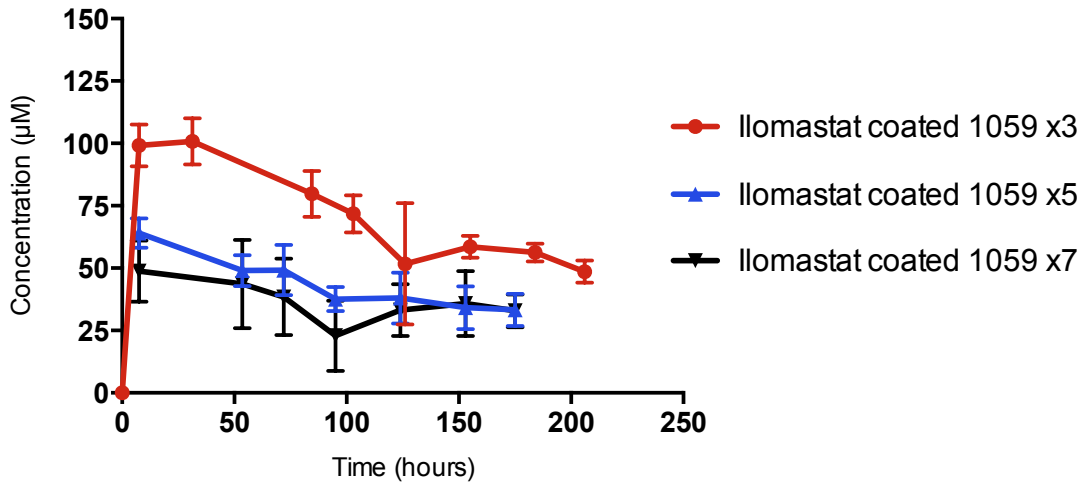

Figure 3-97. Mean concentration of ilomastat released from ilomastat implants coated in PC 1059 multiple times 3 (n = 3), 5 (n = 3), 7 (n = 3). Presumed mean mass of drug = 1 mg. Error bars indicate SD.

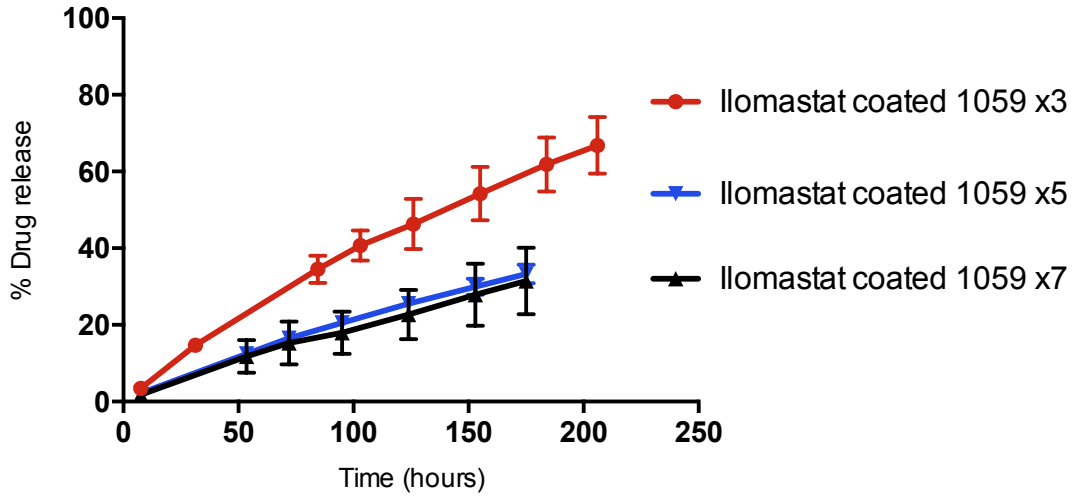

Figure 3-98. Cumulative release of ilomastat over time from implants coated 3, 5 and 7 times in PC 1059. Error bars indicate SD.

3.7.2 In vivo analysis of polymers coated 7 times in PC 1059

Implants coated in PC1059 7 times had the most regular and complete coatings whilst still releasing drug at a therapeutic concentration, thus were chosen as candidates to determine anti-scarring potential. It was postulated that these implants would provide antiscarring efficacy with drug elution through the coating, yet prevent immune cell access and activation. Because we wished to examine distribution of ilomastat in different ocular tissues at the end of the experiment and those globes would not be able to be used for histology the treatment arms and n number were chosen as follows:

The experimental arms chosen were:

1) Ilomastat implants (2 mm 1mg) coated 7 times in PC polymer 1059 (n = 16)
2) MMC (0.2 mg / ml applied for 3 minutes) (n = 10)
3) Sterile water (water applied in the same way as MMC (n = 10)

Two rabbits had to be terminated early: one suffered seizures under anaesthetic (sterile water group) and the other had an intractable hyphaema that resulted in tube blockage and significantly elevated IOP (PC polymer ilomastat implant group). The rabbits treated with MMC had 8 / 10 blebs that were maintained until day 30. Four of these were noted to have an avascular edge at day 18. Ten of fifteen rabbits treated with implants coated in PC polymer 1059 had blebs that appeared to survive until day 30 although the dimensions were smaller than the MMC blebs and in four of these the blebs had a morphology where the implant contributed to the appearance. The animals treated with sterile water all had blebs that failed by day 15. Representative photographs at day 15 and day 24 are shown in Figure 3-99 and Figure 3-100, and a survival curve in Figure 3-101.

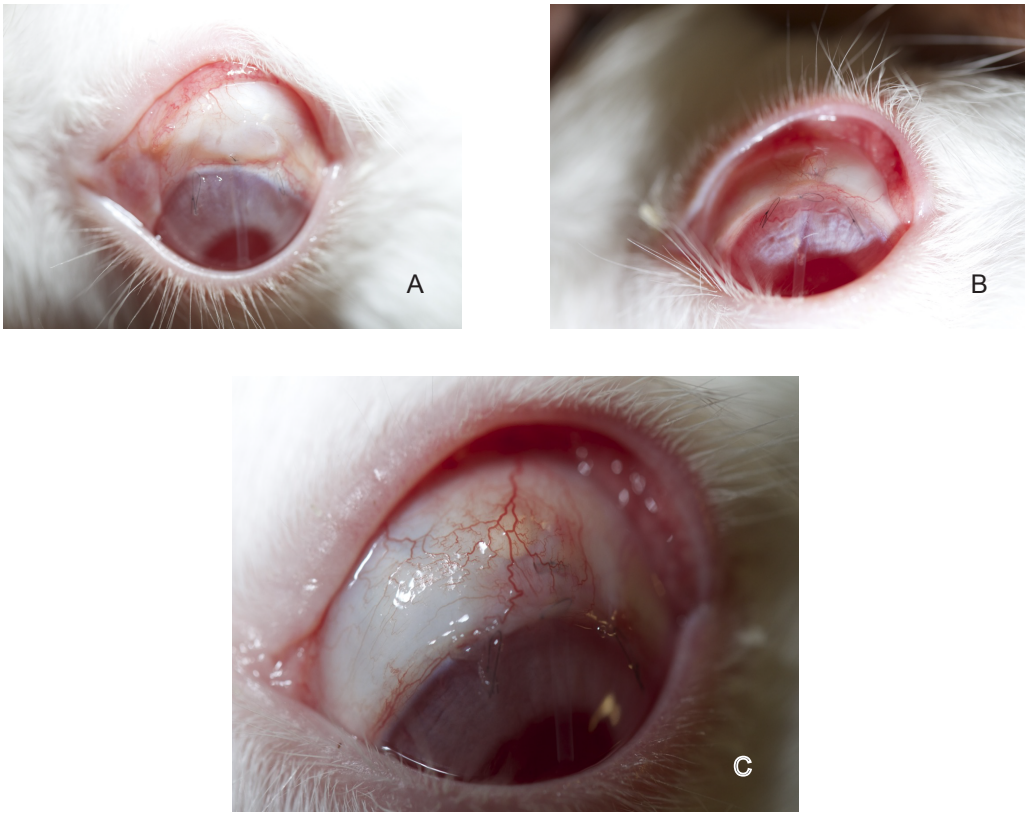

Figure 3-99. Representative photos of blebs at day 15 for each of the treatments: mitomycin C (A), sterile water (B), ilomastat PC 1059 (C). The appearance of blebs A and B were classed as functional and the bleb in C as a failure. The MMC bleb has an avascular edge.

Figure 3-100. Representative photos of blebs at day 24 for each of the treatments: sterile water (A), mitomycin C (B), ilomastat PC 1059 (C and D). The appearance of ilomastat PC 1059 and mitomycin C blebs were classed as functional and the sterile water bleb as a failure. A side view of the ilomastat PC 1059 illustrates how the implant contributes to bleb appearance (D).

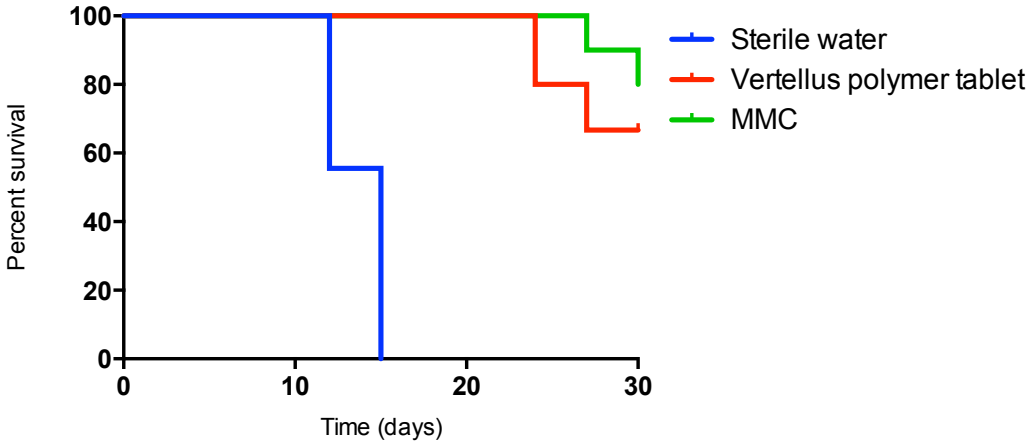

Figure 3-101. Bleb survival of the 3 different groups: ilomastat coated in PC polymer 1059 (n = 15); MMC 0.2 mg / ml applied for 3 minutes (n = 10); sterile water (n = 9).

3.7.3 Intraocular pressure

Intraocular pressures of rabbits treated with MMC were lower than the other two groups at all time points following surgery. The sterile water treated group and PC1059 polymer coated implant treated group had an IOP that returned to baseline by day 9. There was a significant difference between the groups at day 30 (Kruskall-Wallis: (H (2) = 11.76, P = 0.0028). There was little difference in intraocular pressure in the unoperated eye of the three groups.

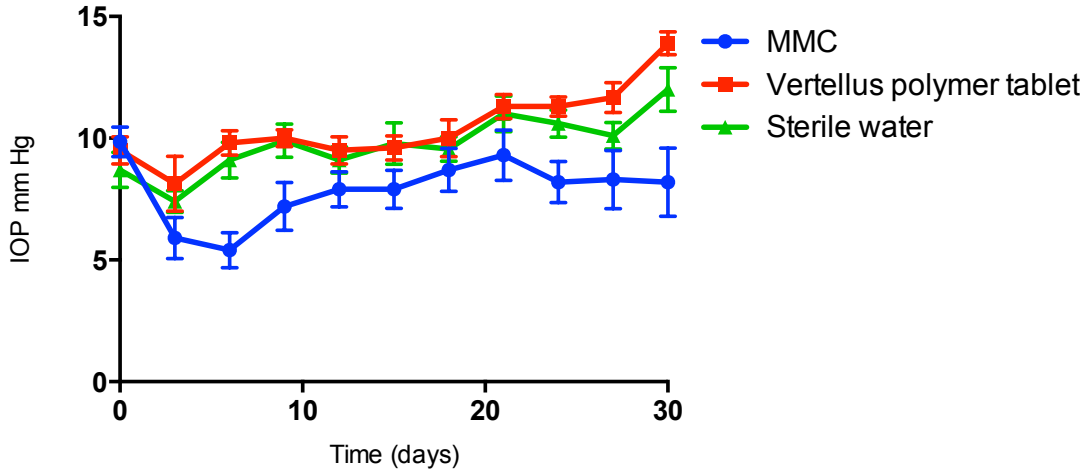

Figure 3-102 IOP for all 3 groups over time. The eyes that received MMC maintained a lower IOP for all postoperative days. Error bars indicate standard error.

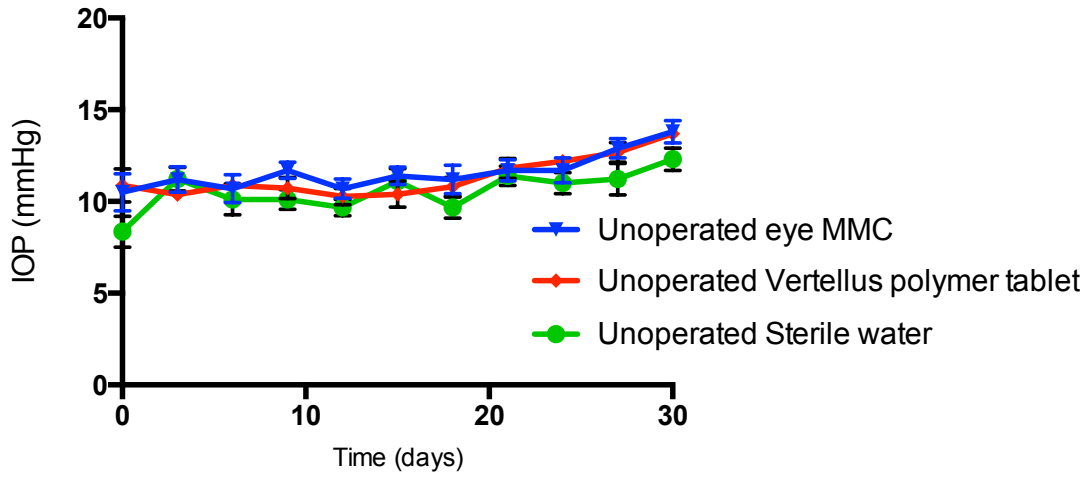

Figure 3-103 IOP for unoperated eye all 3 groups over time. There was little difference between treatment arms. Error bars indicate standard error.

3.7.4 Bleb surface area and height

Blebs of rabbits treated with MMC and the PC1059 polymer coated implants had greater surface area and were classed as 'higher' throughout the experiment.

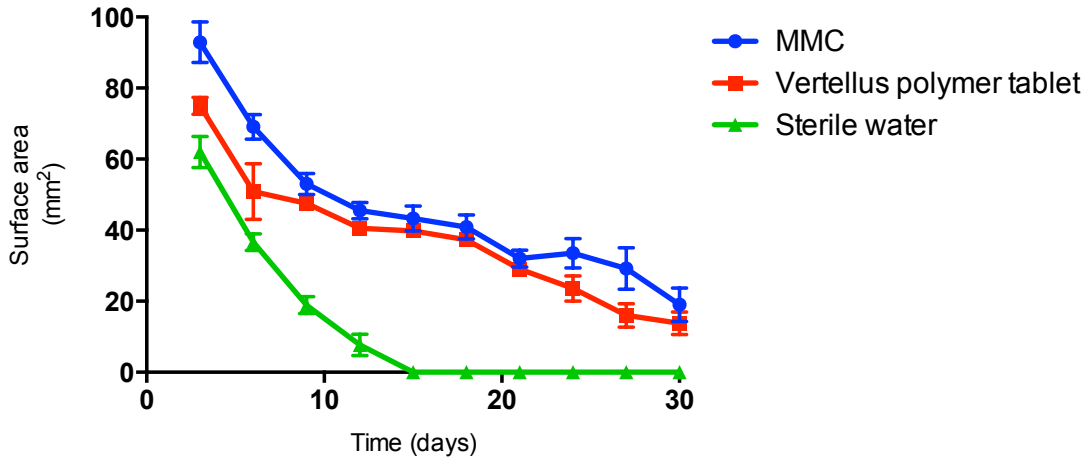

Figure 3-104 Bleb surface area for the 3 groups over time. Rabbits treated with the PC1059 coated implants and MMC had a greater surface area at each time point than the sterile water treated group. Error bars indicate standard error. There was a significant difference between the groups at day 30 (Kruskall-Wallis: (H (2) = 11.02, P = 0.0041)

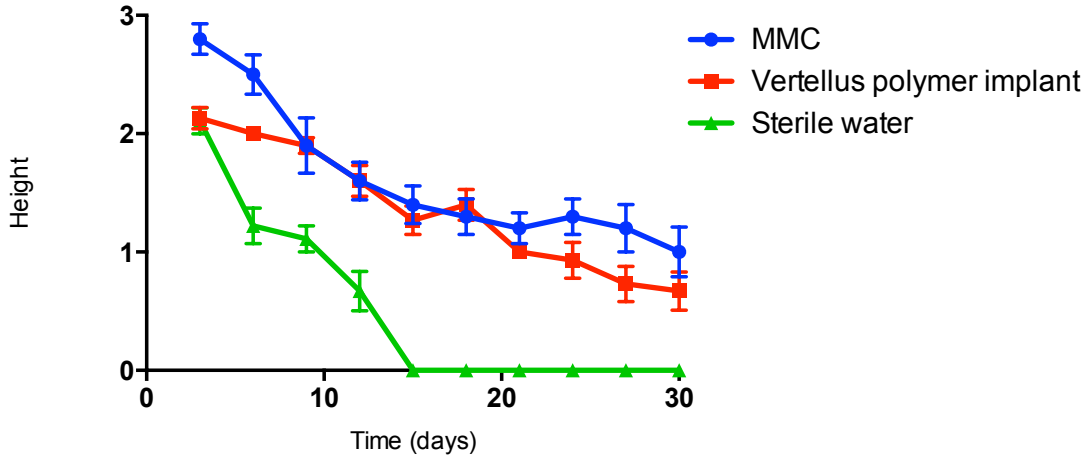

Figure 3-105 Bleb height for the 3 groups over time. Bleb height was graded as 0, flat; 1, shallow/formed; 2, elevated < 2 mm and 3, high > 2 mm. Error bars indicate standard error. There was a significant difference between the groups at day 30 (Kruskall-Wallis: (H (2) = 12.42, P = 0.0020)

3.7.4.1 Bleb vascularity

PC 1059 polymer coated implant treated blebs maintained greater vascularity than the MMC or sterile water treated groups. Little difference in overall vascularity could be distinguished between the MMC and sterile water treatment arms (Figure

3-106). A Kruskall-Wallis test performed at day 15 found a significant difference between the arms (H (2) = 7.68, P = 0.0215).

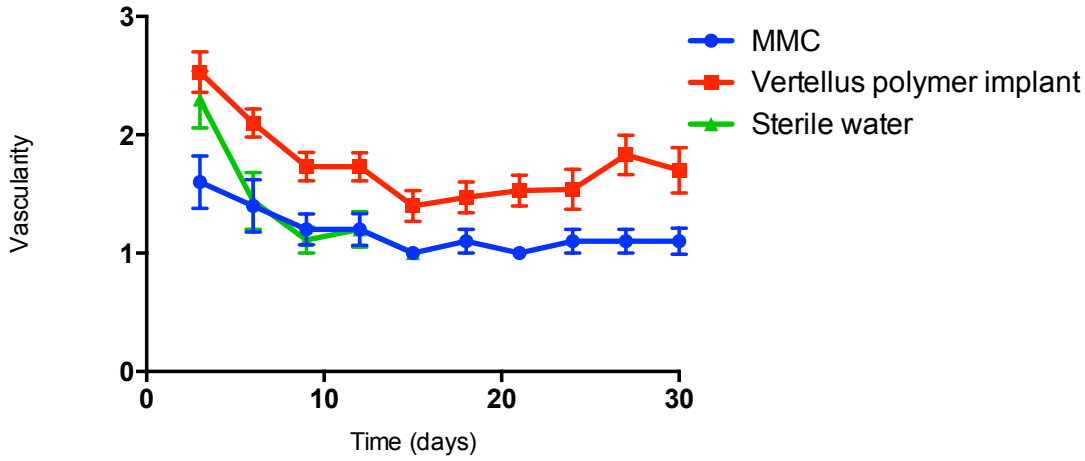

Figure 3-106 Bleb vascularity. The vascularity was graded as 0 = avascular, 1 = normal, 2 = hyperaemic, 3 = very hyperaemic. Data displays vascularity of observed blebs at each time point as mean and standard error of the mean. The implant treated blebs were graded as having greater vascularity at each time point than the blebs treated with MMC and sterile water.

3.7.4.2 Histology

Analysis of the histology for this study was hindered by errors in processing. The processing machine that transfers the globes from one concentration of alcohol to the next broke down in the UCL Institute of Ophthalmology histopathology laboratory. It has subsequently been replaced. Eight of the globes were found to have had their processing interrupted and five of these had extended exposure to air. A number (exact total unknown) were processed at a faster rate than expected.

Of the 29 globes processed for histology, sections could be mounted on slides from 28 globes. The tissue sections of the 5 that had been exposed to air were more compacted, and 4 others were difficult to cut, indicating possible under processing.

In all 9 globes that received PC 1059 coated implants the remains of the implants could be seen as a distinct entities (Figure 3-107, Figure 3-108). An adjacent zone of

inflammatory cells was seen, superior to which there was thickened conjunctiva. Macrophages with a foamy appearance were the predominant cell found within the inflammatory zone. In 4 of the globes inorganic material could be identified and in one section red blood cells were seen nearby.

In the sterile water treated groups the overlying conjunctiva in the bleb area was slightly thickened with a scattering of inflammatory cells (Figure 3-107). In all of the MMC treated group the conjunctiva was noted to have a paucity of nucleated cells in the bleb area. In 3 / 10 of the MMC treated eyes a cavity corresponding to the bleb was found. Epithelial interruptions were seen in these 3 together with apoptotic cells.

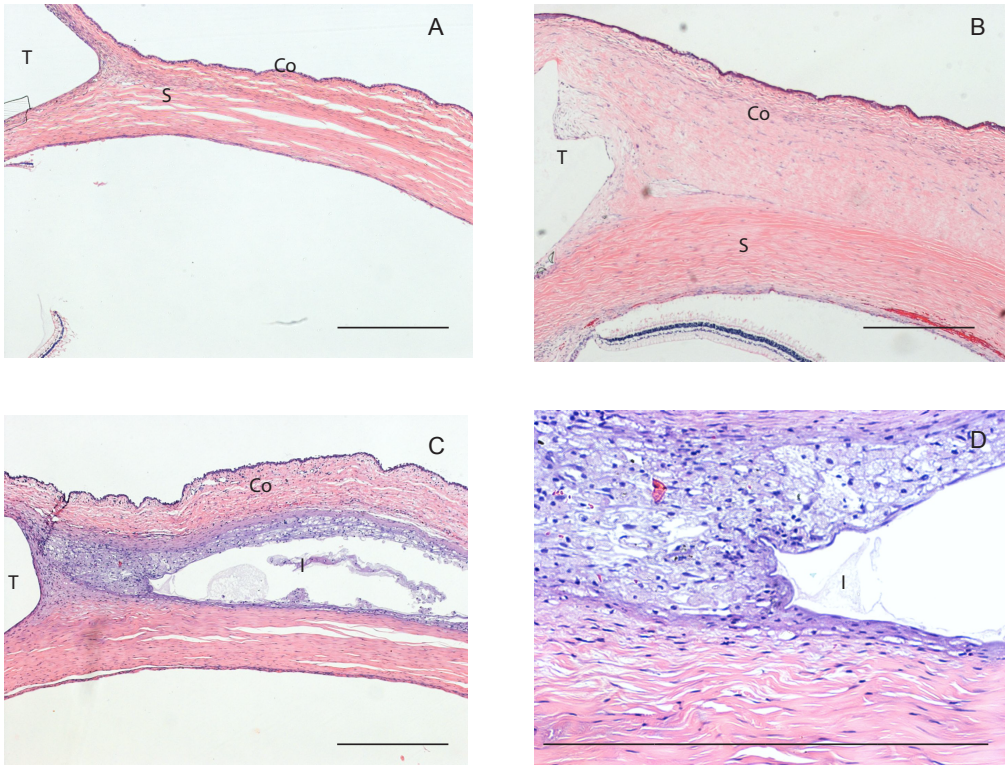

Figure 3-107 Haematoxylin and Eosin staining of bleb areas from rabbits treated with sterile water (A), Mitomycin C (B), PC 1059 coated implants (C) and close (x5) view of PC 1059 (D).
Legends: Co: conjunctiva, T: drainage tube, S: sclera, I: implant remnants. Surrounding the implant remnants were inflammatory cells made up predominantly of macrophages. Scale bars 1 mm.

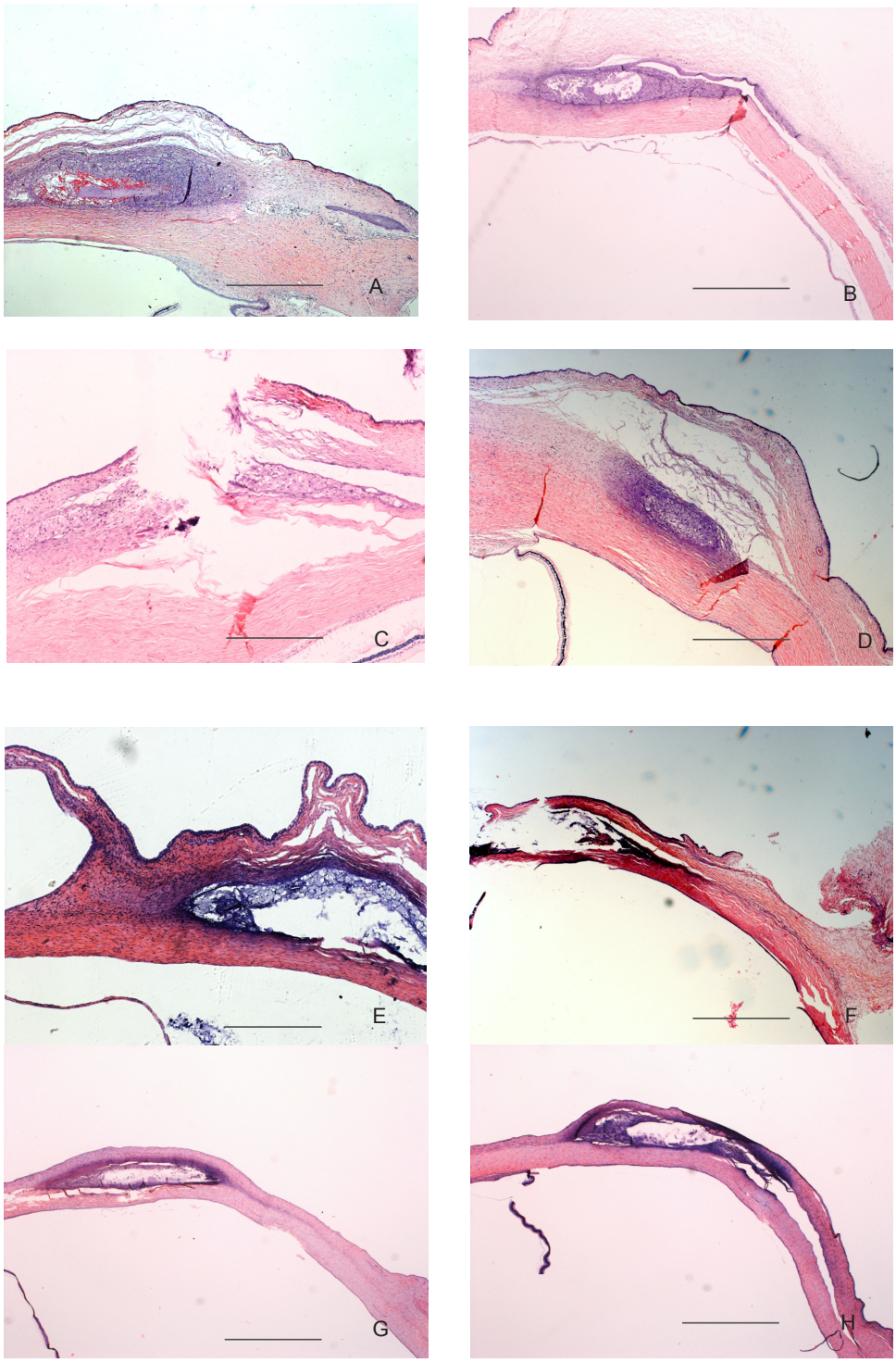

Figure 3-108 Haematoxylin and Eosin staining of all blebs treated with the PC 1059 coated implant. Tiles A, B, C, D, E, F, G, H correspond to rabbits 35, 21, 25, 18, 2, 11, 29, 32. Tiles E, F, G and H also illustrate how the appearance differs when the globes are not processed to plan. Tiles F and G are from globes over exposed to air.

3.7.5 Tissue levels of ilomastat

The concentration of ilomastat in the aqueous, vitreous, bleb conjunctiva, remaining conjunctiva, cornea and sclera were determined at day 30 in 6 of the implant treated blebs Table 3-6. Although I contributed with dissecting tissues at the time of harvesting, Dr Ahmed performed the analysis using facilities at the Royal Free Hospital. It was not possible unfortunately to extract aqueous directly from the bleb.

Table 3-6 Tissue levels of ilomastat at day 30. Tissues where drug was not detected are labelled as ND.

Rabbit number	Aqueous humour (nM)	Vitreous (nM)	Bleb conjunctiva (pg/mg tissue)	Cornea (pg/mg tissue)	Sclera (pg/mg tissue)	Ilomastat remaining after 30 d (µg)
4	14.9	67.1	ND	148.7	ND	46.54
8	ND	3.6	210.7	30.6	644.9	Not found
12	996.5	5.8	871.6	72.1	15838.9	Not found
22	57.7	0.2	33.7	8.5	201.1	Not found
26	15.3	ND	975.6	53.6	1958.9	3.48
30	3.9	0.5	1503.8	0.3	447.1	4.02
Mean ± SD	217.7±195	13.4±12.9	719.1±267.6	52.3±21.9	3818.1±351.1	

3.7.6 Discussion

These experiments showed that it was possible to formulate a PC polymer coated ilomastat implant that would, in theory, allow drug dissolution in an aqueous environment to maintain a therapeutic concentration within the bleb. Similar PC polymers have been used for coating of cardiac stents (Habara, S, et al. 2011). The seven times coating of the non cross-linked polymer appeared to give the smoothest surface, although there was still considerable variability in the coating thickness (Figure 3-92, Figure 3-95). No definitive breaches were seen on SEM of the dry implant, however a zone of foamy type macrophages was found on histology around all implants, and the coating on wet SEM had a somewhat friable appearance.

A foreign body type reaction therefore existed, but much less than seen to naked ilomastat implants in the first in vivo experiment. Whether the remaining reaction was due to the coating becoming spongy and permeable after hydration, allowing immune cell access to solid crystalline drug, whether drug during the coating process had dissolved in the coating itself and recrystallized with drying, or whether this reaction was due to the polymer per se is difficult to say. However, unlike the experiment using the POSS PCU polymer, there were no localised collections of inflammatory cells, suggesting that the coating was unlikely to have cracks or holes.

Vertellus tried many different methods in the coating process, comparing dip coating in a mesh basket to spray painting, using different concentrations of polymer solution and whether to pre clean implants prior to coating with a solvent such as hexane. Given the constraints of time a dip coating method, which yielded the smoothest coatings, was chosen. Pre-cleaning with a solvent, which may have caused significant implant absorption, was deemed not to be necessary. Nonetheless, how much drug absorption took place in the coating process is important to determine in future experiments in coating optimisation. Certainly some drug was absorbed, given that many implants were found to have lost, rather than gained mass after polymer coating. Indeed where multiple coats were applied experiments drug loss is likely to be greater, as ilomastat is readily soluble in ethanol (1mg / mL) and each time a polymer coating, is applied the implant beneath may become wet. Unfortunately there was insufficient time and insufficient number of implants to explore this relationship.

Although smoother and thicker, implants coated seven times still had considerable variability in thickness. Some of the thinnest points were found on corners, as were some of the thickest, suggesting that gravity played a significant influence while the polymer was drying. An analogy might be a cake with wet icing, the thinnest icing being the superior corners, with the thickest icing being found at the edge at the cake bottom next to the cake board. In future experiments alternative methods to dip coating such as fine spraying, might lead to a more uniform polymer thickness.

Vertellus attempted a more viscous polymer solution but the coverage of this implant surface was irregular.

The kinetics of release for 3 coatings were similar to naked implants of the same size and will most likely reflect how thinly coated these implants were. Interestingly, although slower, there was little difference between the kinetics of release for the 5 and 7 coatings. This correlates with the finding that even though variation was greater for 5 coats, overall mean polymer thickness was the same. The drug concentration differences close to the implants (the boundary layer) are likely to be similar for both 5 times and 7 times coatings.

PC 1059 was the polymer of choice for coating in later experiments rather than PC 1036 because preliminary coating experiments showed a greater uniformity of coating, with drug crystals being less apparent beneath and faster release for implants coated in PC 1059. This polymer however is non-crosslinked, which although may have benefited drug release created wider spaces within the polymer matrix, allowing cellular access.

The choice of number and types of treatment arms in an in vivo experiment is difficult to judge. There are significant advantages and disadvantages for each choice and no obvious ‘correct’ answer. In an ideal world where time and money were unlimited and rabbit experience was without discomfort, with therefore little ethical problems, multiple treatment arms with multiple sampling time points would be used (Table 2-5). A negative control, consisting of an implant without active drug, would minimise the number of different variables, and discount the ‘spacer effect’ of the implant. Multiple time points of harvesting post surgery would be able to answer the question of whether negative control arms exhibited greater inflammatory response early on, before remodelling had taken place.

In the real world, however, time and money are limited, and rabbit experience during an experiment is less than pleasant. Indeed it is important to question constantly

animal use, reducing n numbers to obtain maximum information with minimum numbers, refining the experiment to minimise suffering, and replacing animals where able with alternative *in vitro* techniques. In this, as in previous experiments, measures were taken to minimise suffering, for example operating on only one eye. The choice of 3 arms was made to maximise the n number for each treatment arm, and sterile water group chosen as the negative control, because this is similar to a patient clinical trial. No clinical trial currently, unless the Olagen implant (a collagen implant being trialled as a spacer in human trabeculectomies) gains acceptance, would involve insertion of a spacer as a comparator.

The disadvantages in not having a spacer, however is that drug effect cannot be isolated. The histology, and indeed bleb morphology, would be more interpretable if an ethylcelluose arm had been included. If there were minimal macrophage presence around a polymer coated ethylcellulose arm one would be able to exclude the stimulatory influence as the polymer per se, and something to plan in a future experiment

As it happened, because many globes were affected by an error in histological processing, having the greatest n number possible was fortuitous. Interestingly, despite difficulty in sectioning the globes that had been either over processed or under processed, the slides were interpretable. The theme of cellular response to implant was apparent, even though tissues appeared compacted.

The drug levels found in the different ocular tissues were lower than expected. There was also significant variability between one rabbit and another. In the aqueous humour the concentration was 0.02 times the therapeutic concentration found to inhibit fibroblasts *in vitro*. It must be remembered, however, that this was aqueous drawn from the anterior chamber, and not from the bleb, which may have been different. We also do not know the in vivo drug levels required for efficacy, for although in vitro gel contraction experiments found that 10 μM to be the lowest concentration that would fibroblasts, other experiments have found the K_i for

ilomastat to be 20 nM (Grobelny et al., 1992). How toxic ilomastat is to ocular tissues is also an unknown. Published data includes concentrations of up to 100 μM not being toxic to human Tenon fibroblasts *in vitro* (Daniels et al., 2003), and no significant side effects seen in a phase 1 clinical trial when patients were treated with eye drops of 2 mM ilomastat.

That aqueous was not able to be drawn from the bleb might be either due to the tissue architecture being more like a sponge rather than a lake of aqueous. Alternatively, the blebs at this point might have failed and there is no aqueous to be tapped. It is not possible to be certain of which of these options is correct, however an earlier time point might have given a different result. Another test might be to tap the MMC blebs. Of interest in 3 of the MMC treated blebs, there was a cavity seen in the histological cross section that most likely would correspond to a lake of aqueous. These 3 also had fewer cells in their tube although no significant difference in IOP.

The observations during the *in vivo* study deserve careful consideration. As in experiments before the observation of a 'bleb' did not correlate with other published parameters for success. Success according to the Kaplan Meier chart leads one to suppose that those rabbits treated with a polymer coated implant exhibited statistically similar success rates to MMC, yet the vascularity, an indicator of likely failure in humans (Group et al., 2007) was consistently greater in the polymer treatment group than either of the other treatment arms. Only the IOP of the MMC treated group, the positive control, was consistently lower than the other treatment arms. IOP is an indicator of success in clinical trials but frequently unreliable in rabbit GFS (Miller et al., 1989). This finding was something that we did not expect. Was the surgery more consistent? Or was it just that larger numbers meant that pooled data was more accurate? It is difficult to say, however evidence is indicative thus that MMC was more successful than polymer treated group and sterile water treated group, and question further the validity of success using observation of a bleb when a solid implant is used. This will be explored further in the next chapter.

These findings show that coating an implant with a PC polymer reduces the stimulatory effect that the particulate nature has on the adjacent tissues. The PC polymer implant did not prolong glaucoma surgical success, with less scarring than negative control as hypothesised, however that the foreign body response was ameliorated is an exciting development that opens the opportunity to drug delivery for other pathologies, and drainage device implants.

3.8 Investigation into bleb functionality

In all of the in vivo experiments so far, the observational outcome of success has been to use the presence of a 'bleb'. This outcome measure presumes that the bleb's presence is indicative of fluid draining into the subconjunctival space. However, where an implant has been used, the histology has contradicted this relationship. Indeed the histology of blebs where implants are seen appears, sine qua non, the least likely to encourage drainage of aqueous fluid.

An alternative method to determine bleb functionality is needed. In the experiment before last, fluorescent dye was injected into the anterior chamber and the bleb watched to see if dye would pass into the bleb area and delineate the bleb anatomy. Unfortunately the time taken to enter the bleb via the tube was longer than time taken to enter the systemic circulation, with increased bleb fluorescence due to dye in the conjunctival and scleral blood vessels. A different tracer not absorbed into the systemic circulation might be more successful such as the use of radiolabelled beads, however would be likely to contribute to the wound healing process, and as the bleb is more like a sponge rather than an open space, a tracer may not enter freely.

Post cataract surgery, because viscoelastic is used to maintain the anterior chamber shape, postoperative elevation of IOP is not uncommon (Jürgens et al., 1997a). Ingerborg Stalmans's group has demonstrated another method through injection of Healon into the anterior chamber of rabbits (personal communication). The IOP as result increased, enough to test briefly a number of hypotensive drugs, however the effect was short lived, probably due to the break down and excretion of the hyaluronic acid. Cross linked hyaluronic acid, such as Healaflow, is believed to have a longer half-life and has been reported to help maintain bleb structure post filtering surgery in humans (Jürgens et al., 1997a; Roy et al., 2012). Injection of Healaflow into the anterior chamber of the rabbit, because of its more stable structure could, in theory, therefore lead to a permanent disruption of aqueous drainage and persistent elevation of IOP.

The use of micro beads to elevate IOP in murine models of glaucoma to test neuroprotective or neuroregenerative agents has been reported (Sappington et al., 2010). Little data exists for the use of beads in the rabbit. One type of bead that showed promise, used in our group for a murine model to test neuroprotection, is a magnetic coated bead. These have the advantage of being able to be directed into the drainage angle after injection using a powerful magnet.

We therefore tested whether injection of magnetic beads and Healaflow into the anterior chamber were able to elevate the IOP, in a pilot study of six rabbits. Three rabbits received injections of magnetic beads into their left anterior chamber, and three rabbits received injections of Healaflow into their anterior chamber. IOP was then monitored postoperatively.

3.8.1 Results

Injection of Healaflow resulted in a postoperative rise in IOP in two of the rabbits: one after the first injection (peak IOP 24 mm Hg) and one after the second injection (peak IOP 38 mm Hg). This elevation was short-lived however, with IOP returning to baseline after 48 hours. Magnetic bead injection revealed no elevation in IOP; indeed the IOP of operated eyes followed a lower trajectory than the unoperated, although this did not reach statistical significance (Figures 3-110, 3-111).

The globe size was found to increase in all 3 rabbits treated with Healaflow (limbus to limbus horizontal corneal diameter increase of 1 – 2 mm, $P = 0.0075$ unpaired t test). No increase in globe size was seen with magnetic bead injection. Representative photographs of eyes treated with Healaflow injection and magnetic bead injection are shown below (Figure 3-109).

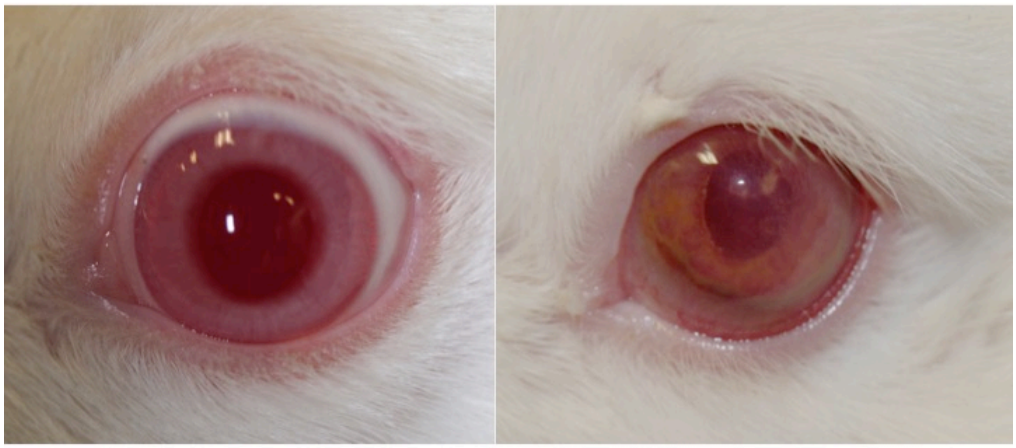

Figure 3-109 The appearance of representative eyes post injection of Healaflow or magnetic beads.

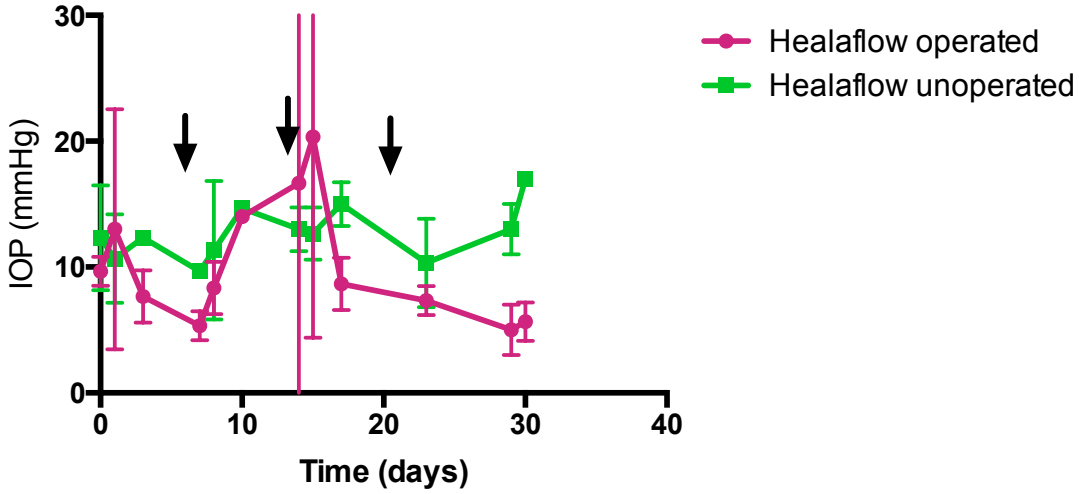

Figure 3-110 Graph to show the IOP of Healaflow injected eyes compared to uninjected eyes over time. Arrows indicate the points of injection. Postoperatively after the first and second injection 1/3 of the rabbits (not the same) showed an increase in IOP. Data shown is the mean ± SD.

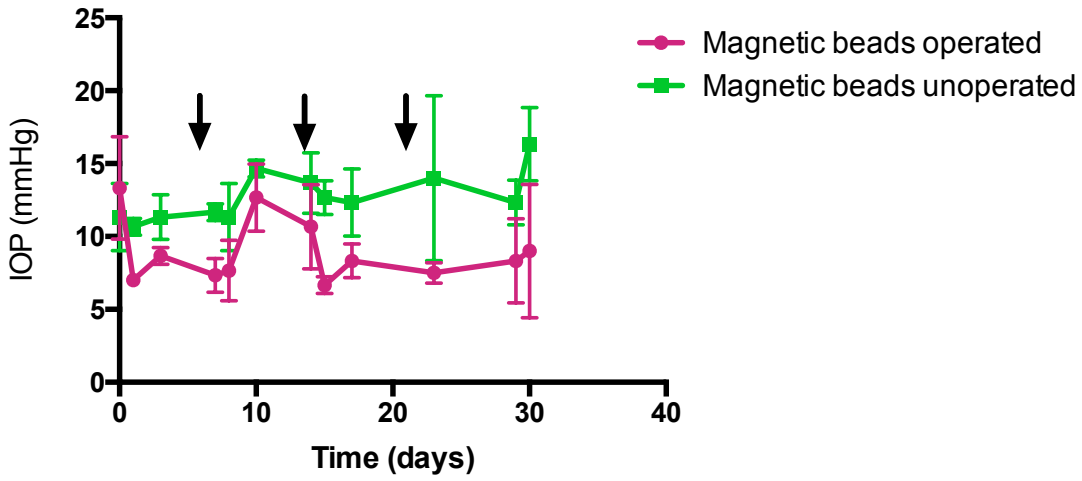

Figure 3-111 Graph to show the IOP magnetic beads over time. Arrows indicate the points of injection. Postoperatively no rabbits showed an increase in IOP. Data shown is the mean ± SD.

3.8.2 Discussion

These results show that repeated anterior chamber injection of microbeads and cross-linked hyaluronic acid in this rabbit model do not lead to sustained elevation of IOP. Indeed only a few rabbits responded to the challenge of an ocular hypertensive stimulant, and in those that did the elevation in IOP was short-lived. That the response was so little and variable is discouraging. Our aim had been to disturb and disrupt aqueous drainage that would lead to a consistently raised IOP for the duration of a 30-day experiment.

The great variability seen in IOP response to challenge between rabbits illustrates the enormous capacity of a healthy rabbit to drain aqueous (Grierson et al., 1986). Even though the anterior chamber was filled with occlusive agent there was incomplete outflow obstruction and sufficient compensation by the remaining outflow areas. This contrasts enormously to experience in humans, where even a little viscoelastic causes a rise in postoperative IOP after cataract surgery. Indeed people have examined the effect of different viscoelastics used for cataract surgery on the postoperative IOP (Jürgens et al., 1997b), despite the aim not leave any in at the end of surgery.

Other animal models have successfully raised the IOP by injection of beads into the anterior chamber or viscoelastic. The injection of magnetic coated beads has been used successfully in the rat to elevate IOP with the aim of testing either neuroprotective agents or stem cell regenerative therapies for the optic nerve (Samsel et al., 2011). Unfortunately a rat has an eye so small that inserting even the smallest of standard cannulas is too large for glaucoma filtration surgery (personal experience with ex vivo rats).

The development of buphthalmos in several animals not only indicates that there was a significant rise in IOP, but also that rabbits of this age react to raised IOP with globe enlargement in a similar way to human infants with congenital glaucoma. Buphthalmos is seen in children suffering from primary congenital glaucoma up to the age of 3 (deLuise and Anderson, 1983). The connective tissues of the sclera and cornea are more plastic at a young age and deform. With the rabbits in this experiment they too had deformable sclera / corneal tissues. Unfortunately not only does this make it more difficult to estimate the intraocular pressure - an enlarged globe will have a thinner cornea, but globe enlargement is unlikely to be identical between rabbits and therefore will add to greater variation between animals for future experiments. Older rabbits may have not had these characteristics. They are unfortunately far more expensive and beyond the scope of this experiment.

The measurement of success for glaucoma filtration surgery in animal models is difficult. Unlike human glaucoma patients, that have a raised IOP to begin with, New Zealand White rabbits do not. Genetic engineering has allowed such strains to be developed (Gelatt, 1977; Lee et al., 1978; Knepper et al., 1991), however they are not freely available. The advantage of IOP use as an outcome measure is that it is objective, has a scale, and is directly reflective of the aim of surgery. The use of observation of the presence of a bleb as an outcome measure is subjective, has no numerical scale, and as seen in previous experiments, may not reflect a bleb's functionality.

This experiment has shown that it is difficult to raise the IOP of a rabbit artificially. Alternative methods of testing glaucoma filtration efficacy may be more successful. A column of water attached to a cannula inserted into the anterior chamber could artificially raise the IOP, and rate of flow could be related to functionality. Alternatively just using sufficient numbers of animals in an experiment may increase the accuracy of IOP measurement even in the presence of a low physiological IOPs, as seen in the previous experiment.

Chapter 4 Discussion

The wound healing response is a complex process. Different cellular responses of different magnitudes occur at different times according to the type, scale and chronicity of insult. A minor insult of short duration leads to tissue restitution. A chronic major insult causes scarring as attempts are made by the tissue to preserve organ and organism function.

With most surgery the aim is to achieve the desired effect with maximum restitution and minimal scarring. Shorter skin incisions such as 'key-hole' surgery for cholecystectomy improve both appearance and reduce recovery times. Smaller gauge ports for vitrectomy obviate the need for sutures and reduce surgery duration. There is even a suggestion that strabismus surgery should be minimally invasive to cause less scarring and improve outcomes (Cambridge Ophthalmological Symposium 2014).

The concept of successful GFS however contradicts the inherent aim of normal wound healing: to return tissues to their normal structure and function. In successful GFS there is constant flow of aqueous through a fistula, an abnormal connection between the inside of the eye and the sub conjunctival space. A delicate balance exists between the constant drive to close this fistula off, and fluid flow maintaining fistula patency. In the patient, too much flow results in hypotony and disruption of visual function. Too 'active' a wound healing process closes off the fistula and halts the drainage of aqueous.

The experiments within this thesis examined the use of implants of antiscarring drug placed within the subconjunctival space. Based on evidence that these would release drug over a prolonged period, it was hypothesised that scarring would be reduced with an associated delay in wound healing, and functional drainage prolonged.

Although our results show that the physical presence of these implants causes an opposite effect on scarring to that hypothesised and are inconsistent with the previous in vivo data, considerable valuable information has been obtained. It is clear that anything particulate, be that suture or undissolved drug, when placed in the subconjunctival space, excites a foreign body response that stimulates scarring in the tissue's attempt to heal. This is not restricted to one particular type of drug, as even the most potent of steroids, dexamethasone, in its non-dissolved state caused a foreign body response. Experiments that made the implants dissolve faster resulted in this response lessening, indicating that if the challenge is removed the scarring is less, but did not preclude it.

Of particular interest, however, was the discovery that the foreign body response could be tempered when implants were coated with a polymer. Although not masked to the point of allowing drug efficacy to overcome the antagonistic particulate effect, different formulations of polymer coating were found to reduce the response by a significant degree.

Where this is pertinent is in the development of drainage devices where the presence of non host material within the subconjunctival space is necessary. Control of scarring may also help to smoothen the pharmacokinetic profile of sustained release implants in other applications and elsewhere in the body.

The early experiments that demonstrated the efficacy of ilomastat, as an antiscarring agent and prolonging bleb survival in GFS, utilised it in solution form by injection. Not yet explored is the potential of topical application of the drug for GFS. Would topical ilomastat result in therapeutic efficacy?

Ilomastat has similar properties to a topical drug that is the first line treatment for glaucoma patients, latanoprost (Figure 4-1)

Both are small molecules: the molecular weight of latanoprost (432.66), and that of ilomastat is (388.47). The water solubility of latanoprost is 50 mg / ml. This is the same concentration as used by patients. The aqueous solubility of ilomastat is 38 mg /ml. Fibroblast mediated gel contraction is inhibited at ilomastat concentrations of between 3.8 to 38 mg / ml (10 – 100 mM). The Ki for a fibroblast is in fact far less (0.16 ng / ml or 0.4 nM). *In vivo* experiments have shown that topical application of latanoprost results in a concentration of 1.49 ng / mg of drug in the sclera (Sjöquis*t et al*., 1998). We do not know what the penetration of ilomastat would be through the conjunctiva, but given the lipophilic nature of the drug it is likely to be comparable. Would there be any toxic effect of ilomastat to the cornea? It is difficult to determine this without performing the experiment, however it was originally designed as a drug to reduce keratits in the setting of corneal ulceration (Galardy *et al.*, 1994).

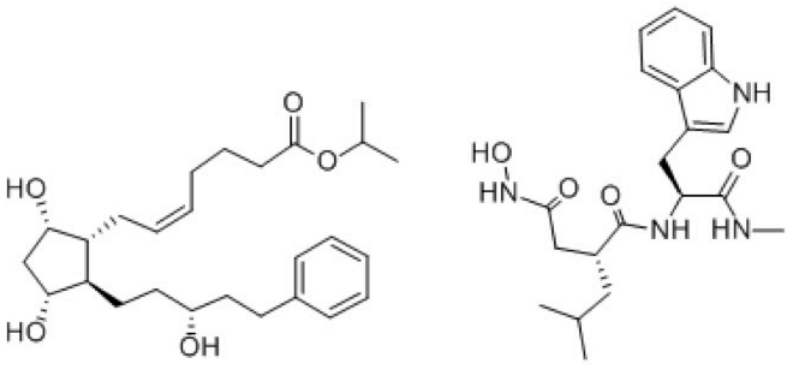

Figure 4-1 Chemical structure of latanoprost (A) and ilomastat (B).

It is my belief that the anti inflammatory efficacy of ilomastat as a topical medication warrants further investigation. Patients, particularly those with glaucoma, are used to applying drops to their eye and would far prefer this method of application than the discomfort of an injection. Furthermore, they would be able to apply the drug themselves, and eliminating the need for all the manpower and inconvenience of multiple hospital visits.

A far wider reaching implication beyond the setting of GFS, if successful, might be the use of topical ilomastat to treat other inflammatory ocular diseases and the prevention of scarring post procedures such as dacrocystorhinostomy. Indeed it may be possible that procedures in other surgical fields would benefit, such as plastic reconstructive surgery. At present the only class of effective potent anti-inflammatory ocular treatments in every day use are steroids. These are not without side effects, such as cataract formation and, as discussed before, raised IOP, particularly in glaucoma patients. A new class of anti inflammatory, MMPis, may even have a synergistic effect if combined with steroids. Unfortunately these experiments were beyond the scope of this PhD.

Interpretation of ‘success’ in experimental animal models is a contentious issue. Historically for glaucoma filtration surgery experiments we rely on the appearance of a ‘bleb’ and the way it looks on a two dimensional wafer thin histological cross section. It is clear that these two parameters are highly dependant on observer interpretation and may vary considerably depending on how the first looks and the orientation and location of the slice of the second.

Without complete objectivity it is not possible to retain an unbiased perspective. The space shuttle ‘Challenger’ exploded shortly after take off on a cold day when the rubber seals in the rocket failed to flex and extend appropriately. The likelihood of this happening was well known to the construction workers who made the seals and as this information was fed up the chain of command a more and more positive interpretation of risk of mechanical failure was taken as juniors wishing to please

their superiors painted an optimistic picture (Feynman RP, 1988). The desire to achieve success in sending a teacher into space outweighed the more sensible decision to delay launch to a warmer day with catastrophic consequences.

These experiments illustrate the importance of understanding material tissue interaction for the development of drug delivery devices. Experimental models are key to allowing the development of new treatments and prevent launching into first time human use without knowledge of how these might behave within a living organism, yet are only useful so long as their limitations are recognised.

Chapter 5 References

Addicks et al., 1983. Histologic characteristics of filtering blebs in glaucomatous eyes. Arch Ophthalmol, 101(5) 795-798.

Al-Shahwan, S. & Edward, D.P., 2005. Foreign body granulomas secondary to retained sponge fragment following mitomycin C trabeculectomy. Graefes Arch Clin Exp Ophthalmol, 243(2) 178-181.

Aulton, M.E. & Taylor, K.M.G., 2013. Pharmaceutics. Elsevier Health Sciences,

Barnes, P.J. & Adcock, I.M., 1995. Steroid resistance in asthma. QJM, 88(7) 455-468.

Bell, E., Ivarsson, B. & Merrill, C., 1979. Production of a tissue-like structure by contraction of collagen lattices by human fibroblasts of different proliferative potential in vitro. Proc Natl Acad Sci USA, 76(3) 1274-1278.

Bijlsma, J.W., 1999. Can we use steroid hormones to immunomodulate rheumatic diseases? Rheumatoid arthritis as an example. Ann N Y Acad Sci, 876366-76; discussion 376.

Bramhall, S.R. et al., 2001. Marimastat as first-line therapy for patients with unresectable pancreatic cancer: a randomized trial. J Clin Oncol, 19(15) 3447-3455.

Bruno, Fisher & Moroi, 2007. Is scarless wound healing applicable to glaucoma surgery? Ex Rev Op, 2(1) 79-90.

Cairns, J.E., 1968. Trabeculectomy. Preliminary report of a new method. Am J Ophthalmol, 66(4) 673-679.

Cannon, G.J. & Swanson, J.A., 1992. The macrophage capacity for phagocytosis. J Cell Sci, 101(Pt 4) 907-913.

Cantrill, H.L. et al., 1975. In vitro determination of relative corticosteroid potency. J Clin Endocrinol Metab, 40(6) 1073-1077.

Caprioli et al., 2010. Blood pressure, perfusion pressure, and glaucoma. Am J Ophthalmol, 149(5) 704-712.

Chang-Lin, J.E. et al., 2011. Pharmacokinetics and pharmacodynamics of a sustained-release dexamethasone intravitreal implant. Investigative Ophthalmology & Visual Science, 52(1) 80-86.

Chen, C.W. et al., 1990. Trabeculectomy with simultaneous topical application of mitomycin-C in refractory glaucoma. J Ocul Pharmacol, 6(3) 175-182.

Cheng, C.K. et al., 1995. Intravitreal sustained-release dexamethasone device in the treatment of experimental uveitis. Investigative Ophthalmology & Visual Science, 36(2) 442-453.

Chun, T.H. et al., 2004. MT1-MMP-dependent neovessel formation within the confines of the three-dimensional extracellular matrix. J Cell Biol, 167(4) 757-767.

Cordeiro et al., 1997. Effect of varying the mitomycin-C treatment area in glaucoma filtration surgery in the rabbit. Investigative Ophthalmology & Visual Science, 38(8) 1639-1646.

Cottone, M. et al., 2011. Medical management of Crohn's disease. Expert Opin Pharmacother, 12(16) 2505-2525.

Coussens, L.M., Fingleton & Matrisian, L.M., 2002. Matrix metalloproteinase inhibitors and cancer: trials and tribulations. Science, 295(5564) 2387-2392.

Crowley, C., Birchall, M. & Seifalian, A.M., 2014. Trachea transplantation: from laboratory to patient. Journal of tissue engineering and regenerative medicine,

Daniels et al., 2003. Matrix metalloproteinase inhibition modulates fibroblast-mediated matrix contraction and collagen production in vitro. Investigative Ophthalmology & Visual Science, 44(3) 1104-1110.

DeBry, P.W. et al., 2002. Incidence of late-onset bleb-related complications following trabeculectomy with mitomycin. Arch Ophthalmol, 120(3) 297-300.

deLuise, V.P. & Anderson, D.R., 1983. Primary infantile glaucoma (congenital glaucoma). Survey of Ophthalmology, 28(1) 1-19.

Demeis, R., 1988. Stick-to-it riblets. Aerospace America, 2648.

Environmental, D., 2011. Recognition, Evaluation, Control.

Dolnik, O. et al., 2004. Ectodomain shedding of the glycoprotein GP of Ebola virus. The EMBO journal, 23(10) 2175-2184.

Doyle et al., 1993. Intraoperative 5-fluorouracil for filtration surgery in the rabbit. Investigative Ophthalmology & Visual Science, 34(12) 3313-3319.

Dziedziczko, A. & Banach-Wawrzeńczyk, E., 1997. Pneumocystis pneumonia in patients with steroid-dependent asthma. Pneumonol Alergol Pol, 65(5-6) 399-405.

Edmunds et al., 2001. The National Survey of Trabeculectomy. II. Variations in operative technique and outcome. Eye (Lond), 15(Pt 4) 441-448.

Eming, S.A., Krieg, T. & Davidson, J.M., 2007. Inflammation in wound repair: molecular and cellular mechanisms. J Invest Dermatol, 127(3) 514-525.

Feynman, R.P., What Do You Care What Other People Think?, 1988, W W Norton, ISBN 0-393-02659-0, 2001 paperback: ISBN 0-393-32092-8

Filho, E. & Sit, 2009. Advances in glaucoma surgery. Ex Rev Op, 4(6) 595-605.

Fluorouracil Filtering Surgery Study Group, 1989. Fluorouracil Filtering Surgery Study one-year follow-up.. Am J Ophthalmol, 108(6) 625-635.

Galardy, R.E. et al., 1994. Low molecular weight inhibitors in corneal ulceration. Ann N Y Acad Sci, 732315-323.

Gálvez, B.G. et al., 2004. Caveolae are a novel pathway for membrane-type 1 matrix metalloproteinase traffic in human endothelial cells. Mol Biol Cell, 15(2) 678-687.

Gedde, S.J. et al., 2007a. Surgical complications in the Tube Versus Trabeculectomy Study during the first year of follow-up. Am J Ophthalmol, 143(1) 23-31.

Gedde, S.J. et al., 2007b. Treatment outcomes in the tube versus trabeculectomy study after one year of follow-up. Am J Ophthalmol, 143(1) 9-22.

Gedde, S.J. et al., 2009. Three-year follow-up of the tube versus trabeculectomy study. Am J Ophthalmol, 148(5) 670-684.

Gelatt, K.N., 1977. Animal models for glaucoma. Investigative Ophthalmology & Visual Science, 16(7) 592-596.

Georgoulas, S. 2010. Novel methods for the moduation of wound healing after glaucoma filtration surgrey. PhD thesis, School of Pharmacy, University of London and UCL Institute of Ophthlamology and Moorfields Eye Hospital.

Georgoulas, S. et al., 2008. Progress in Brain Research. 173237-254.

Georgoulas, S. et al., 2010. A novel single application prolonged release MMP inhibitor is superior to mitomycin in preventing scarrring after experimental glaucoma surgery. Investigative Ophthalmology & Visual Science, 49(5) pp. 4538.

Gooz, M., 2010. ADAM-17: the enzyme that does it all. Crit Rev Biochem Mol Biol, 45(2) 146-169.

Grierson, I. et al., 1986. The effects of various levels of intraocular pressure on the rabbit's outflow system. Experimental Eye Research, 42(4) 383-397.

Grivennikov, Greten & Karin, 2010. Immunity, inflammation, and cancer. Cell, 140(6) 883-899.

Grobelny, D., Poncz, L. & Galardy, R.E., 1992. Inhibition of human skin fibroblast collagenase, thermolysin, and Pseudomonas aeruginosa elastase by peptide hydroxamic acids. Biochemistry, 31(31) 7152-7154.

Gross, J. & Lapiere, C.M., 1962. Collagenolytic activity in amphibian tissues: a tissue culture assay. Proc Natl Acad Sci USA, 481014-1022.

Group, C.A.T.-T.S. et al., 2007. Factors affecting the outcome of trabeculectomy: an analysis based on combined data from two phase III studies of an antibody to transforming growth factor beta2, CAT-152. Ophthalmology, 114(10) 1831-1838.

Hainsworth, D.P. et al., 1996. Sustained release intravitreal dexamethasone. J Ocul Pharmacol Ther, 12(1) 57-63.

Habara, S, et al. 2011. Serial clinical and angiographic follow-up after phosphorylcholine-coated stent implantation. Int Heart Journal, 52(2), 88–91.

Harwerth, R.S., Wheat, J.L. & Rangaswamy, N.V., 2008. Age-related losses of retinal ganglion cells and axons. Investigative Ophthalmology & Visual Science, 49(10) 4437-4443.

Haston, W.S., Shields, J.M. & Wilkinson, P.C., 1982. Lymphocyte locomotion and attachment on two-dimensional surfaces and in three-dimensional matrices. J Cell Biol, 92(3) 747-752.

Hawinkels, L.J. et al., 2008. VEGF release by MMP-9 mediated heparan sulphate cleavage induces colorectal cancer angiogenesis. Eur J Cancer, 44(13) 1904-1913.

Heijl, A. et al., 2002. Reduction of intraocular pressure and glaucoma progression: results from the Early Manifest Glaucoma Trial. Arch Ophthalmol, 120(10) 1268-1279.

Hinz, B. et al., 2007. The myofibroblast: one function, multiple origins. Am J Pathol, 170(6) 1807-1816.

Hitchings & Grierson, 1983. Clinico pathological correlation in eyes with failed fistulizing surgery. Trans Ophthalmol Soc U K, 103(Pt 1) 84-88.

Hu, J. et al., 2007. Matrix metalloproteinase inhibitors as therapy for inflammatory and vascular diseases. Nat Rev Drug Discov, 6(6) 480-498.

Hyung et al., 1994. Effects of postoperative mitomycin C on glaucoma filtration surgery in rabbits treated preoperatively with antiglaucoma medications. Ophthalmic Surg, 25(10) 704-714.

Weller, I., Lockwood, C.M. & chandra, R.K. (1998) Secondary Immunodeficiency. In Immunology, (Eds, Roitt, Brostoff & Male) Mosby, pp. 293-300.

Ichikawa et al., 2006. Matrilysin (MMP-7) degrades VE-cadherin and accelerates accumulation of beta-catenin in the nucleus of human umbilical vein endothelial cells. Oncol Rep, 15(2) 311-315.

Jacob, J.T. et al., 1998. Biocompatibility response to modified Baerveldt glaucoma drains. J Biomed Mater Res, 43(2) 99-107.

Jarvis, B.W. & Qureshi, N., 1997. Inhibition of lipopolysaccharide-induced transcription factor Sp1 binding by spectrally pure diphosphoryl lipid A from

Rhodobacter sphaeroides, protein kinase inhibitor H-8, and dexamethasone. Infection and immunity, 65(5) 1640-1643.

Jimenez, J., 2004. Turbulent flows over rough walls. Annual Review of Fluid Mechanics, 36(1) 173-196.

Jones, R. & Rhee, D.J., 2006. Corticosteroid-induced ocular hypertension and glaucoma: a brief review and update of the literature. Current opinion in ophthalmology, 17(2) 163-167.

Jung, K.I. et al., 2013. Foreign body reaction in glaucoma drainage implant surgery. Investigative Ophthalmology & Visual Science, 54(6) 3957-3964.

Jungebluth, P. et al., 2011. Tracheobronchial transplantation with a stem-cell-seeded bioartificial nanocomposite: a proof-of-concept study. Lancet, 378(9808) 1997-2004.

Junqueira, L.C., Bignolas, G. & Brentani, R.R., 1979. Picrosirius staining plus polarization microscopy, a specific method for collagen detection in tissue sections. Histochem J, 11(4) 447-455.

Jürgens, I., Matheu, A. & Castilla, M., 1997a. Ocular hypertension after cataract surgery: a comparison of three surgical techniques and two viscoelastics. Ophthalmic surgery and lasers, 28(1) 30-36.

Jürgens, I., Matheu, A. & Castilla, M., 1997b. Ocular hypertension after cataract surgery: a comparison of three surgical techniques and two viscoelastics. Ophthalmic surgery and lasers, 28(1) 30-36.

Kamp, D.W. & Weitzman, S.A., 1999. The molecular basis of asbestos induced lung injury. Thorax, 54(7) 638-652.

Karim, R.B. et al., 2006. MMP-2 assessment as an indicator of wound healing: A feasibility study. Adv Skin Wound Care, 19(6) 324-327.

Kawana, K. et al., 2009. Evaluation of trabeculectomy blebs using 3-dimensional cornea and anterior segment optical coherence tomography. Ophthalmology, 116(5) 848-855.

Kawasaki, S. et al., 2009. Evaluation of filtering bleb function by thermography. Br J Ophthalmol, 93(10) 1331-1336.

Kawashima, Y. et al., 1998. Immunolocalization of matrix metalloproteinases and tissue inhibitors of metalloproteinases in human subconjunctival tissues. Curr Eye Res, 17(4) 445-451.

Kennedy, G.L. & Sherman, H., 1986. Acute and subchronic toxicity of dimethylformamide and dimethylacetamide following various routes of administration. Drug and chemical toxicology, 9(2) 147-170.

Khaw et al., 1993. Prolonged localized tissue effects from 5-minute exposures to fluorouracil and mitomycin C. Arch Ophthalmol, 111(2) 263-267.

Kim, K.S. et al., 2011. Expression levels and association of gelatinases MMP-2 and MMP-9 and collagenases MMP-1 and MMP-13 with VEGF in synovial fluid of patients with arthritis. Rheumatol Int, 31(4) 543-547.

King, A.J. et al., 2007. Frequency of bleb manipulations after trabeculectomy surgery. Br J Ophthalmol, 91(7) 873-877.

Kirwan, J.F. et al., 2006. Effect of beta radiation on success of glaucoma drainage surgery in South Africa: randomised controlled trial. BMJ (Clinical research ed), 333(7575) 942.

Knepper, P.A. et al., 1991. Ultrastructural alterations in the aqueous outflow pathway of adult buphthalmic rabbits. Experimental Eye Research, 52(5) 525-533.

Kwak, H.W. & D'Amico, D.J., 1992. Evaluation of the retinal toxicity and pharmacokinetics of dexamethasone after intravitreal injection. Arch Ophthalmol, 110(2) 259-266.

Kwon, D.H. et al., 2014. Myocardial scar burden predicts survival benefit with implantable cardioverter defibrillator implantation in patients with severe ischaemic cardiomyopathy: influence of gender. Heart (British Cardiac Society), 100(3) 206-213.

Lee, P.F. et al., 1978. Correlation of aqueous humor ascorbate with intraocular pressure and outflow facility in hereditary buphthalmic rabbits. Investigative Ophthalmology & Visual Science, 17(8) 799-802.

Leydghecker, W., Akiyama, K. & Neumann, H.G., 1958. Intraocular pressure in normal human eyes. Klin Monbl Augenheilkd Augenarztl Fortbild, 133(5) 662-670.

Lint, V. et al., 2005. Resistance of collagenase-2 (matrix metalloproteinase-8)-deficient mice to TNF-induced lethal hepatitis. J Immunol, 175(11) 7642-7649.

Liu, Z. et al., 2000. The serpin alpha1-proteinase inhibitor is a critical substrate for gelatinase B/MMP-9 in vivo. Cell, 102(5) 647-655.

Lobo, A.-M., Sobrin, L. & Papaliodis, G.N., 2010. Drug delivery options for the treatment of ocular inflammation. Seminars in ophthalmology, 25(5-6) 283-288.

Lockwood, A.J., Kirwan, J.F. & Ashleigh, Z., 2010. Optometrists referrals for glaucoma assessment: a prospective survey of clinical data and outcomes. Eye (Lond), 24(9) 1515-1519.

London, N.J., Chiang, A. & Haller, J.A., 2011. The dexamethasone drug delivery system: Indications and evidence. Adv Ther, 28(5) 351-366.

Luplertlop, N. et al., 2006. Dengue-virus-infected dendritic cells trigger vascular leakage through metalloproteinase overproduction. EMBO Rep, 7(11) 1176-1181.

Manicone & McGuire, 2008. Matrix metalloproteinases as modulators of inflammation. Semin Cell Dev Biol, 19(1) 34-41.

Martinez-de-la-Casa, J.M. et al., 2004. Selective vs argon laser trabeculoplasty: hypotensive efficacy, anterior chamber inflammation, and postoperative pain. Eye (Lond), 18(5) 498-502.

Mastropietro, D.J., Omidian, H. & Park, K., 2012. Drug delivery applications for superporous hydrogels. Expert opinion on drug delivery, 9(1) 71-89.

McCluskey et al., 2009. Otago Glaucoma Surgery Outcome Study: the pattern of expression of MMPs and TIMPs in bleb capsules surrounding Molteno implants. Investigative Ophthalmology & Visual Science, 50(5) 2161-2164.

McLaren, J.W., 2009. Measurement of aqueous humor flow. Exp Eye Res, 88(4) 641-647.

Meyer, P.A., 2006. Avoiding surgery for thyroid eye disease. Eye (Lond), 20(10) 1171-1177.

Mietz et al., 2003. Latanoprost stimulates secretion of matrix metalloproteinases in tenon fibroblasts both in vitro and in vivo. Investigative Ophthalmology & Visual Science, 44(12) 5182-5188.

Miller et al., 1989. Wound healing in an animal model of glaucoma fistulizing surgery in the rabbit. Ophthalmic Surg, 20(5) 350-357.

Molteno, A.C.B. et al., 2009. Otago glaucoma surgery outcome study: tissue matrix breakdown by apoptotic cells in capsules surrounding molteno implants. Investigative Ophthalmology & Visual Science, 50(3) 1187-1197.

Nabih, M. et al., 1991. Toxicity of high-dose intravitreal dexamethasone. Int Ophthalmol, 15(4) 233-235.

Nagase, H., 1997. Activation mechanisms of matrix metalloproteinases. Biol Chem, 378(3-4) 151-160.

Nakada, M.T. et al., 1987. Glucocorticoid regulation of beta-adrenergic receptors in 3T3-L1 preadipocytes. Mol Pharmacol, 31(4) 377-384.

Nish, S. & Medzhitov, R., 2011. Host Defense Pathways: Role of Redundancy and Compensation in Infectious Disease Phenotypes. Immunity, 34(5) 629-636.

Overall, C.M., Wiebkin, O.W. & Thonard, J.C., 1987. Demonstration of tissue collagenase activity in vivo and its relationship to inflammation severity in human gingiva. J Periodont Res, 22(2) 81-88.

Park, J.E. & Barbul, A., 2004. Understanding the role of immune regulation in wound healing. Am J Surg, 187(5A) 11S-16S.

Parkinson, G. et al., 2012. Characterisation of Ilomastat for Prolonged Ocular Drug Release. AAPS PharmSciTech, 13(4) 1063-1072.

Parks, W.C., Wilson, C.L. & López-Boado, Y.S., 2004. Matrix metalloproteinases as modulators of inflammation and innate immunity. Nat Rev Immunol, 4(8) 617-629.

Parmar, D.N. & Sharr, M.M., 1999. Cotton gauze foreign body granuloma following microvascular decompression. Br J Neurosurg, 13(1) 87-89.

Khaw, P.T. et al. The Moorfields Safer Surgery System found at https://www.ucl.ac.uk/impact/case-study-repository/moorfields-safer-surgery-system

Li, Y., Li, D., Ying, X., Khaw, P. T., & Raisman, G. 2015. An energy theory of glaucoma. *Glia*. doi:10.1002/glia.22825 epub ahead of print.

Qin, Y. et al., 2010. A rabbit model of age-dependant ocular hypertensive response to topical corticosteroids. Acta Ophthalmol, 90(6), 559–563.

Quigley & Broman, 2006. The number of people with glaucoma worldwide in 2010 and 2020. Br J Ophthalmol, 90(3) 262-267.

Raidl, M. et al., 2007. Impaired TNFalpha-induced VEGF expression in human airway smooth muscle cells from smokers with COPD: role of MAPkinases and histone acetylation--effect of dexamethasone. Cell Biochem Biophys, 49(2) 98-110.

Rao et al., 2009. New devices in glaucoma surgery. Ex Rev Op, 4(5) 491-504.

Ratner, B.D., 2002. Reducing capsular thickness and enhancing angiogenesis around implant drug release systems. J Control Release, 78(1-3) 211-218.

Razeghinejad, M.R., Fudemberg, S.J. & Spaeth, G.L., 2012. The changing conceptual basis of trabeculectomy: a review of past and current surgical techniques. Surv Ophthalmol, 57(1) 1-25.

Reijerkerk et al., 2006. Diapedesis of monocytes is associated with MMP-mediated occludin disappearance in brain endothelial cells. FASEB J, 20(14) 2550-2552.

Roberts, M.A. et al., 2009. Sympathetic ophthalmia secondary to cyclodiode laser in a 10-year-old boy. J AAPOS, 13(3) 299-300.

Rodrigues, E.B. et al., 2009. The use of vital dyes in ocular surgery. Surv Ophthalmol, 54(5) 576-617.

Rosewicz, S. et al., 1988. Mechanism of glucocorticoid receptor down-regulation by glucocorticoids. J Biol Chem, 263(6) 2581-2584.

Rothman, Liebmann & Ritch, 2000. Low-dose 5-fluorouracil trabeculectomy as initial surgery in uncomplicated glaucoma: long-term followup. Ophthalmology, 107(6) 1184-1190.

Roy, S. et al., 2012. Crosslinked sodium hyaluronate implant in deep sclerectomy for the surgical treatment of glaucoma. European Journal of Ophthalmology, 22(1) 70-76.

Yalkowsky, S.H. & He, Y. (2003) Handbook of aqueous solubility data. CRC press., Boca Raton.

Samsel, P.A. et al., 2011. A novel method for the induction of experimental glaucoma using magnetic microspheres. Investigative Ophthalmology & Visual Science, 52(3) 1671-1675.

Sappington, R.M. et al., 2010. The Microbead Occlusion Model: A Paradigm for Induced Ocular Hypertension in Rats and Mice. Investigative Ophthalmology & Visual Science, 51(1) 207-216.

Saraiya, N.V. & Goldstein, D.A., 2011. Dexamethasone for ocular inflammation. Expert Opin Pharmacother, 12(7) 1127-1131.

Scott, K.A., Wood, E.J. & Karran, E.H., 1998. A matrix metalloproteinase inhibitor which prevents fibroblast-mediated collagen lattice contraction. FEBS Lett, 441(1) 137-140.

Shah, P. et al., 2011. ReGAE 7: long-term outcomes of augmented trabeculectomy with mitomycin C in African-Caribbean patients. Clin Experiment Ophthalmol, 2012; 40: e176–e182.

Shin, M.L. & Firminger, H.I., 1973. Acute and chronic effects of intraperitoneal injection of two types of asbestos in rats with a study of the histopathogenesis and ultrastructure of resulting mesotheliomas. Am J Pathol, 70(3) 291-313.

Sibley, C.H. & Tomkins, G.M., 1974. Mechanisms of steroid resistance. Cell, 2(4) 221-227.

Sjöquist, B., & Stjernschantz, J. 2002. Ocular and systemic pharmacokinetics of latanoprost in humans. *Survey of Ophthalmology*, *47 Suppl 1*, S6–12.

Skuta & Parrish, 1987. Wound healing in glaucoma filtering surgery. Surv Ophthalmol, 32(3) 149-170.

Sledge, G.W. et al., 1995. Effect of matrix metalloproteinase inhibitor batimastat on breast cancer regrowth and metastasis in athymic mice. J Natl Cancer Inst, 87(20) 1546-1550.

SooHoo, J.R. et al., 2012. Bleb morphology and histology in a rabbit model of glaucoma filtration surgery using Ozurdex® or mitomycin-C. Molecular vision, 18714-719.

Srinivas, A. & Ramamurthi, A., 2007. Effects of gamma-irradiation on physical and biologic properties of crosslinked hyaluronan tissue engineering scaffolds. Tissue Eng, 13(3) 447-459.

Stalmans, I. et al., 2006. Safe trabeculectomy technique: long term outcome. Br J Ophthalmol, 90(1) 44-47.

Steffensen, Häkkinen & Larjava, 2001. Proteolytic events of wound-healing--coordinated interactions among matrix metalloproteinases (MMPs), integrins, and extracellular matrix molecules. Crit Rev Oral Biol Med, 12(5) 373-398.

Sudbeck, B.D. et al., 1997. Induction and repression of collagenase-1 by keratinocytes is controlled by distinct components of different extracellular matrix compartments. J Biol Chem, 272(35) 22103-22110.

Sumer, B.M. & Fredsøe, J. (2006) Hydrodynamics Around Cylindrical Strucures. World Scientific Publishing Company Incorporated,

Takeuchi, K. et al., 2009. Solid hyaluronic acid film and the prevention of postoperative fibrous scar formation in experimental animal eyes. Arch Ophthalmol, 127(4) 460-464.

Tan, A. et al., 2013. An anti-CD34 antibody-functionalized clinical-grade POSS-PCU nanocomposite polymer for cardiovascular stent coating applications: a preliminary assessment of endothelial progenitor cell capture and hemocompatibility. PLoS ONE, 8(10) e77112.

Tavolato, M., Babighian, S. & Galan, A., 2006. Spontaneous extrusion of a stainless steel glaucoma drainage implant (Ex-PRESS). Eur J Ophthalmol, 16(5) 753-755.

Tay, E., Aung, T. & Murdoch, I., 2006. Suprachoroidal haemorrhage: a rare complication of cyclodiode laser therapy. Eye (Lond), 20(5) 625-627.

Taylor, 2009. Glaucoma: where to now? Ophthalmology, 116(5) 821-822.

Tham, Y.-C. et al., 2014. Global Prevalence of Glaucoma and Projections of Glaucoma Burden through 2040: A Systematic Review and Meta-Analysis. Ophthalmology, epub ahead of print 10.1016/j.ophtha.2014.05.013

The Advanced Glaucoma Intervention Study (AGIS): 7, 2000. The relationship between control of intraocular pressure and visual field deterioration.The AGIS Investigators. Am J Ophthalmol, 130(4) 429-440.

The Glaucoma Laser Trial (GLT) and glaucoma laser trial follow-up study, 1995: 7. Results. Glaucoma Laser Trial Research Group. Am J Ophthalmol, 120(6) 718-731.

Toriseva & Kähäri, 2009. Proteinases in cutaneous wound healing. Cell Mol Life Sci, 66(2) 203-224.

Tsai, I.Y. et al., 2011. Human macrophage adhesion on polysaccharide patterned surfaces. Soft Matter, 73599-73606.

Vieira, G.M. et al., 2006. Intraocular pressure variation during weight lifting. Arch Ophthalmol, 124(9) 1251-1254.

Wang, Y. et al., 2011. TGF-β1 promoted MMP-2 mediated wound healing of anterior cruciate ligament fibroblasts through NF-κB. Connect Tissue Res, 52(3) 218-225.

Washington, C., 2009. Evaluation of non-sink dialysis methods for the measurement of drug release from colloids: effects of drug partition. International journal of pharmaceutics, 56(1) 71-74.

Watson, P.G. & Barnett, F., 1975. Effectiveness of trabeculectomy in glaucoma. Am J Ophthalmol, 79(5) 831-845.

Wells, A.P. et al., 2003. Cystic bleb formation and related complications in limbus- versus fornix-based conjunctival flaps in pediatric and young adult trabeculectomy with mitomycin C. Ophthalmology, 110(11) 2192-2197.

Wojtowicz-Praga, S. et al., 1998. Phase I trial of Marimastat, a novel matrix metalloproteinase inhibitor, administered orally to patients with advanced lung cancer. J Clin Oncol, 16(6) 2150-2156.

Wolner, B. et al., 1991. Late bleb-related endophthalmitis after trabeculectomy with adjunctive 5-fluorouracil. Ophthalmology, 98(7) 1053-1060.

Wong, E.Y. et al., 2004. Detection of undiagnosed glaucoma by eye health professionals. Ophthalmology, 111(8) 1508-1514.

Wong, T.T., Mead, A.L. & Khaw, 2003. Matrix metalloproteinase inhibition modulates postoperative scarring after experimental glaucoma filtration surgery. Investigative Ophthalmology & Visual Science, 44(3) 1097-1103.

Wong, T.T., Mead, A.L. & Khaw, 2005. Prolonged antiscarring effects of ilomastat and MMC after experimental glaucoma filtration surgery. Investigative Ophthalmology & Visual Science, 46(6) 2018-2022.

Wong, T.T. et al., 2002. Matrix metalloproteinases in disease and repair processes in the anterior segment. Surv Ophthalmol, 47(3) 239-256.

Yong, V.W. et al., 2001. Metalloproteinases in biology and pathology of the nervous system. Nat Rev Neurosci, 2(7) 502-511.

Zacharia, P.T., Deppermann, S.R. & Schuman, J.S., 1993. Ocular hypotony after trabeculectomy with mitomycin C. Am J Ophthalmol, 116(3) 314-326.

Zarković, M. et al., 2008. Cortisol response to ACTH stimulation correlates with blood interleukin 6 concentration in healthy humans. Eur J Endocrinol, 159(5) 649-652.

Zhang, L. et al., 2013. Zwitterionic hydrogels implanted in mice resist the foreign-body reaction. Nature biotechnology, 31(6) 553-556.